LOCKHEED MARTIN ENERGY RESEARCH LIBRARIES
3 4456 0515494 4

CENTRAL RESEARCH LIBRARY

ORNL-4997

Cy/21

NEUTRON PHYSICS DIVISION

Progress Report

Period Ending August 31, 1974

OAK RIDGE NATIONAL LABORATORY
CENTRAL RESEARCH LIBRARY
DOCUMENT COLLECTION
LIBRARY LOAN COPY
DO NOT TRANSFER TO ANOTHER PERSON
If you wish someone else to see this
document, send in name with document
and the library will arrange a loan.
UCN-7969
(3 3-67)

OAK RIDGE NATIONAL LABORATORY
OPERATED BY UNION CARBIDE CORPORATION • FOR THE U.S. ATOMIC ENERGY COMMISSION

Printed in the United States of America. Available from
National Technical Information Service
U.S. Department of Commerce
5285 Port Royal Road, Springfield, Virginia 22151
Price: Printed Copy $7.60; Microfiche $1.45

This report was prepared as an account of work sponsored by the United States Government. Neither the United States nor the United States Atomic Energy Commission, nor any of their employees, nor any of their contractors, subcontractors, or their employees, makes any warranty, express or implied, or assumes any legal liability or responsibility for the accuracy, completeness or usefulness of any information, apparatus, product or process disclosed, or represents that its use would not infringe privately owned rights.

ORNL-4997
UC-34c – Physics–Nuclear

Contract No. W-7405-eng-26

NEUTRON PHYSICS DIVISION PROGRESS REPORT

For Period Ending August 31, 1974

F. C. Maienschein, Director

OCTOBER 1974

OAK RIDGE NATIONAL LABORATORY
Oak Ridge, Tennessee 37830
operated by
UNION CARBIDE CORPORATION
for the
U.S. ATOMIC ENERGY COMMISSION

LOCKHEED MARTIN ENERGY RESEARCH LIBRARIES
3 4456 0515494 4

Reports previously issued in this series are as follows:

ORNL-2081	Period Ending September 10, 1956
ORNL-2389	Period Ending September 1, 1957
ORNL-2609	Period Ending September 1, 1958
ORNL-2842	Period Ending September 1, 1959
ORNL-3016	Period Ending September 1, 1960
ORNL-3193	Period Ending September 1, 1961
ORNL-3360	Period Ending September 1, 1962
ORNL-3499, Vols. I and II	Period Ending August 1, 1963
ORNL-3714, Vols. I and II	Period Ending August 1, 1964
ORNL-3858, Vols. I and II	Period Ending August 1, 1965
ORNL-3973, Vols. I and II	Period Ending May 31, 1966
ORNL-4134	Period Ending May 31, 1967
ORNL-4280	Period Ending May 31, 1968
ORNL-4433	Period Ending May 31, 1969
ORNL-4592	Period Ending May 31, 1970
ORNL-4705	Period Ending May 31, 1971
ORNL-4800	Period Ending May 31, 1972
ORNL-4902	Period Ending May 31, 1973

CONTENTS

Introduction and Summary xi

1. Present Status of Cross-Section Data of the Fissile and Fertile Isotopes for Fast Reactors – G. de Saussure and R. B. Perez 1
2. Recent Measurements on ^{238}U at ORNL – G. de Saussure 1
3. Multilevel Effects in the Unresolved Resonances Region of the Cross Sections of Fissile Nuclides – G. de Saussure and R. B. Perez 11
4. Natural Chromium and ^{52}Cr Neutron Elastic and Inelastic Scattering Cross Sections from 4.07 to 8.56 MeV – W. E. Kinney and F. G. Perey 12
5. Natural Titanium Neutron Elastic and Inelastic Scattering Cross Sections from 4.07 to 8.56 MeV – W. E. Kinney and F. G. Perey 12
6. Neutron-Induced Gamma-Ray Production in Titanium for Incident-Neutron Energies of 4.9, 5.4, and 5.9 MeV – J. K. Dickens 12
7. ^{54}Fe Neutron Elastic and Inelastic Scattering Cross Sections from 5.50 to 8.50 MeV – W. E. Kinney and F. G. Perey 13
8. ^{63}Cu and ^{65}Cu Neutron Elastic and Inelastic Scattering Cross Sections from 4.07 to 8.50 MeV – W. E. Kinney and F. G. Perey 13
9. ^{206}Pb, ^{207}Pb, and ^{208}Pb Neutron Elastic and Inelastic Scattering Cross Sections from 5.50 to 8.50 MeV – W. E. Kinney and F. G. Perey 14
10. Neutron-Capture Cross Sections of the Stable Lead Isotopes – B. J. Allen, R. L. Macklin, R. R. Winters, and C. Y. Fu 14
11. Nitrogen Neutron Elastic and Inelastic Scattering Cross Sections from 4.34 to 8.56 MeV – F. G. Perey and W. E. Kinney 14
12. Natural Nickel and ^{60}Ni Neutron Elastic and Inelastic Scattering Cross Sections from 4.07 to 8.56 MeV – W. E. Kinney and F. G. Perey 14
13. Gamma-Ray Production from Neutron Interactions with Nickel for Incident Neutron Energies Between 1.0 and 10 MeV: Tabulated Differential Cross Sections – J. K. Dickens, T. A. Love, and G. L. Morgan 15
14. Direct-Interaction Interpretation for ^{40}Ca$(n,np\gamma)^{39}$K Reactions at $E_n = 17$ to 20 MeV – J. K. Dickens 15
15. Neutron-Induced Gamma-Ray Production in Calcium in the Energy Range $0.7 \leqslant E_n \leqslant 20$ MeV – J. K. Dickens, T. A. Love, and G. L. Morgan 16
16. Gamma-Ray Production Due to Neutron Interactions with Zinc for Incident Neutron Energies Between 0.85 and 20 MeV: Tabulated Differential Cross Sections – J. K. Dickens, T. A. Love, and G. L. Morgan 16
17. Gamma-Ray Production Due to Neutron Interactions with Zinc. Tabulated Differential Cross Sections for 31 Gamma Rays for Incident Neutron Energies Between 0.9 and 6 MeV – G. G. Slaughter and J. K. Dickens 16

18. Gamma-Ray Production Due to Neutron Interactions with ^{68}Zn and the Level Structure of ^{68}Zn – J. K. Dickens 17

19. ^{28}Si($n,n'\gamma$) Photon Production Cross Sections for $E\gamma = 1.78$ MeV, $5.0 \leqslant E_n \leqslant 9.5$ MeV – J. K. Dickens and G. L. Morgan 17

20. Gamma-Ray Production from Neutron Interactions with Silicon for Incident Neutron Energies Between 1.0 and 20 MeV: Tabulated Differential Cross Sections – J. K. Dickens, T. A. Love, and G. L. Morgan 17

21. Gamma-Ray Production Due to Neutron Interactions with Tin for Incident Neutron Energies Between 0.75 and 20 MeV: Tabulated Differential Cross Sections – J. K. Dickens, T. A. Love, and G. L. Morgan 18

22. Gamma-Ray Production Due to Neutron Interactions with Magnesium for Incident Neutron Energies Between 0.8 and 20 MeV: Tabulated Differential Cross Sections – J. K. Dickens, T. A. Love, and G. L. Morgan 18

23. Gamma-Ray Production Due to Neutron Interactions with Fluorine and Lithium for Incident Neutron Energies Between 0.55 and 20 MeV: Tabulated Differential Cross Sections – J. K. Dickens, T. A. Love, and G. L. Morgan 18

24. Fission-Product Afterheat – A Review of Experiments Pertinent to the Thermal-Neutron Fission of ^{235}U – A. M. Perry, F. C. Maienschein, and D. R. Vondy 19

25. Differential Cross Sections for the Production of Neutrons from the Bombardment of ^{12}C, ^{27}Al, ^{54}Fe, and ^{208}Pb by 40-MeV Protons – J. W. Wachter, R. T. Santoro, T. A. Love, and W. Zobel 19

26. Inelastic Proton Scattering from ^{138}Ba and ^{144}Sm at 30 MeV – D. Larson, S. M. Austin, and B. H. Wildenthal 20

27. Compilation of Phenomenological Optical-Model Parameters, 1969–1972 – C. M. Perey and F. G. Perey 20

28. Calculated Secondary-Particle Spectra from Alpha-Particle- and Carbon-Induced Nuclear Reactions – T. A. Gabriel, R. T. Santoro, H. W. Bertini, and N. M. Larson 20

29. Predicted Proton Spectrum at Forward Angles for 29.4-GeV Nitrogen on Carbon – H. W. Bertini, T. A. Gabriel, and R. T. Santoro 21

30. Comparisons of Predictions from Two Intranuclear-Cascade Models with Measured Secondary Proton Spectra at Several Angles from 62- and 39-MeV Protons on Various Elements – H. W. Bertini, G. D. Harp, and F. E. Bertrand 21

31. HIC-1: A First Approach to the Calculation of Heavy-Ion Reactions at Energies $\geqslant 50$ MeV/Nucleon – H. W. Bertini, T. A. Gabriel, R. T. Santoro, O. W. Hermann, N. M. Larson, and J. M. Hunt 22

32. Intermediate Structure in the Neutron-Induced ^{235}U Cross Sections – G. D. James, G. de Saussure, and R. B. Perez 22

33. Estimated Uncertainties in Evaluated Data – F. G. Perey 23

34. The Formalism for Data Covariance Representation in ENDF/B and Application to the ^{238}U Capture Cross Section for Sensitivity Studies – F. G. Perey, G. de Saussure, and R. B. Perez 25

35. ENDF/B Evaluation of Neutron and Gamma-Ray Production Cross Sections for Calcium – C. Y. Fu and F. G. Perey 27

36. ENDF/B Evaluation of Neutron and Gamma-Ray Production Cross Sections for Iron – F. G. Perey, C. Y. Fu, S. K. Penny, W. E. Kinney, and R. Q. Wright 27

37. ENDF/B Evaluation of Neutron and Gamma-Ray Production Cross Sections for Lead – C. Y. Fu and F. G. Perey 27

38. ENDF/B Evaluation of Neutron and Gamma-Ray Production Cross Sections for Silicon – D. Larson and F. G. Perey 28

39. ENDF/B Evaluation of Neutron and Gamma-Ray Production Cross Sections for Fluorine – C. Y. Fu, D. C. Larson, and F. G. Perey 28

40. Reports to the U. S. Nuclear Data Committee – F. G. Perey 28

41. Defense Nuclear Agency Working Cross-Section Library: Description and Contents (Volume I Revision) – R. W. Roussin and J. B. Wright 29

42. Multigroup Cross-Section Dependence on Weighting Function Model – C. R. Weisbin, J. S. Hendricks, D. E. Cullen, E. M. Oblow, and P. D. Soran 29

43. MINX: A Modular Code System for Processing Multigroup Cross Sections for Nuclear Data in ENDF/B Format – D. R. Harris, R. J. LaBauve, R. E. MacFarlane, P. D. Soran, C. R. Weisbin, and J. E. White 31

44. A New Procedure for the Determination of Neutron Multigroup Transfer Matrices – C. R. Weisbin, P. D. Soran, and J. S. Hendricks 32

45. Multigroup Neutron Transfer Matrix Formulation for Scattering Reactions with Tabulated Secondary Spectra – C. R. Weisbin and P. D. Soran 32

46. Cross Section Processing Codes – Is There a Dollar s Worth of Difference Between Them? – C. R. Weisbin, N. M. Greene, H. Henryson II, R. J. LaBauve, C. Durston, D. E. Cullen, and R. B. Kidman 33

47. The Testing of ^{238}U Photon Production Data from ENDF/B Materials 58, 702, and 4187 – W. E. Ford III 35

48. Anisotropic Inelastic Scattering Matrices from ENDF Data – N. M. Greene 38

49. Effects of Highly Anisotropic Scattering on Monoenergetic Neutron Transport at Deep Penetrations – E. Oblow, K. Kin, H. Goldstein, and J. J. Wagshal 39

50. Processing and Testing of ENDF/B-IV Fission Product and Transmutation Data – C. W. Kee, C. R. Weisbin, and R. E. Schenter 40

51. UKE-III: A Computer Program for Translating Neutron Cross-Section Data from the UKAEA Nuclear Data Library to the Evaluated Nuclear Data File Format – R. Q. Wright, S. N. Cramer, and D. C. Irving 41

52. MACKLIB: 100-Group Neutron Fluence-to-Kerma Factors and Reaction Cross Sections Generated by the MACK Computer Program from Data in ENDF Format – M. A. Abdou and R. W. Roussin 42

53. MANYFILE: A Computer Program for Use in the Manipulation of Data Sets Between Various Input/Output Devices – H. E. Comolander and R. K. Gryder 42

54. Next-Flight Estimation for the Fictitious Scattering Monte Carlo Method – S. N. Cramer 43

55. Approximate Numerical Solutions to the Time-Dependent Neutron Transport Equation Using the TASK Algorithm – E. T. Tomlinson 44

56. The DOT III Two-Dimensional Discrete Ordinates Transport Code – W. A. Rhoades and F. R. Mynatt 45

57. Development of a Code System for Determining Radiation Protection of Armored Vehicles (The VCS Code) – W. A. Rhoades, A. R. Buhl, G. L. Haynes, R. J. Hinton, T. J. Hoffman, J. V. Pace III, L. M. Petrie, R. D. Sharp, and L. R. Williams 45

58. Vehicle Code System (VCS) User's Manual – W. A. Rhoades, M. B. Emmett, G. W. Morrison, J. V. Pace III, and L. M. Petrie 46

59. Calculations of the Transport of Fast Neutrons ($\lesssim$ 50 MeV) Through Matter – R. G. Alsmiller 46

60. Computer Codes and Data Available from the Radiation Shielding Information Center – D. K. Trubey, B. F. Maskewitz, and R. W. Roussin 47

61. Recent Trends in Reactor Shielding in the U.S.A. – D. K. Trubey 48

62. The U.S. Theoretical and Computational LMFBR Program – W. M. Stacey, B. J. Toppel, R. N. Hwang, H. Henryson II, K. D. Lathrop, and F. R. Mynatt 49

63. Comparison of Transport Approximations for Reactor Physics Calculations in a Fast Reactor – G. F. Flanagan, N. M. Greene, W. W. Engle, Jr., and E. T. Tomlinson 50

64. Transport Calculations for Reactivity Measurements in Subcritical Configurations of the FFTF Engineering Mockup Core – G. F. Flanagan, D. B. Simpson, D. L. Selby, and J. T. Mihalczo 53

65. Analysis of Stored-Fuel, Control-Rod, and Inherent-Source Effects on the CRBR Ex-Vessel Source Range Monitoring System – G. F. Flanagan, W. W. Engle, Jr., L. R. Williams, and F. R. Mynatt 54

66. Energy- and Region-Dependent Bucklings for the FFTF Engineering Mockup Core from Monte Carlo – L. M. Petrie and N. F. Cross 56

67. Criticality Calculations for Cylindrical Billets of Uranium-Aluminum Alloy – N. F. Cross, P. B. Fox, and G. E. Whitesides 57

68. Generalized Reactor Sensitivity Analysis Program at ORNL – E. G. Silver, E. M. Oblow, J. M. Kallfelz, C. R. Weisbin, D. E. Bartine, G. F. Flanagan, and F. R. Mynatt 58

69. Reactor Cross-Section Sensitivity Studies Using Transport Theory – E. M. Oblow 60

70. Sensitivity Studies of the Breeding Ratio for the Clinch River Breeder Reactor – J. M. Kallfelz, M. L. Williams, D. Lal, and G. F. Flanagan 61

71. Studies of Sensitivity of Shield Performance to Nuclear Data Variations – F. C. Maienschein 63

72. Fast Reactor Analytical Shielding Progress Reports, March 1973–September 1973 – F. R. Mynatt et al. 66

73. Calculation of Penetrations in the FTR Radial Cavity Shield – M. B. Emmett, W. W. Engle, Jr., and F. R. Mynatt 68

74. Calculations of Coolant-Pipe Neutron Streaming and Secondary Coolant Activation in the Fast Flux Test Facility – B. J. McGregor, F. B. K. Kam, F. R. Mynatt, and L. S. Abbott 70

75. ORNL Cross-Section Sensitivity Analysis Applications for Radiation Shielding – D. E. Bartine, F. R. Mynatt, E. M. Oblow, R. L. Childs, J. V. Pace III, J. R. Knight, and T. M. Sims 71

76. An Evaluation of the Engineering Shield Design for the FFTF Head Compartment – H. C. Claiborne 74

77. The ORNL LMFBR Experimental Shielding Program – C. E. Clifford 75

78. Fast Reactor Experimental Shielding Progress Reports, May 1973–February 1974 – C. E. Clifford et al. 78

79. ORNL TSF Pipe Chase Neutron Streaming Experiment – Phase Two – B. J. McGregor and F. J. Muckenthaler 80

80. Final Report on a Benchmark Experiment for Neutron Transport in Thick Sodium – R. E. Maerker, F. J. Muckenthaler, R. L. Childs, and M. L. Gritzner 81

81. Final Report on a Benchmark Experiment for Neutron Transport Through Iron and Stainless Steel – R. E. Maerker and F. J. Muckenthaler 81

82. Comparisons of Detailed Measured and Calculated Neutron Spectra Behind Thick Samples of Iron – R. E. Maerker and F. J. Muckenthaler 82

83. Calculation of Energy Depositions and Dose Rates in Proposed Shielding Surrounding the TSR-II Reactor – S. Uchida, J. Lewin, and R. E. Maerker 84

84. Experimentally Determined Neutron and Gamma-Ray Spectra from an Encapsulated Cm_2O_3 Power Source – R. M. Freestone, Jr. 84

85. Time-Dependent Neutron and Secondary Gamma-Ray Weapon Output, Including Complete Collision Kinetics – T. A. Gabriel 84

86. Effects of Air-Density Perturbations on the Transport of Gamma Rays Produced by Point Gamma-Ray Sources – B. J. McGregor and F. R. Mynatt 85

87. Calculations of the Penetration of Nuclear Weapons Radiation into a Missile Silo – F. R. Mynatt, T. J. Hoffman, J. V. Pace III, C. E. Burgart, and L. S. Abbott 85

88. A One-Dimensional Calculational Method for an Air-Over-Ground Radiation Field Incident on an Underground Concrete Structure – J. V. Pace III and F. R. Mynatt 86

89. Transport Calculations for 14-MeV and Fission Neutron Sources in Air/Ground and Air/Seawater Geometry – J. V. Pace III and D. E. Bartine 87

90. Time-Dependent Neutron and Secondary Gamma-Ray Transport in the Atmosphere – Sensitivity to Cross Sections – F. R. Mynatt 89

91. Radiation Transport Cross-Section Sensitivity Analysis – A General Approach Illustrated for a Thermonuclear Source in Air – D. E. Bartine, E. M. Oblow, and F. R. Mynatt 90

92. Selection of Group Energy Boundaries Using Sensitivity Theory – E. Oblow, J. Ching, and J. Drischler 90

93. A Cross-Section Sensitivity Study of Radiation Transport in Concrete – D. E. Bartine, J. V. Pace III, and J. R. Knight 92

94. Monte Carlo Analysis of Neutron and Gamma-Ray Transport in Concrete – G. W. Morrison, L. M. Petrie, and F. R. Mynatt 94

95. Calculational Analysis of Neutron and Gamma-Ray Transport Experiments in Nitrogen – S. N. Cramer and E. M. Oblow 97

96. Neutron and Photon Energy Spectrum Calculations for Nitrogen Integral Experiments – S. N. Cramer and E. M. Oblow 97

97. Analyses of Neutron Scattering and Gamma-Ray Production Integral Experiments on Carbon for Neutron Energies from 1 to 15 MeV – S. N. Cramer and E. M. Oblow 100

98. Production and Testing of the DNA Few-Group Cross-Section Library – D. E. Bartine, F. R. Mynatt, R. W. Roussin, J. R. Knight, and R. Q. Wright 100

99. Cross-Section Sensitivity of Breeeding Ratio in a Fusion-Reactor Blanket – D. E. Bartine, R. G. Alsmiller, Jr., E. M. Oblow, and F. R. Mynatt 102

100. Comparison of Cross-Section Sensitivities of Breeding Ratios in Fusion-Reactor Blankets – R. G. Alsmiller, Jr., J. Barish, T. A. Gabriel, and R. T. Santoro 102

101. Shielding Design Calculations for ORMAK-F/BX – T. A. Gabriel, R. T. Santoro, and W. W. Engle, Jr. 103

102. Services to the CTR Community by the Radiation Shielding Information Center – R. W. Roussin, D. K. Trubey, and B. F. Maskewitz 105

103. Bibliography, Subject Index, and Author Index of the Literature Examined by the Radiation Shielding Information Center (Reactor and Weapons Radiation Shielding) – D. K. Trubey, R. W. Roussin, J. Gurney, and A. B. Gustin 105

104. Materials Information in the Radiation Shielding Information Center – B. F. Maskewitz, D. K. Trubey, and R. W. Roussin 105

105. The Development of Radiation Shielding Standards in the U.S.A. – D. K. Trubey 106

106. Calculations Related to the Application of Neutrons, Protons, Negatively Charged Pions, and Heavy Ions in Cancer Radiotherapy – R. G. Alsmiller, Jr. 106

107. Calculations Related to the Use of Photons, Neutrons, Negatively Charged Pions, Protons, and Alpha Particles in Cancer Radiotherapy – R. G. Alsmiller, Jr., R. T. Santoro, T. W. Armstrong, J. Barish, K. C. Chandler, and G. T. Chapman 107

108. Calculations Pertaining to the Use of Fast ($\lesssim$ 50 MeV) Neutrons in Cancer Radiotherapy – R. G. Alsmiller, Jr., and J. Barish 107

109. The Effects of Bone in the Use of Negatively Charged Pions in Cancer Radiotherapy – R. T. Santoro, R. G. Alsmiller, Jr., and K. C. Chandler 108

110. Calculations Related to the Application of Negatively Charged Pions in Radiotherapy: Absorbed Dose, LET Spectra, and Cell Survival – T. W. Armstrong and K. C. Chandler 108

111. Calculated Physical and Biological Results when Negatively Charged Pions are Used to Irradiate a Small and a Large "Tumor" Volume in a Tissue Phantom – R. T. Santoro and R. G. Alsmiller, Jr. 108

112. Calculated Particle-Production Spectra from π^- Captures in Tissue, Tissue-Equivalent Plastic, Silicon, and Germanium – T. W. Armstrong and K. C. Chandler 109

113. Calculations on Tissue Equivalence for Stopping π^- Mesons– T. W. Armstrong and K. C. Chandler 109

114. Calculations Related to the Application of Silicon Detectors in Pion Radiobiology – T. W. Armstrong and K. C. Chandler 109

115. Calculation of the Response of Silicon Detectors of Finite Radius to π^- Mesons Stopping in Tissue – T. W. Armstrong and K. C. Chandler 109

116. Calculation of Residual Nuclei Production by a Beam of Negatively Charged Pions Incident on a Tissue Phantom – T. W. Armstrong and K. C. Chandler 110

117. Response of a Large All-Liquid Scintillation Spectrometer and of a 24-Layer Iron-Plastic Spectrometer to Charged Pions and Protons in the Low-GeV Energy Range – T. A. Gabriel and J. D. Amburgey 110

118. Energy Deposition by High-Energy Electrons (50 to 200 MeV) in Water – R. G. Alsmiller, Jr., J. Barish, and S. R. Dodge 110

119. Energy Deposition by 45-GeV Photons in Hydrogen, Beryllium, Aluminum, Copper, and Tantalum – R. G. Alsmiller, Jr., and J. Barish 111

120. Photon Spectra from Induced Activity in an Orbiting Spacecraft – R. G. Alsmiller, Jr., G. T. Chapman, J. W. Wachter, and J. Barish 111

121. A Technique to Determine the Shape of a Minimum Weight Shield – W. W. Engle, Jr., and F. R. Mynatt 111

122. Nuclear Accident Dosimetry in a Simulated Criticality Accident – R. T. Santoro, R. G. Affel, G. C. Cain, and J. H. Greene 113

123. Differential Cross Sections for Charged-Particle Emission in Reactions of 58-MeV Alpha Particles with ^{12}C, ^{16}O, and ^{54}Fe; Comparison with Exciton Model of Pre-Equilibrium Particle Emission – F. E. Bertrand, R. W. Peelle, and C. Kalbach-Cline 114

124. Feasibility Study of a Honeycomb Vacuum Wall for Fusion Reactors – S. N. Cramer and E. M. Oblow 115

Publications and Papers Presented at Scientific Meetings 116

Organization Chart 129

INTRODUCTION AND SUMMARY

A custom of the Neutron Physics Division that is continued this year is the compilation of a progress report from abstracts of reports or journal articles published during the reporting period and from summaries (or abstracts) of papers presented at scientific meetings during the reporting period. With the considerable delay that invariably exists between the time research is performed and the time it is publicized, a progress report assembled in this manner lags behind the research performed during the months purportedly covered, which in this case is the period between May 31, 1973, and August 31, 1974. Thus to place the Division's current program in perspective, and also to indicate the interrelationship of the various papers included here, we offer the following overview of the Division's general areas of research followed by a summary of the specific program activities recently completed or now under way.

Outline

Areas of Research	Program Activities
Nuclear Data Measurements	LMFBR Program
Nuclear Data Calculations and Evaluations	GCFR Shielding Program
Nuclear Data Processing	CTR Program
Development of Transport Methods	Reactor Safety Studies
Integral Experiments	Neutron Cross-Section Standards
Sensitivity Analyses	High-Energy Accelerator Shielding Program
Nuclear Analyses	NASA Program
Information Dissemination	Cancer Radiotherapy Studies
	DNA Program
	Facility Operations

AREAS OF RESEARCH

The various areas of research in the Neutron Physics Division can be viewed as components of a system designed to provide a capability for performing the nuclear analyses that are required in most of the Division's technical programs. Although the individual programs are diverse, the nuclear analyses in each have a common goal: an understanding of the interaction of specified materials in given arrangements with nuclear particles or radiation from internal or external sources. To meet this goal, vigorous research must be pursued to determine the interaction of the radiations with the pertinent nuclides, to develop methods for following the interactions as the radiations are transported through the various combinations of materials, and to devise techniques for identifying those interactions most important to a particular calculation. The Division's work falls in all these areas, and for some data and methods it is the major contributor. The results obtained, combined with those from similar research performed elsewhere, lead to a nuclear analysis capability that is adaptable to increasingly complex radiation sources and material geometries. In the past year, for example, it has been adapted to reactor cores and shields, to military structures and vehicles exposed to nuclear detonations, to space vehicles passing through radiation fields, to high-energy particle accelerator shields, and even to the human body undergoing radiation therapy.

ORNL-DWG 74-10289

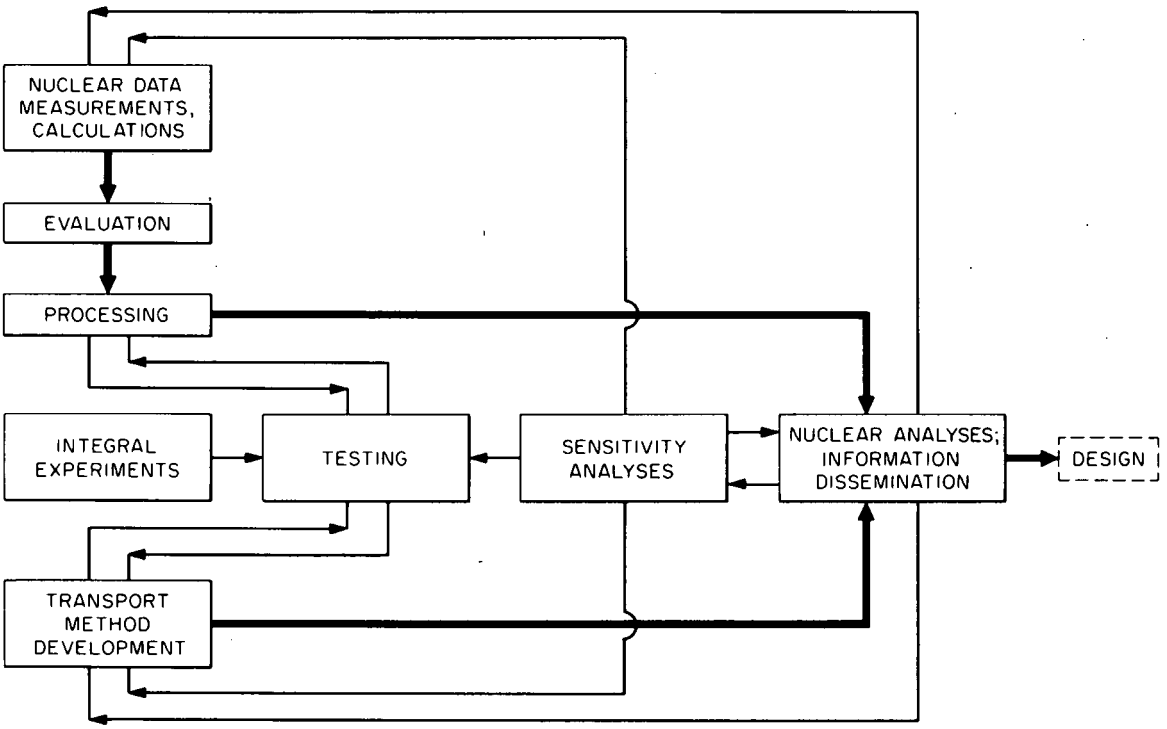

Area of research in Neutron Physics Division, 1974

The interrelationship of the activities in the Division's research areas is shown in the chart above. As indicated in the upper left-hand corner, nuclear (interaction) data are obtained both from measurements and calculations. The data for given nuclides are evaluated to provide "best sets," which are then processed into formats usable in the nuclear analyses. Concurrently, the transport methods are developed and adapted to the particular systems under study. Before the data and methods are applied in a nuclear analysis, however, they are frequently tested through a procedure that involves the analysis of an integral experiment and a "sensitivity" study in which critical areas of the nuclear data are examined in detail. Depending on the results of the testing procedure, iteration of some of the activities may be required before the data and method are confidently applied to the particular system. This interaction of the activities is explained more fully in the following discussion.

Nuclear Data Measurements

The nuclear data measurements performed within the Division are measurements of neutron-interaction and gamma-ray-production cross sections and related data for incident neutron energies up to 20 MeV. Most of the experiments are performed at the Oak Ridge Electron Linear Accelerator (ORELA), where a pulsed source of neutrons and high-speed data acquisition and analysis equipment are available for measurements in 11 different flight paths. The incident neutron energies are determined by time-of-flight techniques. A few specialized measurements are also made at the Oak Ridge Research Reactor. The experimental results from all these measurements are forwarded to the National Neutron Cross Section Center (NNCSC) at Brookhaven National Laboratory, where they are entered as unevaluated data, along with measurements from other facilities.

Nuclear Data Calculations and Evaluations

Nuclear data required for a nuclear analysis but not available from measurements must be estimated in some manner, usually from calculations. For neutron energies below 20 MeV, the calculations performed in our Division are carried out in conjunction with data set evaluations. Evaluating a set of nuclear data entails developing and using nuclear models both to provide preliminary tests of all available measured cross sections and to calculate cross sections for intermediate energies. The evaluations are coordinated with similar activities elsewhere through the Cross Section Evaluation Working Group. Each evaluation considers all available neutron and gamma-ray interaction data on a given nuclide and provides an evaluated set for release through the Center's ENDF/B files. Although in the past the uncertainties associated with the evaluated data have generally not been included with the data sets, at CSEWG's request, estimated data covariance files over the range of data covered are beginning to be released with the evaluations to meet the needs of critical programs. The format used for the covariance files (commonly referred to as "error files") has been developed within the Division.

While the work of the evaluators is a continuing program, updated sets of ENDF/B data are released by NNCSC only infrequently (the latest is ENDF/B-IV). For most of the nuclides important to the nuclear analysis of shields, intermediate versions of the evaluated data sets can be obtained from a Working Cross Section Library established by the Defense Nuclear Agency in the Radiation Shielding Information Center (RSIC), which is an integral part of the Division. Thus not only does the Division participate directly in the evaluation of data sets, it also acts as a repository for some of the evaluations.

In addition to the work on these "low-energy" cross sections, cross sections are generated to describe the interactions of various medium- and high-energy particles, including charged particles. Only a few of these cross sections are available from experiments, making it necessary to rely almost entirely upon values obtained from calculations. As a result, there has been a concentrated effort within the Division over the last several years to develop nuclear models that can be used to predict the energies and angles of particles emerging from particle-nucleus collisions. The models are usually employed to calculate data for specific problems, and in general there has been no organized effort to evaluate or disperse the data as cross sections; however, some data sets are available from a Data Library Collection maintained by RSIC.

Nuclear Data Processing

The evaluated data sets available from NNCSC or RSIC are comprised of microscopic cross sections for specific neutron or gamma-ray interactions with individual nuclides at discrete ("point") energies. For use within a transport calculation, these cross sections must be processed into an appropriate energy structure and then converted to macroscopic cross sections for the various material compositions that will appear in the problem. In some transport calculations the point cross sections are processed and mixed with subroutines in the main computer code, with the energy structure largely being determined by the detail in which the cross sections are known. For other transport calculations the point cross sections must be averaged and weighted within specified energy groups before they can be accepted by the computer program. Cross sections of this latter type are referred to as "multigroup" cross sections and are generally thought of as representing rather broad energy intervals. Recently, however, we have been selectively reducing the widths of the energy groups to the extent that the effective detail of the energy structure approaches that of the point cross sections.

The development and use of computer codes that process multigroup cross sections is an important activity within the Division. In fact, during the last two years a large effort has been devoted to developing

a system of interfaced modular codes for producing "coupled" sets of cross sections (the AMPX system). In such sets, the neutron-interaction and gamma-ray-production cross sections in each energy group are coupled with gamma-ray-interaction cross sections so that the transport of both neutrons and neutron-induced gamma rays can be handled in a single calculation. The Phase I version of AMPX is in use, and some cross-section sets that have been processed for standard materials have been deposited in RSIC's Data Library Collection for general availability. In addition, the code system itself, as well as other cross-section processing codes, is available from a code collection maintained by RSIC. Additional processing work in the Division includes development of the MINX neutron-interaction code (including the adaptation of MINX to the AMPX system) and development of an ENDF capability for the ORIGEN code, which is an isotope generation and depletion code.

Development of Transport Methods

The "transport" methods developed within the Division include Monte Carlo, discrete ordinates, and diffusion theory methods, and more recently finite-element techniques for both diffusion and transport theory.

The Monte Carlo and discrete ordinates methods are the most appropriate for deep-penetration shielding calculations. The discrete ordinates method tends to be more practical in that it yields the most information about a system, but it is limited to systems whose geometries can be described in one or two spatial dimensions. For shield systems that require three-dimensional descriptions, the Monte Carlo method must be used.

Several transport computer codes based on both methods have been developed within the Division. For low-energy radiations, these include the well-known ANISN and DOT-III discrete ordinates codes and the O5R, O6R, and MORSE Monte Carlo codes. For high-energy transport the primary effort has been on a Monte Carlo code identified as the High Energy Transport Code (HETC).

As would be expected, the limitations and advantages of the Monte Carlo and discrete ordinates methods, together with the necessity for considering different nuclear processes at low and high energies, have led to the division of large or complicated problems into parts that are computed in sequence, each with the most appropriate method. The results of one calculation are then used as the radiation source for the next calculation in the series. This "coupling" of techniques, which requires the development of interfacing codes, is done most efficiently and with the greatest confidence when all the transport codes employed in an analysis use the same set of processed cross sections. For many years this was not possible because Monte Carlo codes could accept only point cross sections and discrete ordinates codes could accept only multigroup cross sections. However, the development of a multigroup Monte Carlo code (MORSE) has resulted in coupled calculations becoming routine.

In addition to the development of Monte Carlo and discrete ordinates methods, the Division is now responsible for ORNL's efforts in the development of diffusion-theory approximations for calculating transport in reactor cores. While diffusion theory is not applicable for calculating the strongly directed fluxes in shields, it provides the most practical approach for calculating the nearly isotropic fluxes in cores. The diffusion-theory code now under development is identified as the VENTURE code, and the objective of this work is to provide a useful tool for the difficult three-dimensional core problems, as well as for the more routine one- and two-dimensional problems.

Advanced transport method development only recently undertaken is aimed at improving numerical techniques, especially the finite-element approach for both diffusion and transport equations. An

experimental finite-element code for the two-dimensional discrete-angle transport equation is operational, and work is soon to begin on a finite-element approach to the two-dimensional P_1 transport equation.

As each version of a computer code is completed, it is made generally available through RSIC's Computer Code Collection. In most cases the development of codes continues in order to increase the accuracy, efficiency, and range of applicability of the method. This further development frequently consists of the adaptation of a code system for a particular nuclear analysis, which can constitute a major effort, especially if the problem geometry is complicated.

Integral Experiments

Ideally the use of the processed cross sections and the adapted method for a particular nuclear analysis would be delayed until both are tested for the given application. In reality the degree of testing is determined by several factors, including the uncertainty associated with the data and/or method and the importance and urgency of the proposed problem, not to mention the availability of funding for the tests.

Data-checking experiments. A test of a cross-section set can be carried out only by using the data in a transport calculation performed as an analysis of an integral experiment on the material of interest. In our Division we analyze two types of integral experiments: those performed at accelerator facilities, involving relatively small samples of the materials, and those performed at a reactor facility, involving bulk quantities of the materials. The small integral experiments are designed (often with the aid of transport calculations) to emphasize the testing of differential data. The large experiments are designed as severe tests of the adequacy of full data sets for deep-penetration calculations. In all the analyses an attempt is made to duplicate the responses of the detectors used in the experiments, which in turn requires independent studies of detector response functions.

Some of the small integral experiments are performed at ORELA, and others are performed at the Intelcom Rad Tech accelerator facility. The bulk experiments are performed at the Tower Shielding Facility. In the TSF experiments a large sample of the material of interest is positioned against a collimated beam from the Tower Shielding Reactor II, and measurements of the spectra of neutrons and gamma rays penetrating through the material are made on the opposite side at various angles from the reactor-sample axis. One of the major difficulties in such experiments is ensuring that a sufficiently large thickness of the material is used while at the same time a measurable flux is maintained. A new TSR-II beam shield now being constructed will provide a more intense beam source for future experiments.

Experiments for method tests. Other integral experiments performed at the TSF are designed for method testing – or more specifically for the adaptability of a particular method for transport calculations involving complicated geometric regions and/or various combinations of materials. In such experiments a region similar to that in question is mocked up; however, in general, prototypic mockups limited to a single design are avoided. Whereas in the past such mockups were tested to obtain design data directly, we now largely rely on the transport methods to support the design and on the experiments to confirm the methods.

Benchmark cases. If the analysis of an experiment produces complete agreement between the measured and calculated detector responses, not only are the data sets and transport method verified, but also the experimental results themselves. The experiment may then be classified as a "benchmark" case (standard) for testing other transport methods or refinements in the cross-section data. Official recognition of a data-testing benchmark experiment is given by CSEWG, which has placed two TSF experiments in this

category this year. In addition, a Shielding Benchmark Committee of the American Nuclear Society selects benchmark cases both for data testing and method testing, and this Committee has also recognized a TSF experiment this year. The ANS benchmarks are described in documents issued through RSIC.

Other benchmark cases are developed on the basis of calculations alone – some through the intercomparison of methods for the same problem and others through the use of detailed data set structures. These benchmarks, some of which are being produced within our Division, can also be used in tests.

Sensitivity Analyses

Sensitivity analyses are a relatively recent and increasingly important activity of the Division, interacting both with the integral experiment analyses and with other types of nuclear analyses, including those performed for specific systems. Unfortunately the term "sensitivity analysis" has more than one meaning, even within our Division, but basically it implies a study of the relative contributions to a calculated response by various particle interactions. In its most sophisticated context, it refers to a computerized sensitivity analysis program which determines the rate of change in a calculated response per percent change in any individual cross section as a function of the energy. Thus sensitivity analyses indicate how important particular cross sections are to a calculation, and they may be used to determine the degree of accuracy to which cross sections should be known to achieve a specified accuracy in a calculation, thereby guiding the selection of cross-section experiments.

Division efforts on the development of sensitivity code systems are extensive. They began with the development of a sensitivity analysis program called SWANLAKE that is limited in application to responses calculated with the one-dimensional discrete ordinates code ANISN. Since many nuclear analyses require a minimum of two dimensions, an additional code (the VIP code) has recently been developed which allows SWANLAKE to be linked with the two-dimensional code DOT-III. Work on extending sensitivity analyses to three-dimensional diffusion-theory calculations is currently under way. This ambitious undertaking is aimed at substantially improving reactor shield and core designs, as well as the design of many military systems.

One important application of sensitivity analysis is in the area of nuclear data testing. When an experiment is designed primarily for data testing, it is assumed that both the experimental techniques and the transport method as adapted for the analysis have already been verified. Any disagreement between the measured and calculated responses is then attributed to inadequacies of the cross-section set. A sensitivity analysis is performed to pinpoint the trouble.

If the calculated response is shown to have a large sensitivity to cross sections in particular energy groups, the question arises as to whether those cross sections, which in the calculation are averaged and weighted values, are truly representative of their groups. Thus it should not be assumed that the cross sections themselves are in error until the effect of using other multigroup structures has been investigated. This will provoke an iteration with the cross-section processing activity and eventually a reanalysis of the experiment. Continued disagreement between the experiment and the analysis will ultimately call for a reevaluation of the cross-section data and possibly a new series of cross-section measurements. The iteration continues, in many cases over a period of years, until resolution of the problem is obtained.

Part of the resolution of the problem which is hoped for but not now easily attained is the determination of the uncertainty associated with a calculated response due to experimental and other unavoidable uncertainties inherent in the evaluated cross-section sets. As was pointed out earlier in this introduction, the ENDF/B sets now being released are accompanied by data covariance (uncertainty) files

for at least some of the data. This has prompted an interest in automated techniques for determining the effects of the uncertainties on calculated transport results. The Division is currently engaged in developing codes which will read and process the ENDF/B uncertainty files and construct multigroup covariance matrices representing the different types of experimental uncertainties and their correlations for a particular nuclide. With these programs the uncertainties in the cross sections that are input into a calculation will be available for use by a sensitivity analysis program, which can then estimate the total uncertainty in a problem solution due to the combined cross-section uncertainties. When this technique is applied to an experiment analysis, the disagreement between calculated and measured responses due to data uncertainties can be separated from the disagreement attributable to inadequacies of the transport method; that is, the disagreement due to data uncertainties will be indicated from the sensitivity analysis, and the remainder can be attributed to inadequacies of the method. If the latter are significant, the development of pertinent features of the method may be iterated and a reanalysis of the experiment performed.

Nuclear Analyses

The preceding discussion has described the various Division activities which when merged together lead to the nuclear analysis of various systems with a state-of-the-art technology. The particular systems analyzed within the Division are discussed below in conjunction with the specific technical programs.

Information Dissemination

In addition to developing and applying a state-of-the-art technology, the Division has an additional goal of making this technology, as well as the results obtained from its application, available to industry, contractors, universities, and other interested groups. Some of the nuclear analyses are performed specifically to aid the design of proposed systems, in which case the results are immediately transmitted informally to the designers. Other nuclear analyses, including those performed during the testing of the data and methods, are of more general interest. As formal descriptions of the analyses become available, those that describe radiation shielding work are reviewed, indexed, and entered into RSIC's Storage and Retrieval Information System (SARIS), along with shielding literature produced by other organizations. The documents are simultaneously publicized through the RSIC monthly newsletter. Upon request, RSIC will search SARIS for specific information, and under its Selective Dissemination of Information system, RSIC routinely forwards information from SARIS to subscribers who have indicated a continuing interest in particular types of information. Thus RSIC acts as a clearinghouse for all available shielding literature, interacting with various groups throughout the world.

RSIC similarly acts as a clearinghouse for transport computer codes and other types of codes useful in shielding studies. As pointed out earlier, RSIC maintains a computer code collection. Transport codes are identified as CCC codes, and other codes, such as auxiliary routines and miscellaneous programs for data manipulation and conversion, are identified as PSR codes (peripheral shielding routines). Many organizations contribute to the collection, but before one is accepted, RSIC ensures that it is operable for simple test cases and that it is sufficiently documented for general use.

Another RSIC service mentioned earlier is its Data Library Collection, from which sets of nuclear data can be obtained. In addition, RSIC provides problem assistance that may vary from a response to a simple letter request to studying a problem to the extent that an approach to its solution is recommended and help is given in assimilating the necessary material.

With RSIC in our midst and with the prominent role we play in radiation shielding studies, it is understandable that the Neutron Physics Division is thought of primarily as a shielding division. While we profess expertise in shielding, we are also active in other areas, as will be apparent from the following discussion of the Division's technical programs.

PROGRAM ACTIVITIES

LMFBR Program

A major program in the Division, and one which involves all the research areas of the Division, provides direct support to the nuclear design of liquid-metal fast breeder reactors. This includes not only the design of the core and the shield but also the design of other structural and mechanical components of the system.

Cross-section studies for the fissile and fertile materials. Basic to the design of LMFBR cores are accurate values of the neutron fission and capture cross sections of the fertile and fissile materials over the full energy range of the significant flux (about 1 keV to a few MeV). Experiments performed at ORELA have as their goal reducing the existing uncertainties, some as great as 10% or more, among the cross-section values for the most utilized fertile and fissile nuclides. In the experiments, which are concentrated at neutron energies below 0.5 MeV, fission and capture cross sections are measured directly, as well as the parameters α (the capture-to-fission ratio) and $\bar{\nu}$ (the number of neutrons per fission).

The Division's work in this area is reflected in the ENDF/B-IV releases, the results having greatly influenced or even dominated some of these most recent evaluations. ORELA measurements are referred to in File 1 of the ENDF/B-IV evaluation for ^{240}Pu and ^{241}Pu, and a detailed comparison of ORELA ^{239}Pu fission and capture data with a parametric description of these cross sections was used in the determination of the final set of resonance parameters in the ENDF/B-IV evaluation for ^{239}Pu. In addition, neutron transmission measurements with four different thicknesses of ^{239}Pu were used for determining the structure that should be included for the ^{239}Pu neutron cross sections.

The ENDF/B-IV evaluation of the fission and capture cross sections for ^{235}U from 0.082 to 25 keV was performed within the Division, and the energy dependence of the cross sections in the thermal energy range was tested through comparisons of the evaluation with data from ORELA. In addition, a large effort was directed to comparisons of published and unpublished ORELA data on the ^{238}U resonance parameters with calculations made by the Monte Carlo technique using various sets of resonance parameters. This led to modifications of the parameters incorporated in the ENDF/B-IV evaluation for the resonances representing the cross section below 4 keV.

Cross-section studies for low- and medium-*A* nuclides. Cross-section studies for the nuclides included in LMFBR structural, coolant, control, and shield materials are also carried out at ORELA. For these materials the cross sections most needed are neutron-scattering and gamma-ray-production cross sections. Since the production cross sections have support from another program (see discussion of DNA program), the scattering cross sections have received the most attention in the LMFBR studies.

The scattering cross-section measurements were originated several years ago at the ORNL Van de Graaff Facility under other reactor programs, and a number of the reports published during the past year cover Van de Graaff data obtained on elements of interest to the LMFBR program (N, Ti, Cr, Ni, Fe, Cu, and Pb). At the same time, a 40-m ORELA flight-path station was equipped with a specially designed scattering chamber and associated electronics, and scattering data were acquired on Na, Si, and Fe. In the ORELA technique, measurements are made of the deexcitation gamma rays from the $(n,n'\gamma)$ reaction. In this way the energy resolution for inelastic scattering can be made comparable with that for the total cross section for the same nuclide and energy region.

This work is closely coordinated with CSEWG and NNCSC, and in some cases, specific measurements are made to aid cross-section evaluators. The need for such data prompted measurements of gamma-ray-production data for nickel, which formed the basis for the ENDF/B-IV gamma-ray-production files for this nuclide. It also prompted measurements of total cross sections for thick samples of iron, nickel, and chromium.

In addition, evaluations are performed for several elements. During the past year the ^{12}C ENDF/B-IV evaluation was completed, and an update of the ENDF/B-III version for sodium was recommended for Version IV. An evaluation for iron, still under way, is partially covered by this program, as is the development of a formalism to represent the covariance matrix of uncertainties associated with the evaluated nuclear data.

Reactor core studies. The size and complexity of the proposed fast breeder systems require the economical application of advanced, flexible, high-precision reactor codes for LMFBR core calculations. This has prompted the development of the three-dimensional multigroup diffusion-theory code VENTURE for use by LMFBR designers. The first version of VENTURE and an associated cross-section processor have already been routinely used by General Electric. Subsequently, the capability of treating a simplified P_1 formulation has been included. When Version I is completed for general release, it is expected to have capabilities for criticality search, for basic perturbation analysis, and for calculations of reaction rates and fuel conversion ratios (i.e., breeding ratios). Other refinements will be introduced in Version II. The finite-element code now being developed is also for LMFBR reactor core applications.

The development of a cross-section sensitivity code system for reactor core studies based on transport methods is also under way. It will include a generalized perturbation theory code interfaced with the sensitivity code SWANLAKE and with a code (PUFF) that processes ENDF/B uncertainty files into multigroup covariance matrices. The outputs of these codes can be combined to translate cross-section uncertainties into uncertainties on calculated reactor parameters. The system is eventually to be interfaced with VENTURE and also with DOT-IV (see next section). In the meantime, a preliminary system has been applied to generate cross-section sensitivity profiles for the breeding ratio for the Clinch River Breeder Reactor (CRBR).

In another area, calculations have been performed in support of experiments performed on the Engineering Mockup Core of the Fast Flux Test Facility (FFTF) set up on the ZPR-9 at Argonne National Laboratory. The purpose of these tests was to look at the subcritical multiplication, inverse rod drop kinetics, and noise analysis as techniques for measuring the shutdown reactor level with an in-vessel low-level flux monitor (LLFM). This work indicated that the LLFM is satisfactory for measuring the subcritical reactivity using modified source multiplication techniques provided adequate calculations of detection efficiencies are made. We are currently analyzing a reverse-approach-to-criticality experiment, the purpose of which is to indicate the adequacy of the LLFM system for monitoring the approach to criticality during initial startup of the FFTF.

Shielding studies. The LMFBR shielding studies conducted within the Division have the long-range goal of providing shielding design methods (transport codes) for general application to fast breeder systems and the intermediate goal of assisting in the shield designs for the FFTF and the CRBR. Throughout, the method development, including the testing of the needed cross sections, is verified by experiments performed at the Tower Shielding Facility.

Current work in the area of transport code development is centering on Version IV of the two-dimensional discrete ordinates code DOT, which will have the capability for solving larger problem meshes with less fast memory and allowing the radial spatial mesh and directional quadrature to vary with axial position so that the computation work can be concentrated in the most important

spatial regions. In the meantime, DOT-III and the MORSE Monte Carlo code are being routinely applied to LMFBR calculations. Coupled calculations that require that the outgoing boundary fluxes calculated with DOT-III be converted to other angular and spatial grids before being used as the source in a second calculation have been facilitated by a recently improved version of the FACT surface-to-surface coupling code. In addition, the SWANLAKE sensitivity code has now been made compatible with the DOT-III code, and the COMGOM combinatorial geometry routines used with MORSE have been improved.

ORNL calculations specifically for the FFTF, begun approximately five years ago and now nearing completion, have significantly affected the shield design of that facility. Many of the calculations have been concerned with the doses on the maintenance deck, with those performed during this reporting period concentrating on the effect of holes through a magnetite concrete shield surrounding the reactor guard vessel near the top of the sodium pool. The size of these calculations, together with the necessity for describing the reactor cavity shield in three dimensions, required that they be coupled DOT-MORSE-DOT calculations. Another complicated problem which has been attacked both with DOT and with MORSE has been the study of the neutron fluxes in the reactor cavity due to fissions produced in the stored-fuel modules inside the reactor vessel. Studies of the neutron streaming and the concomitant sodium activation doses in the FFTF sodium coolant system have also continued into this reporting period, as have analyses of a revised head compartment shield and center island shield. All the FFTF work to date has been summarized in a draft report forwarded to Westinghouse Electric Corporation for inclusion in an FFTF project report.

Calculations specifically in support of the CRBR design were initiated during this reporting period with DOT-III calculations to investigate the effectiveness of the lower axial shield in reducing the fluxes to which the grid plate could be subjected. The adaptation of DOT-III to calculations of neutron fluxes throughout the reactor vessel and surrounding cavity has also progressed, with considerable emphasis given to the tailoring of coupled cross-section sets to the CRBR system.

A large calculational effort was carried out to predict the signal-to-background ratio at the location of an ex-vessel LLFM in an early CRBR design that included 34 in-vessel stored-fuel locations. The resulting ratio was 20/1, which was prohibitive. These results contributed to a design update in which most of the stored fuel inside the vessel was removed, and calculations were performed to assist in the specification of the number and location of contingency stored-fuel modules within the vessel. The resulting design included an array of four unshielded fuel modules that were located 120° from the LLFM's and a B_4C shield placed on the guard vessel up to a half angle of 45°. With this configuration, the background was only 3%. On the basis of this study and the well-known shielding problems caused by stored fuel in the FFTF, it can be concluded that no commercial plant design should include in-vessel fuel storage.

Studies were also performed to assess the spatial and spectral effects on the CRBR ex-vessel LLFM of control rod removal and inherent source changes in the core during and immediately following refueling. Only the source changes resulted in appreciable asymmetry effects, indicating that procedural controls are required to assure that the inherent source is not locally depleted in any one region of the core during refueling.

A number of TSF experiments and accompanying analyses have been performed to support the methodology applied to the FFTF and CRBR systems, as well as to provide direct information. Two extensive experiments were designed to investigate the fission rates in simulated stored-fuel modules for the FFTF. In the first, the radial regions between the core and a stored-fuel module were mocked up, and the responses of ^{235}U and ^{239}Pu fission detectors just beyond the configuration were interpreted as representing the fission rate in the stored fuel. A factor of 2 difference between

the experimental and calculated fission rates resulted in modifications of the calculational method. In the second experiment, three cylindrical arrays of ^{235}U mocked up the stored fuel, and the spectrum of fast neutrons leaking from the array was measured. The complicated geometry of this experiment will require that the analysis, which is as yet incomplete, be performed with a coupled DOT-MORSE system.

A similar TSF experiment was performed to study the adequacy of the calculational technique for predicting the counting rate of the LLFM in the CRBR. This experiment provided information pertinent to the decision to use an ex-vessel detector in the CRBR rather than an in-vessel detector, which would have increased the cost of the system significantly.

In another TSF experiment a lower axial shield mockup with changeable plugs was studied to evaluate streaming of neutrons through control rod penetrations in the CRBR. In addition to providing data for checking the calculational method for the proposed shield (uranium oxide, stainless steel, and sodium), this experiment indicated that the streaming would be negligible for the intermediate-energy neutrons that will dominate the neutron spectrum in number.

A study of the heating of LMFBR shields due to secondary gamma-ray production within the shields has also been undertaken. Energy-deposition measurements within an iron shield were made both with thermoluminescent dosimeters (TLD's) and with a specially designed ionization chamber, the latter filled with high-pressure Ar-Kr simulating the energy absorption cross section of iron. Additional TLD measurements were made within the shield by Argonne National Laboratory and by Massachusetts Institute of Technology in a program aimed at achieving an accuracy within 5%. It is expected that this experiment and its accompanying analysis will be designated as a benchmark case. (Earlier measurements of neutron penetration through iron and sodium have recently been announced as benchmarks.)

In other experiments and calculations during this reporting period, the neutron-attenuating and gamma-ray-production properties of Inconel have been investigated, and total cross-section checks have been made for a number of elements.

RSIC-LMFBR activities. RSIC is heavily committed to promoting communication among the various groups engaged in LMFBR shielding studies and receives direct support from the AEC Reactor Research and Development Division for this purpose. As pointed out earlier in this paper, its activities center on facilitating the exchange of nuclear data, transport codes, and shielding literature.

GCFR Shielding Program

In recent months (as of March 1974) the Division has begun a shielding study for the 300-MW(e) demonstration model of the Gas Cooled Fast Reactor proposed by General Atomic Corporation. We have been charged with identifying shielding problem areas, of which six have already been located, and with ensuring that radiation shielding methods and data are verified for the accurate calculation of these problems. The approach is the same as that used in the LMFBR shielding program, with GCFR studies benefiting from and overlapping with the LMFBR studies in many cases. In particular, TSF experiments are being designed to represent the individual problems, and analyses of the experiments will be performed with the available transport methods adapted to the problem. Depending on the outcome of the analyses, recommendations for further refinements in the transport methods and nuclear data will be made.

A basic two-dimensional DOT-III calculation of the model provided by GA has already been made, and work has begun on the first problem area: axial neutron streaming to the grid support plate. This involves developing a streaming calculational ability and designing a basic streaming

experiment. In preparation for the calculations, a cross-section library has been produced which consists of 51 neutron groups and 25 gamma-ray groups especially tailored for the GCFR.

CTR Program

Cross-section studies. Neutron-scattering and gamma-ray-production cross-section studies similar to those performed for the LMFBR program (see above) have been initiated for nuclides and neutron energy ranges of interest for Controlled Thermonuclear Reactor applications. The nuclei of particular concern are those expected to be included in the blanket and shield assembly surrounding the confined plasma. One element already under study is fluorine. The cross sections for fluorine were reevaluated this past year and will be updated on the basis of recent total cross-section measurements made at ORELA under this program and gamma-ray-production cross-section measurements carried out under the DNA program (see below). Other elements scheduled for investigation are niobium, vanadium, and molybdenum, some preliminary measurements for niobium having already been made.

Neutronics studies. Calculations of the transport of the 14-MeV neutrons emitted from the plasma into the first wall, the blanket, and the shield are also under way. During the past year, ANISN calculations and accompanying sensitivity analyses were performed for four different reactor-blanket configurations to determine the sensitivity of the breeding ratio for each to various neutron cross sections. Current studies are directed toward developing calculational techniques for transport problems unique to the CTR. The resulting capability will serve as a basis for the blanket and shield design and also for predictions for radiation damage to the superconducting magnet and other components.

Neutral atom transport. A program has also been initiated to develop atomic cross-section sets for neutral atom interactions (ionization, charge exchange, etc.) and to adapt the available processing and transport codes to calculations of the transport of the particles within the plasma and up to the first wall. When the initial particles (hydrogen atoms) interact with the wall, some will rebound into the plasma and some will cause "sputtering" – that is, wall material (high-Z atoms) will be knocked into the plasma. Since the presence of these particles in the plasma will cause it to cool, the wall must be designed to minimize the effect of backscattering and sputtering. One proposal is to use a honeycomb wall design, the feasibility of which is being investigated through Monte Carlo calculations.

RSIC-CTR activities. During FY-1974 a modestly funded RSIC-CTR program resulted in a 15% increase in requests to the Center for services, data, computer codes, and other information. Subsequently the program has been considerably expanded. Plans for establishing a CTR evaluated cross-section library similar to the DNA Working Cross Section Library are being developed. In addition, processed data sets for CTR neutronics studies will be designed, generated, and distributed.

Reactor Safety Studies

Since the amount of information on radiochemical yields and radionuclide decay schemes immediately following fission is inadequate for reactor safety and accident analyses, studies to determine the energy release rate versus time from fission product decay are required. A series of studies recently initiated within the Division (in February 1974) is expected to determine the total beta-ray and gamma-ray energy release rates from fission product decay during the period from 2 to 2000 sec after the thermal-neutron fission of ^{235}U and ^{239}Pu. The procedure now being developed and tested will be to irradiate samples of the fuels in the Oak Ridge Research Reactor and via a pneumatic transport system withdraw and

position the samples for gamma-ray or beta-ray counting within 2 sec following irradiation. The gamma-ray spectrometer is based on a NaI(Tl) crystal–photomultiplier assembly, and the beta-ray spectrometer will be based either on an organic scintillator or on a large-volume solid-state device. The goal of the project is to reduce the uncertainty on the energy release rates to ±3% on ^{235}U and to ±4% on ^{239}Pu. The method used will also yield spectra of the beta and gamma rays with a modest resolution.

This work will be coordinated with a CSEWG Fission Product Subcommittee, within which an interlaboratory Decay Heat and Burnup Task Force is compiling radiochemical yield and radioactive decay information. Relative to the CSEWG effort, these measurements will provide a benchmark case.

Neutron Cross-Section Standards

A small effort recently begun at ORELA will help develop the standards required for measurements of fast-neutron cross sections. In the first experiment the average number of prompt neutrons ($\bar{\nu}$) per spontaneous fission of ^{252}Cf will be studied to help establish its value to within ¼%. This parameter is a frequently used standard for studying $\bar{\nu}$ of other materials such as ^{235}U and ^{239}Pu.

High-Energy Accelerator Shielding Program

For a number of years the Division has been engaged in a program originated to support the design of shields for high-energy particle accelerators. Since essentially no experimental data existed to describe the interactions that would occur in the shields, the work began with the development of a Monte Carlo intranuclear cascade code for calculating the needed cross sections. Now in its seventh version, this code, called the Medium Energy Cascade Code (MECC-7), is capable of giving reliable estimates of the energies and angular distributions of nucleons and pions produced from nucleon-nucleus and pion-nucleus collisions at energies below about 3 GeV. Development of a high-energy code (HECC-1) that will be capable of calculating the cross sections for particles having energies on the order of hundreds of GeV is now in progress. In the meantime, high-energy cross sections are estimated by a method which uses the intranuclear cascade code with an "extrapolation" method.

The accelerator shielding program has also included the development of the Monte Carlo high-energy transport code HETC. HETC has the ability to account for the energy and angular distributions of all particles produced in nuclear interactions, and at each nonelastic collision site a calculation with subroutine versions of MECC-7 and an evaporation program, plus an extrapolation program if needed, is performed to describe the results of the collision to HETC. Other codes, in particular an electron-photon cascade code and several of the low-energy transport codes discussed earlier, use information generated by HETC as the source for additional transport calculations.

Calculations based on these methods have yielded design data for several accelerators, in earlier years for the National Accelerator Laboratory and the Massachusetts Institute of Technology accelerator and this past year for the University of Indiana accelerator. The most recent calculations have consisted of a series to determine the depth and radial distributions of the energy deposited by 45-GeV photons in a variety of thick targets and a series to provide the energy and angular distributions of neutrons produced when 50-, 100-, and 200-MeV protons are incident on thick targets. In addition, calculations of the energy and angular distributions of the photoprotons produced by 400-MeV bremsstrahlung in a variety of elements were made for comparison with measurements performed at the University of Lund, Sweden.

Much of the current work in this program is performed to aid in the design of instruments to be used by the experimental groups at the accelerator facilities. In this area the responses of several different ionization spectrometers to pions and protons in the range from 3 to 50 GeV are being calculated with the HETC code

and the electron-photon cascade code. They include both all-liquid and multimedia spectrometers, the latter consisting of thin plastic scintillators embedded in thick absorbers or alternate layers of iron and liquid. For the multimedia-type spectrometers it was necessary to modify the electron-photon cascade code so that it could treat nonhomogeneous media.

Several additional calculations pertinent to this program have been performed in conjunction with the NASA and cancer radiotherapy studies discussed below.

NASA Program

A space shielding program for the National Aeronautics and Space Administration also began several years ago with the generation of the cross sections needed for transport calculations, those of primary concern being the cross sections required for calculations in which the incident particles were protons. For this program the energy range covered by MECC-7 is adequate, and a moderate amount of experimental data has been available for checking its results. During the past year the validity of MECC-7 has been further investigated through intercomparisons with a similar code developed at Brookhaven National Laboratory, the results from both being compared with experimental secondary proton spectra for 62- and 39-MeV protons incident on carbon, iron, and bismuth.

Although the decreasing emphasis on space missions has decelerated the effort in this program, calculations supporting spacecraft shield designs are still under way, a recent one being a calculation of the spectra of photons emitted from activated materials in a spacecraft passing through the Van Allen proton belt. In addition, work performed in conjunction with the cancer radiotherapy studies described below has been directed toward the development of a nuclear model for predicting the interactions of heavy ions with nuclei (the HIC-1 code). Such a model is a prerequisite to the calculation of the shielding required to protect against the high-energy heavy galactic cosmic rays and to study the use of heavy ions in cancer radiotherapy.

Cancer Radiotherapy Studies

Probably the most significant recent work performed in the Division's cancer radiotherapy studies sponsored by the National Science Foundation has been a series of transport calculations to study the relative effectiveness of various types of radiations incident on a tissue phantom. The particles considered were photons, neutrons, negatively charged pions, protons, and alpha particles, and for each type the beam parameters were chosen so that the same tissue volume was irradiated. The results obtained were absorbed doses, linear-energy-transfer (LET) spectra, cell survival probabilities, relative biological effectiveness (RBE's), and oxygen enhancement ratios (OER's) as a function of position in the tissue.

Several additional studies have yielded information specifically of interest to those using negatively charged pion beams for cancer treatment. In one the effect of bone in the path of a pion beam traversing a tissue phantom was predicted, and in another the effect of using different beam sizes to irradiate specific tumor volumes in a tissue phantom was studied. In addition, calculations of the energy deposition by high-energy electrons in a water phantom were performed for use in studying the effect of electron contamination in the pion beams.

Other calculations have been performed to aid in the development of techniques for monitoring the radiation delivered to the tissue volume under treatment. In particular, the depth dependence and energy spectra of the residual nuclei produced by negative pions in tissue, tissue-equivalent plastic, silicon, and germanium were predicted, and the responses of silicon detectors of various radii and thicknesses to negative pions stopping in tissue were studied.

The current use of fast neutrons in clinical trials prompted another series of calculations. In these, a variety of neutron spectra incident on a tissue-equivalent phantom were considered, and the corresponding absorbed doses, LET spectra, cell survival probabilities, RBE's, and OER's were predicted.

All of the above calculations were performed with calculational techniques developed under the accelerator and NASA shielding programs, and some of the above calculations were partially supported by the accelerator shielding program. In another cooperative effort, the development of the HIC-1 code discussed under the NASA program has been partially supported under this program (see above).

DNA Program

The Division program sponsored by the Defense Nuclear Agency is primarily concerned with providing the nuclear data and methods needed for the radiation transport analysis of systems exposed to radiations from nuclear detonations. In addition, specific radiation transport analyses requested by DNA are performed in order to demonstrate and effectively use the new methods on important problems. As in the case of the LMFBR program, essentially all areas of research in the Division are associated with the DNA program.

Cross-section studies. The DNA cross-section studies comprise both cross-section measurements (at ORELA) and cross-section evaluations, the latter including the development of nuclear models and their application in cross-section calculations. The nuclei of concern are those appearing in the atmosphere and ground, and in the structural materials used in buildings and equipment. Because gamma rays produced by neutron interactions in shield materials have been shown in many cases to be the most important radiation component to be dealt with, the experiments to date have concentrated on measurements of gamma-ray-production cross sections for fast neutrons using a small (5-in.) NaI gamma-ray detector; the neutron interactions involved have predominantly been inelastic scatterings. Production cross sections based on these measurements have been reported for 16 elements, and techniques have been developed for additional measurements of inelastic-scattering gamma rays at lower energies with a germanium detector. In addition a large (9 × 12 in.) NaI crystal has been tested for detecting the higher gamma-ray energies produced by epithermal neutron capture reactions. A technique employing an NE-213 spectrometer has also been developed for measuring neutron scattering cross sections.

Cross-section evaluations have been performed or updated for the elements silicon, calcium, iron, and lead. In addition, evaluations of the gamma-ray-production cross sections for fluorine and zinc have been completed, and responsibility for a magnesium evaluation has been accepted. This work is coordinated both with the ENDF/B files and with the DNA Working Cross Section Library maintained by RSIC.

Cross-section processing. The basic development work on AMPX, the system of interfaced modular codes that produces coupled neutron and gamma-ray multigroup cross sections for transport codes, has largely been carried out under the DNA program. During the past year a Phase I IBM-360 version of AMPX was released through RSIC, and an upgraded Phase II version was subsequently completed and frozen. As released, the system contains six basic modules, but work on additional modules has begun. These new modules are for the purposes of checking data and for processing photon scattering with bound electron effects included. An important goal in the forthcoming work is the implementation of the AMPX Phase II version on CDC computers.

Throughout the year, AMPX has been used to produce multigroup cross sections needed for the various nuclear analyses under way within the Division. In addition, it was used to produce a few-group cross-section library tailored for DNA contractors depending largely on small computers. The set contains 37 neutron groups and 21 gamma-ray groups, with appropriate weighting functions. The selection of the

group structure was based on extensive study of transport calculations that had been performed for air and concrete with a cross-section set consisting of 129 neutron groups and 42 gamma-ray groups. As a secondary result of the study, a high-energy gamma-ray group was added to the many-group set. It is planned to release both the 37-21 set and the 129-43 set through RSIC's Data Library Collection.

Transport method development. The DNA program has supported much of the Division's transport method development work, including the development of the discrete ordinates codes ANISN, TDA (time-dependent ANISN), and DOT, and the Monte Carlo code MORSE. During the past year, documentation of the versions of DOT and MORSE as they are now supplied to users was completed, and improvements on both systems were continued. In the case of DOT, the work on the improved version (DOT-IV) is being carried out under the LMFBR program. The later versions for both codes will result in an ability of the systems to handle larger problems with reduced computer demands. In MORSE this is being accomplished by restructuring the cross-section input to reduce the memory storage requirements during input and to remove information not needed after it has been used. Core storage requirements are also being reduced through a new option that allows "supergrouped" cross sections to be successively input into a problem.

Another code whose development has been partially sponsored by DNA is a special version of ANISN referred to as the "point ANISN" code. In point ANISN the multigroup structure is very fine, simulating a point structure, and the required computing time is minimized by the use of a fast numerical scheme to generate the cross sections. With the cross-section detail that can be used in point ANISN, it is particularly suitable for calculating one-dimensional benchmark cases which are independent from multigroup approximation.

In addition, a coupled code system has been developed to handle a particular class of problems. Called the SCS code, it uses ANISN throughout but changes geometries. It has been developed as a one-dimensional approach for calculating the penetration of radiation from an in-air detonation into a missile silo lid – a problem that has required two dimensions in the past. In SCS the transport through air is calculated for a sphere and the transport through the silo lid is calculated for an infinite slab.

Under a project sponsored by the Ballistics Research Laboratory, a Vehicle Code System (VCS) was developed for the problem of an armored vehicle in an air-over-ground radiation environment. This code uses the DNA-developed DOT and MORSE transport codes as the major components of the system. As developed, VCS is useful for almost any vehicle or structure in a radiation environment requiring two-dimensional transport.

Integral experiments and analyses. DNA-supported integral experiments to check differential cross-section data are performed both at ORELA and at the Intelcom Rad Tech accelerator, with analyses of all the experiments performed within our Division. In general the experiments have been sufficiently coordinated that the analyses on a particular element from the two facilities can be performed concurrently. In the experiments, measurements are made of scattered neutrons and secondary gamma rays at various angles from a pulsed neutron beam incident on a sample of the material of interest. The design of the experiment and the techniques employed in the calculations are influenced by continued interaction between the experimental and calculational programs. A preliminary experimental run at one scattering angle and a corresponding calculation confirm the design of the experiment and guide the selection of a fine-group cross-section structure for the final (MORSE) analysis. Unexplained discrepancies between the calculated and measured neutron and gamma-ray spectra at various angles are attributed to errors in the cross sections, and a subsequent examination of the results indicates the contributions of individual partial cross sections to the response in the vicinity of the discrepancies. These partial cross sections are then selected for special study in the sensitivity analyses of applied problems (see below). Those cross sections

found to be the most important for DNA problems are thus identified for the cross-section evaluators, who reexamine and update the corresponding data files. If, following an iteration of the various activities, complete agreement between the calculated and measured responses is attained, the experiment can serve as a benchmark for testing multigroup cross-section sets for that element as they are developed.

During the past year this procedure was applied to ORELA and IRT experiments on carbon with resulting good agreement. A similar study for nitrogen has a few unresolved discrepancies. Studies for oxygen, iron, and SiO_2 are still in progress. The SiO_2 sample has been designed to have a cross-section sensitivity similar to that of concrete.

In addition to the "differential" experiments, ORELA experiments are performed to test total neutron cross-section sets. When the experimental data are corrected for the transmission through the samples, they can be compared directly with the total cross-section set. During the past year, reduction of the data obtained for nine different materials was completed, and, with the exception of oxygen, all the total cross-section sets were found to be deficient in some energy regions.

Development of sensitivity analysis techniques. The SWANLAKE sensitivity analysis program, referred to in previous paragraphs, was developed under DNA sponsorship. During the past year the ability of this program to calculate and plot the normalized rate of change of one-dimensional discrete ordinates (ANISN) results with respect to changes in any partial cross section as a function of energy has been checked out by its application to the calculation of the transport of radiation from two different weapons through infinite air. In each case the sensitivity of the calculated responses to the cross sections for nitrogen and oxygen was determined. Work was subsequently begun on the VIP code to extend SWANLAKE to a two-dimensional capability. In addition, SWANLAKE was successfully linked up with the point ANISN code and to a limited extent with the SCS code. (Studies with SWANLAKE and point ANISN are useful in selecting optimum multigroup structures for applied transport problems.)

Work has also been done in developing a code system which with specified cross-section uncertainties would allow SWANLAKE to calculate the total uncertainty in a problem solution. As a first attempt, a ±1 correlation between measured and derived cross-section values for a given reaction was assumed over the entire energy range, and no correlation between reactions of different types was considered. This technique was applied to the two infinite-air calculations performed this year and also to an earlier infinite-air calculation for a thermonuclear source.

The development of a more sophisticated cross-section error analysis package was also initiated. In this system the PUFF cross-section error-processing code is to be linked with SWANLAKE. PUFF is developed within the MINX code and can be an optional overlay within the neutron multigroup module in the AMPX system; it was successfully used to process the ENDF total cross-section error file for carbon this past year.

Application of methodology to military problems. In previous years, two major DNA studies involving coupled DOT, ANISN, TDA, and MORSE calculations were carried out to determine the radiation intensities incident upon and penetrating into missile silos, the first a time-dependent study for a simple idealized silo configuration and the second a time-integrated study for a more realistic configuration. Since these two studies are directly applicable to missile silo design and since they also provide a catalog of data that can be used to estimate radiation intensities at comparable positions in similar silo configurations, considerable effort has been spent during the past year in determining the effect that revisions in the cross-section data and in the multigroup structure used in the calculations would have on the time-integrated results. At the same time the usefulness of the one-dimensional SCS code system to problems of this type was investigated.

A series of benchmark-quality calculations with the DOT code were also performed for a 14-MeV neutron source and a pure fission weapon neutron source in an air-over-ground geometry and in an

air-over-seawater geometry. The ground range was 1500 m, and the source heights were 1, 50, 100; and 300 m above the ground and 50 m above the seawater. The latest DNA cross sections for nitrogen and oxygen were used in a 22-18 neutron-gamma group structure, and the results were obtained as Henderson neutron tissue doses, gamma-ray tissue doses, and silicon neutron and gamma-ray ionizations as a function of distance from the source. In performing these calculations it was noted that the usual finite-difference scheme in DOT produced fluctuations in the fluxes, particularly for the 14-MeV source. After much study the entire series of calculations was repeated using the weighted-difference scheme, thereby producing excellent results.

One-dimensional benchmark calculations were made with the point ANISN code for a standard thermonuclear source in an iron sphere and in an air sphere. SWANLAKE sensitivity analyses were performed for both cases.

In a SAMSO-sponsored study, a series of calculations which were very similar to the first silo study were performed using the latest air and concrete cross sections in the few-group structure developed for DNA contractor use. In a BRL-sponsored study a series of calculations were completed in which the penetration of weapons radiation into several tank configurations was calculated with the VCS code.

RSIC-DNA activities. All of the RSIC services contribute to the DNA program, but perhaps the most significant is the service offered through the DNA Working Cross Section Library. As of August 31, 1974, it includes the latest evaluations for 25 nuclides important for weapons shielding problems. In addition, RSIC has initiated a DNA Processed Cross Section Library with the few-group set developed within the Division and with a set of MAGI's point data for use in the Monte Carlo code SAM-CE. It is also through RSIC that the various transport, processing, and sensitivity codes developed under the DNA program, at ORNL and elsewhere, are made available to DNA contractors. In addition, the detailed results from some DNA transport calculations are available from RSIC on magnetic tape.

Facility Operation

The Division is responsible for the operation of the Tower Shielding Facility and the Health Physics Research Reactor, the same team handling both reactors. We also share responsibility with the Physics Division for the operation of the Oak Ridge Electron Linear Accelerator. As pointed out above, most of the Division's experimental research is performed either at the TSF or at ORELA, and support for these facilities is given by the user programs. Only rarely do we participate in experiments at the HPRR, our responsibility being limited to the safe operation of the reactor for experiments conducted by the Health Physics Division.

TSF. The radiation source at the TSF is a spherical 1-MW water-cooled reactor having an aluminum-uranium core approximately 3 ft in diameter. The control rods for the reactor are also spherically symmetrical and are contained within a 2-ft-diam water-filled region in the center of the core. This reactor configuration simplifies calculations of the radiation leakage from the source, which is an integral part of the analysis of the experiments.

The facility is designed to allow very high radiation levels in the operating area so that experiments can be carried out on very thin materials as well as on thick materials. During the experiments the reactor is surrounded by a spherical lead-water reactor shield through which a 15-in.-diam radiation beam port extends, providing a collimated beam for the experiments. A new beam shield recently constructed for the reactor will provide a beam having a larger diameter (3 ft) and shorter length (1 ft) than the old shield, and it is expected to extend the range of attenuation that can be measured by a factor of 50 to 100.

ORELA. ORELA was designed to simultaneously accommodate a number of neutron cross-section experiments utilizing the time-of-flight technique. The neutrons are produced when bursts of electrons that

have been injected into one end of a 75-ft-long accelerator are boosted by an electromagnetic wave to average energies as high as 140 MeV before they interact with a tantalum target at the opposite end of the accelerator. Bursts of neutrons are emitted from the target in all directions, and they travel along each of the flight tubes to the experiments located at the various stations. The width of the neutron burst, governed by the width of the electron burst, can be varied from a microsecond down to 2 nsec. In practice, it is usually varied in the range from 3 to 50 nsec. With a maximum of 1000 bursts per second, sufficient time is available between bursts for measurements to be made of the time required for the neutrons from one burst to reach the experiment before those from the following burst arrive. Each burst results in the production of about 10^{11} neutrons having an energy spectrum determined by the energies of the interacting electrons. The experimental results are fed into a specially designed data acquisition system which, through the use of three computers, can handle data from several experiments totaling as many as 15,000 events/sec. Several of the flight stations are being used by the Division.

Other Activities

In addition to the programmatic activities already described, the Division has provided aid to other agencies during the reporting period. These have included a study of the core physics characteristics for the Aberdeen Pulse Reactor, calculations of the radiation shielding requirements for a radar site defense unit, and a recently initiated study of the shielding requirements for areas containing radioactive materials in commercial power reactors.

Finally, RSIC has extended its services to the utilities, for which the Electric Power Research Institute has now authorized funding, and it is also beginning work on a computing technology information center for the Society of Nuclear Medicine.

Additional information on the programmatic activities of the Neutron Physics Division is provided in the following papers, and the organizational responsibility for the various areas of research is shown in a chart presented on p. 129.

Lorraine S. Abbott

1. PRESENT STATUS OF CROSS-SECTION DATA OF THE FISSILE AND FERTILE ISOTOPES FOR FAST REACTORS[1,2]

G. de Saussure R. B. Perez

The most important cross-section data for the development of fast reactors are the fission cross section of ^{235}U and the fission and capture cross sections of ^{238}U and ^{239}Pu. The fission cross section of ^{235}U is widely used as a standard with respect to which other fission and capture cross sections are measured, and the fission and capture cross sections of ^{238}U and ^{239}Pu control the neutron balance in a fast breeder reactor.

In this paper we will review the status of these data and compare our present knowledge of these cross sections to that available four years ago, when W. G. Davey reviewed the status of cross sections and other nuclear data for the Second International Conference on Nuclear Data for Reactors.

Since 1970, a very large number of cross-section measurements for the fissile and fertile isotopes have been completed, and our knowledge of the cross sections has become much more detailed. This is particularly true for the energy region below a few hundred keV, where measurements done by the time-of-flight technique and with "white spectrum" neutron sources have revealed a considerable amount of intermediate structure. Some of the consequences of this structure have been explored and have led to a reevaluation of measurements done with nearly monoenergetic sources of neutrons.

The error quoted by Allen and Ferguson for their 1957 measurement of the fission cross section of ^{235}U was 3 to 5%. The error estimate of the most recent U.S. evaluation (ENDF/B-IV) of this cross section is still 4%. This does not indicate that no improvement in accuracy has been achieved in the past 17 years; rather, it indicates that as more measurements of the same cross section become available, the evaluators and experimenters are forced to a more precise evaluation of the probable errors.

An examination of recent measurements and a comparison of the latest evaluations indicate that the present accuracy of fission data is of the order of 4% up to 5 MeV. The capture data have uncertainties of the order of 10 to 15%.

The uncertainties in the data are strongly correlated: uncertainties in normalization, particularly below a few hundred keV, introduce correlations over wide energy ranges; measurements of α and measurements relative to the fission cross section of ^{235}U and other standards introduce correlations between the errors on different cross sections.

As in 1970, the cross sections which still require the most improvement, from the reactor point of view, are the capture cross section of ^{238}U and the fission cross section of ^{235}U. Recent unpublished data and measurements in progress should considerably improve our knowledge of these cross sections in the near future, but much more work will be needed to attain the accuracy requirements of nuclear designers.

---

1. Summary of paper presented at American Nuclear Society meeting, Atlanta, Ga., September 8–11, 1974.
2. Research sponsored by AEC-LMFBR program.

2. RECENT MEASUREMENTS ON ^{238}U AT ORNL[1,2]

G. de Saussure

In 1972, R. B. Perez, E. G. Silver, and I completed a series of measurements at the Oak Ridge Electron Linear Accelerator (ORELA) in which we used a large liquid scintillator[3] and the time-of-flight technique to determine the capture cross section of ^{238}U in the neutron energy range from 5 eV to 100 keV. When we compared our results with two earlier sets of data also obtained by the time-of-flight technique – by Moxon[4] at Harwell and by Friesenhahn et al.[5] at Gulf General Atomic – we discovered systematic

discrepancies between the sets that were larger than the known uncertainties of the measurements. In an attempt to resolve these discrepancies, Perez and I have joined R. L. Macklin and J. Halperin in a new series of time-of-flight measurements, using an entirely different detector. It is my intent here to compare the two experimental techniques and then to point out the discrepancies which we hope the latest measurements will explain.

The detector (ORELAST) used in the 1972 ORNL measurements is shown in Fig. 2.1. It consisted of 3000 liters of liquid scintillator (NE-224 poisoned with trimethyl borate) viewed by 32 photomultipliers, each 5 in. in diameter. The ^{238}U sample, a disk about 8 cm in diameter, was placed in the center of the tank and was decoupled from the scintillator by a 2.5-cm-thick ^{6}LiH liner. An aluminized Mylar foil (not shown in the figure) separated the tank into two halves, and coincidences between the signals from the two halves were required for a capture event. This requirement resulted in a high signal-to-background ratio, since gamma rays from capture in ^{238}U have a high multiplicity and hence a high probability per event of being detected in both halves of the scintillator.

ORNL-DWG 68-10873R

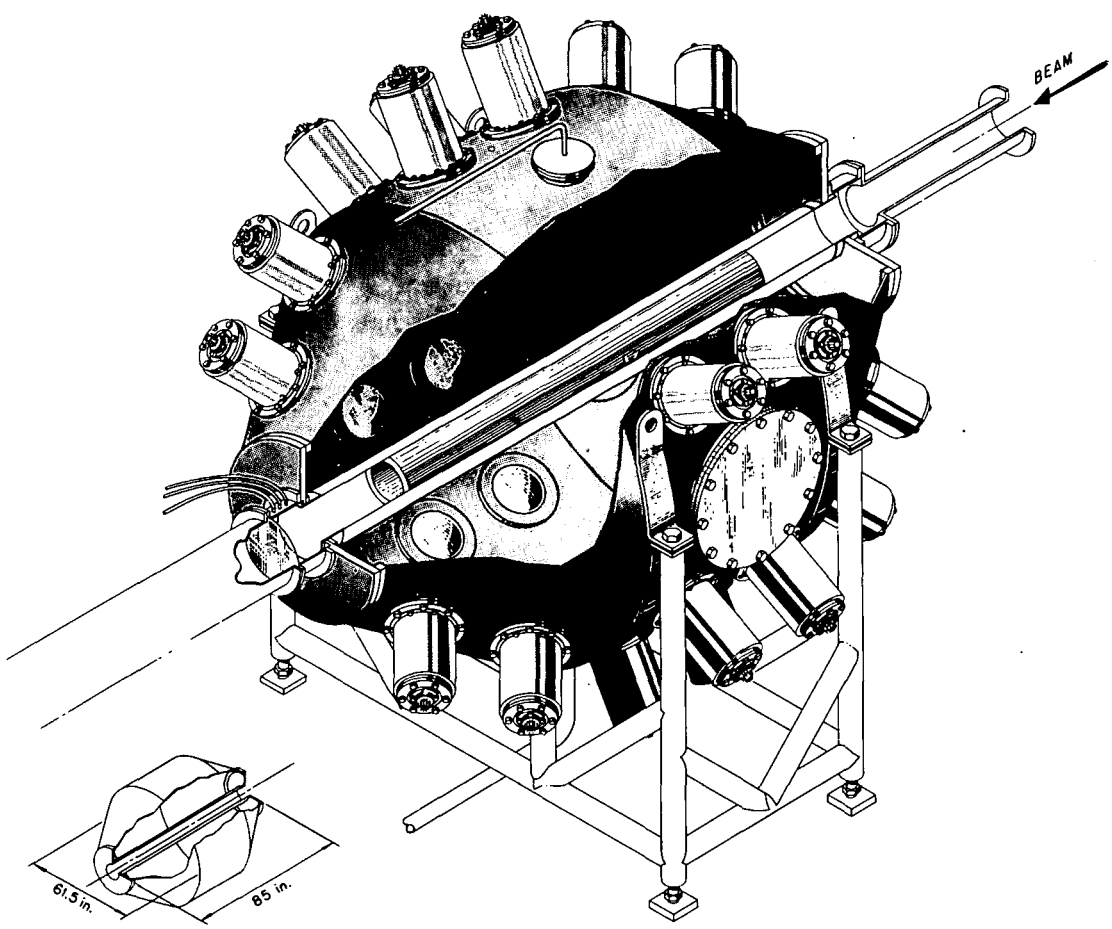

Fig. 2.1. Sketch of the liquid scintillator tank (ORELAST) used in 1972 ^{238}U capture cross-section measurements. Located at ORELA 40-m flight-path station.

The pulses from the scintillator were divided into two pulse-height groups corresponding to equivalent total gamma-ray energies between 2.8 and 4.5 MeV and between 4.5 and 10 MeV. In turn, each of these pulse-height groups was divided into two subgroups according to whether or not signals were received in coincidence from both halves or a single signal was received from only one of the halves. We did not observe significant systematic changes in the ratio of coincidences to singles or in the pulse-height distribution either with the neutron energy or from level to level in the resolved range.

Figure 2.2 shows that the signal-to-background ratio was about eight times better for the coincidence signals than for the single signals and that the ratio of single to coincidence signals remained constant from level to level within our accuracy of approximately 5%.

Figure 2.3 illustrates how the background was determined. The level of the background was obtained in the notches of a set of resonance filters. In between these notches the shape of the background was obtained from a run in which the uranium sample was replaced by a lead sample (with minor corrections for the capture in lead). This background shape was mostly determined by the lifetime of the scattered neutrons in the tank and was not a sensitive function of the thickness of lead used. From the runs with the notch filters, we determined the net counts per incident neutron away from the notches. From a second set of runs without notch filters, we then obtained the net count rate over the regions with notches.

Figure 2.4 shows the incident neutron spectrum with and without the notch filters. This spectrum was measured with a BF_3 ionization chamber and with a 1-mm-thick ^6Li glass. The two measurements agreed within 3% over decimal intervals up to 100 keV. The structure above 20 keV was caused by the filtering of the beam by a 20-mm aluminum housing surrounding the ORELA moderator. (This housing was later

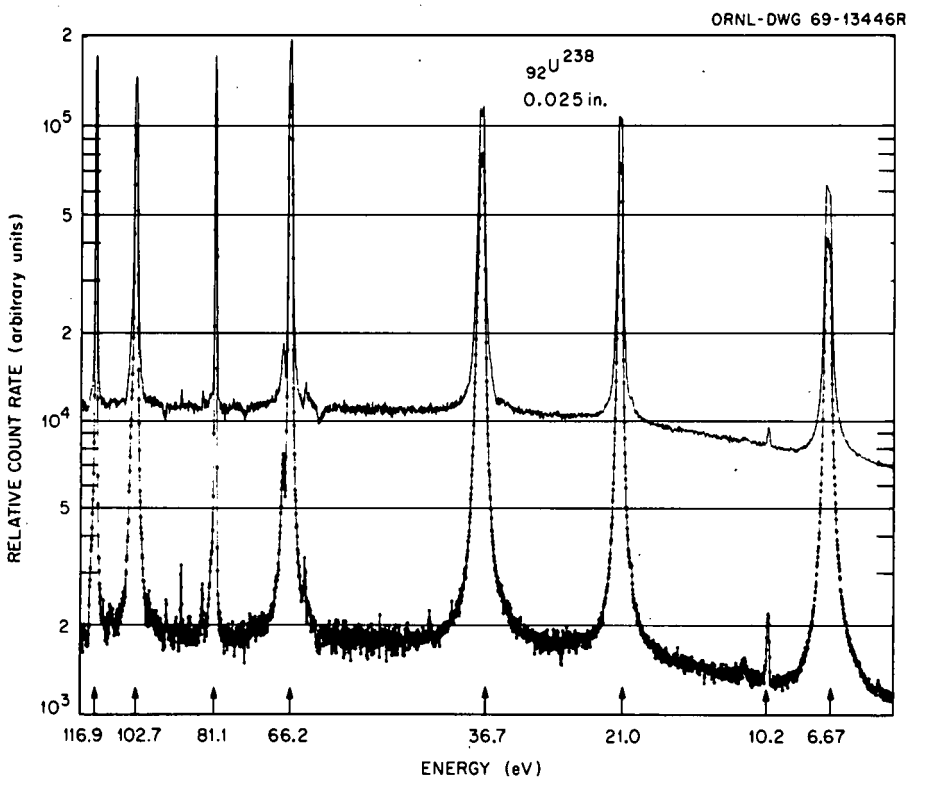

Fig. 2.2. Count rates observed with a 25-mil-thick sample of ^{238}U in the ORELAST. The upper curve represents events observed in one of the halves of the ORELAST but not in the other. The lower curve represents coincidences between the two halves of the ORELAST. The signal-to-background ratio is approximately eight times better for the concidence signals (lower curve) than for the single signals (upper curve).

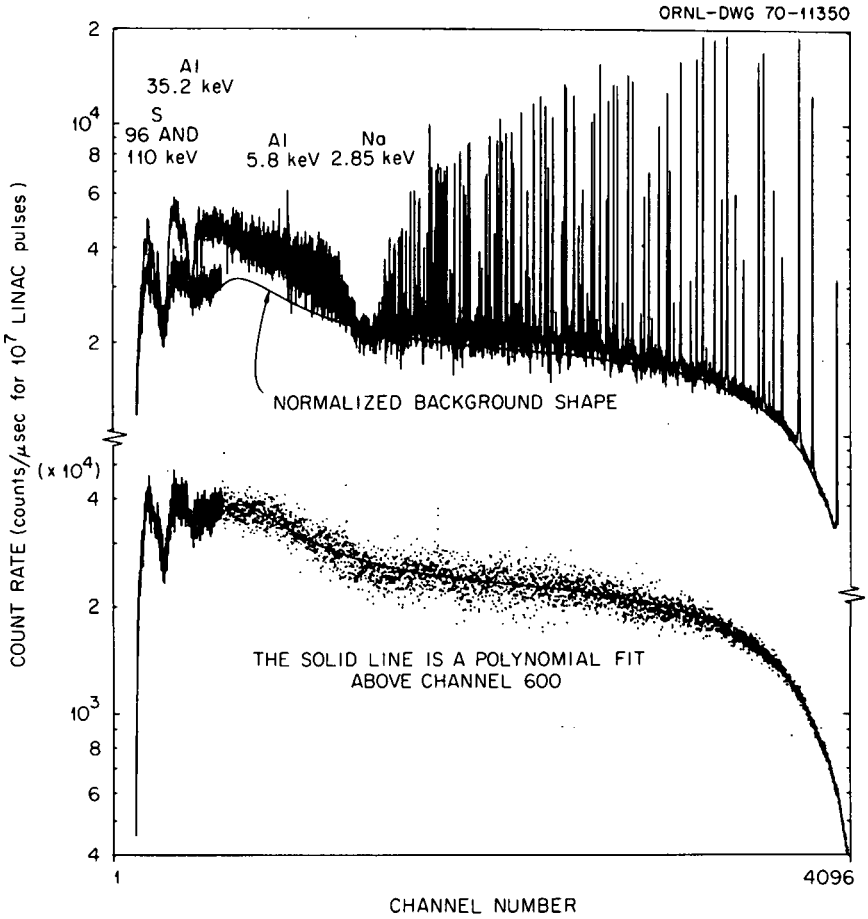

Fig. 2.3. Shape of background – measured with a 0.003-in. lead sample.

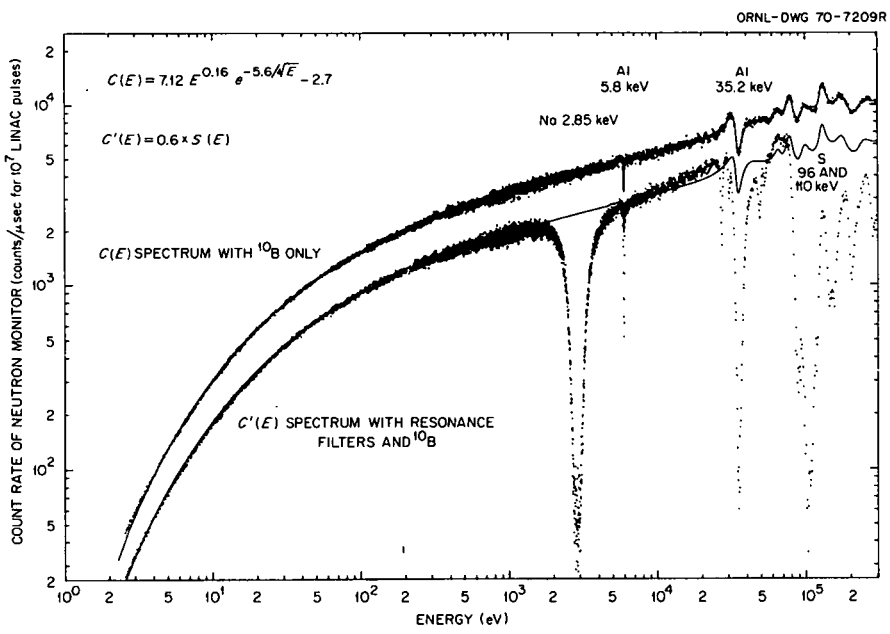

Fig. 2.4. Incident neutron energy spectrum with and without the resonance filters.

replaced by beryllium, and the spectrum became much smoother.) The neutron spectrum decreased at low energies due to a ^{10}B overlap filter.

Figure 2.5 illustrates the normalization of the data by the saturated resonance technique. The solid line was obtained by a Monte Carlo calculation, which is insensitive to the exact value of the resonance parameters. It is difficult to see how this normalization could be in error by more than 2%. In order to obtain average capture cross sections, it was necessary to correct the data for multiple scattering and resonance self-shielding. Above 4 keV this correction was less than 4% for the two sample thicknesses used. (It was evaluated by a method due to L. Dresner and coded by R. L. Macklin, both of ORNL.) Below 4 keV, and particularly over the 100-eV-wide intervals, the statistical approach breaks down, and we used the

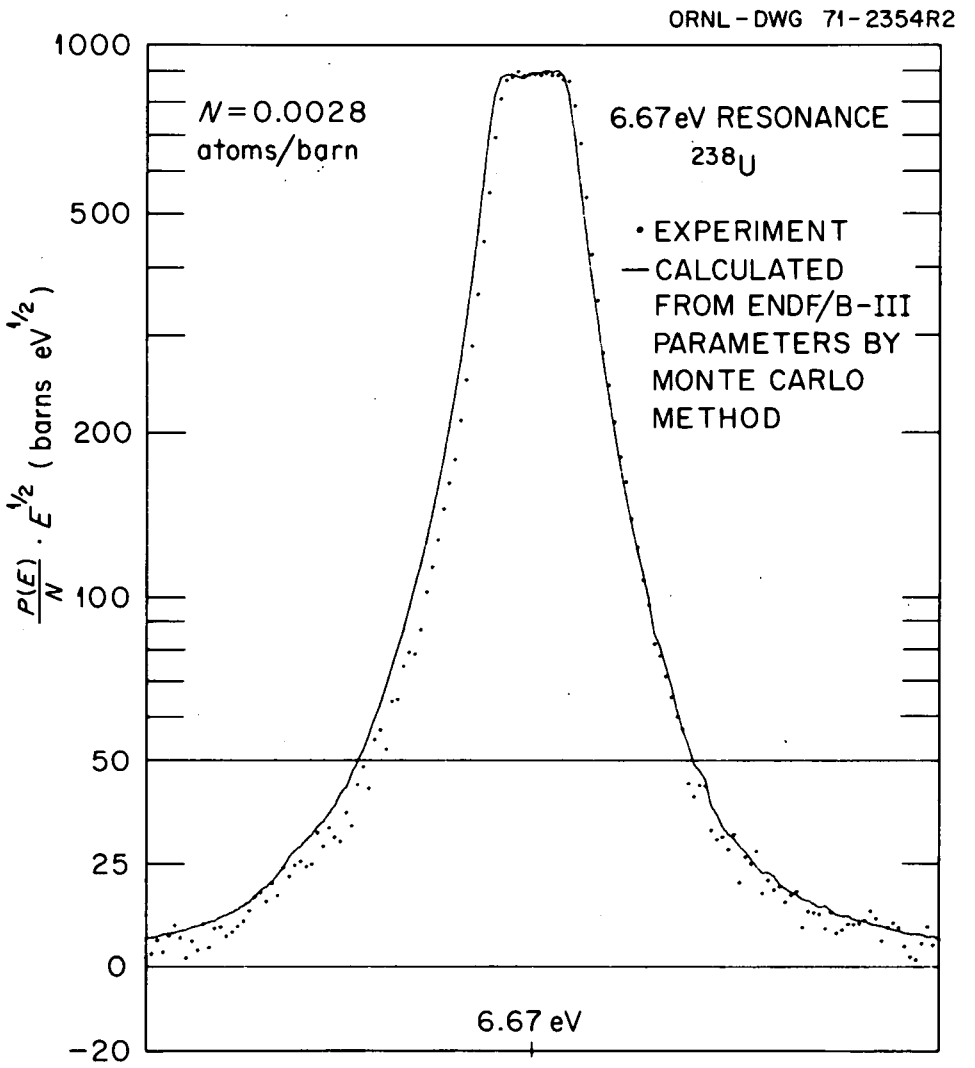

Fig. 2.5. Probability of capture in a 25-mil-thick sample of ^{238}U at the 6.67-eV resonance. The ordinate is the probability of capture multiplied by the square root of the energy and divided by the sample thickness (in atoms per barn). The calculation was done with the Monte Carlo code MULTSCA using the resonance parameters of ENDF/B-III. Note that the ordinate is linear from −20 to +50 b·eV$^{1/2}$ and logarithmic above 50 b·eV$^{1/2}$.

ENDF/B-III resonance parameters (which are in fair agreement with our data) to compute both corrections by a Monte Carlo technique. For the thick samples used in the measurement (0.0028 atom/b), the correction was as large as 300%; for the thin sample (0.0004 atom/b), it was always smaller than 40%.

The detector being used in our second series of measurements was designed by Macklin and is illustrated in Fig. 2.6. The rectangular sample, perpendicular to the neutron beam, is placed between a pair of nonhydrogenous scintillator cells (NE-226) viewed by photomultipliers. On-line pulse-height weighting ensures that the capture detection efficiency is independent of multiplicity and is a function only of the total energy released (binding energy). The BF_3 and proton-recoil monitors shown in the figure have since been replaced by a 0.5-mm ^{6}Li glass monitor. The normalization is done by the saturated resonance technique. The scattering background is obtained by replacing the uranium sample with a lead sample, and it is normalized to the main run by the ratio of the monitor counts.

We turn now to the discrepancies among our 1972 measurements and those of Moxon and of Friesenhahn et al. Figure 2.7 shows the three data sets averaged over decimal intervals in the range 0.5 to 100 keV. Our data agree, more or less within errors, with the data of Moxon up to 10 keV and with the data of Friesenhahn et al. above 50 keV. From 10 to 50 keV, the three sets of data are inconsistent, and over most of the range 0.5 to 100 keV at least one set of data is inconsistent with the others. Note also that in the interval 0.9 to 1 keV our capture is 25% larger than that of Moxon.

In Fig. 2.8 we compare our data averaged over 50-eV intervals (solid line) with data obtained with a Van de Graaff source and other monoenergetic sources.[6] Within the rather large uncertainties of these

ORNL DWG 69-14021

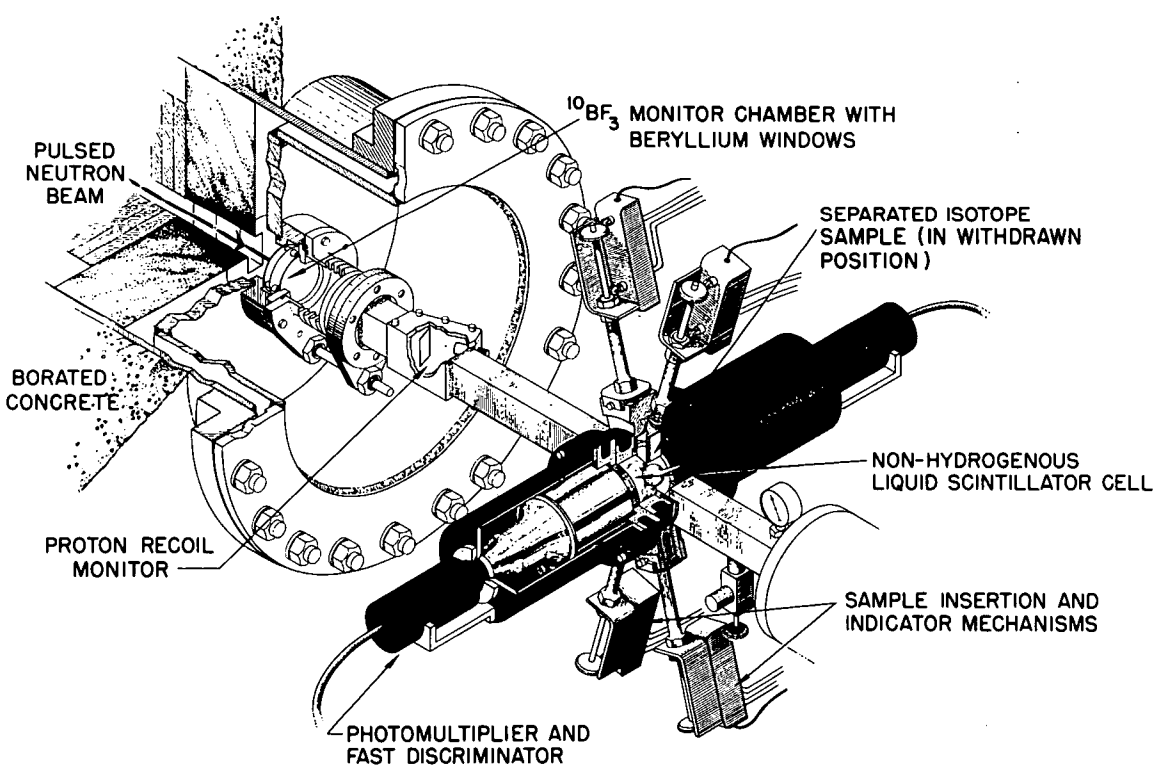

Fig. 2.6. Experimental arrangement for current ^{238}U capture cross-section measurements located at ORELA 40-m flight-path station.

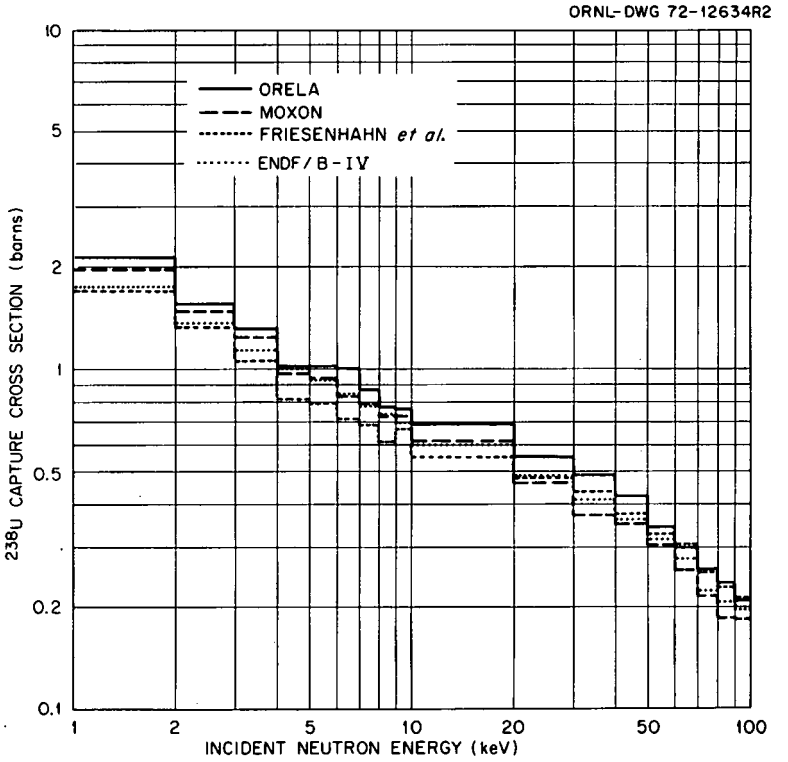

Fig. 2.7. Comparison of three sets of data on the capture cross section of ^{238}U. The three sets have been averaged over the decimal intervals and are relative to the same standard, the ^{10}B($n\alpha$) cross section.

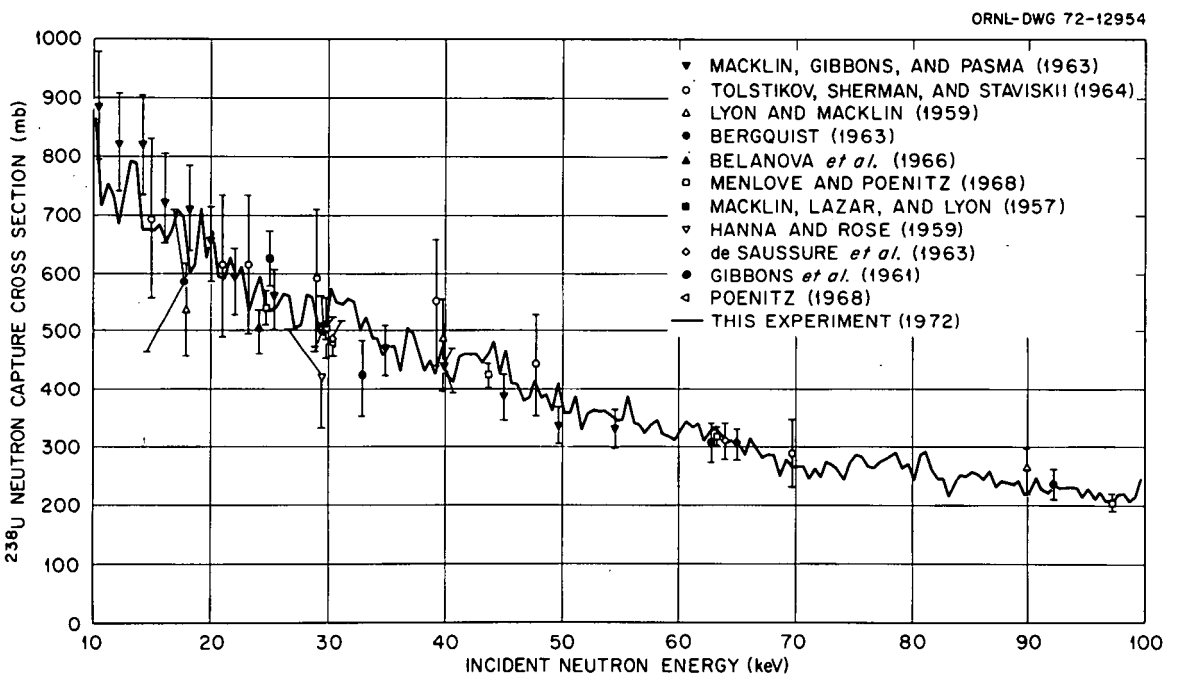

Fig. 2.8. Comparison of various measured values of the ^{238}U capture cross section in the energy range from 10 keV to 100 keV. The solid line was obtained by averaging the data from run R0031901 over 500-eV intervals and applying a sample thickness correction of 0.962. The other data were taken from Table XIX of Davey's evaluation (ref. 6).

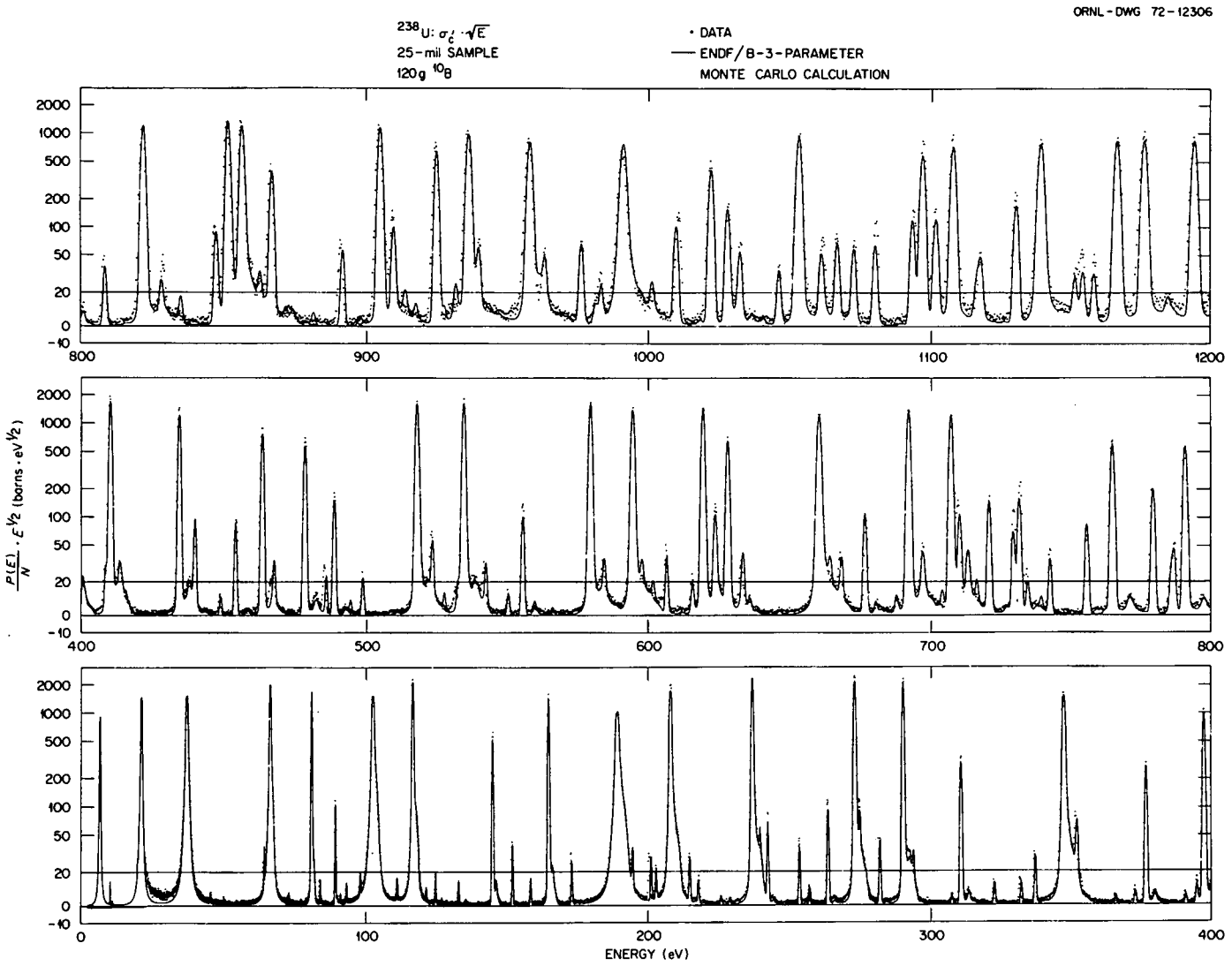

Fig. 2.9. Comparison of the measured and computed capture probabilities for a ^{238}U sample of 0.0028 atom/b and for incident neutron energies up to 1.2 keV. The ordinate is the probability of capture multiplied by the square root of the energy and divided by the sample thickness (in atoms per barn). The calculation was done with the Monte Carlo code MULTSCA using the resonance parameters of ENDF/B-III. Note that the ordinate is linear from −10 to +20 b·eV$^{1/2}$ and logarithmic above 20 b·eV$^{1/2}$.

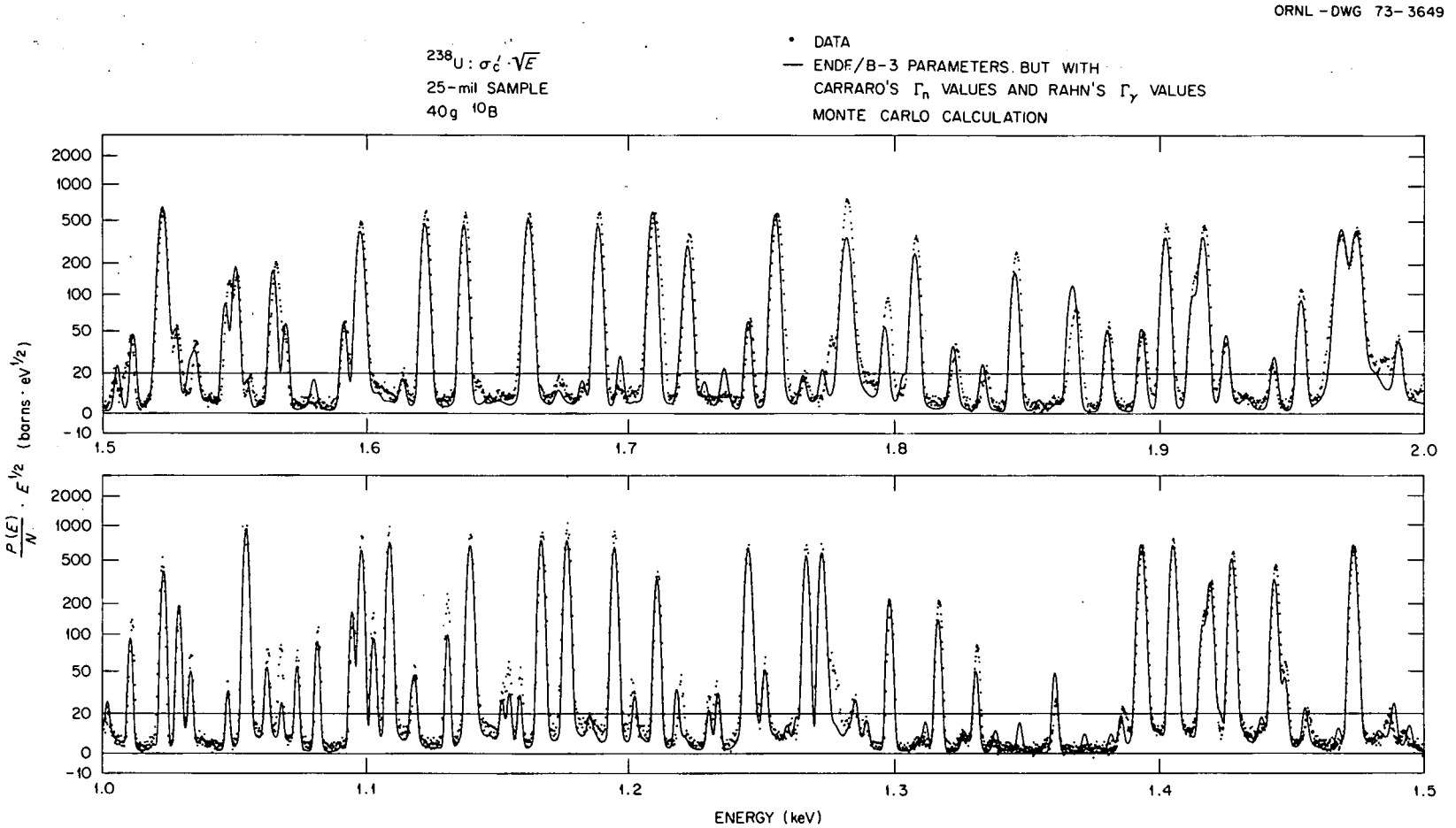

Fig. 2.10. Comparison of the measured and computed capture probabilities for a ^{238}U sample of 0.0028 atom/b and for incident neutron energies from 1 to 2 keV. The ordinate is the probability of capture multiplied by the square root of the energy and divided by the sample thickness (in atoms per barn). The calculation was done with the Monte Carlo code MULTSCA using the resonance parameters of ENDF/B-III. Note that the ordinate is linear from −10 to +20 b·eV$^{1/2}$ and logarithmic above 20 b·eV$^{1/2}$.

ORNL - DWG 73-4917

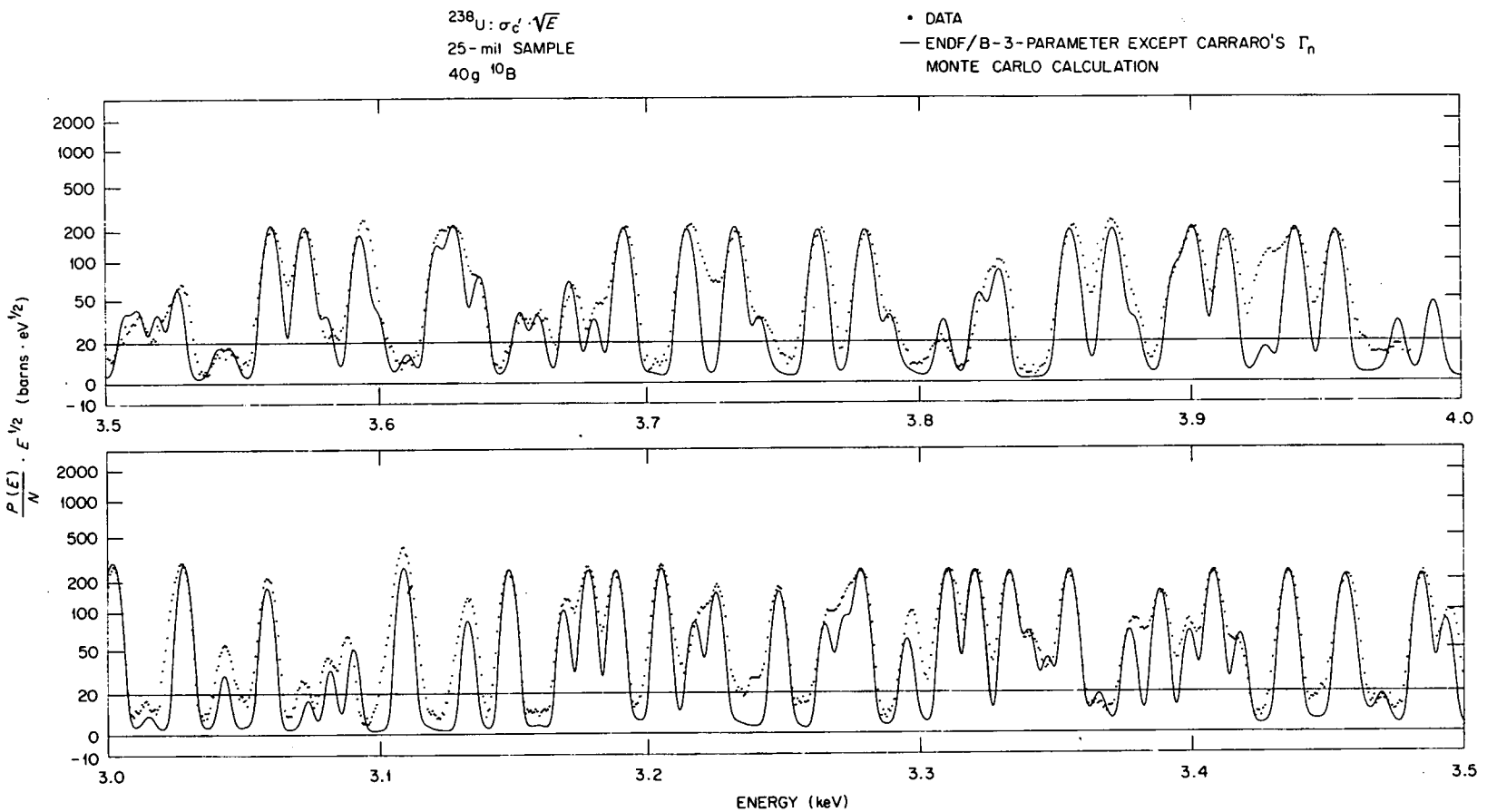

Fig. 2.11. Comparison of the measured and computed capture probabilities for a ^{238}U sample of 0.0028 atom/b and for incident neutron energies from 3 to 4 keV. The ordinate is the probability of capture multiplied by the square root of the energy and divided by the sample thickness (in atoms per barn). The calculation was done with the Monte Carlo code MULTSCA using the resonance parameters of ENDF/B-III. Note that the ordinate is linear from −10 to +20 b·eV$^{1/2}$ and logarithmic above 20 b·eV$^{1/2}$.

earlier data and the large fluctuations of the cross section, the various sets of data are consistent with ours. A comparison of our more recent time-of-flight data on a scale that shows these fluctuations could probably help in identifying sources of discrepancies such as errors in energy scale or in backgrounds.

Figure 2.9 is a comparison between our results and a calculation based on ENDF/B-III. The discrepancies are mostly in the area and peak values of particular levels, such as those near 1100 eV and some small levels at lower energies. In the range 0.9 to 1 keV, our value of the average capture is 27 $b \cdot eV^{1/2}$ higher than that of Moxon. The figure seems to rule out that the discrepancy could be due to an underestimate of the background.

Figures 2.10 and 2.11 show comparisons between our data and calculations based on the neutron widths published by Carraro.[7] Again our data indicate more capture than predicted by the resonance parameters, and the discrepancy is not systematic but concentrated on a few levels.

In conclusion, we are still puzzled by the discrepancies between the different measurements. We are attempting to better identify the source of these discrepancies by new measurements using different techniques and followed by detailed comparisons of the data from the different measurements. We shall also shortly do some transmission experiments and analyze our low-energy data for resonance parameters.

We are indebted to R. Ingle, N. Hill and H. Weaver for much of the experimental work described above.

1. Paper presented at Specialists Meeting on Resonance Parameters of Fertile Nuclei [ ] and ^{239}Pu, Saclay, France, May 20–22, 1974.
2. Research sponsored by AEC-LMFBR program.
3. G. de Saussure, E. G. Silver, R. B. Perez, R. Ingle, and H. Weaver, *Measurement of the ^{238}U Capture Cross Section for Incident Energies Up to 100 keV*, ORNL-TM-4059 (February 1973); see also *Nucl. Sci. Eng.* 51, 385 (1973).
4. M. C. Moxon, *The Neutron Capture Cross Sections of ^{238}U in the Energy Region 0.5 to 100 keV*, AERE-R-6074 (1969).
5. S. J. Friesenhahn et al., *Neutron Capture Cross Sections on Molybdenum, Tantalum, and ^{238}U*, GA-10194 (1970).
6. W. G. Davey, *Nucl. Sci. Eng.* 39, 337 (1970).
7. G. Carraro and W. Kolar, "Total Neutron Cross Section Measurements of ^{238}U," *Proceedings of Third Conference on Neutron Cross Sections and Technology, March 1971, Knoxville, Tennessee*, vol. II, USAEC report CONF-710301 (August 1971), p. 701.

3. MULTILEVEL EFFECTS IN THE UNRESOLVED RESONANCES REGION OF THE CROSS SECTIONS OF FISSILE NUCLIDES[1,2]

G. de Saussure R. B. Perez

For the specification of the cross sections of the fissile isotopes in the neutron energy region of unresolved resonances, the single-level formalism is often used, while an analysis of the cross sections in the resolved region indicates that a multilevel formula may be more appropriate. In this paper, we compare the statistical properties of the cross sections generated using the single-level formalism with those obtained by a multilevel formulation. The multilevel parameters were chosen to give the same average cross sections as the single-level formalism. The comparison indicates that there are small, but significant, differences between the statistical properties of the cross sections obtained with the multilevel formalism and those obtained with the single-level formula. The differences are probably too small, particularly when Doppler broadening is considered, to affect reactor calculations.

1. Abstract of published paper: *Nucl. Sci. Eng.* 52, 382 (1973).
2. Research sponsored by AEC-LMFBR program.

4. NATURAL CHROMIUM AND ^{52}Cr NEUTRON ELASTIC AND INELASTIC SCATTERING CROSS SECTIONS FROM 4.07 TO 8.56 MeV[1,2]

W. E. Kinney F. G. Perey

Measured neutron elastic and inelastic scattering cross sections for natural chromium between 4.07 and 8.56 MeV and for ^{52}Cr between 6.44 and 8.56 MeV are presented and compared with the elastic differential cross sections of Holmqvist and Wiedling and with ENDF/B MAT 1121. Our elastic scattering differential cross sections are in fair agreement with those of Holmqvist and Wiedling. Our angle-integrated differential elastic scattering cross sections are systematically higher by as much as 17% than those of Holmqvist and Wiedling above 4.6 MeV, a situation similar to that found in comparing the two sets of data for other elements. The ENDF/B III MAT 1121 elastic angular distributions are found to be in poor agreement with experimental results from 4 to 8.5 MeV, though the ENDF/B III MAT 1121 angle-integrated differential elastic scattering cross sections agree within experimental uncertainties with our results over this energy range. An evaporation model of inelastic scattering is found to be of questionable validity if applied to levels in the residual nucleus of excitation energy less than 6 MeV.

1. Abstract of ORNL-4806 (ENDF-198) (January 1974).
2. Research sponsored by AEC-LMFBR program.

5. NATURAL TITANIUM NEUTRON ELASTIC AND INELASTIC SCATTERING CROSS SECTIONS FROM 4.07 TO 8.56 MeV[1,2]

W. E. Kinney F. G. Perey

Measured cross sections per atom of natural titanium for neutron elastic scattering and for inelastic scattering to levels in ^{48}Ti for incident neutron energies between 4.07 and 8.56 MeV are given and compared with previous results. ENDF/B III MAT 1144 angular distributions are in reasonably good agreement with experimental results at angles less than 40° but differ by as much as an order of magnitude at larger angles. The ENDF/B III MAT 1144 angle-integrated elastic scattering cross sections agree within experimental uncertainties with experimental results at energies below 6.44 MeV but rise 20% above measured values at 8.56 MeV. ENDF/B III MAT 1144 inelastic scattering cross sections to discrete levels in ^{48}Ti are in poor agreement with experimental data because of the predominance of continuum inelastic scattering in ENDF/B III MAT 1144. An evaporation model of inelastic scattering to the continuum is found to be valid for inelastic scattering to levels of excitation energy greater than 6 MeV but is questionable for inelastic scattering to levels of lower excitation energy.

1. Abstract of ORNL-4810 (October 1973).
2. Research sponsored by AEC-LMFBR program.

6. NEUTRON-INDUCED GAMMA-RAY PRODUCTION IN TITANIUM FOR INCIDENT-NEUTRON ENERGIES OF 4.9, 5.4, AND 5.9 MeV[1,2]

J. K. Dickens

Interactions of neutrons with titanium have been studied by measuring gamma-ray production cross sections. For a sample of natural titanium, spectra were obtained for incident mean neutron energies E_n = 4.9, 5.4, and 5.9 MeV with gamma-ray detector systems utilizing coaxial Ge(Li) detectors. Nearly monoenergetic neutrons were obtained from the $D(d,n)$ reaction using deuterons obtained from the

(pulsed) Oak Ridge National Laboratory 5-MV Van de Graaff accelerator. Time of flight was used with the detector to discriminate against pulses due to neutrons and background radiation. Gamma-ray identification was aided by obtaining several spectra for samples enriched in the isotopes ^{46}Ti and ^{48}Ti, and new information on the level structures of these two isotopes was obtained. Absolute differential cross sections for production of gamma rays were obtained and are reported. These cross sections have been compared, where possible, with previous (n,n') measurements and with cross sections derived from the current ENDF/B evaluation.

1. Abstract of published paper: *Nucl. Sci. Eng.* **54**, 191 (1974).
2. Research sponsored by Defense Nuclear Agency.

7. ^{54}Fe NEUTRON ELASTIC AND INELASTIC SCATTERING CROSS SECTIONS FROM 5.50 TO 8.50 MeV[1,2]

W. E. Kinney F. G. Perey

Measured ^{54}Fe neutron elastic scattering cross sections and cross sections for inelastic scattering to seven discrete levels or groups of levels in ^{54}Fe in the incident neutron energy range from 5.50 to 8.50 MeV are presented. The elastic data are in good agreement with our previously reported natural iron results. Inelastic scattering to the 1.409-MeV level shows evidence of direct reaction contributions at the higher incident neutron energies. ENDF/B III MAT 1180 natural iron cross sections for inelastic scattering to the 1.409-MeV level in ^{54}Fe are higher by a factor of 2 than our data. Cross sections for inelastic scattering to levels in the residual nucleus of excitation energy greater than 4.29 MeV are presented as continuum cross sections. It is found that an evaporation model of continuum inelastic scattering is adequate above 6.2 MeV excitation energy but is questionable in describing inelastic scattering to lower-lying levels.

1. Abstract of ORNL-4907 (ENDF-203) (February 1974).
2. Research sponsored by AEC-LMFBR program.

8. ^{63}Cu AND ^{65}Cu NEUTRON ELASTIC AND INELASTIC SCATTERING CROSS SECTIONS FROM 4.07 TO 8.50 MeV[1,2]

W. E. Kinney F. G. Perey

Measured neutron elastic and inelastic scattering cross sections for ^{63}Cu and ^{65}Cu between 5.50 and 8.50 MeV are presented and compared with elastic data of Holmqvist and Wiedling and with ENDF/B III MAT 1085 and 1086. Our elastic differential cross sections are in fair agreement with those of Holmqvist and Wiedling in shape. Our angle-integrated differential elastic cross sections are systematically higher by as much as 28% than those of Holmqvist and Wiedling above 5 MeV, a situation similar to that found in comparing the two sets of data for other elements. ENDF/B III MAT 1085 and 1086 angular distributions underestimate the elastic forward peak below 20° when compared with experimental results and display unphysical fluctuations due to the use of a Legendre series of order 20 where order 9 is the highest required by the data. An evaporation model with temperature ranging from 0.8 to 1.05 MeV reasonably describes inelastic scattering to levels in the residual copper nuclei of excitation energy above 3.2 MeV.

1. Abstract of ORNL-4908 (ENDF-204) (February 1974).
2. Research sponsored by AEC-LMFBR program.

9. ^{206}Pb, ^{207}Pb, AND ^{208}Pb NEUTRON ELASTIC AND INELASTIC SCATTERING CROSS SECTIONS FROM 5.50 TO 8.50 MeV[1,2]

W. E. Kinney F. G. Perey

Measured neutron ^{208}Pb differential elastic scattering cross sections at 5.50, 7.00, and 8.50 MeV are given and compared with previous results. Measured ^{206}Pb, ^{207}Pb, and ^{208}Pb neutron inelastic scattering cross sections are given at roughly 0.5-MeV intervals from 5.50 to 8.50 MeV and also compared with previous results. ENDF/B III MAT 1136 elastic angular distributions, angle-integrated elastic and inelastic scattering cross sections, and nuclear temperatures are in generally good agreement with experiment over this energy range.

1. Abstract of ORNL-4909 (ENDF-206) (June 1974).
2. Research sponsored by AEC-LMFBR program.

10. NEUTRON-CAPTURE CROSS SECTIONS OF THE STABLE LEAD ISOTOPES[1,2]

B. J. Allen[3] R. L. Macklin[4] R. R. Winters[5] C. Y. Fu

Neutron-capture yields for several samples of separated lead isotopes were obtained at the Oak Ridge Electron Linear Accelerator in the neutron energy range above 2.5 keV. These were analyzed for resonance-capture areas and parameters. The data are included in a new evaluation of lead cross-section data.

1. Abstract of published paper: *Phys. Rev.* C8(4), 1504 (1973).
2. Research partially sponsored by Defense Nuclear Agency.
3. Present address: Australian Atomic Energy Commission, Lucas Heights, Australia.
4. Physics Division.
5. Present address: Denison University, Granville, Ohio.

11. NITROGEN NEUTRON ELASTIC AND INELASTIC SCATTERING CROSS SECTIONS FROM 4.34 TO 8.56 MeV[1,2]

F. G. Perey W. E. Kinney

Measured nitrogen neutron elastic and inelastic cross sections at incident neutron energies from 4.34 to 8.56 MeV are presented and compared with previous results. Our elastic data are systematically lower than the data of Bostrum et al. and systematically higher than the data of Bauer et al. but generally agree with the data of Chase et al. and Phillips. Our angle-integrated differential inelastic scattering cross sections are in reasonable agreement with previous results. Agreement of our data and ENDF/B III MAT 1133 is reasonable.

1. Abstract of ORNL-4805 (ENDF-205) (February 1974).
2. Research sponsored by AEC-LMFBR program.

12. NATURAL NICKEL AND ^{60}Ni NEUTRON ELASTIC AND INELASTIC SCATTERING CROSS SECTIONS FROM 4.07 TO 8.56 MeV[1,2]

W. E. Kinney F. G. Perey

Measured neutron elastic and inelastic scattering cross sections for natural nickel between 4.07 and 8.56 MeV are presented and compared with the elastic differential cross sections of Holmqvist and Wiedling and

with ENDF/B III MAT 1123. Our elastic differential cross sections are in general agreement with those of Holmqvist and Wiedling but our angle-integrated differential elastic cross sections are systematically higher by about 10% than those of Holmqvist and Wiedling above 4.6 MeV, a situation found in comparing the two sets of data for other elements. The ENDF/B III MAT 1123 elastic angular distributions are found to be in poor agreement with experimental results from 4 to 8.5 MeV, though the ENDF/B III MAT 1123 angle-integrated differential elastic cross sections agree generally within experimental uncertainties with our results over this energy range. Additional measurements of ^{60}Ni neutron elastic and inelastic scattering cross sections at 4.34 and 4.92 MeV are given and compared with our previous results from 6 to 8.5 MeV and with our natural-nickel results. Agreement is shown to be excellent. Inelastic scattering cross sections to the 1.450-MeV level in ^{58}Ni are computed from the natural nickel and ^{60}Ni data. An evaporation model of inelastic scattering to levels of excitation energy in the residual nucleus below 6 MeV is found to be of questionable validity.

1. Abstract of ORNL-4807 (ENDF-198) (January 1974).
2. Research sponsored by AEC-LMFBR program.

13. GAMMA-RAY PRODUCTION FROM NEUTRON INTERACTIONS WITH NICKEL FOR INCIDENT NEUTRON ENERGIES BETWEEN 1.0 AND 10 MeV: TABULATED DIFFERENTIAL CROSS SECTIONS[1,2]

J. K. Dickens T. A. Love G. L. Morgan

Numerical values of differential cross sections for gamma rays produced by neutron reactions with nickel have been obtained for neutron energies between 1.0 and 20 MeV. These data were obtained using two different experimental systems: (*a*) $d^2\sigma/d\omega dE$ values were obtained for $\theta_\gamma = 125°$ using an NaI spectrometer. These data are presented as gamma-ray production group cross-section values of $d^2\sigma/d\omega dE$ for $0.7 \leqslant E_\gamma \leqslant 10.5$ MeV, with gamma-ray intervals ranging from 20 keV for $E_\gamma \leqslant 1$ MeV to 160 keV for $E_\gamma \sim 9$ MeV. Neutron energy intervals varied from 0.5 MeV for $E_n = 1$ to 8 MeV to 3 MeV for $E_n = 14$ to 20 MeV. (*b*) Discrete line values of $d\sigma/d\omega$ for transitions due to neutron interactions with nickel were obtained at $\theta_\gamma = 55$ or 125° for $E_n = 4.85$, 5.4, and 5.9 MeV, using Ge(Li) spectrometers.

1. Abstract of ORNL-TM-4379 (November 1973).
2. Research sponsored by AEC-LMFBR program.

14. DIRECT-INTERACTION INTERPRETATION FOR ^{40}Ca($n,np\gamma$)^{39}K REACTIONS AT E_n = 17 TO 20 MeV[1,2]

J. K. Dickens

Gamma-ray production cross sections measured for the ^{40}Ca(n,np)^{39}K reactions are interpreted using a model based upon the 2-particle–2-hole configuration mixing in the ground-state wave function of ^{40}Ca and a direct knockout reaction mechanism.

1. Abstract of paper to be published in the *Physical Review.*
2. Research sponsored by Defense Nuclear Agency.

15. NEUTRON-INDUCED GAMMA-RAY PRODUCTION IN CALCIUM IN THE ENERGY RANGE $0.7 \leqslant E_n \leqslant 20$ MeV[1,2]

J. K. Dickens T. A. Love
G. L. Morgan

Gamma-ray spectra were obtained at $\theta_\gamma = 125°$ for reactions involving neutron interactions with a sample of natural calcium. Cross sections for the production of gamma rays have been deduced from these spectra as a function of both neutron and photon energy. The data were obtained using an NaI spectrometer system and the Oak Ridge Electron Linear Accelerator as the neutron source. The experimental results have been compared with predictions based on the gamma-ray files of the current Defense Nuclear Agency evaluation for calcium (Mat 4152 Mod 3) and with previous experimental data. Although there is generally good (15%) agreement, important differences are discussed.

1. Abstract of published paper: *Nucl. Sci. Eng.* **53**, 277 (1974); see also *Bull. Amer. Phys. Soc.* **18** (10), 1402 (1973).
2. Research sponsored by Defense Nuclear Agency.

16. GAMMA-RAY PRODUCTION DUE TO NEUTRON INTERACTIONS WITH ZINC FOR INCIDENT NEUTRON ENERGIES BETWEEN 0.85 AND 20 MeV: TABULATED DIFFERENTIAL CROSS SECTIONS[1,2]

J. K. Dickens T. A. Love
G. L. Morgan

Numerical values of differential cross sections for gamma rays produced by neutron reactions with tin have been obtained for neutron energies between 0.85 and 20 MeV for $\theta_\gamma = 125°$. The $d^2\sigma/d\omega dE$ values were obtained using an NaI spectrometer. These data are presented as gamma-ray production group cross-section values of $d^2\sigma/d\omega dE$ for $0.7 \leqslant E_\gamma \leqslant 10.5$ MeV, with gamma-ray intervals ranging from 20 keV for $E_\gamma \leqslant 1$ MeV to 160 keV for $E_\gamma \sim 9$ MeV. Neutron energy intervals varied from 0.15 MeV for $E_n = 0.85$ to 1 MeV to 3 MeV for $E_n = 14$ to 20 MeV.

1. Abstract of ORNL-TM-4464 (February 1974).
2. Research sponsored by Defense Nuclear Agency.

17. GAMMA-RAY PRODUCTION DUE TO NEUTRON INTERACTIONS WITH ZINC. TABULATED DIFFERENTIAL CROSS SECTIONS FOR 31 GAMMA RAYS FOR INCIDENT NEUTRON ENERGIES BETWEEN 0.9 AND 6 MeV[1,2]

G. G. Slaughter[3] J. K. Dickens

Numerical values of differential cross sections for gamma rays produced by neutron interactions with zinc have been measured for neutron energies between 0.9 and 6 MeV for $\theta_\gamma = 120°$. The $d\sigma/d\omega$ data were obtained using a 35-cm^3 Ge(Li) detector. The data consist of cross-section values for 31 gamma rays having E_γ between 300 and 2780 keV. Neutron energy intervals varied between a minimum of ~50 keV at $E_n \sim$ 900 keV and a maximum of ~1.5 MeV for $E_n \sim 5.8$ MeV.

1. Abstract of ORNL-TM-4523 (April 1974).
2. Data reduction partially sponsored by Defense Nuclear Agency.
3. Physics Division.

18. GAMMA-RAY PRODUCTION DUE TO NEUTRON INTERACTIONS WITH ^{68}Zn AND THE LEVEL STRUCTURE OF ^{68}Zn[1,2]

J. K. Dickens

Numerical values of differential cross sections for gamma rays produced by neutron interactions with ^{68}Zn have been measured for an incident energy of 5.4 MeV and gamma-ray scattering angle of 55°. The $d\sigma/d\omega$ data were obtained using a 60-cm^3 Ge(Li) detector. The data consist of cross-section values for 164 gamma rays or gamma-ray groups having gamma-ray energies between 413 and 4998 keV. These data were analyzed to obtain information on the level structure of ^{68}Zn, and 131 transitions were assigned among 78 known or postulated new levels in ^{68}Zn.

1. Abstract of ORNL-4985 (August 1974).
2. Research supported by Defense Nuclear Agency.

19. ^{28}Si$(n,n'\gamma)$ PHOTON PRODUCTION CROSS SECTIONS FOR E_γ = 1.78 MeV, 5.0 $\leqslant E_n \leqslant$ 9.5 MeV[1,2]

J. K. Dickens G. L. Morgan

The excitation function for the production of the 1.78-MeV gamma ray due to neutron interactions with ^{28}Si has been measured for incident neutron energies between 5 and 9.5 MeV with neutron energy resolution ~35 keV for E_n = 5 MeV to ~80 keV for E_n = 9.5 MeV. These data are compared with previously reported values and with the current ENDF/B evaluation.

1. Abstract of paper published in *Phys. Rev.* C10, 958 (1974).
2. Research sponsored by Defense Nuclear Agency.

20. GAMMA-RAY PRODUCTION FROM NEUTRON INTERACTIONS WITH SILICON FOR INCIDENT NEUTRON ENERGIES BETWEEN 1.0 AND 20 MeV: TABULATED DIFFERENTIAL CROSS SECTIONS[1,2]

J. K. Dickens T. A. Love
G. L. Morgan

Numerical values of differential cross sections for gamma rays produced by neutron reactions with silicon have been obtained for neutron energies between 1.0 and 20 MeV. The cross-section values were obtained using an NaI spectrometer. These data consist of (*a*) the production of gamma rays by neutron reactions with values of $d^2\sigma/d\omega dE$ for θ_γ = 125 and 90° and for 0.7 $\leqslant E_\gamma \leqslant$ 10.5 MeV, with gamma-ray intervals ranging from 20 keV for $E_\gamma \leqslant$ 1 MeV to 160 keV for $E_\gamma \approx$ 9 MeV and with neutron energy intervals varying from 0.25 MeV for E_n = 1.0 to 2.0 MeV to 3 MeV for E_n = 14 to 20 MeV; and (*b*) values of $d\sigma/d\omega$ for E_n = 1.78 MeV for θ_γ = 125° and for E_n between threshold and 9.6 MeV.

1. Abstract of ORNL-TM-4389 (December 1973).
2. Research sponsored by Defense Nuclear Agency.

21. GAMMA-RAY PRODUCTION DUE TO NEUTRON INTERACTIONS WITH TIN FOR INCIDENT NEUTRON ENERGIES BETWEEN 0.75 AND 20 MeV: TABULATED DIFFERENTIAL CROSS SECTIONS[1,2]

J. K. Dickens T. A. Love
G. L. Morgan

Numerical values of differential cross sections for gamma rays produced by neutron reactions with tin have been obtained for neutron energies between 0.75 and 20 MeV for $\theta_\gamma = 125°$. The $d^2\sigma/d\omega dE$ values were obtained using an NaI spectrometer. These data consist of neutron and gamma-ray production group cross-section values of $d^2\sigma/d\omega dE$ for $0.7 \leqslant E_\gamma \leqslant 10.5$ MeV, with gamma-ray intervals ranging from 20 keV for $E_\gamma \leqslant 1$ MeV to 160 keV for $E_\gamma \sim 9$ MeV. Neutron energy intervals varied from 0.25 MeV for $E_n = 0.75$ to 2 MeV to 3 MeV for $E_n = 14$ to 20 MeV.

1. Abstract of ORNL-TM-4406 (November 1973).
2. Research sponsored by Defense Nuclear Agency.

22. GAMMA-RAY PRODUCTION DUE TO NEUTRON INTERACTIONS WITH MAGNESIUM FOR INCIDENT NEUTRON ENERGIES BETWEEN 0.8 AND 20 MeV: TABULATED DIFFERENTIAL CROSS SECTIONS[1,2]

J. K. Dickens T. A. Love
G. L. Morgan

Numerical values of differential cross sections for gamma rays produced by neutron reactions with magnesium have been obtained for neutron energies between 0.76 and 20 MeV. The cross-section values were obtained using an NaI spectrometer. These data consist of (*a*) the production of gamma rays by neutron reactions with values of $d^2\sigma/d\omega dE$ for $\theta_\gamma = 125$ and 90° and for $0.7 \leqslant E_\gamma \leqslant 10.5$ MeV, with gamma-ray intervals ranging from 20 keV for $E_\gamma \leqslant 1$ MeV to 160 keV for $E_\gamma \approx 9$ MeV and with neutron energy intervals varying from ~0.25 MeV for $E_n = 0.76$ to 1.5 MeV to 3 MeV for $E_n = 14$ to 20 MeV; and (*b*) values of $d\sigma/d\omega$ for $E_\gamma = 1.37$ MeV for $\theta_\gamma = 125°$ and for E_n between threshold and 6.0 MeV and for $E_\gamma = 1.81$ MeV for $\theta_\gamma = 125°$ and for E_n between threshold and 3.2 MeV.

1. Abstract of ORNL-TM-4544 (May 1974).
2. Research sponsored by Defense Nuclear Agency.

23. GAMMA-RAY PRODUCTION DUE TO NEUTRON INTERACTIONS WITH FLUORINE AND LITHIUM FOR INCIDENT NEUTRON ENERGIES BETWEEN 0.55 AND 20 MeV: TABULATED DIFFERENTIAL CROSS SECTIONS[1,2]

J. K. Dickens T. A. Love
G. L. Morgan

Numerical values of differential cross sections for gamma rays produced by neutron reactions with lithium fluoride have been obtained for neutron energies between 0.55 and 20 MeV for $\theta_\gamma = 125°$. The cross-section values were obtained using an NaI photon spectrometer and the Oak Ridge Electron Linear Accelerator as the neutron source. The data for neutron interactions with fluorine are presented as gamma-ray production group cross-section values of $d^2\sigma/d\omega dE$ for $0.7 \leqslant E_\gamma \leqslant 10.5$ MeV, with gamma-ray

intervals ranging from 20 keV for $E_\gamma \leqslant 1$ MeV to 160 keV for $E_\gamma \sim 9$ MeV; for these data, neutron energy intervals varied from 0.25 MeV for $1.25 \leqslant E_\gamma \leqslant 2$ MeV to 3 MeV for $14 \leqslant E_n \leqslant 20$ MeV. The data for neutron interactions with lithium are presented as gamma-ray production cross-section values of $d\sigma/d\omega$ for the 0.478-MeV gamma ray; for the data, the neutron energy intervals varied between 10 keV at threshold and 1 MeV for $E_n \geqslant 14$ MeV.

1. Abstract of ORNL-TM-4538 (April 1974).
2. Research sponsored by Defense Nuclear Agency.

24. FISSION-PRODUCT AFTERHEAT – A REVIEW OF EXPERIMENTS PERTINENT TO THE THERMAL-NEUTRON FISSION OF ^{235}U[1,2]

A. M. Perry[3] F. C. Maienschein
D. R. Vondy

We have reviewed experimental data relating to beta and gamma energy release rates following thermal-neutron fission of ^{235}U. We have proposed an afterheat function based on these experiments, for after-shutdown times from 1 sec to 5×10^5 sec, compared this function with the proposed ANS Standard ANS-5.1, and estimated the uncertainty in our proposed function. Our proposed function varies between 0.98 and 1.08 times the proposed standard function; we estimate the standard deviation to be between 10% and 15%.

1. Abstract of ORNL-TM-4197 (October 1973).
2. Research sponsored by AEC Division of Reactor Research and Development.
3. Reactor Division.

25. DIFFERENTIAL CROSS SECTIONS FOR THE PRODUCTION OF NEUTRONS FROM THE BOMBARDMENT OF ^{12}C, ^{27}Al, ^{54}Fe, AND ^{208}Pb BY 40-MeV PROTONS[1,2]

J. W. Wachter T. A. Love
R. T. Santoro W. Zobel

Differential cross sections in energy and angle have been obtained using time-of-flight spectroscopy for secondary neutrons produced in the reactions of 39.3- and 40.8-MeV protons with ^{12}C, ^{27}Al, ^{54}Fe, and ^{208}Pb. Neutron energy spectra are given for laboratory angles of 90°, 20°, 45°, 60°, 90°, and 135° for energies $\geqslant$6 MeV. The NE-213 efficiency was calculated using the 05S Monte Carlo code.[3] Comparisons with the predictions of the intranuclear-cascade model of Bertini[4] show good agreement at medium angles. As with the earlier 63-MeV measurements,[5] the data do not show the predicted quasi-free scattering peak at small angles. The calculated cross sections at 135° are low by factors of 3 to 6.

1. Abstract of paper presented at American Physical Society Meeting, Berkeley, Calif., December 27–29, 1973.
2. Research sponsored by NASA.
3. R. E. Textor and V. V. Verbinski, ORNL-4160 (1968).
4. H. W. Bertini, *Phys. Rev.* **131**, 1801 (1963), with erratum *Phys. Rev.* **138**, AB 2 (1965).
5. J. W. Wachter, *Bull. Amer. Phys. Soc.* **18**, 118 (1973).

26. INELASTIC PROTON SCATTERING FROM ^{138}Ba AND ^{144}Sm AT 30 MeV[1,2]

D. Larson S. M. Austin[3]
B. H. Wildenthal[3]

Differential cross sections for elastic and inelastic scattering of 30-MeV protons by ^{138}Ba and ^{144}Sm have been measured with a total energy resolution for the inelastic peaks of 7 to 10 keV, full width at half maximum. This permitted the observation of 20 excited states in ^{138}Ba and 18 excited states in ^{144}Sm below E_x = 3.4 MeV, and the determination of excitation energies accurate to 2 keV or less for these states. Based on characteristic shapes derived from angular distributions to states of known J^π, spin-parity assignments were made for the majority of the observed states. Collective-model distorted-wave Born-approximation calculations for the observed transitions were compared to the data, and deformation parameters were extracted for all states to which J^π could be assigned. The energy-level structures of these nuclei, obtained by combining the present results with information in the literature, are compared to the predictions of structure calculations based on the assumption of a closed $N = 82$, $Z = 50$ core.

1. Abstract of *Phys. Rev.* C9(4), 1574 (1974).
2. Research performed at Michigan State University and sponsored by National Science Foundation.
3. Michigan State University.

27. COMPILATION OF PHENOMENOLOGICAL OPTICAL-MODEL PARAMETERS 1969–1972[1,2]

C. M. Perey F. G. Perey

A compilation is presented, with bibliography, of optical-model parameters determined by fitting elastic-scattering angular distributions for various incident particles including heavy ions. Only parameters published in the period 1969–1972 are included.

1. Abstract of *Atomic Data and Nuclear Data Tables* **13**, 293–337 (1974).
2. Work supported by AEC Division of Reactor Research and Development.

28. CALCULATED SECONDARY-PARTICLE SPECTRA FROM ALPHA-PARTICLE- AND CARBON-INDUCED NUCLEAR REACTIONS[1,2]

T. A. Gabriel H. W. Bertini
R. T. Santoro N. M. Larson[3]

A newly developed calculational model for nucleus-nucleus collisions has been applied to obtain secondary-neutron spectra from 100-MeV/nucleon alpha particles incident on ^{12}C and from 100-MeV/nucleon ^{12}C incident on ^{12}C. These data can be used in estimating shielding requirements for medium-energy heavy-ion machines. Also included is a comparison between a previous model used only for calculating secondary-particle spectra from alpha-particle nuclear reactions and the new, more general nucleus-nucleus collision model.

1. Abstract of ORNL-TM-4334 (October 1973) and of paper published in *Nucl. Sci. Eng.* **53**, 323 (1974).
2. Work jointly funded by the National Aeronautics and Space Administration under Order H-38280A and the AEC Division of Physical Research.
3. Computer Sciences Division, UCC Nuclear Division.

29. PREDICTED PROTON SPECTRUM AT FORWARD ANGLES FOR 29.4-GeV NITROGEN ON CARBON[1,2]

H. W. Bertini T. A. Gabriel
R. T. Santoro

The proton spectrum over the angular interval of 0 to 10 milliradians from the interactions of 29.4-GeV nitrogen on carbon has been calculated. The differential cross section for the emission of protons indicates that there is a significant number of emitted protons with energies greater than the energy per nucleon of the incident projectile (2.1 GeV). A description of the calculational method is included.

1. Abstract of *Phys. Rev.* C9(2), 522 (1974); see also *Predicted Proton Spectrum at Forward Angles for 29.4-GeV N on C Collisions,* ORNL-TM-4311 (September 1973).
2. Work jointly funded by the National Aeronautics and Space Administration, Order H-38280A, and by the National Science Foundation, Order NSF/RANN AG-399.

30. COMPARISONS OF PREDICTIONS FROM TWO INTRANUCLEAR-CASCADE MODELS WITH MEASURED SECONDARY PROTON SPECTRA AT SEVERAL ANGLES FROM 62- AND 39-MeV PROTONS ON VARIOUS ELEMENTS[1,2]

H. W. Bertini G. D. Harp[3]
F. E. Bertrand[4]

Detailed comparisons of correlated energy-angle proton spectra corresponding to continuum-state transitions have been made between experimental data and two versions [Brookhaven National Laboratory (BNL) and Oak Ridge National Laboratory (ORNL)] of the intranuclear-cascade model for 62- and 39-MeV protons incident on carbon, iron, and bismuth. These energies were selected because detailed experimental data are available and because the energy limit of validity of the intranuclear-cascade approach could be examined. The calculated spectra are in good agreement ($\leqslant$30%) with the shapes and magnitudes of the measured integral spectra for the 62-MeV reactions. However, the comparisons of the spectra at angles $\leqslant 20°$ and $>90°$ poor. There is a much greater discrepancy in the correlated energy-angle data from reactions at 39 MeV. The BNL version, which contains the greater physical detail, tends to reduce the discrepancies in the spectral shape at small and large angles between the experimental data and the simpler intranuclear-cascade version (ORNL). Examples of these discrepancies are a high estimated quasi-free peak at small angles and a small scattering intensity at back angles. However, the BNL version reduces the particle yield for heavy targets so that the comparisons of the predicted absolute cross sections with the experimental data are often poor. The effects of reflection and refraction, which are included in the BNL version only, appear to be in the right direction to compensate for the discrepancies of the ORNL version, but some modification in the manner that this phenomenon is incorporated may be required to avoid the discrepancies in absolute cross sections.

1. Abstract of ORNL-TM-4638 (in press); submitted for journal publication.
2. Work was partially funded by the National Aeronautics and Space Administration, Order H-38280A, under Union Carbide Corporation's contract with the U.S. Atomic Energy Commission, and by Brookhaven National Laboratory under Associated Universities' contract with the U.S. Atomic Energy Commission.
3. Chemistry Department, Brookhaven National Laboratory.
4. Physics Division.

31. HIC-1: A FIRST APPROACH TO THE CALCULATION OF HEAVY-ION REACTIONS AT ENERGIES ≥50 MeV/NUCLEON[1,2]

H. W. Bertini O. W. Hermann[3]
T. A. Gabriel N. M. Larson[3]
R. T. Santoro J. M. Hunt[4]

A preliminary version of a heavy-ion-interaction model is described in detail. The basic assumption of the model is that heavy-ion reactions can be described by the interactions of the individual nucleons of the projectile and target with one another. Transitions to the eigenstates of the target and projectile are ignored. Encouraging results are obtained when comparisons with experimental data are made on an absolute basis, even though there are differences of factors of 3 or more in these comparisons for some of the data. Several ways of improving the model and extending its applicability to lower energies are also presented.

1. Abstract of ORNL-TM-4134 (January 1974).
2. Work jointly funded by the National Aeronautics and Space Administration, Order H-38280A, and by the National Science Foundation, Order NSF/RANN AG-399.
3. Computer Sciences Division, UCC Nuclear Division.
4. Oak Ridge Associated Universities Undergraduate Research Trainee. Present address: University of Wisconsin Medical School, Madison, Wis.

32. INTERMEDIATE STRUCTURE IN THE NEUTRON-INDUCED ^{235}U CROSS SECTIONS[1,2]

G. D. James[3] G. de Saussure
R. B. Perez

The ^{235}U fission cross section exhibits large fluctuations in the unresolved resonance region.[4-7] One asks whether this phenomenon can be explained in terms of the statistical nuclear model, or whether, on the contrary, these fluctuations represent departures from this model, in certain energy regions,[8] where enhancements of the reaction widths may occur.

Two statistical tests have been proposed[9,10] to determine whether these fluctuations are of a random nature: the Wald-Wolfowitz[11] and the Levene-Wolfowitz[11] tests. In the former, one counts the number of runs, R, of consecutive observed values which lie above or below a reference value (ideally the median); in the latter, one counts the number of consecutive observed pairs of values of increasing or decreasing magnitude (runs up or down), thus creating a set of runs, $R(l)$, of length, l. Both statistics provide the number of runs, $E(R)$, expected from random statistical data, as well as the standard deviation, $\sigma(R)$, and the probability, $P(R)$, for R to depart from its expected value by more than F standard deviations.

To utilize these tests with confidence, one has to prove that cross sections obtained from the statistical nuclear model do indeed satisfy both statistics. The ^{235}U fission cross section was simulated by Monte Carlo techniques for neutron energies between 10 and 40 keV and averaged over 100-eV energy intervals. The result of the statistical tests, Table 32.1, shows the adequacy of both statistics.

The capability of detecting the presence of intermediate structure was tested by mocking up fission width enhancement on the basis of the double-humped fission barrier model.[12] In this case the fission widths, $\Gamma_{\lambda' f}$, of fine structure resonances (Class I levels) are modulated by the presence of levels in the second fission potential barrier minimum[13] (Class II levels), according to the equation[14]

$$\Gamma_{\lambda' f} = \Gamma_{\lambda f} + \sum_{\mu} \frac{A^2_{\lambda\mu}\,\Gamma_{\mu}}{(E - E_{\mu})^2 + (1/4)\Gamma^2_{\mu}}\,, \tag{1}$$

Table 32.1. Results of statistical tests of ^{235}U fission cross section fluctuations

Function	Wald and Wolfowitz statistics					Levene and Wolfowitz statistics				
	R	$E(R)$	(R)	F	Probability	$R(l)^{(a)}$	$E(Rl)$	$\sigma(Rl)$	F	Probability
σ_f	94	150.2	8.60	6.48	$<10^{-7}$	85	123.4	11.2	3.38	3.6×10^{-4}
σ_c	122	150.7	8.62	3.27	$5.4 \times 10^{-}$	110	123.8	11.2	1.19	0.117
α	126	150.9	8.64	2.82	2.37×10^{-3}	111	123.8	11.2	1.10	0.136
σ_{abs}	109	150.8	8.63	4.79	85×10^{-7}	111	123.4	11.2	1.06	0.144
σ_f (simulated)	149	151.0	8.65	0.17	0.43	122	123.0	11.2	0.043	0.48
σ_f (simulated with modulation)	79	143.3	8.20	7.78	$<10^{-7}$	90	120.9	11.1	2.74	3.04×10^{-3}
σ_c (simulated with modulation)	67	150.0	8.59	9.61	$<10^{-7}$	92	123.8	11.2	2.79	2.62×10^{-3}

[a]Only the runs of length $l = 1$ are shown.

where $\Gamma_{\lambda f}$ belongs to the Class I levels, Γ_μ and E are the fission widths and level energies for the Class II levels, and $A_{\lambda\mu}$ is the coupling between the two potential wells. Data generated according to Eq. (1) show large departures from random statistical behavior in both statistical tests (Table 32.1).

Next, the ^{235}U fission and capture cross sections measured at ORELA[15] were averaged over 100-eV intervals between 10 and 40 keV and tested as shown in Table 32.1 The significant deviations from random statistical behavior confirm the presence of an intermediate structure in both the ^{235}U fission and capture cross sections. This finding has implications in regard to our understanding of the unresolved resonance region and treatment of cross sections in this region for reactor design.

1. Summary of paper presented at American Nuclear Society Meeting, San Francisco, November 11–15, 1973; published in *Trans. Amer. Nucl. Soc.* **17**, 495 (1974).
2. Research partially sponsored by AEC-LMFBR program.
3. Harwell, England.
4. B. H. Patrick et al., *J. Nucl. Energy* **24**, 269 (1970).
5. J. R. Lemley et al., *Nucl. Sci. Eng.* **43**, 281 (1971).
6. C. D. Bowman et al., *Proc. Second Conf. Nuclear Data for Reactors*, Helsinki, IAEA (1970).
7. G. de Saussure et al., *Trans. Amer. Nucl. Soc.* **14**, 370 (1971).
8. C. Mahaux, *Statistical Properties of Nuclei*, p. 545, J. B. Garg, ed., Plenum Press, New York, (1972).
9. G. D. James, *Nucl. Phys.* **A170**, 309 (1971).
10. Y. Baundinet-Robinet and C. Mahaux, *Phys. Lett.* **42B**, 392 (1972).
11. A. Wald and J. Wolfowitz, *Annal. Math. Stat.* **XI**, 2 (1940); also *Documenta Geigy, Scientific Tables*, K. Diem, ed., Geigy Pharmaceuticals, Ardsley, New York.
12. V. M. Strutinsky, *Nucl. Phys.* **A95**, 420 (1967).
13. J. E. Lynn, AERE-R-5891, Atomic Energy Research Establishment, Harwell, England (September 1968).
14. R. B. Perez et al., *Symposium on the Physics and Chemistry of Fission*, Paper SM/122/121, Vienna, July, 1969.
15. R. B. Perez et al., *Simultaneous Measurements of the Neutron Fission and Capture Cross Sections for ^{235}U for Neutron Energies from 8 eV to 10 keV*, ORNL-TM-3696 (1972).

33. ESTIMATED UNCERTAINTIES IN EVALUATED DATA[1,2]

F. G. Perey

During the last decade large efforts have gone into preparing microscopic neutron cross-section data files, called evaluated data files, to serve as basic input data for various neutron transport applications. A prime example of such evaluated microscopic cross sections is the ENDF/B set, a cooperative effort of the

Cross Section Evaluation Working Group (CSEWG). The ENDF/B cross-section reference set is updated periodically to provide increased coverage of nuclei, energy range, reaction types, etc., and generally to upgrade the data files to reflect our improved knowledge of the cross sections due to new measurements or theoretical calculations and also to remove deficiencies discovered in the analysis of integral experiments (Phase II data testing). The data files are intended to represent as accurately as possible our knowledge of the microscopic cross sections and, therefore, should be application independent. However, because this evaluation work has been funded almost exclusively out of various applied programs, invariably the content of the ENDF/B set has been influenced by the applications for which the different evaluations were needed. The most efficient use of limited financial resources devoted to this aspect of nuclear technologies, the different stages of development of these technologies with respect to nuclear data needs, and the varying importance of the nuclei of the set in different applications have caused the "intrinsic quality" of the data in the files to vary widely as a function of nuclei, reaction types, and energy ranges. The fact that an evaluated file exists for a nuclide in the official CSEWG reference set at a given time is not a proof of its adequacy for any specific application, but only represents the collective judgment of the CSEWG members that it was the best overall evaluation available in this format at that time, and it meets a minimum of procedural requirements (Phase I review).

At the moment, possibly only one evaluation, the one for hydrogen, is generally thought to exceed the accuracy requirements in the microscopic data for most present, or contemplated, applied uses. For most important neutron transport applications, it is generally conceded that many of the neutron cross sections will not be known for a long time to such a high degree of accuracy that uncertainties in the basic microscopic data can be ignored. Several studies have been made, for a few applications, of the cost and design penalties associated with nuclear data uncertainties, and these studies yielded what we could call "target accuracies" in the various microscopic data as acceptable for these applications. These studies have had to assume what were acceptable design parameter uncertainties and, on the basis of the then-known cross sections, make assumptions on what would be the "correlations of the uncertainties" in the final acceptable data set. At present, it is thought that for some applications a few of the very important partial cross sections may be known to within a factor of 2 of the target accuracies of these studies. There is, however, no consensus on the question of whether or not the present estimated uncertainties are sufficiently uncorrelated.

To answer most of the questions regarding the adequacy of nuclear data for different applications in a credible manner, we require a knowledge of the estimated uncertainties, and their correlations, in the evaluated data. This information at the present time is sometimes to be found in the documentation of the evaluations, is very incomplete, difficult to extract, and sufficiently ill-defined as to the nature of the correlations in the data so as to prevent very credible quantitative statements to be made regarding the adequacy of the data. With ENDF/B-IV, a start has been made toward implementation of the complete description of the estimated covariances of the microscopic data on the tape. We will present the concepts and major features of the ENDF/B-IV format for representing the covariance matrices of the pointwise microscopic cross sections as a function of energies, of different partial cross sections for a given nuclide, and of cross sections for different nuclei. We will show how the method of representation chosen allows the computation of covariance matrices of group cross sections as a straightforward additional step to most present group-cross-section processing codes. The problems of representing these covariances and their handling by processing codes for the resolved and unresolved resonance regions are under active investigation and will be alluded to.

---

1. Summary of paper presented at American Nuclear Society Meeting, Philadelphia, June 23–27, 1974; published in *Trans. Amer. Nucl. Soc.* 18, 337 (1974).
2. Research sponsored by AEC-LMFBR program.

34. THE FORMALISM FOR DATA COVARIANCE REPRESENTATION IN ENDF/B AND APPLICATION TO THE ^{238}U CAPTURE CROSS SECTION FOR SENSITIVITY STUDIES[1,2]

F. G. Perey G. de Saussure
R. B. Perez

In many radiation transport calculations a significant fraction of the uncertainties in the calculated results comes from the uncertainties in the basic cross-section data used as input. The implications of such uncertainties for the design of reactors and their significant economic impacts have been discussed by Greebler,[3] Barré and Chaudat,[4] Usachev et al.,[5] and others. Recent cross-section sensitivity studies[6] have underscored the importance of correlations in the errors of different cross sections or of a given cross section at different energies. These error correlations arise because the nuclear data are often derived from "shape measurements" normalized at a given energy or from the measurements of ratios or differences of cross sections. Furthermore, different cross sections are often measured with the same or similar experimental techniques so that errors in the determination of backgrounds or detector efficiencies, for instance, may introduce correlated errors in the microscopic data.

In the past, no attempt has been made to include estimated covariances of the evaluated microscopic cross sections in the ENDF/B files for the purpose of propagating these estimated uncertainties to the final results of the transport calculations. However, for ENDF/B-IV, the Cross-Section Evaluation Working Group[7] has decided that formats should be adopted to allow a precise representation of estimated covariances in some of the microscopic data.

An appropriate formalism to represent the covariance matrix of errors associated with evaluated nuclear data has been developed[8] and is outlined in this paper. The determination of the components of the covariance matrices usually requires an intimate knowledge of the experimental techniques used in the measurements of the data leading to the evaluated values. When all the errors associated with the measurements are well understood, the covariance matrix may be obtained by the standard methods of error propagation,[9] although this is not an easy task and requires familiarity with the experimental techniques, as has been pointed out by Peelle.[10] Often, data must be evaluated from measurements which are not consistent within the errors quoted by the experimenters. In such cases, some of the errors contributing to the evaluation are obviously not properly identified. Yet, an estimate of the components of the covariance matrix may still be obtained by an appropriate analysis of the discrepancies between the various measurements.

The basic concept used in the proposed formalism is the expansion of the covariances of the energy-dependent cross sections into elements which are fully correlated over a stated energy range. Let X_i and Y_j be two energy-dependent cross sections at E_i and E_j. The covariance $\mathrm{cov}(X_i, Y_j)$ is first expanded as a sum of components $\mathrm{cov}^n(X_i, Y_j)$:

$$\mathrm{cov}(X_i, Y_j) = \sum_n \mathrm{cov}^n(X_i, Y_j) .$$

Each component $\mathrm{cov}^n(X_i, Y_j)$ represents elements which are correlated over some energy range of $X(E)$ and $Y(E)$ as described below.

Let the energy range of $X(E)$ and $Y(E)$ be broken up into nonoverlapping consecutive energy intervals E_k^n and associate with each such energy interval an element $F^n_{XY,k}$, thereby creating an $(E_k^n, F^n_{XY,k})$ table of values.

Let S_i^k be an operator which is unity when the energy E_i is within the energy interval E_k^n of the table and zero otherwise.

Depending upon the value of a flag associated with each such $(E_k^n, F_{XY,k}^n)$ table, the following three types of covariance components are defined:

1. Absolute elements correlated only within each E_k^n interval,

$$\mathrm{cov}^n(X_i, Y_j) = \sum_k S_i^k S_j^k F_{XY,k}^n \cdot$$

2. Fractional elements correlated only within each E_k^n interval,

$$\mathrm{cov}^n(X_i, Y_j) = \sum_k S_i^k S_j^k F_{XY,k}^n X_i Y_j \cdot$$

3. Fractional elements correlated over all E_k^n intervals,

$$\mathrm{cov}^n(X_i, Y_j) = \sum_{k,k'} S_i^k S_j^{k'} F_{XY,k}^n F_{XY,k'}^n X_i Y_j \cdot$$

The complete formalism for ENDF/B-IV allows up to two such tables to be defined over the energy range of $X(E)$ and $Y(E)$ for each $\mathrm{cov}^n(X_i, Y_j)$ component, thereby allowing other correlation patterns to be defined as well.

The advantages of this formalism are threefold: (1) It gives the covariance information about the microscopic cross sections in the files in a compact form, (2) it follows very closely the method used by most experimentalists to analyze the estimated uncertainties in their data, and (3) group cross-section processing codes can easily be adapated to process the covariance files of the microscopic data to generate the covariance matrices of group cross sections for use in sensitivity studies.

As an important example of this technique, we have evaluated the principal components of the energy covariance matrix of the capture cross section of ^{238}U in the range 1 keV to 10 MeV. The discrepancies among the most recent and complete measurements[11] of the capture cross section of ^{238}U were investigated by averaging each set of data over the energy ranges over which significant correlations may be expected. A set of simultaneous equations was then obtained for the components of the covariance matrix. Finally, the numerical values of the components of the covariance matrix were computed and reported in the format described above. The results can be used in future reactor cross-section sensitivity studies.

---

1. Summary of paper presented at American Nuclear Society Meeting, Atlanta, September 8–11, 1974.
2. Research sponsored by AEC-LMFBR program.
3. P. Greebler, B. A. Hutchins, and C. L. Cowan, "Implications of Nuclear Data Uncertainties to Reactor Design," *Nuclear Data for Reactors*, vol. I, International Atomic Energy Agency, Vienna, 1970, pp. 17–33.
4. J. Y. Barré and J. P. Chaudat, "Roles Respectifs des Evaluations et des Expériences Intégrales pour la Physique des Réacteurs Rapides," *Applications of Nuclear Data in Science and Technology*, International Atomic Energy Agency, Vienna, paper IAEA/SM-170/69, 1973.
5. L. N. Usachev, V. N. Manokhin, and Y. G. Bokkov, "Nuclear Data Accuracies and Their Implications on the Design of Fast Reactors," *Applications of Nuclear Data in Science and Technology*, International Atomic Energy Agency, Vienna, paper IAEA/SM-170/91, 1973.
6. E. M. Oblow, *Reactor Cross-Section Sensitivity Studies Using Transport Theory*, ORNL-TM-4437 (1974).
7. Minutes of the Spring and Fall 1973 Meetings of the Cross-Section Evaluation Working Group; F. G. Perey, *Formats and Procedures for ENDF/B Data Covariance Files* (to be published).
8. F. G. Perey, *Formats and Procedures for ENDF/B Error Files*, proposed to Cross-Section Evaluation Working Group (1973) (to be published).
9. W. C. Hamilton, *Statistics in Physical Science*, Ronald Press, New York, 1964.

10. R. W. Peelle, *Generation of Uncertainty Quantities for Evaluated Neutron Cross Sections ENDF/B-IV* (1973) (to be published in revised form).
11. See paper 2 of this report.

35. ENDF/B EVALUATION OF NEUTRON AND GAMMA-RAY PRODUCTION CROSS SECTIONS FOR CALCIUM[1,2]

C. Y. Fu F. G. Perey

A complete evaluation is given of the neutron and photon production cross sections of natural calcium from 0.00001 eV to 20 MeV. The results of nuclear model calculations were used where applicable. In particular, as gamma-ray branching ratios are mostly known, (n,x) and $(n,x\gamma)$ cross-section data were examined together to arrive at consistent data sets. The data files include those for resonance parameters, neutron cross sections, angular and energy distributions of secondary neutrons, multiplicity of secondary gamma rays, and angular and energy distributions of secondary gamma rays.

1. Abstract of paper to be included in *ENDF/B Summary Documentation,* ENDF-201, issued by National Neutron Cross Section Center.
2. Research sponsored by Defense Nuclear Agency.

36. ENDF/B EVALUATION OF NEUTRON AND GAMMA-RAY PRODUCTION CROSS SECTIONS FOR IRON[1,2]

F. G. Perey S. K. Penny[3]
C. Y. Fu W. E. Kinney
R. Q. Wright[3]

A complete evaluation is given of the neutron and photon production cross sections of natural iron from 0.00001 eV to 20 MeV. The results of nuclear model calculations were used where applicable. In particular, as gamma-ray branching ratios are mostly known, (n,x) and $(n,x\gamma)$ cross-section data were examined together to arrive at consistent data sets. The data files include those for resonance parameters, neutron cross sections, angular and energy distributions of secondary neutrons, multiplicity of secondary gamma rays, and angular and energy distributions of secondary gamma rays.

1. Abstract of paper to be included in *ENDF/B Summary Documentation,* ENDF-201, issued by National Neutron Cross Section Center.
2. Research sponsored by Defense Nuclear Agency.
3. Computer Sciences Division, UCC Nuclear Division.

37. ENDF/B EVALUATION OF NEUTRON AND GAMMA-RAY PRODUCTION CROSS SECTIONS FOR LEAD[1,2]

C. Y. Fu F. G. Perey

A complete evaluation is given of the neutron and photon production cross sections of natural lead from 0.00001 eV to 20 MeV. The results of nuclear model calculations were used where applicable. In particular, as gamma-ray branching ratios are mostly known, (n,x) and $(n,x\gamma)$ cross-section data were examined together to arrive at consistent data sets. The data files include those for resonance parameters, neutron cross sections, angular and energy distributions of secondary neutrons, multiplicity of secondary gamma rays, and angular and energy distributions of secondary gamma rays.

1. Abstract of paper to be included in *ENDF/B Summary Documentation*, ENDF-201, issued by National Neutron Cross Section Center.
2. Research sponsored by Defense Nuclear Agency.

38. ENDF/B EVALUATION OF NEUTRON AND GAMMA-RAY PRODUCTION CROSS SECTIONS FOR SILICON[1,2]

D. Larson F. G. Perey

A complete evaluation is given of the neutron and photon production cross sections of natural silicon from 0.00001 eV to 20 MeV. The results of nuclear model calculations were used where applicable. In particular, as gamma-ray branching ratios are mostly known, (n,x) and $(n,x\gamma)$ cross-section data were examined together to arrive at consistent data sets. The data files include those for resonance parameters, neutron cross sections, angular and energy distributions of secondary neutrons and charged particles, multiplicity of secondary gamma rays, and angular and energy distributions of secondary gamma rays.

1. Abstract of paper to be included in *ENDF/B Summary Documentation*, ENDF-201, issued by National Neutron Cross Section Center.
2. Research sponsored by Defense Nuclear Agency.

39. ENDF/B EVALUATION OF NEUTRON AND GAMMA-RAY PRODUCTION CROSS SECTIONS FOR FLUORINE[1,2]

C. Y. Fu D. C. Larson
F. G. Perey

A complete evaluation is given of the neutron and photon production cross sections of fluorine from 0.00001 eV to 20 MeV. The results of nuclear model calculations were used where applicable. In particular, as gamma-ray branching ratios are mostly known, (n,x) and $(n,x\gamma)$ cross-section data were examined together to arrive at consistent data sets. The data files include those for resonance parameters, neutron cross sections, angular and energy distributions of secondary neutrons, multiplicity of secondary gamma rays, and angular and energy distributions of secondary gamma rays.

1. Abstract of paper to be included in *ENDF/B Summary Documentation*, ENDF-201, issued by National Neutron Cross Section Center.
2. Research sponsored by Defense Nuclear Agency and the AEC Division of Physical Research.

40. REPORTS TO THE U.S. NUCLEAR DATA COMMITTEE[1,2]

F. G. Perey

These are collections of recent, not generally publicized, cross-section work done at ORNL and recent papers which have been submitted for publication. The reports are prepared for the USNDC and include only material which the author thinks might be of interest to the USNDC Subcommittee members. The reports cover the periods between the USNDC meetings.

1. Two reports were issued during the year: ORNL-TM-4390 (November 1973) and ORNL-TM-4589 (June 1974).
2. Work sponsored by the AEC Division of Physical Research.

41. DEFENSE NUCLEAR AGENCY WORKING CROSS-SECTION LIBRARY: DESCRIPTION AND CONTENTS (Volume I Revision)[1,2]

R. W. Roussin J. B. Wright

The Radiation Shielding Information Center serves as a repository for the Defense Nuclear Agency (DNA) cross-section library. This is a working library in ENDF format, and each cross-section set can be revised whenever the authorized evaluator deems changes to be necessary. This report lists the current contents of the library, describes the data formats and procedures to be used, gives a history of the modifications made to DNA evaluations to date, and gives the listings of file 1 from each tape in the library. Liaison with the ENDF/B library is maintained, and the evaluations are identified with numbers that correspond to similar data in the ENDF/B library. In this revised issue, complete data sets are included for ^{14}N, ^{16}O, ^{27}Al, Pb, ^{1}H, Si, Ca, ^{9}Be, ^{23}Na, ^{3}H, ^{181}Ta, Fe, ^{238}U, ^{235}U, ^{12}C, ^{4}He, Mg, Cu, ^{239}Pu, ^{240}Pu, ^{182}W, ^{183}W, ^{184}W, and ^{186}W. In addition, gamma-ray-production data only are included for F, Zn, Ag, and Sn.

1. Abstract of ORNL-RSIC-34, vol. I (Rev.) (June 1974).
2. Work sponsored by Defense Nuclear Agency.

42. MULTIGROUP CROSS-SECTION DEPENDENCE ON WEIGHTING FUNCTION MODEL[1,2]

C. R. Weisbin D. E. Cullen[4]
J. S. Hendricks[3] E. M. Oblow
P. D. Soran[5]

The multigroup cross-section dependence on weighting function model has important ramifications in at least two strong research efforts currently under way. The first of these is an attempt to specify a generally useful multigroup structure for a wide range of nuclear design applications.[6] One such fine multigroup structure may ultimately be proposed in the ANSI Standard N411.[7] For general applicability, it is suggested that such a structure be chosen so group constants are relatively insensitive to reasonable choices of the within-group weighting spectra; that is, a spread of values is observed that does not exceed the recognized uncertainties in nuclear data. A second development program is directed toward obtaining multigroup sets with uncertainty bounds. The multigroup processing code MINX[8] is being developed to enable the user to obtain multigroup sets known to be accurate to within an input specified tolerance, provided one assumes that the data base and weighting function are known explicitly. Since the weighting spectrum can never be known exactly, it is vital to perform a parametric study to determine the importance of the uncertainty in spectral shape relative to that of other known processing errors such as integration tolerances, angular distribution fitting, etc.

Recently, Stacey et al.[9] found a single weighting function to be adequate for the purpose of generating broad-group cross sections for similar cores and blankets. However, they did experience difficulty applying such a library to problems with radically different compositions.

The present work considers group structures both broader and finer than those previously employed. It is comprehensive in terms of the variety of weighting functions, temperatures, and compositions examined and differential in the sense of observing the effects on each of the partial cross sections rather than a single integral measurable (for which cancellation of effects can sometimes go unobserved).

Some highlights of the study are presented in Tables 42.1 and 42.2. The results indicate that for the proposed[6] 239-group structure, the multigroup cross-section variations observed for three different smooth Bondarenko weighting functions are of the same order as (and generally much less than) the uncertainties in the original microscopic data. The few groups in which significant differences were noted are at energies near thresholds and resolved resonances. Much larger differences have been noted for a typical 30-group structure.[10]

Table 42.1. Average percent deviation for infinitely dilute cross sections and f factors obtained for constant, $1/E$, and $1/E$ + fission spectrum smooth Bondarenko weighting[a]

	$\sigma(0^\circ, \infty)$	$f(2100^\circ, \infty)$	$f(300^\circ, 50)$	$f(2100^\circ, 50)$	$f(300^\circ, 0)$
			^{239}Pu		
Total	0.187	0.036	0.137	0.097	0.166
Elastic	0.118	0.011	0.072	0.056	0.082
$(n, 2n)$	0.127	0.000	0.000	0.000	0.000
Fission	0.257	0.031	0.058	0.055	0.090
1st level	0.056	0.001	0.001	0.001	0.001
Capture	0.290	0.029	0.078	0.073	0.115
			Fe		
Total	0.152	0.007	0.016	0.014	0.069
Elastic	0.159	0.003	0.006	0.008	0.032
$(n, 2n)$	0.557	0.000	0.000	0.000	0.001
1st level	0.081	0.005	0.002	0.002	0.010
Capture	0.253	0.006	0.616	0.006	0.016
			^{235}U		
Total	0.188	0.026	0.082	0.070	0.123
Elastic	0.029	0.004	0.009	0.008	0.010
$(n, 2n)$	0.224	0.000	0.000	0.000	0.000
Fission	0.225	0.028	0.057	0.048	0.087
1st level	0.197	0.001	0.000	0.001	0.001
Capture	0.276	0.031	0.044	0.049	0.086

[a]Computations performed in proposed CSEWG group structure. The f factor is defined by:

$$f(T, \sigma_0) \equiv \frac{\sigma(T, \sigma_0)}{\sigma(0^\circ, \infty)},$$

where

$\sigma(T, \sigma_0)$ = cross section (barns) at temperature T and dilution σ_0,

σ_0 = background total cross section per absorber atom,

T = temperature ($^\circ$K).

Table 42.2. Average and maximum percent deviations between multigroup constants obtained with different weight functions for proposed CSEWG group structure[a]

Reaction	Energy region					
	Unresolved		Resolved		All	
	Av	Max	Av	Max	Av	Max
Total	0.126	1.689	1.457	6.299	0.187	6.299[b]
Elastic	0.091	1.517	0.920	4.338	0.118	4.338[b]
$(n,2n)$					0.127	3.057[c]
Fission	0.186	1.761	2.053	7.521	0.257	7.521[b]
1st level	0.765	6.174			0.056	6.174[d]
2nd level					0.035	1.239[d]
3rd level					0.040	2.070[d]
4th level					0.045	1.917[d]
5th level					0.040	1.032[d]
Capture	0.211	2.624	2.040	5.668	0.290	5.668[b]
(n,p)					0.580	4.133[d]
(n,d)					0.912	9.012[d]
(n,t)					0.619	5.787[d]
(n,α)					0.279	2.643[d]

[a]Legend: ^{239}Pu, $\sigma_0 = 10^{10}$, $T = 0°$K,
$C(E) = 1/E$, const, $1/E$ + fission spectrum

[b]Difference of this magnitude observed in only two groups in resolved energy region.

[c]Difference appears at energies > 19 MeV.

[d]Difference appears only in threshold group where cross section is generally $<10^{-3}$ b.

1. Summary of paper presented at American Nuclear Society Meeting, San Francisco, November 11–15, 1973; *Trans. Amer. Nucl. Soc.* 17, 483 (1974).
2. ORNL participation sponsored by Defense Nuclear Agency and AEC-LMFBR program.
3. Massachusetts Institute of Technology.
4. Lawrence Livermore Laboratory.
5. Los Alamos Scientific Laboratory.
6. C. R. Weisbin and R. J. LaBauve, *Specification of a Generally Useful Multigroup Structure for Neutron Transport*, LA-5277-MS, Los Alamos Scientific Laboratory (May 1973).
7. R. A. Dannels, Westinghouse Nuclear Energy Systems, personal communication (June 1973).
8. C. R. Weisbin, P. D. Soran, D. R. Harris, R. J. LaBauve, and J. S. Hendricks, "MINX – A Multigroup Interpretation of Nuclear X-Sections," *Trans. Amer. Nucl. Soc.* **16**, 127 (1973); see also paper 43.
9. W. M. Stacey et al., "Studies of Methods for Fast Neutron Multigroup Cross Section Generation and Their Effect upon the Neutronic Properties of LMFBR Critical Assemblies," CONF-72091, Book 2, U.S. Atomic Energy Commission Technical Information Center (1972).
10. T. J. Hirons and M. E. Battat, *Calculations of Fast Critical Assemblies Using LASL and ENDF/B Version II Data*, LA-DC-12369, Los Alamos Scientific Laboratory (June 1971).

43. MINX: A MODULAR CODE SYSTEM FOR PROCESSING MULTIGROUP CROSS SECTIONS FROM NUCLEAR DATA IN ENDF/B FORMAT[1,2]

D. R. Harris[3] P. D. Soran[3]
R. J. LaBauve[3] C. R. Weisbin
R. E. MacFarlane[3] J. E. White[4]

MINX is a modular code system for computation of multigroup nuclear data from evaluated nuclear data in ENDF/B format. High-order Legendre group-to-group transfer matrices are computed accurately.

Resonance shielding and streaming effects are treated by Bondarenko techniques. Nuclear data sets are computed by MINX to be useful in widely used methods for design of fission and fusion devices.

1. Abstract of paper presented at Seminar on Codes for Nuclear Data Processing, NEA-CPL, Ispra, Italy, December 5–7, 1973.
2. ORNL participation sponsored by AEC-LMFBR program.
3. Los Alamos Scientific Laboratory.
4. Computer Sciences Division, UCC Nuclear Division.

44. A NEW PROCEDURE FOR THE DETERMINATION OF NEUTRON MULTIGROUP TRANSFER MATRICES[1,2]

C. R. Weisbin P. D. Soran[3]
J. S. Hendricks[4]

A new technique has been employed to generate Legendre components of group-to-group neutron scattering cross-section matrices for two-body interactions. This semianalytic procedure, which treats the rapidly fluctuating cross-section behavior analytically, has been incorporated in the MINX processor, a code for the multigroup interpretation of nuclear x-sections. The algorithm requires only a minimum of numerical approximations and employs a flexible energy integration mesh so that localized resonance phenomena may be adequately represented.

1. Abstract of paper to be published in *Nuclear Science and Engineering.*
2. ORNL participation sponsored by AEC-LMFBR program.
3. Los Alamos Scientific Laboratory.
4. Massachusetts Institute of Technology.

45. MULTIGROUP NEUTRON TRANSFER MATRIX FORMULATION FOR SCATTERING REACTIONS WITH TABULATED SECONDARY SPECTRA[1,2]

C. R. Weisbin P. D. Soran[3]

In this note, the calculation of multigroup neutron transfer matrices for multibody breakup reactions is considered, wherein the secondary spectral representation is tabulated and uncoupled from the outgoing angular distribution.

It is shown for tabular ENDF/B spectral formulations that integration over the sink group, for arbitrary incident energy, may be performed analytically, incorporating directly the data set and energy meshes provided by the evaluator. This is achieved by linearly interpolating between two successive tabulated incident energies, the respective integrals over the sink group. This is particularly important for the case of tabulated energy distributions, where reconstruction of the two-dimensional density function can require large amounts of unnecessary interpolation. Finally, the proposed method is examined with regard to recent suggestions for more accurate unit base transformation interpolation procedures not yet incorporated in ENDF/B.

1. Abstract of paper submitted for journal publication.
2. ORNL participation sponsored by AEC-LMFBR program.
3. Los Alamos Scientific Laboratory.

46. CROSS-SECTION PROCESSING CODES – IS THERE A DOLLARS WORTH OF DIFFERENCE BETWEEN THEM?[1,2]

C. R. Weisbin R. J. LaBauve[5]
N. M. Greene[3] C. Durston[6]
H. Henryson II[4] D. E. Cullen[7]
R. B. Kidman[8]

Since we do not live in an idealized world with infinite computational and monetary resources, the question of dollars worth of difference between cross-section processing codes must be evaluated both from the viewpoint of how much "accuracy" is required and how much "money" is available to obtain the answer. It would be desirable if a single processing code gave the best answers at the least cost; however, this is presently not the case. Therefore this paper will discuss the range of applicability and the effort that must be expended in processing ENDF/B cross sections with several multigroup averaging programs in wide use in the United States. Examples drawn from the authors' experience include AMPX,[9] MINX[10]/SPHINX,[11] MC^2-2/SDX,[12] ETOX[13]/IDX,[14] ENDRUN[15]/TDOWN,[16] SUPERTOG,[17] ETOG,[18] and MC^2.[19] These codes are typical and by no means all inclusive. For example, the GAF/GAR/GAND[20] system is not explicitly discussed. Often these programs are, in fact, systems of linked computer codes, and such distinctions will be highlighted. This paper will demonstrate that there are significant differences between the algorithms employed and that there is considerable variation in the versatility of several of these codes. Since the practical effect of different processing techniques on important reactor parameters is problem dependent, this paper will emphasize approximations introduced, areas of validity, computing time required, and experience, while leaving it to further study to determine *how* one might best get his "dollar's worth."

Two types of considerations are examined with respect to the aforementioned codes. The first involves programmatic and logistic concerns which first confront the prospective user. These include:

1. the types of computers for which demonstrated experience is available in the generation of multigroup cross sections, using such a processor;
2. the transport codes and associated formats for which the processor is designed to generate multigroup data sets;
3. the necessity for accurate representation of cross-section minima, as well as resonances, and extremes in neutron energy range, in addition to requirements for high-order matrices and neutron-gamma coupled sets;
4. the appropriateness of flux estimates from previously measured spectra in similar reactors, physical models, interpolative shielding factor techniques, etc., as opposed to a more detailed flux calculation;
5. the ability to properly treat all ENDF/B formats; and
6. the availability of desirable options such as built-in standard weighting functions and group structures, internal group collapsing mechanisms, and flexible dimensioning.

The more sophisticated user will consider the algorithms and associated approximations introduced during (*a*) resonance reconstruction, (*b*) Doppler broadening, (*c*) flux estimation and self-shielding, (*d*) groupwise numerical averaging, (*e*) computation of group-to-group transfer matrices, (*f*) gamma-ray interaction and production calculation, (*g*) space-energy collapse to few groups, and (*h*) quantification of numerical uncertainties.

As an example, the methods by which various processing codes treat Doppler broadening tend to differ considerably. At least four different techniques have been employed: these include (ψ, χ)[19] methods, J*

improvements,[21] TEMPO[22] procedures, and the σ^1 (refs. 23 and 24) technique. The last approach is, at least potentially, the most accurate and the most time consuming.

If the nuclei in the medium are assumed to be distributed according to a Maxwellian distribution with temperature T, the Doppler broadening equation can be reduced to the form[22]

$$\sigma(E, T) = \frac{1}{E}\sqrt{\alpha/4\pi} \int_0^\infty \sqrt{E'}\, \sigma(E', 0) \left[e^{-\alpha(\sqrt{E'}-\sqrt{E})^2} - e^{-\alpha(\sqrt{E'}+\sqrt{E})^2} \right] dE' , \tag{1}$$

where

T = temperature of medium (°K),

$\alpha = M/(mkT)$,

m, M = masses of the neutron and target nucleus respectively,

k = Boltzmann's constant,

$\sigma(E', 0)$ = cross section for incident neutrons of energy E' at temperature $T = 0$°K.

In deriving (ψ, χ) formulations, the second exponential in Eq. (1) is neglected, and the major contribution from the remaining exponential

$$e^{-\alpha(\sqrt{E'}-\sqrt{E})^2}$$

is assumed to come from a narrow region about $E' = E$. This is consistent with expanding regions of integration to ∞ and neglecting the energy dependence of the Doppler width. In existing codes, using this method, the cross section $\sigma(E', 0)$ is assumed to be composed of a series of isolated single-level Breit-Wigner resonances; thus a background file or generalized cross-section formulation is not considered. Generally, these approximations are adequate for reactor problems but may be unsuitable for shielding applications where appropriate consideration of the background file is important. This approach may be inadequate for CTR core or military applications, where temperatures are much higher.

Improvements have been proposed[21] to extend the J* treatment for evaluating the generalized form of the resonance integral. Herein, rational transformations and Gauss-Jacobi quadrature are invoked to derive expressions for integrals of the flux-weighted Doppler-broadened cross section directly based on the nuclear resonance approximation. Several mathematical approximations are introduced with regard to asymptotic properties, parameter selection, etc., but these have been demonstrated to be negligible. For a system typical of fast-reactor compositions, the newer procedure was shown to be approximately a factor of 100 faster than the corresponding MC[2] for the same problem and equivalent in accuracy.

The TEMPO approach starts from Eq. (1), neglects the second exponential, and assumes that the reaction rate $[\sqrt{E}\, \sigma(E, 0)]$ is given as a table of values with linear-linear interpolation between entries. The algorithm has the same limitations as the (ψ, χ) technique concerning E large compared to $1/\alpha$, and the energy dependence of the Doppler width is ignored. However, it has the advantage that it can handle and tabulate reaction rate, not just Breit-Wigner resonances.

The σ^I method starts from Eq. (1) and makes only one assumption: the cross section (not the reaction rate) is assumed piecewise linear between entries. This technique has all the advantages of the TEMPO method and is applicable to all energies, not just $E \gg 1/\alpha$.

Comparison between these four techniques illustrates just one of a multitude of trade-offs between accuracy and cost. Selection of one method over the other depends upon how accurate one requires the data and how much one is willing to pay for it.

1. Summary of paper presented at American Nuclear Society Meeting, Atlanta, September 8–11, 1974.
2. ORNL participation jointly sponsored by AEC-LMFBR program and Defense Nuclear Agency.
3. Computer Sciences Division, UCC Nuclear Division.
4. Argonne National Laboratory.
5. Los Alamos Scientific Laboratory.
6. Westinghouse Advanced Reactors Division.
7. Lawrence Livermore Laboratory.
8. Hanford Engineering Development Laboratory.
9. N. M. Greene and F. R. Mynatt, "The AMPX Modular Code System for Generating Coupled Neutron-Gamma Multigroup Cross-Section Sets," *Trans. Amer. Nucl. Soc.* **15**, 568 (1972).
10. C. R. Weisbin, P. D. Soran, D. R. Harris, R. J. LaBauve, and J. S. Hendricks, "MINX – a Multigroup Interpretation of Nuclear X-Sections," *Trans. Amer. Nucl. Soc.* **16**, 127 (1973); see also C. R. Weisbin, P. D. Soran, R. E. MacFarlane, D. R. Harris, R. J. LaBauve, and J. S. Hendricks, *MINX, a Multigroup Interpretation of Nuclear Cross Sections from ENDF/B*, Los Alamos Scientific Laboratory report to be published.
11. N. C. Paik, C. Durston, W. Davis, and M. B. Yarbrough, *Physics Evaluations and Applications – Quarterly Progress Report for Period Ending January 31, 1974*, WARD-XS-3045-5 (March 1974).
12. B. J. Toppel and H. Henryson II, "Methodology and Application of the MC^2-2/SDX Cross Section Capability," *Trans. Amer. Nucl. Soc.* **16**, 126 (1973).
13. R. E. Schenter, J. L. Baker, and R. B. Kidman, *ETOX – a Code To Calculate Group Constants for Nuclear Reactor Calculations*, BNWL-1002 (1969).
14. R. W. Hardie and W. W. Little, Jr., *IDX, a One-Dimensional Diffusion Code for Generating Effective Nuclear Cross Sections*, BNWL-954 (March 1969).
15. B. A. Hutchins, C. L. Cowan, M. D. Kelley, and J. E. Turner, *ENDRUN-II, a Computer Code to Generate a Generalized Multigroup Data File from ENDF/B*, GEAP-13704 (1971).
16. C. L. Cowan, B. A. Hutchins, and J. E. Turner, *TDOWN, a Code to Generate Composition and Spatially Dependent Cross Sections*, GEAP-13740 (1971).
17. R. Q. Wright, N. M. Greene, J. L. Lucius, and C. W. Craven, Jr., *SUPERTOG: A Program to Generate Fine Group Constants and P_n Scattering Matrices from ENDF/B*, ORNL-TM-2679 (1969).
18. D. E. Kusner, R. A. Dannels, and S. Kellman, *ETOG-I, a FORTRAN IV Program to Process Data from the ENDF/B File to the MUFT, GAM, and ANISN Formats*, WCAP-3845-1 (1969).
19. B. J. Toppel, A. L. Rago, and D. M. O'Shea, *MC^2, a Code to Calculate Multigroup Cross Sections*, ANL-7318 (1967).
20. R. J. Archibald and D. R. Mathews, *The GAF/GAR/GAND Fast Reactor Cross Section Preparation System, GAND – a Computer Program for Preparing Input Data for the GAFGAR Code from an ENDF/B Format Nuclear Data File*, GA-7542, vol. II (1972).
21. R. N. Hwang, "Efficient Methods for the Treatment of Resonance Cross Sections," *Nucl. Sci. Eng.* **52**, 157 (1973).
22. K. Gregson and M. F. James, "TEMPO – a General Doppler Broadening Programme for Neutron Cross Sections," Atomic Energy Establishment, Winfrith, England, AEEW-M518 (1965).
23. D. E. Cullen, O. Ozer, and C. R. Weisbin, "Exact Doppler Broadening of Evaluated Neutron Cross Sections," *Trans. Amer. Nucl. Soc.* **16**, 320 (1973).
24. D. E. Cullen, *Program SIGMA1 (Version 74-1)*, UCID-16426 (January 1974).

47. THE TESTING OF ^{238}U PHOTON PRODUCTION DATA FROM ENDF/B MATERIALS 58, 702, AND 4187[1,2]

W. E. Ford III[3]

Photon production data from three sets of ^{238}U ENDF/B data, MAT 58 (ref. 4), MAT 702 (ref. 5), and MAT 4187, mod 1 (ref. 6), were tested by using the data to calculate secondary gamma-ray pulse-height spectra (SGRPHS) that could be compared with measured spectra. This project also provided a test of the AMPX modular code system for generating coupled neutron-gamma multigroup cross-section sets.[7]

The measured SGRPHS used as the standards for comparison were obtained from a series of unreported ORNL experiments by Maerker and Muckenthaler. Using procedures described for other materials,[8,9] a 5-ft X 5-ft X 1½-in.-thick depleted uranium slab [$N_{235} = 1.201 \times 10^{-4}$, $N_{238} = 4.718 \times 10^{-2}$ atoms/(b cm)] was exposed to filtered and unfiltered collimated neutron beams from the ORNL TSR-II reactor, and resulting SGRPHS were measured with a NaI(Tl) detector system.

AMPX was used to prepare coupled P_3 neutron-gamma cross sections from MATs 58, 702, and 4187, mod 1, and from the ^{235}U ENDF/B data set MAT 57 (ref. 4) in a 100-neutron-group structure ($0 \leqslant E_n \leqslant$ 14.9182 MeV) and a 60-gamma-group structure ($0.01 \leqslant E_\gamma \leqslant 11.0$ MeV). The point ENDF/B neutron interaction cross sections were weighted using a Maxwellian-$1/E$-fission spectrum, and the secondary gamma-ray-production cross sections (SGRPXSs) were weighted with a $1/E$ spectrum. Sets of macroscopic cross sections were prepared for the depleted uranium slab by mixing a ^{238}U AMPX coupled cross-section set and the ^{235}U AMPX set. Multigroup delayed fission SGRPXSs prepared with POPOP4 using data set 925804 from the POPOP4 library and the multigroup fission cross sections from the AMPX calculations were mixed with the AMPX cross sections.[10,11] (The importance of augmenting ENDF/B photon production data with delayed gamma-ray data when analyzing experiments has been previously reported.[12])

Using multigroup representations of the TSR-II beams[13] and the coupled cross sections, the intensity of secondary gamma rays emitted from the depleted uranium slab was calculated with ANISN.[14] After

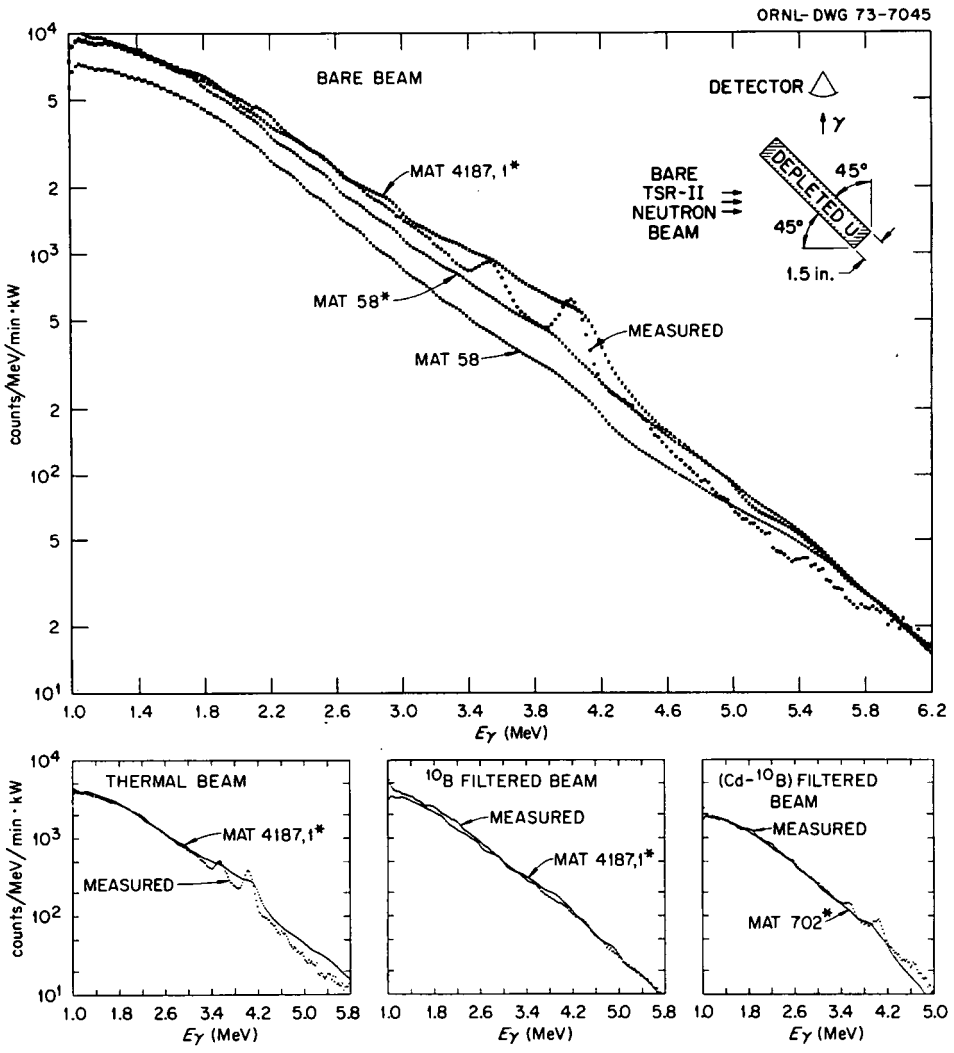

* INCLUDES DELAYED FISSION GAMMA RAYS

Fig. 47.1. Secondary gamma-ray pulse-height comparisons for 1.5-in.-thick depleted uranium slab.

Table 47.1. Ratios of areas under curves in Fig. 47.1

Beam	^{238}U cross-section set	E_γ, Energy range (MeV)	Ratio of area: calculated/measured
Bare	MAT 58	1.0–6.2	0.70
Bare	MAT 58[a]	1.0–6.2	0.91
Bare	MAT 4187, 1[a]	1.0–6.2	0.99
Thermal	MAT 4187, 1[a]	1.0–5.8	1.03
^{10}B filtered	MAT 4187, 1[a]	1.0–5.8	0.89
(Cd – ^{10}B) filtered	MAT 702[a]	1.0–5.0	0.99

[a]Includes delayed fission gamma rays.

being corrected for the geometric attenuation and for the attenuating effect of a detector neutron shield, the calculated intensity was folded with Maerker and Muckenthaler's response functions for the detection system[8] to give the calculated SGRPHS for comparison with the measured spectra. These last calculational steps were done with LINFOLD2.[13]

Examples of measured and calculated SGRPHS comparisons resulting from the bare, Cd-filtered minus ^{10}B-filtered, bare minus Cd-filtered (thermal), and ^{10}B-filtered TSR-II beams are shown in Fig. 47.1. Ratios of the areas under the calculated curves to the areas under the measured curves are listed in Table 47.1. Delayed fission gamma rays contribute 23% of the MAT 58 bare beam spectrum.

1. Summary of paper presented at American Nuclear Society Meeting, San Francisco, November 11–15, 1973; published in *Trans. Amer. Nucl. Soc.* **17**, 545 (1973).

2. Research sponsored by Defense Nuclear Agency.

3. Computer Sciences Division, UCC Nuclear Division.

4. L. Stewart and R. E. Hunter, *Evaluated Neutron-Induced Gamma-Ray Production Cross Section for ^{235}U and ^{238}U,* LA-4918, Los Alamos Scientific Laboratory (July 1972); ENDF/B data tape for MATs 57 and 58 obtained from L. Stewart (LASL).

5. H. Takahashi, *Gamma-Ray Production Cross Sections of Neutron-Induced ^{238}U Reactions,* NNCSC, Brookhaven National Laboratory (paper prepared for journal submission); ENDF/B data tape for MAT 702 obtained from H. Takahashi (BNL) through the Radiation Shielding Information Center (RSIC).

6. R. W. Roussin, ed., *Defense Nuclear Agency Working Cross Section Library: Description and Contents,* ORNL-RSIC-34 (October 1972); ENDF/B data tape for Howerton and MacGregor's (LLL) MAT 4187, mod 1 obtained from RSIC's Defense Nuclear Agency Working Cross-Section Library.

7. N. M. Greene and F. R. Mynatt, "The AMPX Modular Code System for Generating Coupled Neutron-Gamma Multigroup Cross-Section Sets," *Trans. Amer. Nucl. Soc.* **15**, 568 (1972).

8. R. E. Maerker and F. J. Muckenthaler, *Gamma-Ray Spectra Arising from Thermal Neutron Captures in Elements Found in Soils, Concretes, and Structural Materials,* ORNL-4382 (August 1969).

9. R. E. Maerker and F. J. Muckenthaler, *Gamma-Ray Spectra Arising from Fast-Neutron Interactions in Elements Found in Soils, Concretes, and Structural Materials,* ORNL-4475 (April 1970).

10. W. E. Ford III and D. H. Wallace, *POPOP4 – a Code for Converting Gamma-Ray Spectra to Secondary Gamma-Ray Production Cross Sections,* CTC-12, Computer Technology Center, Oak Ridge, Tenn. (May 1969).

11. W. E. Ford III *The POPOP4 Library of Neutron-Induced Secondary Gamma-Ray Yield and Cross Section Data,* CTC-42, Computer Technology Center, Oak Ridge, Tenn. (Sept. 10, 1970).

12. W. E. Ford III, "The Testing of Photon Production Data from ENDF/B-III Material 1135 (^{27}Al)," *Trans. Amer. Nucl. Soc.* **15**, 963 (1972).

13. W. E. Ford III and J. S. Gillen, *The Testing of ^{238}U Secondary Gamma-Ray Production Data Sets from the POPOP4 Library,* ORNL-TM-3482 (February 1972).

14. W. W. Engle, *A User's Manual for ANISN – a One-Dimensional Discrete Ordinates Transport Code with Anisotropic Scattering,* K-1693, Union Carbide Corp. (Mar. 30, 1967).

48. ANISOTROPIC INELASTIC SCATTERING MATRICES FROM ENDF DATA[1,2]

N. M. Greene[3]

The recent upsurge of interest in multigroup cross-section processing has led to the implementation of treatments which, heretofore, have largely been ignored. One of these is an anisotropic treatment for discrete level inelastic scattering.

It has been established that elastic scattering cannot be treated isotropically in high accuracy calculations.[4,5] A recent experiment[6] at Gulf Radiation Technology demonstrates a case where the difference between isotropic vs anisotropic inelastic scattering for carbon leads to spectral differences on the order of 15% in Monte Carlo calculational mockups.[7] The procedure used to generate the multigroup cross sections for the Monte Carlo calculations is described below. It is used in the AMPX[8] modular system developed at Oak Ridge National Laboratory. The method has the following important characteristics:

1. It treats both elastic and level model inelastic scattering.
2. It is tailored toward treating the full energy and angular detail with which cross sections are represented in ENDF/B.[9]
3. Error bounds on the multigroup numbers can be established before the potentially time-consuming transfer matrix calculation is made.
4. It is especially efficient for the large group problem; the 141-energy-group P_8 cross sections for carbon used in the calculations noted above required 2 min vs 8 min for 141-group P_8 elastic and P_0 inelastic matrices via an older and widely used technique.[10]
5. Calculations are made in the LAB system.
6. It is simple to program.

In the laboratory system, a group-to-group transfer term can be written

$$\sigma_l^x(g \to g') = \frac{\int_{E \epsilon g} dE\, \phi_l(E) \int_{E' \epsilon g'} dE' \int_{\vec{\Omega}} d\Omega\, \sigma_l^x(E \to E', \Omega)}{\int_{E \epsilon g} dE\, \phi_l(E)}, \tag{1}$$

where $\sigma_l^x(E \to E', \Omega)$ is the lth term in a Legendre fit to the differential process x cross section for an E to E' transfer through an angle Ω. The weighting flux $\phi_l(E)$ has been assumed isotropic. The differential cross section can be written

$$\sigma_l^x(E \to E', \Omega) = \sigma^x(E) \int_{-1}^{1} d\mu \frac{2l+1}{4\pi} P_l(\mu)\, \delta(E, E', \mu)\, f_l(E), \tag{2}$$

where $\delta(E, E', \mu)$ relates the initial and final energies for a transfer through the laboratory angle μ. The δ-function is a rather formidable expression which, when combined with all the possible forms of ENDF data,

1. Legendre expansion coefficients in the LAB or CM system, or
2. tabulated distributions in the LAB or CM system, leads to a set of complicated expressions for Eq. (1).

These equations present a large job to provide processing for all cases.

Consider a single LAB angle μ_m. The δ-function, which now is only in energy, reduces Eq. (1) to a series of line integrals in group g; that is, given a group g' and μ_m, one can back-calculate through the δ-function to find which part of group g scatters to g'. This suggests a mechanical quadrature in LAB angle

which reduces Eq. (1) to

$$\sigma_l^x(g \to g') = \frac{\frac{2l+1}{4\pi} \sum_{m=1}^{M} w_m P_l(\mu_m) \int_{E_{\text{low}}(\mu_m, g')}^{E_{\text{high}}(\mu_m, g')} dE\, \sigma_l^x(E, \mu_m)\, \phi_l(E)}{\int_{E \epsilon g} dE\, \phi_l(E)}; \tag{3}$$

all the "physics" in this expression is contained in the limits of the integral. The remaining detail is to calculate $\sigma_l^x(E, \mu_m)$. When ENDF data are given in the LAB, it can be calculated directly. When the CM is used, the CM angle, ω_m, corresponding to μ_m is determined; the cross section evaluated there and a Jacobian multiplication give the required value.

The method makes it trivial to change integration schemes. Trapezoidal, Simpson's, and Gauss-Legendre quadratures have all been tried, with the latter, as expected, being considerably more economical and accurate.

When a quadrature is chosen, certain "summed" quantities can be compared to calculate moment values to give an indication of the error introduced by the quadrature; for example,

$$\frac{1}{4\pi} \sum_{m=1}^{M} w_m\, \sigma_0^x(E, \mu_m)$$

should closely sum to $\sigma^x(E)$ at all points where the differential cross section is specified.

Elastic scattering is treated as a special case, namely, with a Q-value of zero, and uses the same programming as does inelastic scattering.

Check cases, such as the 141-group calculation noted earlier, indicate the new method is well behaved and should eliminate some of the known "numerical" problems from the earlier treatment.[10]

1. Summary of paper presented at American Nuclear Society Meeting, San Francisco, November 11–15, 1973; *Trans. Amer. Nucl. Soc.* **17**, 549 (1974).
2. Research sponsored by Defense Nuclear Agency.
3. Computer Sciences Division, UCC Nuclear Division.
4. F. R. Mynatt, N. M. Greene, and W. W. Engle, Jr., "On the Application of Discrete-Ordinates Transport Theory to Deep-Penetration Calculations in Water," *Trans. Amer. Nucl. Soc.* **9**, 366 (1966).
5. N. M. Greene and W. R. Cobb, "A Calculational Sensitivity Study for a Selected LMFBR Using S_n Theory," *Trans. Amer. Nucl. Soc.* **13**, 172 (1970).
6. L. Harris, Jr., G. D. Trimble, and J. C. Young, *Integral Experiment to Test Gamma-Ray Production and Neutron Scattering Cross Sections*, Gulf-RT-A12292 (September 1972).
7. S. N. Cramer and E. M. Oblow, "Calculational Analysis of Neutron and Gamma-Ray Transport Experiments in Carbon," *Trans. Amer. Nucl. Soc.* **16**, 349 (1973).
8. N. M. Greene, J. L. Lucius, W. E. Ford III, J. E. White, R. Q. Wright, and L. M. Petrie, *AMPX: A Modular Code System for Generating Coupled Multigroup Neutron-Gamma Libraries from ENDF/B*, ORNL-TM-3706 (AMPX-1) (to be published).
9. M. K. Drake, ed., *Data Format and Procedures for the ENDF Neutron Cross Section Library*, BNL-50279, Battelle Northwest Laboratories (October 1970).
10. C. W. Craven, Jr., and J. L. Lucius, *TRANSFER: A Program to Calculate P_n Multigroup Scattering Matrices*, ORNL-TM-1537 (May 1966).

49. EFFECTS OF HIGHLY ANISOTROPIC SCATTERING ON MONOENERGETIC NEUTRON TRANSPORT AT DEEP PENETRATIONS[1,2]

E. Oblow H. Goldstein[3]
K. Kin[3] J. J. Wagshal[4]

The sensitivity of the flux in deep-penetration problems to anisotropic scattering was studied within the framework of monoenergetic transport theory. Several parameterized anisotropic-scattering kernels were

used to represent a general class of anisotropies. The representation of these kernels in Legendre polynomial series of various orders was explored to determine their effect on calculated discrete eigenspectra and infinite medium fluxes. Eigenspectra for several kernels are presented as a function of the kernel parameter. Conclusions were drawn about the order of the Legendre expansion of the kernels required for accurate deep-penetration calculations and the possible existence of multiple diffusion decay modes in realistic problems. In general, rather low-order Legendre expansion was found to be adequate for problems in which the scalar flux was the primary quantity of interest.

1. Abstract of ORNL-TM-4408 (December 1973); also abstract of *Nucl. Sci. Eng.* 54, 72 (1974).
2. ORNL participation sponsored by Defense Nuclear Agency.
3. Division of Nuclear Science and Engineering, Columbia University.
4. Hebrew University, Jerusalem, Israel.

50. PROCESSING AND TESTING OF ENDF/B-IV FISSION PRODUCT AND TRANSMUTATION DATA[1,2]

C. W. Kee[3] C. R. Weisbin
R. E. Schenter[4]

Isotope generation and depletion calculations used in the analysis of fission product decay heat following thermal-neutron fission of ^{235}U have been suspect[5,6] due to the limited nuclear decay information available for yields, decay energies, half-lives, etc., particularly for times less than 100 sec after shutdown. Since the credibility of this technique is important to the successful analysis of the loss-of-coolant accident (LOCA) in light-water nuclear reactors, the United States Atomic Energy Commission, through the Cross Section Evaluation Working Group, has sponsored the generation of an extensive library of radioactive decay data for inclusion in ENDF/B-IV. The purposes of this paper are to report the first results of summation calculations using this newer library, to establish the precision of the calculational technique by comparing the decay power computed by different programs using this same data base, to quantify the agreement observed with regard to relevant experimental data (and reviews thereof) of the integral afterheat function, and, finally, to place in perspective these newer results with regard to the proposed American Nuclear Society Standard[5] on the same subject.

The data library employed for this study was derived from preliminary ENDF/B-IV tapes numbered 969 and 970; the former contained fission product yield information for more than 1000 nuclides, while the latter included nuclear decay systematics for more than 800 nuclides of interest. No significant change is anticipated for this type of information in the final release of ENDF/B-IV. Initial studies with a new data base of this magnitude generally require substantial modifications to existing programs such as RIBD,[7] ORIGEN,[8] and CINDER.[9] For example, the calculations with ORIGEN required redimensioning and the development of a translation program[10] to expand and update the ORIGEN library. The translation program was also used to quantify the degree to which the data were modified from that previously used.

Calculations using the pre-ENDF/B-IV data have been performed for several different irradiation times and flux levels, using the ORIGEN and RIBD codes. The total $(\beta + \gamma)$ integral afterheat for a 60,000-day irradiation ($\sim$ infinite) at a flux level of 10^6 neutrons cm^{-2} sec^{-1} (low enough to neglect capture) is given in Table 50.1 along with ORIGEN calculations using earlier data,[10] the Perry et al.[6] evaluation, and the ANS-5 standard.[5] The calculations of ORIGEN and RIBD, using the pre-ENDF/B-IV data base, agree to within the three figures printed on output. The largest difference between these calculations and the Perry et al. evaluation is 12% for times less than 1 sec following discharge. At 10 sec, the difference is less than

Table 50.1. Fission product afterheat for thermal neutron fission of ^{235}U following "infinite" operation at constant power

Time after shutdown, t(sec)	Total afterheat ($\beta + \gamma$) [(MeV/sec)/(fission/sec)]			
	ORIGEN (earlier data)	ANS-5	Perry et al.	ORIGEN/RIBD, present work[a]
1×10^0	10.0	12.50	13.52	11.99
1×10^1	9.05	10.00	10.05	9.72
1×10^2	6.82	6.62	6.54	6.74
1×10^3	4.00	3.70	3.941	4.12
1×10^4	2.01	1.93	2.001	1.96
1×10^5	1.05	0.95	1.012	0.977
1×10^6	0.583	0.534	0.561	0.553

[a]Neither code, at present, treats transitions to second excited states. Therefore, the decay schemes of eight nuclides in the ORIGEN-ENDF/B library were modified to conform with the ad hoc convention used by RIBD, namely, the transition is treated as though it passed to the first excited state.

4%. The calculated results will increase if transitions to second excited states are properly included. (At present, they are approximated as though the decay passes to the first excited state.)

It is concluded that for decay heat calculations of this type, ORIGEN and RIBD give essentially the same results (provided they start from the identical data base), even though the calculations use different numerical methods. The data represented by the preliminary ENDF/B-IV evaluated decay file represent a substantial improvement over previous libraries that are associated with codes of this type. Isotope generation and depletion calculations based upon such extensive libraries are feasible for determining beta and gamma energy release rates. The uncertainties associated with the proposed ANS-5 standard[5] appear to be conservative.

1. Summary of paper to be presented at American Nuclear Society Meeting, Washington, D.C., October 27–November 1, 1974.
2. Neutron Physics Division participation sponsored by AEC-LMFBR program.
3. Chemical Technology Division.
4. Hanford Engineering Development Laboratory.
5. American Nuclear Society, *Proposed ANS Standard Decay Energy Release Rates Following Shutdown of Uranium-Fueled Thermal Reactors,* Draft Standard ANS 5.1, approved by Subcommittee ANS-5 of the ANS Standards Committee, October 1971, revised October 1973.
6. A. M. Perry, F. C. Maienschein, and D. R. Vondy, *Fission-Product Afterheat – a Review of Experiments Pertinent to the Thermal-Neutron Fission of ^{235}U,* ORNL-TM-4197 (October 1973); see also paper 24.
7. R. O. Gumprecht, *Mathematical Basis of Computer Code RIBD,* DUN-4136, Douglas United Nuclear (1968).
8. M. J. Bell, *ORIGEN – the ORNL Isotope Generation and Depletion Code,* ORNL-4628 (May 1973).
9. T. R. England, *CINDER – a One-Point Depletion and Fission-Product Program,* WAPD-TM-334 (revised) (1964).
10. C. W. Kee, C. R. Weisbin, and R. E. Schenter, *Processing and Testing of ENDF/B-IV Fission Product and Transmutation Data,* report to the Fission Product Task Force of the Cross Section Evaluation Working Group (June 1974).

51. UKE-III: A COMPUTER PROGRAM FOR TRANSLATING NEUTRON CROSS-SECTION DATA FROM THE UKAEA NUCLEAR DATA LIBRARY TO THE EVALUATED NUCLEAR DATA FILE FORMAT[1,2]

R. Q. Wright[3] S. N. Cramer
D. C. Irving[4]

A computer program, UKE, has been written to translate neutron cross sections on computer tape from the United Kingdom Atomic Energy Authority Nuclear Data Library to the Evaluated Nuclear Data File,

ENDF/B. The code will translate UK library smooth cross-section data, secondary angular distributions, and secondary energy distributions to the ENDF/B format. No resonance parameters, thermal scattering data, or photon data are considered, however. The secondary angular distributions are translated as differential scattering probabilities only, and no Legendre expansion coefficients are given.

General information is presented concerning the format of the two libraries, along with a detailed description of the translation from the UK secondary energy distribution laws to those of ENDF/B. Programming details and a user's guide are also presented.

1. Abstract of ORNL-TM-2880 (revised) (ENDF-134R) (October 1973).
2. Research jointly sponsored by the AEC Division of Reactor Research and Development, the AEC Division of Controlled Thermonuclear Research, and the Defense Nuclear Agency.
3. Computer Sciences Division, UCC Nuclear Division.
4. Science Applications, Inc., Huntsville, Ala.

52. MACKLIB: 100-GROUP NEUTRON FLUENCE-TO-KERMA FACTORS AND REACTION CROSS SECTIONS GENERATED BY THE MACK COMPUTER PROGRAM FROM DATA IN ENDF FORMAT[1,2]

M. A. Abdou[3] R. W. Roussin

The computer code MACK was used to produce averaged neutron reaction cross sections and kerma factors in the 100-group GAM structure. Data are included for materials commonly used in CTR neutronics studies. The basic evaluated cross-section data from which the resulting group-averaged values were derived was ENDF/B-III. The weighting spectrum used in the energy averaging accounts for the energy distribution of D-T neutrons. The effect of radioactive decay was included for reaction product nuclei with half-lives less than 50 days.

The data library and a suitable retrieval program are available upon request as DLC-29/MACKLIB from the Radiation Shielding Information Center at Oak Ridge National Laboratory.

1. Abstract of ORNL-TM-3995 (August 1974).
2. Research jointly supported by the AEC Division of Controlled Thermonuclear Research and the Defense Nuclear Agency.
3. Nuclear Engineering Department, University of Wisconsin.

53. MANYFILE: A COMPUTER PROGRAM FOR USE IN THE MANIPULATION OF DATA SETS BETWEEN VARIOUS INPUT/OUTPUT DEVICES[1,2]

H. E. Comolander R. K. Gryder[3]

MANYFILE was designed to serve the need of the Radiation Shielding Information Center (RSIC) for a utility program to be used in the daily activities of writing master tapes, adding files to tapes, and copying tapes to fill requests from RSIC customers.

This program has been used extensively with the PDP-10 (via remote terminal) to update and rewrite data sets on the IBM-360.

This program resides on a permanently mounted disk on the IBM-360 computers at the ORNL Computing Center and can be accessed as shown by the examples contained herein.

The MANYFILE program in source card form is available from the Radiation Shielding Information Center.

1. Abstract of ORNL-TM-4377 (October 1973).
2. Work jointly sponsored by AEC Division of Reactor Research and Development and the Defense Nuclear Agency.
3. Computer Sciences Division, UCC Nuclear Division.

54. NEXT-FLIGHT ESTIMATION FOR THE FICTITIOUS SCATTERING MONTE CARLO METHOD[1,2]

S. N. Cramer

The fictitious scattering model has been used to reduce computing time and simplify input data for geometrically complex reactor calculations by eliminating boundary crossings in the random walk process,[3-6] and its extension to the estimation process provides a useful method for deep-penetration calculations in spatially complex systems. By applying a one-dimensional fictitious scattering calculation along the line from collision site to detector point, the spatial integration in the exponential attenuation term of the next-flight estimator can be eliminated.

The model can be illustrated by adding a fictitious collision term, $\Sigma_M \Phi$, to the transport equation in the following form:

$$\Omega \cdot \nabla \Phi(\mathbf{r}, E, \Omega) + \Sigma_M(E)\, \Phi(\mathbf{r}, E, \Omega) = S(\mathbf{r}, E, \Omega) + \iint \left\{ \frac{\Sigma_T(\mathbf{r}, E')\, \Sigma_S(\mathbf{r}, E')}{\Sigma_M(E')\, \Sigma_T(\mathbf{r}, E')} f(E' \to E, \Omega' \to \Omega) \right.$$

$$\left. + \left[1 - \frac{\Sigma_T(\mathbf{r}, E')}{\Sigma_M(E')} \right] \delta(E', \Omega' \to E, \Omega) \right\} \times \Sigma_M(E')\, \Phi(\mathbf{r}, E', \Omega') dE' d\Omega' .$$

All flight paths are selected using the spatially independent Σ_M, and their medium boundary intercepts are no longer relevant [$\Sigma_M \geqslant \Sigma_T(\mathbf{r})$ for all $\mathbf{r}$, otherwise negative contributions are introduced]. At each collision site, a real collision occurs with probability $\Sigma_T(\mathbf{r})/\Sigma_M$, and analog collision mechanics are employed. With probability $1 - \Sigma_T(\mathbf{r})/\Sigma_M$, the collision is fictitious and a new flight path is chosen with no change in energy or direction. In Table 54.1, two fictitious scattering methods are shown for evaluating

Table 54.1. One-dimensional fictitious scattering calculation

Method 1

```
    START
    Set λ = 0
    Set r = r0
1   Select ri (from ΣM exp(−ΣM ri))
    Set r = r + ri
    If r ⩾ R, set λ = 1 and STOP
    If r is in external void, set λ = 1 and STOP
    If RN > ΣT(r)/ΣM, go to 1 (0 ⩽ RN ⩽ 1)
    STOP
```

Method 2

```
    START
    Set λ = exp(−ΣM R)
    Set W = 1
    Set r = r0
1   Select ri from ΣM exp(−ΣM ri)
    Set r = r + ri
    If r ⩾R, STOP
    If r is in external void, set λ = λ + W and STOP
    Set W = W[1 − ΣT(r)/ΣM]
    Set λ = λ + W exp[−ΣM(R − r)] and go to 1
```

Table 54.2. One-dimensional sample problem results[a]

Method	$\langle\lambda\rangle$[b]	Variance	Time[c]	Variance × time
1	0.040840	0.038532	15	0.5780
2	0.039878[d]	0.006817	58	0.3954
1 modified[e]	0.040251	0.015271	42	0.6416
2 modified[f]	0.039987[d]	0.013708	23	0.3153

[a] $\mathbf{r}_i$ = 0.0, 1.0, 2.0, 3.0, 4.0, 5.0; $\Sigma_T(\Delta\mathbf{r}_i)$ = 0.8, 0.6, 1.0, 0.3, 0.5; Σ_M = 1.0.
[b] Analytic answer is 0.040762.
[c] IBM 360/91 time in seconds.
[d] Low due to machine roundoff from 150,000 histories.
[e] Method 1 with $1 - \Sigma_T(\mathbf{r})/\Sigma_M$ weighting instead of random number test.
[f] Method 2 with random number test instead of $1 - \Sigma_T(\mathbf{r})/\Sigma_M$ weighting.

one-dimensional problems, and the results of a sample problem showing the relative merits of the methods are given in Table 54.2. It can be shown that these techniques give the correct mean value for the attenuation along a line

$$\langle\lambda\rangle = \exp\left[-\int_{\mathbf{r}_0}^{R} \Sigma_T(\mathbf{r}')d\mathbf{r}'\right] .$$

In a fictitious scattering, next-flight estimation calculation $\mathbf{r}_0$ is the site of a source, real collision, or fictitious collision with $\Sigma_T(\mathbf{r})/\Sigma_M$ weighting in the random walk, and an "estimation history" is started along the line toward the detector site R (usually in an external void). Using the λ from either method in Table 54.1 as the exponential attenuation factor, the rest of the estimator is determined in the usual manner and the random-walk history continues. In a point detector Monte Carlo calculation, the computing time saved by using fictitious scattering in both random walk and estimation over analog methods has been shown to increase as the geometrical complexity of the system increases.

1. Summary of paper presented at American Nuclear Society Meeting, Philadelphia, June 23–27, 1974; *Trans. Amer. Nucl. Soc.* 18, 400.
2. Research sponsored by AEC-LMFBR program.
3. E. Woodcock et al., *Proc. Conf. Application of Computing Methods to Reactor Problems,* ANL-7050, Argonne National Laboratory (1965).
4. N. R. Candelore and R. C. Gast, *RECAP-2: A Monte Carlo Program for Estimating Epithermal Capture Rates in Rod Arrays,* WARP-TM-427, Bettis Atomic Power Laboratory (1964).
5. S. N. Cramer, *Monte Carlo Analysis of the Exact Geometric Mockup of ZPR-III Assembly 48,* ORNL-TM-3596 (1971).
6. S. N. Cramer, "Heterogeneous Calculations of ZPR-III Assembly 48 by Monte Carlo," *Trans. Amer. Nucl. Soc.* 15, 460 (1972).

55. APPROXIMATE NUMERICAL SOLUTIONS TO THE TIME-DEPENDENT NEUTRON TRANSPORT EQUATION USING THE TASK ALGORITHM[1,2]

E. T. Tomlinson[3]

The purpose of this work is to develop a method for obtaining approximate solutions to the time-dependent Boltzmann neutron transport equation. A transfer-scattering algorithm is used to solve the equation in the spatial, energy, and angular domains. The temporal operator is removed by assuming the neutron flux behaves as the product of a linear function and an exponential function between two given time planes. This assumed behavior is substituted into the multigroup, one-dimensional, slab-geometry

discrete-ordinate form of the transport equation. The resultant equations are forward differenced and then cast into a form making them amenable to solution by the transfer-scattering algorithm.

An exponential extrapolation of the flux is used as a convergence acceleration device. An approximation is made for the magnitude of rod-drop transients to alleviate the need to use small time steps during the initial transient.

Finally, a number of numerical experiments are performed to illustrate the validity of the method. These results are compared with results obtained from already existing methods. In all cases, agreement is excellent.

1. Abstract of ORNL-TM-4595 (July 1974).
2. Research sponsored by AEC-LMFBR program.
3. University of Tennessee.

56. THE DOT III TWO-DIMENSIONAL DISCRETE ORDINATES TRANSPORT CODE[1,2]

W. A. Rhoades F. R. Mynatt

The DOT III program uses the method of discrete ordinates to solve radiation transport problems in two spatial dimensions. While suitable for neutral particle transport analysis in fission reactor, CTR, and weapons studies, DOT has been especially developed for large shielding problems involving the transport of neutrons and/or photons. The document gives a full description of input and output data, as well as code implementation information and a description of a few demonstration problems.

1. Abstract of ORNL-TM-4280 (June 1973).
2. Research jointly supported by Defense Nuclear Agency and the AEC Division of Space Nuclear Systems.

57. DEVELOPMENT OF A CODE SYSTEM FOR DETERMINING RADIATION PROTECTION OF ARMORED VEHICLES (THE VCS CODE)[1,2]

W. A. Rhoades T. J. Hoffman[6]
A. R. Buhl[3] J. V. Pace III[5]
G. L. Haynes[4] L. M. Petrie[5]
R. J. Hinton[5] R. D. Sharp[5]
L. R. Williams

A system of coupled computer codes has been developed for the calculation of the protection from nuclear radiation provided by an armored vehicle. The code system uses a discrete-ordinates air transport calculation coupled to an adjoint Monte Carlo calculation. The vehicle description is supplied in combinatorial geometry form. Elements of the method were tested against experimental data. A realistic tactical nuclear weapon problem is demonstrated.

1. Abstract of ORNL-TM-4664 (in press).
2. Work supported by Ballistics Research Laboratories, Aberdeen, Md.
3. Now with the U.S. Atomic Energy Commission, Division of Reactor Research and Development, Washington, D.C.
4. University of Tennessee.
5. Computer Sciences Division, UCC Nuclear Division.
6. Science Applications, Inc., Huntsville, Ala.

58. VEHICLE CODE SYSTEM (VCS) USER'S MANUAL[1,2]

W. A. Rhoades G. W. Morrison[3]
M. B. Emmett[3] J. V. Pace III[3]
L. M. Petrie[3]

The Vehicle Code System calculates radiation protection factors for armored military vehicles by coupling a forward discrete-ordinates air transport calculation with an adjoint Monte Carlo treatment of the vehicle geometry. Efficiency and moderate use of computer time are emphasized. The code system includes special versions of the DOT III and MORSE codes, together with peripheral codes as required.

The user's manual includes notes describing the input format and sample input listings for each code.

1. Abstract of ORNL-TM-4648 (August 1974).
2. Work supported by Ballistics Research Laboratories, Aberdeen, Md.
3. Computer Sciences Division, UCC Nuclear Division.

59. CALCULATIONS OF THE TRANSPORT OF FAST NEUTRONS ($\lesssim$50 MeV) THROUGH MATTER[1,2]

R. G. Alsmiller, Jr.

In considering the transport of fast neutrons through matter, it is necessary to distinguish between neutrons with energies of $\lesssim$15 to 20 MeV and neutrons with higher energies since the amount of information available concerning the transport of neutrons in the different energy ranges is quite different. In the lower energy range there are rather extensive cross-section libraries, and computer codes exist which allow transport calculations to be carried out using discrete-ordinates techniques (e.g., ANISN[3] and DOT[4]) and Monte Carlo techniques (e.g., MORSE[5]).[6] These codes do not in general provide any information on the charged-particle spectra produced by nuclear interactions, which is needed to obtain quantities of biological interest such as linear energy transfer (LET) spectra and cell-survival probabilities.

There is one generally available code, HETC,[7] which contains the differential particle-production cross-section data necessary to transport neutrons with energies of $\lesssim$50 MeV through matter. The cross-section data used in the code at the higher energies are supplied by a subroutine version of the intranuclear-cascade-evaporation code of Bertini et al.[8] The low-energy ($\lesssim$15 to 20 MeV) neutrons produced during the transport of high-energy neutrons may be transported by a variety of methods, but HETC includes a modified version of O5R[9] which is usually used. HETC utilizes Monte Carlo techniques and is capable of treating complex geometries and very general material compositions. A major advantage of HETC is that it is capable of providing the type and energy distribution of all of the charged particles from nuclear reactions, and from this information spatially dependent LET spectra and cell-survival probabilities may be obtained. The code is also capable of treating the transport of high-energy protons and negatively charged pions and their nuclear-reaction products.

The data and methods which may be used to carry out coupled neutron-photon transport calculations at all energies of interest will be discussed to some extent, but the emphasis will be on HETC, and most of the results presented will be those which have been obtained with HETC.[10-12]

1. Abstract of paper to be presented at Second Symposium on Neutron Dosimetry in Biology and Medicine, Munich, Germany, September 30–October 4, 1974.
2. Research jointly sponsored by the National Science Foundation, Order NSF/RANN Ag-399, and the AEC Division of Physical Research.
3. W. W. Engle, Jr., *A Users Manual for ANISN, a One-Dimensional Discrete Ordinates Transport Code with Anisotropic Scattering*, K-1693, Computing Technology Center, Union Carbide Corp. (1967).

4. W. A. Rhoades and F. R. Mynatt, *The DOT III Two-Dimensional Discrete Ordinates Transport Code*, ORNL-TM-4280 (1973).

5. E. A. Straker, P. N. Stevens, D. C. Irving, and V. R. Cain, *The MORSE Code – a Multigroup Neutron and Gamma-Ray Monte Carlo Transport Code*, ORNL-4585 (1970).

6. The codes are those developed at the Oak Ridge National Laboratory, but similar codes exist at other installations in the U.S. and in Europe.

7. K. C. Chandler and T. W. Armstrong, *Operating Instructions for the High-Energy Nucleon-Meson Transport Code HETC*, ORNL-4744 (1972).

8. H. W. Bertini, M. P. Guthrie, and O. W. Hermann, *Instructions for the Operation of Codes Associated with MECC-3, a Preliminary Version of an Intranuclear-Cascade Calculation for Nuclear Reactions*, ORNL-4564 (1971).

9. D. C. Irving, R. M. Freestone, Jr., and F. B. K. Kam, *O5R, a General-Purpose Monte Carlo Neutron Transport Code*, ORNL-3622 (1965).

10. T. W. Armstrong and K. C. Chandler, "Calculations Related to the Application of Negatively Charged Pions in Radiotherapy: Absorbed Dose, LET Spectra, and Cell Survival," *Radiat. Res.* 58, 293–328 (1974).

11. R. G. Alsmiller, Jr., and J. Barish, *Calculations Pertaining to the Use of Fast Neutrons ($\lesssim$50 MeV) in Cancer Radiotherapy*, ORNL-TM-4442 (1974).

12. R. G. Alsmiller, Jr., R. T. Santoro, T. W. Armstrong, J. Barish, K. C. Chandler, and G. T. Chapman, *Calculations Related to the Use of Photons, Neutrons, Negatively Charged Pions, Protons, and Alpha Particles in Cancer Radiotherapy*, ORNL-TM-4369 (1974).

60. COMPUTER CODES AND DATA AVAILABLE FROM THE RADIATION SHIELDING INFORMATION CENTER[1,2]

D. K. Trubey B. F. Maskewitz
R. W. Roussin

The Radiation Shielding Information Center (RSIC) is a technical institute serving the international shielding community.[3,4] It acquires, selects, stores, retrieves, evaluates, analyzes, synthesizes, and disseminates information on shielding and ionizing radiation transport. The major activities include: (1) operating a computer-based information system and answering inquiries on radiation analysis; (2) collecting, checking out, packaging, and distributing large computer codes; and (3) handling evaluated and processed data libraries. The data packages include multigroup coupled neutron–gamma-ray cross sections and kerma coefficients, other nuclear data, and radiation transport benchmark problem results.

As an integral part of its information processing activities, RSIC collects, makes operable, packages, and distributes computer code packages to nuclear scientists and engineers engaged in shielding research or design.[5–7] The various codes are designed for calculations related to radiation from fission and fusion reactors, radioisotopes, weapons, and accelerators and to radiation occurring in space.

For convenience, the available codes are grouped into two classes: (1) those which treat radiation transport, identified by Computer Code Collection (CCC) numbers, and (2) those performing auxiliary data processing useful for other radiation analysis purposes, identified by Peripheral Shielding Routine (PSR) numbers. The numerical methods applied in the CCC codes are primarily discrete ordinates, Monte Carlo, and kernel integration. The remainder include removal-diffusion (Spinney), moments, spherical harmonics, and invariant imbedding transport theory codes and miscellaneous codes to calculate fission product buildup, release and resulting dose, stopping power, optimization, sensitivity analysis, and others.

The PSR codes include multigroup cross section generation and handling, nuclear models, experimental energy spectra unfolding, optimization, plotting, coupling discrete ordinates results to Monte Carlo, random number generation, and others.

As an adjunct to the computer code exchange, RSIC is involved in many data activities, with most emphasis being placed on nuclear cross-section data. The Center's role in the Evaluated Nuclear Data File (ENDF) development is to assist in the acquisition, checkout, and review of "shielding" cross sections in ENDF format, which may ultimately be placed in the ENDF/B file. RSIC maintains and distributes the

Defense Nuclear Agency (DNA) cross-section library. This is a working library in ENDF format whose content can be modified and revised as often as the evaluator deems such changes to be necessary.

For workaday problem solving, it has been found useful to generate and collect multigroup cross-section sets, and package, document, and distribute them in a format suitable as input to the most-used computer codes.[8] Each data set, packaged as a unit, carries a Data Library Collection (DLC) number. As with the code packages, a particular data package does not remain static but is subject to revision, updating, and expansion as required. Other data in the collection include gamma-ray interaction cross sections, neutron-induced gamma-ray production spectra, fluence-to-kerma coefficients, radioactive decay spectra and decay schemes, and detailed output from transport calculations.

A continuing project, in cooperation with the American Nuclear Society, is to collect, edit, and publish reference data in the form of "benchmark problems."[9] The objective is to compile in convenient form a limited number of well-documented problems in radiation transport which will be useful in testing computational methods used in shielding analysis.

Lists of the available codes and data packages are given, and selected ones are discussed.

---

1. Summary of paper to be presented at International Symposium on Radiation Physics, 1974, Bose Institute, Calcutta, November 30–December 4, 1974.

2. Work jointly supported by the AEC Division of Reactor Research and Development, the AEC Division of Controlled Thermonuclear Research, and the Defense Nuclear Agency.

3. D. K. Trubey, "The Radiation Shielding Information Center – a Technical Information Service for Nuclear Engineers," *Nucl. Eng. Design* 9, 392–95 (1969).

4. B. F. Maskewitz, D. K. Trubey, R. W. Roussin, and F. H. Clark, "The Radiation Shielding Information Center: A Unifying Force in the International Shielding Community," *Proc. Fourth Int. Conf. Reactor Shielding, Paris, France, October 9–13, 1972,* CONF-721018, vol. I, pp. 215–25.

5. D. K. Trubey and Betty F. Maskewitz, "Computer Codes for Shielding Calculations – 1969," *Nucl. Eng. Design* **10**, 505–17 (1969).

6. Betty F. Maskewitz and D. K. Trubey, "Computer Codes for Shielding Calculations – 1970," *Nucl. Eng. Design* **13**, 448–49 (1970).

7. Betty F. Maskewitz, Francis H. Clark, and D. K. Trubey, "Computer Codes for Shielding and Related Calculations – 1972," *Nucl. Eng. Design* **22**, 334–41 (1972).

8. R. W. Roussin, D. K. Trubey, and Betty F. Maskewitz, "Data Activities of The Radiation Shielding Information Center," *Proc. Fourth Int. Conf. Reactor Shielding, Paris, France, October 9–13, 1972,* CONF-721018, vol. 4, pp. 1191–1201.

9. A. E. Profio, ed., *Shielding Benchmark Problems,* ORNL-RSIC-25 (ANS-SD-9) (June 1969), Suppl. 1 (1970).

61. RECENT TRENDS IN REACTOR SHIELDING IN THE U.S.A.[1,2]

D. K. Trubey

In attempting to compile and analyze recent trends, one realizes that any description is highly dependent on one's perspective. This paper will be based on observations from the Radiation Shielding Information Center, which has gathered shielding information for some 12 years.

The trends to be listed here are partly technical and partly socio-organizational. They are in the research and development areas, principally liquid-metal fast breeder reactor (LMFBR) programs, and in the commercial nuclear power sector, principally light-water reactor (LWR) and high-temperature gas-cooled reactor (HTGR) industry.

The trends to be discussed are not listed in order of importance.

1. Diminishing use of empirical and approximate computational methods in favor of discrete ordinates (one and two dimensions) and Monte Carlo (up to three dimensions). Increasing sophistication in the use of these methods, for example, successive problems with different geometry description, coupling discrete-ordinates results to a Monte Carlo treatment of more detailed geometry. Increasing use of systematic variance reduction in Monte Carlo.

2. Great advances in cross-section availability and application, including use of common format, greater emphasis on elaborate and sophisticated evaluations guided by sensitivity analysis, greater attention to photon production and high neutron energies, interagency cooperation, data centers for cross-section processing and distribution, common reference libraries, integral experiments for data testing, coupling of neutron and gamma-ray cross-section sets for routine application, and generation and exchange of energy-group cross-section libraries. Group cross-section specifications guided by sensitivity analysis.

3. U.S. Atomic Energy Commission financial support of breeder reactor (LMFBR) and fusion reactor shielding research and development. The program includes experiments, methods development, cross-section evaluation and testing, and analysis of actual designs.

4. Greater sophistication in the nuclear power industry. The architect-engineering firms doing most of the shielding design have increased their capability partly by absorbing experienced engineers from the declining space programs. Environmental and regulatory pressures have increased the importance of balance-of-plant shielding and radiation protection, including maintenance dose accumulation. Shielding people have become increasingly involved in all aspects of radiation protection.

5. Increasing emphasis in the nuclear industry on standards. There is increased interest in benchmark data, both experimental and pure computational, integral data testing and methods, and computer code and method validation.

---

1. Summary of paper to be presented at International Symposium on Radiation Physics, 1974, Bose Institute, Calcutta, November 30–December 4, 1974.

2. Work supported by the AEC Division of Reactor Research and Development and the AEC Division of Controlled Thermonuclear Research.

62. THE U.S. THEORETICAL AND COMPUTATIONAL LMFBR PROGRAM[1,2]

W. M. Stacey[3] H. Henryson II[3]
B. J. Toppel[3] K. D. Lathrop[4]
R. N. Hwang[3] F. R. Mynatt

The intent of this paper is to review the recent methods and code development activities which have taken place within the U.S. LMFBR physics program. These activities fall within nine general areas: (1) resonance theory, (2) multigroup cross-section generation, (3) sensitivity methods and studies, (4) fuel cycle, (5) Monte Carlo, (6) dynamics, (7) multidimensional diffusion theory, (8) transport theory, and (9) code systems and coordination. The authors have attempted to comply with the symposium instructions regarding the exclusion of work related exclusively to shielding and have elected to exclude material which would logically appear in other papers in this symposium or which might be considered as proprietary by industrial contractors.

Although the discussion of each area necessarily will be brief, a summary of the high points seems in order. Efficient numerical algorithms for constructing group-averaged cross sections and the introduction of a probability table method have significantly reduced the computational time required for heavy-element resonance calculations. Continuous slowing-down theory has been extended to treat the wide scattering resonances occurring in LMFBR mixtures. Two major multigroup cross-section preparation codes are in advanced stages of development. A variational extension to perturbation theory which accounts for flux and adjoint changes has been developed and applied to sensitivity studies. The effect of current nuclear data uncertainties and of the evolution of ENDF/B upon the integral properties of an LMFBR critical assembly has been assessed. A fuel cycle code with equilibrium and nonequilibrium capabilities which features an interchangeable neutronics module is in an advanced stage of development. A Monte Carlo code intended primarily for the analysis of critical assemblies is under development. A two-dimensional, quasi-static

space-time dynamics code is at an advanced stage of development, three direct solution methods for the multigroup diffusion theory kinetics equations have been developed and implemented on an experimental basis, and a variational method for estimating the effect of flux shifts on point kinetics parameters has been developed. Two three-dimensional static diffusion theory codes are under development, one based on spatial synthesis and the other based on direct solution methods. Two new techniques have been developed for defining diffusion coefficients to improve the accuracy of diffusion theory. A two-dimensional triangular-mesh discrete-ordinates code based upon the finite-element method is at an advanced stage of development. Coupling of transport calculations to extend the range of solution techniques or to join together different solution techniques has been examined theoretically, and several codes based on this concept have been developed. Experience with a modular code system which is in production use at one installation has validated the concept. Code coordination efforts among the participants in the U.S. LMFBR physics program have been formalized through the specification of interface data file structures, data management procedures, and other considerations related to standardization of practices.

---

1. Summary of paper presented at International Symposium on Physics of Fast Reactors, Tokyo, October 16–23, 1973.
2. Paper sponsored by AEC-LMFBR program.
3. Argonne National Laboratory.
4. Los Alamos Scientific Laboratory.

63. COMPARISON OF TRANSPORT APPROXIMATIONS FOR REACTOR PHYSICS CALCULATIONS IN A FAST REACTOR[1,2]

G. F. Flanagan W. W. Engle, Jr.
N. M. Greene[3] E. T. Tomlinson[4]

In the current design of large fast reactors, the control monitoring during subcritical and low-power operation will be based on data received from ex-core detectors. Since the fluxes to which these detectors are exposed are anisotropic, reaction rates are difficult to calculate inexpensively. Several transport approximations have been developed for this purpose. Five of these will be compared here. The first two approximations are the well-known discrete-ordinate transport forms with different expansions of the Legendre polynomials. The third approximation is the combined S_2 or P_1 approximation,[5,6] which can be expressed for one dimension in the following differential form:

$$\frac{\partial J}{\partial x} + (\Sigma_T - \Sigma_{gg}^0)\Phi = S - \Sigma_{gg}^0\Phi \tag{1}$$

$$\frac{\partial \Phi}{\partial x} + 3(\Sigma_T - \Sigma_{gg}')J = 3(S' - \Sigma_{gg}'J)\,, \tag{2}$$

where

Φ = scalar flux

J = neutron current

S = isotropic fixed plus scattering source

S' = first Legendre moment of the fixed plus scattering source.

The fourth approximation is the usual transport-corrected diffusion approximation, where σ_{tr} is defined as shown:

$$\sigma_{tr}(E) = \sigma_t(E) - \bar{\mu}_{os}(E)\,\sigma_s(E)\,, \tag{3}$$

where $\bar{\mu}_{os}\sigma_s$ can be defined in a variety of ways. In the so-called "inflow approximation" used here,

$$\bar{\mu}_{os}(\bar{E})\,\sigma_s(E) = \frac{1}{3}\,\frac{\int_E^\infty \sigma_1(E' \to E)\,J(E')\,dE'}{J(E)}\,. \tag{4}$$

The fifth approximation is simply uncorrected diffusion theory.

Several calculations were performed on the IBM 360/91 using ANISN.[7] These calculations were based on a one-dimensional model of the fast test reactor.[8] The cross sections were created using the XSDRN processor from the AMPX[9] system. The results of eigenvalue calculations including running time, number of iterations for convergence, and reaction rates are shown in Tables 63.1 and 63.2. The reaction rates are expressed as ratios of nuclide reaction rates to fission rates in the core. The S_8P_3 transport calculation was considered exact for these case comparisons.

Table 63.1. Detection efficiencies

Reaction type/location	S_8P_3	S_8P_1	P_1 (combined S_2)	P_0 corrected	P_0 uncorrected
		Rods withdrawn			
^{10}B/4th row core	6.4947 – 5	6.4978 – 5	6.5156 – 5	6.5121 – 5	6.5930 – 5
^{10}B/6th row core	4.7873 – 5	4.7873 – 5	4.7786 – 5	4.6987 – 5	4.7192 – 5
^{10}B/inner shield (LLFM location)[a]	8.8128 – 6	8.8121 – 6	8.8154 – 6	8.5160 – 6	6.7993 – 6
^{235}U/4th row core	1.9598 – 6	1.9611 – 6	1.9678 – 6	1.9689 – 6	1.9768 – 6
^{235}U/6th row core	1.3646 – 6	1.3638 – 6	1.3800 – 6	1.3520 – 6	1.3477 – 6
^{235}U/inner shield (LLFM location)[a]	9.2817 – 8	9.2766 – 8	9.2550 – 8	8.9656 – 8	6.9529 – 8
		Control rods inserted			
^{10}B/4th row core	7.43937 – 5	7.43931 – 5	7.42502 – 5	6.46112 – 5	7.52770 – 5
^{10}B/6th row core	3.32607 – 5	3.32808 – 5	3.34992 – 5	4.08258 – 5	3.23320 – 5
^{10}B/inner shield (LLFM location)[a]	7.06627 – 6	7.06461 – 6	7.05711 – 6	8.28039 – 6	5.13032 – 6
^{235}U/4th row core	2.29644 – 6	2.29637 – 6	2.29217 – 6	2.03404 – 6	2.32484 – 6
^{235}U/6th row core	1.07957 – 5	1.08020 – 5	1.08779 – 5	1.22515 – 6	1.04568 – 5
^{235}U/inner shield (LLFM location)[a]	7.44149 – 8	7.43562 – 8	7.40490 – 8	8.73626 – 8	5.23883 – 8
		Safety rods inserted			
^{10}B/4th row core	5.75438 – 5	5.75886 – 5	5.77285 – 5	5.77388 – 5	5.75726 – 5
^{10}B/6th row core	5.14535 – 5	5.14432 – 5	5.12623 – 5	5.03747 – 5	5.08495 – 5
^{10}B/inner shield (LLFM location)[a]	1.01573 – 5	1.01574 – 5	1.01752 – 5	9.82336 – 6	7.99702 – 6
^{235}U/4th row core	1.181629 – 6	1.81789 – 6	1.82499 – 6	1.82704 – 6	1.81922 – 6
^{235}U/6th row core	1.49697 – 6	1.49561 – 6	1.48564 – 6	1.47849 – 6	1.49491 – 6
^{235}U/inner shield (LLFM location)[a]	1.07168 – 7	1.07121 – 7	1.07025 – 7	1.03607 – 7	8.19470 – 8
		All rods inserted			
^{10}B/4th row core	5.63229 – 5	5.63683 – 5	5.64118 – 5	5.64371 – 5	5.64457 – 5
^{10}B/6th row core	4.60553 – 5	4.60376 – 5	4.57145 – 5	4.49072 – 5	4.53612 – 5
^{10}B/inner shield (LLFM location)[a]	1.01574 – 5	1.01544 – 5	1.01525 – 5	9.79804 – 6	7.94789 – 6
^{235}U/4th row core	1.85672 – 6	1.85823 – 6	1.86187 – 6	1.86392 – 6	1.86187 – 6
^{235}U/6th row core	1.39692 – 6	1.39518 – 6	1.38011 – 6	1.37353 – 6	1.38041 – 6
^{235}U/inner shield (LLFM location)[a]	1.07415 – 7	1.07335 – 7	1.07031 – 7	1.03569 – 7	8.16520 – 8

[a]Low-level flux monitor (radius = 113 cm).

Table 63.2. Eigenvalue comparison

Approximation (mode)	Eigenvalue (K_{eff})	Percent error	CPU time (min)	Number of outers	Number of inners
S_8P_3 (transport)	1.0753	0	3.92	9	684
S_8P_1 (transport)	1.0750	0.03	3.89	9	689
P_1 combined S_2 (diffusion)	1.0729	0.22	1.88	8	
P_0 corrected (diffusion)	1.0534	2.04	1.86	8	
P_0 uncorrected (diffusion)	1.0964	−1.96	1.85	8	
		Control rods inserted			
S_8P_3 (transport)	0.9820	0	5.30	11	1000
S_8P_1 (transport)	0.9817	0.03	5.20	11	989
P_1 combined S_2 (diffusion)	0.9796	0.24	2.33	11	
P_0 corrected (diffusion)	0.9544	2.80	2.30	11	
P_0 uncorrected (diffusion)	1.005	−2.34	2.42	12	
		Safety rods inserted			
S_8P_3 (transport)	0.9923	0	3.80	8	681
S_8P_1 (transport)	0.9919	0.04	3.72	8	677
P_1 combined S_2 (diffusion)	0.9887	0.37	1.62	7	
P_0 corrected (diffusion)	0.9717	2.08	1.69	7	
P_0 uncorrected (diffusion)	1.011	−1.83	1.79	8	
		All rods inserted			
S_8P_3 (transport)	0.8938	0	4.27	9	779
S_8P_1 (transport)	0.8935	0.04	4.22	9	780
P_1 combined S_2 (diffusion)	0.8908	0.33	2.00	9	
P_0 corrected (diffusion)	0.8770	1.87	2.06	9	
P_0 uncorrected (diffusion)	0.9079	−1.58	2.16	9	

As can be seen from the results, one can obtain accurate reaction rates and eigenvalues using the combined S_2 approximation in ANISN with approximately the same computing costs as ordinary diffusion theory.

Two-dimensional forms of the combined S_2 approximation are currently being developed for use in DOT III. It is expected that most ex-core fast reactor calculations, such as those required in safety, control, and blanket management, for which the transport-corrected diffusion approximation is inadequate, can be correctly calculated using the combined S_2 approximations.

1. Summary of paper presented at American Nuclear Society Meeting, San Francisco, November 11–15, 1973; *Trans. Amer. Nucl. Soc.* 17, 486 (1974).
2. Research sponsored by AEC-LMFBR program.
3. Computer Sciences Division, UCC Nuclear Division.
4. University of Tennessee.
5. G. Bell and S. Glasstone, *Nuclear Reactor Theory,* Van Nostrand Reinhold (1970).
6. B. Carlson, *Numerical Formulation and Solution of Neutron Transport Problems,* LA-2996, Los Alamos Scientific Laboratory (1964).
7. W. W. Engle, Jr., *A Users Manual for ANISN – a One-Dimensional Discrete Ordinates Transport Code with Anisotropic Scattering,* K-1693, Union Carbide Corp. (1967).
8. G. F. Flanagan, D. B. Simpson, and A. R. Buhl, *One-Dimensional Calculations in Support of the Reactivity Surveillance Procedures for the Fast Test Reactor,* ORNL-TM-4014 (1973).
9. N. M. Greene, J. L. Lucius, W. E. Ford III, J. E. White, R. Q. Wright, and L. M. Petrie, *AMPX: A Modular Code System for Generating Coupled Multigroup Neutron-Gamma Libraries from ENDF/B,* ORNL-TM-3706 (AMPX-1) (to be issued).

64. TRANSPORT CALCULATIONS FOR REACTIVITY MEASUREMENTS IN SUBCRITICAL CONFIGURATIONS OF THE FFTF ENGINEERING MOCKUP CORE[1,2]

G. F. Flanagan D. L. Selby[3]
D. B. Simpson J. T. Mihalczo[4]

All reactivity measurement methods described in several earlier papers[5] depend on the ratio of calculated parameters to infer the reactivity from the measurements. The required parameters are: (*a*) for breakfrequency noise analysis measurements, the ratio of the prompt-neutron lifetime at delayed criticality to that at the subcritical state for which the reactivity is desired; (*b*) for inverse kinetics rod-drop measurements (IKRD), the delayed-neutron effectiveness factors for each delayed-neutron group for each fissionable isotope and the ratio of detection efficiency before the drop to that after; (*c*) for modified source-neutron multiplication measurements, both the ratio of the detection efficiency at the subcritical state to that of a known initial state, in which the relationship between the count rate and a known reactivity (obtained from independent measurements, usually IKRD) is established, and the ratio of the effective source strengths between the subcritical state and the initial state. The last techniques use ratios of calculated quantities and the calibration at a known initial state to avoid the requirement of calculating absolute values of the source strength and detection efficiencies.

Fifty-group cross sections for the calculations were obtained from ENDF/B-III data with a modified version of the AMPX[6] system available at ORNL. In this version, the unresolved resonance region was weighted using the Nordheim method available in the XLACS module. The resolved resonance region was weighted using the narrow-resonance treatment with an energy-dependent potential scattering cross section. The latter required a modification of the NITAWL module of AMPX. The cross sections were spatially cell weighted to account for drawer heterogeneity effects. Neglect of heterogeneity effects reduces the neutron multiplication factor 1.5%.

Both *R-Z* and *X-Y* forward and adjoint were performed. In the *R-Z* calculations, the FTR absorber rods were smeared into annuli with the atomic density of boron reduced to give the same absorptions at the midplane as were obtained from the *X-Y* calculations. Zone- and energy-dependent bucklings for the *X-Y* calculations were obtained from three-dimensional Monte Carlo calculations with the KENO code, discussed in another paper.[7] Calculations were performed using DOT III. Previous studies[8,9] indicated the necessity of using either the discrete ordinate transport for P_1 diffusion approximation for analysis of ex-core detection systems. Since P_1 capability is presently not available in two dimensions, the analysis was carried out using S_4P_3 discrete ordinate calculations. To obtain a multiplication factor of 1.0 for the delayed critical configuration, the total bucklings from the Monte Carlo calculation were increased by 6%.

Delayed-neutron effectiveness factors for each fissionable isotope and delayed-neutron group, which were required for the IKRD algorithms that determined the reactivity from the neutron density as a function of time, were obtained from the usual expressions[10] using forward and adjoint fluxes from the transport theory calculations. It was assumed that these fluxes were products of the *X-Y* and *R-Z* fluxes. These fluxes were also used to calculate the prompt-neutron lifetime, detector efficiencies, and effective source strengths that were required for interpretation of the measurements. Effective source strengths were determined from the spatial distribution of sources in the assembly weighted with the neutron importance, which is an integral over energy of the product of the adjoint flux and energy distribution of source neutrons.

The average delayed-neutron effectiveness factor was 0.86. The changes in the effective source strength, detection efficiency, and prompt-neutron lifetime between the delayed critical and the fully shut down

(~$30 subcritical) configuration were 25, 25, and 10.7%, respectively. Thus, neglect of these changes in these calculated parameters can lead to errors of 25% in the reactivity obtained from the measurements.

1. Summary of paper presented at American Nuclear Society Meeting, Philadelphia, June 23–27, 1974; published in *Trans. Amer. Nucl. Soc.* 18, 268 (1974).
2. Research sponsored by AEC-LMFBR program.
3. University of Tennessee.
4. Instrumentation and Controls Division.
5. J. T. Mihalczo, V. K. Paré, and M. V. Mathis, *Trans. Amer. Nucl. Soc.* 18, 344–346 (1974).
6. N. M. Greene, J. L. Lucius, W. E. Ford III, J. E. White, and R. Q. Wright, *AMPX: An Interface System to Generate Coupled Multigroup Neutron-Gamma Cross Sections from ENDF/B*, ORNL-TM-3706 (in press).
7. L. M. Petrie and N. F. Cross, "Energy- and Region-Dependent Bucklings for the FFTF Engineering Mockup Core from Monte Carlo," *Trans. Amer. Nucl. Soc.* 18, 348 (1974); see also paper 66.
8. G. F. Flanagan, D. B. Simpson, and A. R. Buhl, *One-Dimensional Calculations in Support of the Reactivity Surveillance Procedures for the Fast Test Reactor*, ORNL-TM-4014 (1973).
9. G. F. Flanagan, N. M. Greene, W. W. Engle, Jr., and E. T. Tomlinson, "Comparison of Transport Approximations for Reactor Physics Calculations in a Fast Reactor," *Trans. Amer. Nucl. Soc.* 17, 486 (1973).
10. G. R. Keepin, *Physics of Nuclear Kinetics*, p. 178 (1965).

65. ANALYSIS OF STORED-FUEL, CONTROL-ROD, AND INHERENT-SOURCE EFFECTS ON THE CRBR EX-VESSEL SOURCE RANGE MONITORING SYSTEM[1,2]

G. F. Flanagan L. R. Williams
W. W. Engle, Jr. F. R. Mynatt

Early in the design of the Clinch River Breeder Reactor (CRBR), it was found advantageous to proceed with an ex-vessel low-level flux monitoring (LLFM) system instead of the ex-core system used in the Fast Flux Test Facility (FFTF). The design also called for an in-vessel stored-fuel area containing 34 stored-fuel locations and two transfer ports. FFTF experience indicated that the stored-fuel inherent source dominated the count rate of ex-vessel LLFM's during the refueling sequence, and therefore the design used in the CRBR called for extensive shielding to be placed around the stored fuel with large "windows" in the shield for monitoring the core.

This design was analyzed at ORNL using DOT III. The model consisted of a 60° R-θ section with S_6 quadrature and a P_1 expansion of the 50-group cross sections. The results for various subcritical configurations are summarized in Table 65.1. A 1/10 stored-fuel-to-core count rate background ratio was required. Thus, the 17/1 stored-fuel-to-core ratio was unacceptable, and the design was subsequently changed to exclude in-vessel fuel storage except for four contingency locations.

A second analysis was performed at ORNL to assist in the azimuthal location of these contingency storage locations and the shielding required. The analysis consisted of a 180° R-θ DOT III adjoint

Table 65.1. Effect of stored fuel

Configuration	$\frac{1}{1-K}$	^{235}U fissions per gram per second			
		Ex-vessel detector		Outside core barrel	
		Core	Stored fuel	Core	Stored fuel
−1 $	345	17	11	123	20
−3 $	115	5.5	10	41	13
−10 $	35	1.7	9.7	12	11
−30 $	11.3	0.54	9.7	4.1	9.5

calculation folded with the leakage from an ANISN calculation of four stored fuel elements shielded with 6 and 12 in. of SS 304. The adjoint source was the ^{235}U fission cross section distributed over the graphite block surrounding the LLFM. The results are summarized in Table 65.2. Confirmatory analysis on the final design with the contingency stored fuel located at 120° with 45° guard vessel shielding indicated a 3% background from the stored fuel, well within the 10% requirement.

Additional analysis was required in order to assess the spatial/spectral effect on the LLFM of control-rod removal and inherent-source changes in the core during and immediately following refueling. In this analysis, a DOT III R-θ adjoint problem was run using a 50-group S_6-P_1 transport approximation. The adjoint geometry extended from the blanket-reflector interface to 1 ft inside the concrete shield. The adjoint source was the same as used in the stored-fuel analysis. The block was centered at 0° in R-θ geometry. A forward 360° R-θ DOT model which included the core, the blanket, and the reflector was created and run in 50 groups with an S_2-P_1 transport approximation.

Three forward cases were analyzed. In case 1, all of the safety and control rods were inserted except a safety rod located at +30°. The forward and adjoint angular fluxes were folded using the FACT code. The response was the reaction rate of a detector located at 0°. The forward problem fluxes were rotated −120° and folded with the adjoint. The response represented the reaction rate of a detector located at 120°.

Case 2 was similar to case 1 except the rod at 30° was inserted and a rod at +150° was removed. Similar folding was performed.

Case 3 was a forward calculation with all rods inserted. In this case, the magnitude of the inherent source in the segment 0° to 60° was reduced by 50%, representing a portion of the refueling sequence. The forward fluxes were again folded with the adjoint, rotated −120°, and folded again. The results are summarized in Table 65.3.

Table 65.2. Minimum angle of stored fuel relative to ex-vessel detector

Inherent Source	BOL source 1
Core component at −30 $	1.7 fissions g^{-1} sec^{-1}
Background limit	0.17 fission g^{-1} sec^{-1}

12 in. of B_4C shield on guard vessel	Stored fuel SS304 shield (in.)	Minimum angle (deg)
No	0	140
No	6	100
No	12	90
Yes	0	100
Yes	6	85
Yes	12	77

Table 65.3. Rod and source effects

Case	Detector response at 0° / Detector response at 120°
1	0.998
2	1.002
3	0.760

The results indicate little control-rod shadowing of an LLFM detector, but considerable source effects.

1. Summary of paper presented at American Nuclear Society Meeting, Atlanta, Ga., September 8–11, 1974.
2. Research sponsored by AEC-LMFBR program.

66. ENERGY- AND REGION-DEPENDENT BUCKLINGS FOR THE FFTF ENGINEERING MOCKUP CORE FROM MONTE CARLO[1,2]

L. M. Petrie[3] N. F. Cross[3]

In an effort to eliminate discrepancies observed between measured and calculated reaction rate ratios for BOL-REF-5S,[4] the KENO[5,6] code was used to calculate buckling cross sections for use in the DOT[7] code. These buckling cross sections were calculated with both space and group dependence to account for effects caused by the three-dimensional nature of the experiment. Other information obtained from the Monte Carlo calculations included k_{eff} and the generation time.

The BOL-REF-5S mockup was divided into four regions: the inner core, the outer core, the radial reflector, and the shield. The buckling cross sections, Σ, were calculated by

$$\Sigma_{gi} = J_{gi}/\Phi_{gi} \,, \tag{1}$$

Table 66.1. Buckling cross sections for BOL-REF 5S

Group	Inner core	Outer core	Reflector	Group	Inner core	Outer core	Reflector
1	0.0	0.0	0.0	26	1.1156–3	9.2752–4	5.1379–4
2	0.0	0.0	0.0	27	1.5150–4	–1.3242–4	1.0031–5
3	2.7941–3	3.2713–3	4.7636–2	28	4.6774–4	7.6160–4	1.1202–4
4	3.7801–3	4.8118–3	0.0	29	2.9719–4	1.6815–5	3.0939–4
5	4.1363–3	4.4923–3	3.7558–3	30	7.3670–4	5.6020–4	2.2455–4
6	4.3293–3	3.6451–3	3.2526–3	31	7.0531–4	5.5997–4	8.4975–4
7	3.6631–3	4.5020–3	2.3166–3	32	2.5709–5	6.5530–5	1.8503–4
8	3.3327–3	4.4263–3	2.2478–3	33	–6.0671–4	–3.9373–4	–2.2336–4
9	4.6398–3	3.6246–3	8.0073–4	34	–1.0773–3	–1.2710–3	1.8361–4
10	2.5519–3	3.0225–3	2.0876–3	35	–4.3172–3	1.1526–3	3.6676–4
11	2.7432–3	2.5106–3	1.1857–3	36	–5.4067–4	–1.2082–3	1.3081–4
12	2.5626–3	2.4230–3	1.8469–3	37	–1.7173–4	–6.8156–4	1.9316–4
13	2.1456–3	1.7722–3	1.2753–3	38	–2.6279–4	–1.2363–3	1.1033–4
14	1.4082–3	1.1789–3	7.5212–4	39	–1.1773–3	–1.8887–4	–3.1851–4
15	1.8246–3	1.8130–3	1.4075–3	40	–1.3681–3	–1.6636–3	–4.1003–5
16	1.6120–3	1.9977–3	1.3498–3	41	–2.9057–3	–3.1140–3	7.1646–5
17	1.1662–3	1.3239–3	9.8077–4	42	–8.1476–3	–7.1405–3	1.9903–4
18	1.2990–3	8.9408–4	6.6073–4	43	–1.0842–2	–8.3310–3	–1.5376–4
19	1.0281–3	1.4688–3	9.3858–4	44	–1.9677–2	–1.5384–2	–2.9705–5
20	1.0336–3	1.4319–3	4.4021–4	45	–3.4884–2	–1.8845–2	1.3062–4
21	1.3717–3	9.7153–4	5.4640–4	46	–5.8532–2	–1.3306–2	–3.4858–4
22	1.0850–3	9.5743–4	9.1469–4	47	–8.8982–3	–5.4213–3	–2.5750–4
23	9.7805–4	1.0262–3	2.7896–4	48	–2.1013–2	–1.4954–2	5.2116–4
24	3.7230–4	4.4267–4	5.7842–4	49	–9.4376–1	–5.3161–1	–2.6707–4
25	7.1749–4	4.2816–4	4.3976–4	50	0.0	1.3224–1	3.0465–3

where J_{gi} is the net axial current in group g between a region i and the axial reflector and Φ_{gi} is the volume-integrated flux in region i for group g. The results for the first three regions are presented in Table 66.1. Note that the bucklings decrease with decreasing energy eventually becoming negative due to slowing down and outward radial transport in the axial reflector.

The buckling cross sections for the shield were set to zero because they were considerably lower in magnitude than for the core or reflector and their statistical variance was large. The deviations in the inner core, outer core, and reflector ranged upward from 5, 8, and 25% respectively. Zero bucklings occurred in a few groups where the flux was so small no current was tabulated. KENO calculated a k_{eff} of 0.986 ± 0.006 for a critical three-dimensional mockup. This subcritical result was probably due to the way the heterogeneities were averaged into the cross sections. The generation time was calculated to be 0.58 μsec, compared with a measured value of 0.6 μsec. The time used for these calculations was <10 min on an IBM 360/91 computer.

The buckling cross sections presented in Table 66.1 were used in DOT to calculate reaction-rate ratios. The ^{235}U reaction-rate ratio error when compared to experimental results ranged from 0% for the reflector-shield ratio to 30% for the core-shield ratio. The ^{239}Pu reaction-rate ratio error ranged from <1 to 6%. The reaction-rate ratios before using the bucklings calculated by KENO were in error by as much as a factor of 2. The eigenvalue calculated by DOT using these bucklings and an improved cross-section set was 1.006. Increasing the bucklings by 6%, the eigenvalue was reduced to 1.0. A change of this magnitude is well within the statistical error of the bucklings. This study demonstrates the influence the spatial energy dependence of the bucklings can exert on the flux shape in a two-dimensional calculation.

1. Summary of paper presented at American Nuclear Society Meeting, Philadelphia, June 23–27, 1974; published in *Trans. Amer. Nucl. Soc.* 18, 348 (1974).
2. Research sponsored by AEC-LMFBR program.
3. Computer Sciences Division, UCC Nuclear Division.
4. J. T. Mihalczo, V. K. Paré, M. V. Mathis, and F. Shahrokhi, "Breakfrequency Noise Analysis Measurements for Subcritical Configurations of the FFTF Engineering Mockup Core," *Trans. Amer. Nucl. Soc.* 18, 346 (1974).
5. G. E. Whitesides and N. F. Cross, *KENO – a Multigroup Monte Carlo Criticality Program,* CTC-5, Union Carbide Corp., Nuclear Division (September 1969).
6. L. M. Petrie and N. F. Cross, *KENO II – an Improved Monte Carlo Criticality Program,* ORNL-4938 (1974).
7. W. A. Rhoades and F. R. Mynatt, *The DOT III Two Dimensional Discrete Ordinates Transport Code,* ORNL-TM-4280 (September 1973).

67. CRITICALITY CALCULATIONS FOR CYLINDRICAL BILLETS OF URANIUM-ALUMINUM ALLOY[1,2]

N. F. Cross[3] P. B. Fox[3]
G. E. Whitesides[3]

The KENO and CHERI Monte Carlo codes were used to analyze various arrangements of uranium-aluminum alloy billets. A maximum of 15 billets were used with optimum interspersed water moderation. It was concluded that the units were safe as long as they were confined to a configuration resulting in three 36-in.-long cylinders. Without further investigation, the 15 individual units cannot be considered safe under all circumstances.

1. Abstract of ORNL-CF-74-4-21 (Apr. 9, 1974).
2. Research sponsored by AEC-LMFBR program.
3. Computer Sciences Division, UCC Nuclear Division.

68. GENERALIZED REACTOR SENSITIVITY ANALYSIS PROGRAM AT ORNL[1,2]

E. G. Silver C. R. Weisbin
E. M. Oblow D. E. Bartine
J. M. Kallfelz[3] G. F. Flanagan
F. R. Mynatt

A capability for sensitivity analysis applicable to transport models of power reactors and shields, and in particular the LMFBR, plays a central role in guiding the production, evaluation, and utilization of the nuclear data entering into reactor design and optimization studies.

Sensitivity analysis serves as a guide to priority assignments for the remaining needs for basic cross-section measurements to set confidence limits on calculated integral parameters, and to apportion correctly the importance of the various contributing uncertainties to the variance of such integral parameters. In addition, sensitivity analysis embodying transport-theory calculations finds application in the optimizing of transport calculations and extracting maximum information from benchmark spectral data. It can importantly influence reactor design optimization by permitting the reduction of dyseconomic allowances for input uncertainties.

The ORNL group has made use of the SWANLAKE[4] program, developed originally to perform ANISN-transport-calculation-based sensitivity analysis for shielding problems, to develop a coherent approach to generalized reactor sensitivity analysis.[5–8] The work to be described here makes use of this approach to develop methods for calculating sensitivity profiles and associated estimators for reactors.

The basic mathematical approach is based on the perturbation methods already applied to reactor sensitivity studies by Stacey, employing a variational approach,[9,10] and by Gandini, using generalized perturbation theory.[11] Here, as in the approach by Usachev[12] and Lewins,[13] the generalized adjoint flux is interpreted as importance function for the particular reactor parameter specified by the generalized source.

The calculation methods are based on the use of quite general bilinear function ratios, R, of the form

$$R(\phi, \phi^*) = \frac{\langle \phi^*, H_1 \phi \rangle}{\langle \phi^*, H_2 \phi \rangle} , \tag{1}$$

where H_1 and H_2 are arbitrary operators. R may also reduce for an important class of cases to the linear form

$$R(\phi) = \frac{\langle H_1 \phi \rangle}{\langle H_2 \phi \rangle} . \tag{2}$$

The bilinear form is suitable for defining, for example, reactivity worth, Doppler coefficient, void coefficient, and neutron lifetime, whereas reaction rate ratios, such as breeding ratio, are formulated in the linear form.

Writing the Boltzmann equation in the symbolic form

$$P\phi = A\phi - \lambda B\phi = 0 , \tag{3}$$

where A and B are the neutron transport (leakage and scattering) operator and fission source operator, respectively, and using Pomraning's variational principle for R, one finds that the stationary conditions lead

to generalized perturbation equations of the following form:

$$P\Gamma, = \frac{dR}{d\phi^*} \; ; \; P^*\Gamma^* = \frac{dR}{d\phi} ; \tag{4}$$

$$\langle \Gamma, B^*\phi^* \rangle = 0 \; ; \; \langle \Gamma^*, B\phi \rangle = 0 \, . \tag{5}$$

In implementing the solution of these equations with ANISN, new problems particular to transport theory arise involving the contamination of the generalized functions Γ and Γ^* with the homogeneous equation solutions ϕ and ϕ^*. It can be shown that a unique solution for Γ^* is possible only if the orthogonality conditions $\langle S^*, \phi \rangle$ and Eq. (5) are rigorously zero. At present, the only method available for

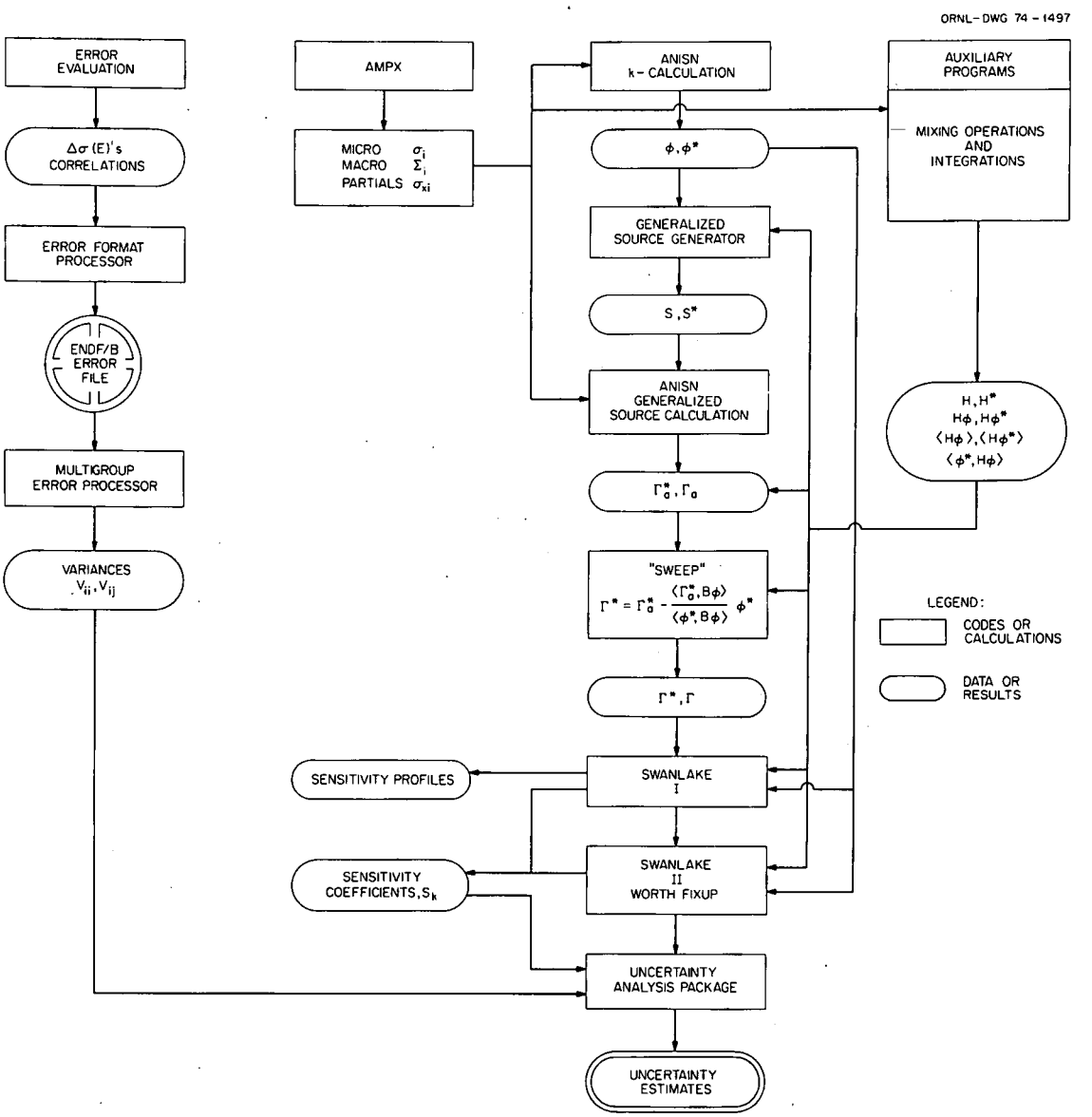

Fig. 68.1. Logical block diagram, ORNL sensitivity analysis.

eliminating the contamination-causing nonorthogonality is "sweeping" the fundamental mode out with an equation of the form

$$\Gamma^* = \Gamma_a^* - \frac{\langle \Gamma_a^*, B\phi \rangle}{\langle \phi^*, B\phi \rangle} \cdot \phi^* \tag{6}$$

(for the adjoint case), where Γ_a^* is the contaminated adjoint. Figure 68.1 illustrates the entire set of procedures needed for sensitivity analysis calculations on reactors, including the sweep.

A parallel development effort, also indicated in Fig. 68.1, has been under way to generate and standardize the format of uncertainties and covariances in the cross-section data for the ENDF/B error file, and the multigroup processor to generate the variance matrix in group form. These data are combined with the sensitivity profiles generated by SWANLAKE to produce the uncertainty estimates.

To have a basis of comparison of the sensitivity results with diffusion-theory calculations, the Italian-origin code sequence TAIM, CIAP, GLOBPERT has been implemented at ORNL. Comparison of some results permits assessment of the importance of transport effects on the significant parameters.

Results with transport methods are currently being applied to a model of the LMFBR demonstration reactor.

---

1. Paper presented at American Nuclear Society Meeting, Philadelphia, June 23–27, 1974; published in *Trans. Amer. Nucl. Soc.* **18**, 341 (1974).
2. Research supported by AEC-LMFBR program.
3. Georgia Institute of Technology.
4. D. E. Bartine, E. M. Oblow, and F. R. Mynatt, *SWANLAKE – a Computer Code Utilizing ANISN Radiation and Transport Calculations for Cross-Section Sensitivity Analysis,* ORNL-TM-3809 (1973).
5. E. M. Oblow, *General Sensitivity Theory for Radiation Transport,* ORNL-TM-4110 (1973).
6. D. E. Bartine, E. M. Oblow, and F. R. Mynatt, *Neutron Cross-Section Sensitivity Analysis: A General Approach Illustrated for a Na-Fe System,* ORNL-TM-3944 (1972).
7. D. E. Bartine, E. M. Oblow, and F. R. Mynatt, *Radiation Transport Sensitivity Analysis – a General Approach Illustrated for a Thermonuclear Source in Air,* ORNL-TM-4335, 1973; see also paper 91.
8. D. E. Bartine, R. G. Alsmiller, Jr., E. M. Oblow, and F. R. Mynatt, *Cross-Section Sensitivity of Breeding Ratio in a Fusion Reactor Blanket,*" ORNL-TM-4208 (1973); see also paper 99.
9. W. M. Stacey, Jr., "Variational Estimates and Generalized Perturbation Theory for the Ratios of Linear and Bilinear Functionals," *J. Math. Phys.* **13**, 1119 (1972).
10. W. M. Stacey, Jr., "Variational Estimates of Reactivity Worths and Reaction Rate Ratios in Critical Nuclear Reactors," *Nucl. Sci. Eng.* **48**, 444 (1972).
11. A. Gandini, "A Generalized Perturbation Method for Bilinear Functionals of the Real and Adjoint Neutron Fluxes," *J. Nucl. Energy* **21**, 755 (1967).
12. L. N. Usachev, "Perturbation Theory for the Breeding Factor and Other Ratios of a Number of Different Processes in a Reactor," *At. Energ.* **15**, 472 (1963).
13. J. Lewins, *Importance: The Adjoint Function,* Pergamon Press (1965).

69. REACTOR CROSS-SECTION SENSITIVITY STUDIES USING TRANSPORT THEORY[1,2]

E. M. Oblow

An approach to making reactor sensitivity studies and reactor parameter uncertainty analysis using transport theory is developed. Sensitivity functions based on variational principles are reviewed and compared with an alternate approach using generalized perturbation theory. The computational implementation of the method using transport codes is also discussed. Finally, the use of cross-section error

files in conjunction with sensitivity coefficients in estimating uncertainties in reactor parameters is described.

1. Abstract of ORNL-TM-4437 (April 1974).
2. Research sponsored by AEC-LMFBR program.

70. SENSITIVITY STUDIES OF THE BREEDING RATIO FOR THE CLINCH RIVER BREEDER REACTOR[1,2]

J. M. Kallfelz[3] D. Lal[3]
M. L. Williams[3] G. F. Flanagan

It is well known that significant uncertainties exist in neutron cross-section values of importance for the design of LMFBRs. The influence of these uncertainties on significant fast breeder integral design parameters, such as the breeding ratio, can be determined by:

1. direct calculations in which a particular cross section is changed and the integral parameter is calculated and compared with the value obtained with the unaltered cross section,
2. calculations with "generalized perturbation theory," which allows one to determine in a single run the influence on the integral parameter of changes to many different cross-section values.

Because of the necessity of a complete reactor calculation for each cross-section change and the large number of cross-section values in a typical multigroup cross-section set, method 1 is somewhat impractical for a comprehensive study of present cross-section and integral-parameter uncertainties.

Generalized perturbation theory, first developed by Usachev,[4] utilizes the "generalized adjoint function," which represents the importance of neutrons at a particular space and energy point to some integral parameter of interest. Using this function, first-order perturbation theory expressions have been derived which give changes in integral reactor parameters associated with cross-section and design changes.

Gandini[5] extended the formalism of Usachev to include not only integral parameters that are functions of the real neutron flux, such as the breeding ratio, but also functions of both the real and adjoint flux, such as "worths," or changes in the reactor multiplication constant caused by changes in reactor constituent densities. The methods and codes developed by Gandini and his co-workers have been used in many studies[6–8] of the correlation between cross-section changes and values of integral reactor parameters.

The generalized perturbation theory codes developed and used in the previous studies usually employ diffusion theory. Currently an effort is under way at Oak Ridge National Laboratory to develop the codes necessary to perform such investigations of reactor core and blanket parameters in S_n transport theory.[10,11] The work reported here is a part of a larger task at ORNL, which has as a goal the determination of uncertainties in present LMFBR design parameters, based on current estimates of cross-section uncertainties. It consists of two parts: (*a*) model investigation and (*b*) generation of sensitivity profiles for the CRBR.

Model investigation. The goal of these studies was to determine one-dimensional (1D) models that are appropriate for breeding ratio sensitivity investigations of a reactor which can only be described completely with a three-dimensional model.

The causes for interest in determining such a model were twofold: (1) At present, the transport theory sensitivity calculations being pursued at ORNL are limited to the 1D case; (2) the diffusion theory sensitivity code package,[12–14] which is presently in production status at ORNL and Georgia Tech, is also limited to 1D. Hence, our sensitivity studies of the CRBR breeding ratio required appropriate 1D models to ensure that the values resulting from the investigations are meaningful.

Most 1D sensitivity studies[8,9,15–18] have employed either spherical or infinite-cylinder geometry, and we have considered both these geometries in our model studies. For the spherical model, problems are involved in defining the "average" blanket and in suitably describing the two-radial-region core (with different fissile/fertile ratios) of the CRBR. Infinite cylindrical models obviously require appropriate corrections for the axial blanket influence.

For these model studies, a simple four-region (inner core, outer core, radial blanket, axial blanket) model of the CRBR was employed. One of the first tasks was to demonstrate that with appropriate corrections utilizing 1D cylindrical calculations, the axial blanket contribution to the breeding ratio could be correctly accounted for. This was accomplished; the result for the corrected 1D calculations of the breeding ratio utilizing MACH-1[19] was within 1% of the result with the 2D model using EXTERMINATOR.[20]

In the model studies, comparisons are made between the 1D values and results from 2D generalized perturbation theory codes[21] recently developed at CNEN. The goal of the 1D model is to "conserve sensitivity," and region-by-region comparison is made for various components (e.g., absorption, leakage) of the expression for the integral parameter change. For 1D cylindrical models uncorrected for the axial blanket, the breeding ratio and energy shape of the generalized adjoint function can be quite different from that of the actual reactor; to correct for this fact, a method is discussed which uses weighted cross sections rather than the usual regional values in the definition of the fixed source term of the generalized adjoint equation. Further problems with 1D models are illustrated and discussed.

Generation of sensitivity profiles for the CRBR. The second part of the reported work contains a set of "sensitivity profile" curves representing the changes in the CRBR breeding ratio for arbitrary 1% changes in the group cross sections of selected nuclides which have a significant influence on this ratio. The runs to determine these curves utilize the Italian diffusion theory sensitivity codes.[12–14] The cross-section values used, generated at ORNL, are a 26-group set with 10 downscatter groups for ENDF/B Version III. The models used for these studies are based on the latest (April 1974) model of CRBR, as defined by Westinghouse. The reported profiles include both the "indirect effect" (i.e., that caused by the spectrum change) and the "direct effect" of changing the cross sections involved in the breeding ratio. In general, the direct effect is the much larger of the two effects.

Arbitrary cross-section standard deviations can be folded into the sensitivity profiles to obtain the variance of the integral parameter of interest. In another paper presented at this meeting, Perey et al.[22] discuss a method of representing estimated uncertainties and correlations in evaluated data (covariances) in the ENDF/B file. We have folded covariance values based on the work of Perey et al. into our sensitivity profiles for several cross sections for which such values are now available; the results illustrate the influence of the "off-diagonal" covariance values, which describe correlations between group cross-section values, on the calculated variance of the integral parameter.

The presented results are analyzed, giving the physical reasons for the shapes of the curves.

---

1. Summary of paper presented at American Nuclear Society meeting, Atlanta, September 8–11, 1974.
2. Research sponsored by AEC-LMFBR program.
3. Georgia Institute of Technology.
4. L. N. Usachev, "Perturbation Theory for the Breeding Factor, and Other Ratios of a Number of Different Processes in a Reactor," *At. Energ.* 15(6), 472 (December 1963).
5. A. Gandini, "A Generalized Perturbation Method for Bilinear Functionals of the Real and Adjoint Neutron Fluxes," *J. Nucl. Energy, Parts A/B* 21, 755 (1967).
6. Bitelli, G. Cecchini, A. Gandini, and M. Salvatores, "Analysis and Correlation of Integral Experiments in Fast Reactors with Nuclear Parameters," *Proc. Int. Conf. Physics of Fast Reactor Operation and Design, London, England, June 23–26, 1969.*

7. Y. Yamamoto et al., *Effect of Uncertainty in Nuclear Constants on Nuclear Characteristics Sensitivity Analysis of Nuclear Constants for the Core of the Monju Reactor,* Hitachi report PNC-SJ-202-72-5 (May 1972), issued by USAEC TIC as JAPFNR-78.

8. M. Salvatores, "Adjustment of Multigroup Neutron Cross Section by a Correlation Method," *Nucl. Sci. Eng.* **50,** 345 (1973).

9. A. Gandini and M. Salvatores, "Effects of Plutonium-239 Alpha Uncertainties on Some Significant Integral Quantities of Fast Reactors," *Nucl. Sci. Eng.* **41,** 452 (1970).

10. E. M. Oblow, *Cross-Section Sensitivity Studies for Critical Reactors Using Transport Theory,* ORNL-TM-4437 (April 1974).

11. E. G. Silver, E. M. Oblow, J. M. Kallfelz, C. R. Weisbin, D. E. Bartine, G. F. Flanagan, and F. R. Mynatt, "Generalized Reactor Sensitivity Analysis Program at ORNL," invited paper presented at the June 23–27, 1974, American Nuclear Society meeting, Philadelphia.

12. I. Dal Bono, *TAIM – Multigroup Diffusion Code,* Internal CNEN report, Doc. CEC(66)12, Casaccia, Italy (1966).

13. I. Dal Bono et al., *The CIAP-1D Code,* CNEN report RT/FI(68)9, Casaccia, Italy (1969).

14. I. Dal Bono et al., *The GLOBPERT-1D Code,* CNEN report RT/FI(68)10, Casaccia, Italy (1968).

15. G. P. Cecchini and M. Salvatores, "Advances in Generalized Perturbation Theory," *Nucl. Sci. Eng.* **46,** 304 (1971).

16. W. Stacey, Jr., "Variational Estimates of Reactivity Worths and Reaction Rate Ratios in Critical Nuclear Reactors," *Nucl. Sci. Eng.* **48** (1972).

17. G. P. Cecchini and M. Salvatores, "Advances in the Generalized Perturbation Theory," *Nucl. Sci. Eng.* **46,** 304 (1971).

18. A. Gandini et al., "Use of Generalized Perturbation Methods for Optimization of Reactor Design," *J. Nucl. Energy, Parts A/B* **23,** 469 (1969).

19. D. A. Meneley, et al., *MACH-1, a One-Dimensional Diffusion-Theory Package,* ANL-7223, pp. 58–60 (1966).

20. T. B. Fowler, M. L. Tobias, and D. R. Vondy, *EXTERMINATOR – a Multi-Group Code for Solving Neutron Diffusion Equations in One- and Two-Dimensions,* ORNL-TM-842 (July 1966).

21. M. Salvatores, DDV, SORC-1, CIAP-2D, GLOBPERT-2D, Two-Dimensional CNEN Sensitivity Code Package, private communication.

22. F. R. Perey, G. de Saussure, and R. B. Perez, paper presented at American Nuclear Society meeting, Atlanta, September 8–11, 1974; see paper 34 of this report.

71. STUDIES OF SENSITIVITY OF SHIELD PERFORMANCE TO NUCLEAR DATA VARIATIONS[1,2]

F. C. Maienschein

The question of the sensitivity of shield performance to neutron cross sections may be restated as: How will the solution to a radiation transport problem change as a result of changes in input cross-section parameters? Most past attempts to provide quantitative answers to this question for reactor shields have depended upon substitution of modified input parameters to obtain a new solution to the problem. In view of the number of parameters which may be involved and their energy dependence, this approach must generally be either incomplete or inordinately time-consuming, or both. Furthermore, this technique is only accurate to first order, and attempts to account for the correlations of input data are awkward.

In an attempt to avoid the above problems and allow an objective identification of the important parameters in a radiation transport problem, E. M. Oblow, D. E. Bartine, and F. R. Mynatt of ORNL have applied techniques based on linear perturbation theory. Usachev[3] and others have, of course, used linear perturbation theory for sensitivity calculations of the performance of LMFBR's to nuclear data and, in an approximate treatment, have shown the apparent importance of error correlations.

A major feature of the ORNL approach is the concept of the cross-section sensitivity profile vs energy. The sensitivity, $P_X(E)$, of a result, R, to a particular cross section, Σ_X, at energy E may be expressed as:

$$P_X(E) = \frac{\int_{\bar{r}} dr \int_{\bar{\Omega}} d\Omega \left[-\Phi^+(\bar{r}, E, \bar{\Omega})\, \Sigma_{X_T}(\bar{r}, E)\, \Phi(\bar{r}, E, \bar{\Omega}) \right.}{R}$$

$$\left. + \frac{\int_{\bar{\Omega}'} \int_{\bar{E}'} d\bar{\Omega}'\, dE'\, \Phi^+(\bar{r}, E', \bar{\Omega}')\, \Sigma_X(\bar{r}, E \to E', \bar{\Omega}\cdot\bar{\Omega}')\, \Phi(\bar{r}, E, \bar{\Omega}) \right]}{R},$$

where $\Phi^+(\bar{r}, E, \bar{\Omega})$ is the unperturbed adjoint flux, $\Phi(\bar{r}, E, \bar{\Omega})$ is the unperturbed forward flux, $\Sigma_{X_T}(E)$ is the total cross section for reaction type X, $\Sigma_X(\bar{r}, E, \rightarrow E', \bar{\Omega}\cdot\bar{\Omega}')$ is the transfer cross section from energy E to E' for reaction type X, and R is the integrated response defined as:

$$R = \int_E dE \int_{\bar{r}} dr \int_{\bar{\Omega}} d\Omega\, D(\bar{r}, E, \bar{\Omega})\, \Phi(\bar{r}, E, \bar{\Omega}) ,$$

where $D(\bar{r}, E, \bar{\Omega})$ is the response function, for example, a flux-to-dose conversion factor. All of the above quantities are defined for the specific problem (source, materials, geometry, and detector) under consideration.

A mathematically consistent formulation leading to the sensitivity function shown has been presented by Oblow.[4] The relationship of the sensitivity function to the partial derivatives of the result of the radiation transport calculation with respect to variations in input parameters is also indicated.

A complete description of the computer code SWANLAKE, which is used for sensitivity calculations, has been prepared by Bartine.[5] Basically, SWANLAKE takes the forward and adjoint angular flux solutions for a given problem and combines them with the cross section to be studied. Sensitivity profiles are obtained for the entire input cross-section data field as a function of spatial zone and summed over all zones. The referenced report includes descriptions of data input and output, a sample problem, and typical running times and computer core requirements.

While the current version of SWANLAKE is applicable to a wide range of problems, limitations should be noted. Problems must be time-independent and one-dimensional. The present sensitivity function only allows for downscatter of particles and does not include the effects of fission cross sections. It is anticipated that most, if not all, of the above restrictions will be removed in future versions.

The sensitivity profile directly indicates cross-section importance as a function of energy of the incident particles as is indicated by the results included below. This type of identification can and should guide future evaluations and measurements of neutron cross sections toward the partial cross sections and energy regions of highest importance. The sensitivity profile should be applied even more specifically in the design of integral experiments for data testing, since it provides a quantitative link between the experimental results and design calculations.

The sensitivity profile may be used to determine the effect of Legendre series truncation for a multigroup P_ℓ cross-section set by examining the sensitivity as a function of the number of expansion terms. Group-dependent choices of the number of Legendre moments used in the angular expansion can be considered for two-dimensional problems.

The sensitivity profile can be integrated over specific energy intervals to give the sensitivity of the result to a constant fractional change in the cross section for reaction type X over the specified energy interval. Using the best estimate of the uncertainties in the data and summing the product of uncertainty and sensitivity then gives the uncertainty in the result due to this reaction type. In the summation, one has to correctly account for correlations of uncertainties in the input data. For radiation transport problems, correlations introduced during cross-section evaluation are "strong" or complete; for example, partial cross sections, such as those for elastic scattering, may be obtained by subtraction of inelastic scattering from the total cross section. Work to date has included only uncorrelated and completely correlated errors.

To generally implement the use of sensitivity functions in predicting the overall uncertainties in radiation shield (or reactor) designs, much more complete and meaningful error or uncertainty information must be incorporated into the data files. Correlations over energy (both local and distant), among reaction types, and among related data for different materials will be required. It is planned that first steps will be taken in incorporating error files in ENDF/B-IV, but they will be far from complete.

Results

Sodium-Iron. A problem of interest for LMFBR's has been examined. The neutron tissue dose was determined after penetration of neutrons from an FTR radial shield simulation through 15 ft of sodium followed by 3 ft of iron. The 50 energy groups used in making the forward and adjoint calculations are tabulated, together with the source spectrum and response functions.

Sensitivity profiles are obtained for the various cross-section reaction types. Each profile shows for each energy group the variation in the neutron tissue dose per unit lethargy for a variation of the indicated cross section. For example, a 1% increase in the iron total cross section in energy group 30 (~19 to 25 keV) leads to a −3% change per unit lethargy interval in the neutron tissue dose after 15 ft of sodium followed by 3 ft of iron. An increase of 1% in the iron elastic cross section for group 40 leads to +0.005% change per unit lethargy in the neutron dose. The absolute change in the dose is obtained in either case by multiplying the change per unit lethargy by the lethargy width of the group in which the cross-section change was made.

The profiles show quantitatively how sensitive the penetration is to the minima in the total cross sections, especially at 24.5 keV in iron and from 1 to 3 MeV in sodium. It should be noted, however, that the detailed structure in the cross-section minima may be masked by the group structure used. If such structure is important as indicated, tailored group structures or point cross sections may be required to adequately represent important cross sections exhibiting marked minima.

Air transport. Other sensitivity results have been obtained for the transport of neutrons and secondary gamma rays through air at a thickness of 2000 m. Neutron-dose profiles for three neutron source spectra (fission, 14-MeV, and thermonuclear) are shown for changes in the total cross sections.[6] A later paper[7] for the same problem gives the energy-integrated sensitivities for 13 partial cross sections for both nitrogen and oxygen. Each of these values was determined from an energy-dependent sensitivity profile.

CTR blanket. An example of the many problems which can be treated with the sensitivity function approach is provided by the calculations of tritium breeding in an assumed geometry for a controlled thermonuclear reactor.[8] The system contains a niobium structure, lithium coolant, and graphite shield. The niobium cross sections are especially uncertain, and sensitivities and profiles were obtained for six geometrical regions and five niobium cross-section types for breeding in both ^{6}Li and ^{7}Li and their sum (90 combinations) from one set of forward and adjoint calculations. The results show little sensitivity (less than 0.2 in the units indicated above) for any of the niobium cross sections. They agree with limited checks made by direct substitution.

Future Developments

For those cases in which linear perturbation theory is inadequate, higher-order approximations may be considered. The simplicity of using the unperturbed adjoint for all cross-section changes is lost, however, and treating error correlations may no longer be practical.

Further use of sensitivity calculations for assessing the accuracy of design calculations will depend upon the availability of error and error correlations for all nuclear data files. In general, all new evaluations of nuclear data should include this information, and the data files should be revised to accommodate it. However, it would be a mistake to underestimate the magnitude of the task of preparing meaningful error files.

Currently, sensitivity methods are being applied to the design of integral experiments for checking radiation-transport calculations. Benchmark experiments, no matter how elegant, are of little value unless they bear reasonable relationship to problems of design interest. Past experiments were designed as (always imperfect) mockups or were based upon intuitive judgments of sensitivities to parameters important in

design. Now such evaluations can be made quantitatively, and the experiments, whether benchmark or simulative, can be designed accordingly.

For some experiment design and many other applications, restrictions to one space dimension and time independence limit the usefulness of the results. Therefore, efforts are under way to extend the sensitivity profile calculations to two dimensions using as a basis the DOT two-dimensional discrete-ordinates code and time dependence using the TDA time-dependent ANISN code.

It is planned to extend the SWANLAKE approach to predictions of LMFBR core performance changes with nuclear-data uncertainties. It is necessary to quantify the apparent great importance of correlations in nuclear-data uncertainties[9] in order to establish the real need for additional nuclear-data measurements and evaluations.

---

1. Paper presented at 16th Meeting of the European-American Committee on Reactor Physics, June 4–8, 1973, Chicago.

2. The research reported in this paper has been jointly supported by the Defense Nuclear Agency, the AEC Division of Reactor Research and Development, and the AEC Division of Controlled Thermonuclear Research.

3. L. N. Usachev, "Perturbation Theory for the Breeding Ratio," *J. Nucl. Energy A/B* **18**, 571 (1964).

4. E. M. Oblow, *General Sensitivity Theory for Radiation Transport,* ORNL-TM-4110 (March 1973).

5. D. E. Bartine, F. R. Mynatt, and E. M. Oblow, *SWANLAKE, a Computer Code Utilizing ANISN Transport Calculations for Cross-Section Sensitivity Analysis,* ORNL-TM-3809 (May 1973).

6. D. E. Bartine, F. R. Mynatt, and E. Oblow, "A Sensitivity Analysis of Neutron and Gamma Transport in Air," *Trans. Amer. Nucl. Soc.* 15(2), 959 (1972).

7. D. E. Bartine, E. M. Oblow, and F. R. Mynatt, "Cross Section Sensitivity Analysis for Discrete Ordinates Calculations," *Trans. Amer. Nucl. Soc.* **16**, 345 (1973).

8. D. E. Bartine, R. G. Alsmiller, Jr., E. Oblow, and F. R. Mynatt, "Cross-Section Sensitivity of Breeding Ratio in a Fusion-Reactor Blanket," *Trans. Amer. Nucl. Soc.* **16**, 8 (1973); see also paper 99.

9. L. N. Usachev and Yu. G. Bobkov, *Planning an Optimum Set of Microscopic Experiments and Evaluations to Obtain a Given Accuracy in Reactor Parameter Calculations,* INDC(CCP)-19/U, English translation of a Russian original (January 1972).

72. FAST REACTOR ANALYTICAL SHIELDING PROGRESS REPORTS, MARCH 1973–SEPTEMBER 1973[1]

Reports written by:
F. R. Mynatt
L. S. Abbott
R. L. Childs[2]
W. W. Engle, Jr.
R. E. Maerker

Work done by:
D. E. Bartine
R. L. Childs[2]
H. C. Claiborne[3]
M. B. Emmett[2]
W. W. Engle, Jr.
G. Haynes[4]
F. B. K. Kam[5]
J. E. Knight[2]
J. Lewin
R. E. Maerker
B. J. McGregor[6]
J. V. Pace III[2]
W. A. Rhoades
T. M. Sims[5]
J. H. Swanks[5]
S. Uchida[7]
L. R. Williams

March and April 1973, ORNL-TM-4400 (February 1974)

Analytical shielding work performed for the fast reactor program during the months of March and April 1973 consisted of several calculations supporting the design of various regions of the FFTF and the analyses of three Tower Shielding Facility experiments. The FFTF studies were for the branch-arm pipe shielding, the FTR radial cavity shield and head compartment, and the HTS pipeway and IHX vault. In addition, the calculation of the power of the stored fuel modules, needed for accurate calculations of other FFTF regions, were repeated for a revised fuel-element composition. The three TSF experiments being analyzed

were performed to study the penetration of neutrons in large thicknesses of sodium, the streaming of neutrons through a mockup of the FTR pipeway, and the production of secondary gamma rays in iron/polyethylene configurations. Of these, the analysis of the first experiment (the sodium-penetration experiment) was completed.

May and June 1973, ORNL-TM-4401 (February 1974)

Analytical shielding work performed for the fast reactor program during the months of May and June consisted of a continuation of the FFTF studies in progress during the March–April period, an analysis of the second phase of the TSF-FTR pipe-chase neutron-streaming experiment, two cross-section sensitivity studies, a continuation of the analysis of the TSF iron/polyethylene secondary gamma-ray experiment, and calculations supporting the use of thermoluminescent dosimeters for gamma-ray heating measurements. The FFTF studies included a general review of the branch-arm pipe shielding; calculations of the penetration of neutrons, secondary gamma rays, and sodium-activation gamma rays through the radial cavity shield and head compartment; design support calculations for the HTS pipeway and IHX vault; and calculations of the stored-fuel power. The first sensitivity study investigated the sensitivity of the calculated neutron tissue dose at the exit face of a large sodium-iron system to all the cross sections used in the calculations, and the second study investigated the sensitivity of the calculated neutron damage to the FTR grid plate to the nickel cross sections used in the calculations.

July and August 1973, ORNL-TM-4402 (November 1973)

Analytical shielding work performed for the fast reactor program during the months of July and August included calculations for both the FFTF and the Demo plant, computer code development, analyses of TSF experiments, and a cross-section sensitivity study of a TSF experiment. Most of the FFTF studies were aimed at determining the effect of various design changes on the dose rates at the maintenance deck during reactor operation – in particular, the effects of penetrations through the radial cavity shield and the effect of a new design for the head temperature control system shield. Gamma-ray dose rates due to the activated sodium coolant were also calculated for two locations in the system: around one of the branch-arm piping shields and near the entrances of the 28-in. and 16-in. coolant lines into the IHX cell. The main Demo plant study was for the lower axial shield region; another study has been initiated to calculate the Demo stored-fuel power and the ex-vessel detector response. The code development consisted in setting forth a set of specifications for the fourth version of the discrete-ordinates code DOT. The TSF experiments that were analyzed were an experiment in which secondary gamma-ray production in iron-polyethylene configurations was investigated and another in which the transmission of the Westinghouse spectrum modifier and 5-in. radial blanket was measured. The sensitivity study was performed to demonstrate that estimates of the accuracy of calculations for the FFTF and Demo plant can be deduced from a sensitivity study of an experimental configuration that only roughly mocks up the real system.

September and October 1973, ORNL-TM-4482 (May 1974)

Analytical shielding work performed for the fast reactor program during the months of September and October consisted of calculations for both the FFTF and the CRBR plants, continued computer code development, the partial analysis of three different TSF experiments, and calculations supporting the design of a new TSR-II beam shield. In the FFTF studies, the combined effect of multiple penetrations through the reactor cavity shield was determined, additional predictions of the ^{24}Na gamma-ray dose rates in the heat exchanger vault were made, and a preliminary three-dimensional calculation of the reactor cavity

fluxes produced by the FTR stored fuel was carried out. In the CRBR studies, predictions were made of the effect of stored-fuel neutrons on the response of the ex-vessel RSP detectors. The code development work centered on selecting features to be included in the DOT-IV code. The analyses for the TSF experiments consisted of calculations of the fission detector responses observed in the TSF-FTR first-fission stored-fuel experiment, calculations of the neutron fluxes measured in the TSF Inconel experiment, and calculations of the energy deposition by ^{60}Co gamma rays in iron (as measured with thermoluminescent detectors). Several calculations were also performed to predict the heating deposition and leakage dose rates associated with a proposed large-beam TSR-II shield.

---

1. Research supported by AEC-LMFBR program.
2. Computer Sciences Division, UCC Nuclear Division.
3. Chemical Technology Division.
4. University of Tennessee.
5. Operations Division.
6. On assignment from the Australian Atomic Energy Commission.
7. On assignment from Hitachi Research Laboratory, Hitachi, Ltd., Hitachishi, Ibaraki-ken, Japan.

73. CALCULATION OF PENETRATIONS IN THE FTR RADIAL CAVITY SHIELD[1,2]

M. B. Emmett[3] W. W. Engle, Jr.
F. R. Mynatt

The DOMINO[4] computer code has been used in the solution of the FTR radial cavity shield problem. These calculations were performed to study the effect of three different major penetrations in the radial cavity shield on the dose rate at the top of the maintenance deck. The DOT-III[5] discrete-ordinates code was run for that portion of the geometry up to the bottom of the radial cavity shield, and a boundary angular flux tape was written. The DOMINO code used this tape and other information from the DOT run to generate tables of probabilities for selecting the source group, position, and direction in a forward MORSE[6] run. Four geometrical configurations, including the SOLID case which has no penetrations, were mocked up using the combinatorial geometry package[7] in MORSE.

Four adjoint DOT cases were run for that portion of the geometry from the maintenance deck down to the top of the radial cavity shield, and the resulting angular flux tapes were processed by DOMINO. The source for the adjoint calculations was either the neutron or gamma-ray flux-to-dose conversion factors. The source was placed at the top of the maintenance deck and was distributed radially from 260 to 450 cm in one pair of cases and from 325 to 400 cm in the second set. The DOMINO tapes generated from these adjoint calculations were used as scoring functions for the MORSE run. Figure 73.1 shows the DOT geometrical mockup in *R-Z* geometry and indicates the positions of the DOMINO coupling surfaces. The result of the analysis is the integrated dose over that surface area occupied by the adjoint source. Because of the existence of multiple DOT adjoints and one MORSE forward run, a collision tape was written for subsequent analysis, with each adjoint DOMINO tape as a scoring function.

Preliminary calculations indicated that the number of boundary crossings occurring in the significant groups and regions was quite small. To limit the amount of machine time required to obtain acceptable statistics, source energy biasing parameters were calculated using fluxes from an adjoint DOT run, and the source position was restricted to the most significant spatial regions.

Table 73.1 gives an indication of the results obtained for each geometry and for both neutron and gamma adjoints. As a result of these calculations, which show a maximum increase of 20% in the integrated dose rate at the maintenance deck, it appears that the penetrations have no significant effect.

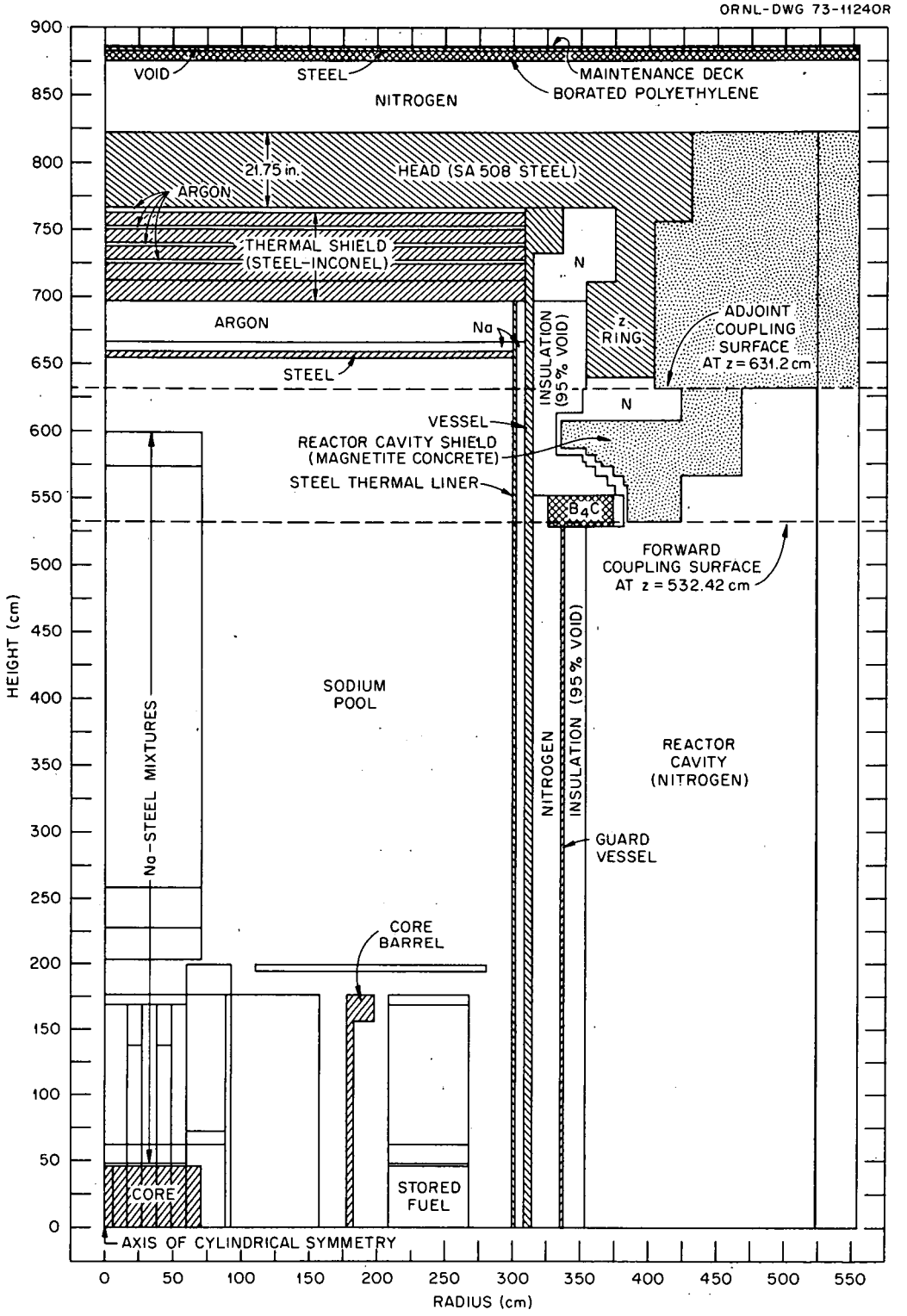

Fig. 73.1. DOT *R-Z* geometry for FTR.

Table 73.1. Typical results of radial cavity shield calculations

Adjoint/geometry (cm)	Integrated dose rate at maintenance deck (cm^2-millirems/hr)				
	Solid		SISI transporter duct, MORSE	16-in. inlet line, MORSE	6-in. overflow line, MORSE
	DOT	MORSE			
GAMMA (260–450)	5.81 + 5[a]	5.82 + 5 (0.06)[b]	6.12 + 5 (0.05)	6.33 + 5 (0.08)	6.61 + 5 (0.14)
NEUTRON (260–450)	7.64 + 5	7.68 + 5 (0.11)	9.25 + 5 (0.06)	8.83 + 5 (0.10)	6.97 + 5 (0.11)
GAMMA (325–400)	3.0 + 5	3.01 + 5 (0.06)	3.02 + 5 (0.05)	3.28 + 5 (0.08)	3.43 + 5 (0.14)
NEUTRON (325–400)	4.65 + 5	4.72 + 5 (0.11)	5.64 + 5 (0.06)	5.4 + 5 (0.10)	4.25 + 5 (0.11)

[a]Read as 5.81×10^5.

[b]Read as 5.82×10^5 with 6% fractional standard deviation.

1. Summary of paper presented at American Nuclear Society Meeting, San Francisco, November 11–15, 1973; *Trans. Amer. Nucl. Soc.* 17, 561 (1974).
2. Research supported by AEC-LMFBR program.
3. Computer Sciences Division, UCC Nuclear Division.
4. M. B. Emmett, C. E. Burgart, and T. J. Hoffman, *DOMINO, a General Purpose Code for Coupling Discrete Ordinates and Monte Carlo Radiation Transport Calculations*, ORNL-4853 (1973).
5. W. A. Rhoades and F. R. Mynatt, *The DOT III Two-Dimensional Discrete Ordinates Transport Code*, ORNL-TM-4280 (1973).
6. E. A. Straker et al., *The MORSE Code – a Multigroup Neutron and Gamma-Ray Monte Carlo Transport Code*, ORNL-4585 (1970).
7. E. A. Straker et al., *The MORSE Code with Combinatorial Geometry*, DNA 2860T (May 1972).

74. CALCULATIONS OF COOLANT-PIPE NEUTRON STREAMING AND SECONDARY COOLANT ACTIVATION IN THE FAST FLUX TEST FACILITY[1,2]

B. J. McGregor[3] F. R. Mynatt
F. B. K. Kam[4] L. S. Abbott

Two series of calculations were performed with the DOT discrete-ordinates code in two-dimensional cylindrical geometry to predict the neutron streaming along the sodium coolant pipes of the Fast Flux Test Facility to the heat exchanger vault. The results were used to predict the sodium activation that could be expected in the heat exchanger, the criterion for the secondary loop sodium being a maximum of 0.06×10^{-9} Ci/cm^3. The first DOT study was performed in the fall of 1972 for the then-current design of the coolant system for the 28-in.-diam pipe penetrations; the second study was performed in February of 1973 for a later design of both the 28-in.-diam and the 16-in.-diam pipe penetrations. The second study was backed up with a few Monte Carlo calculations performed for more realistic three-dimensional geometries to determine the validity of using the symmetrically cylindrical geometry in the DOT calculations. The results indicated that the DOT calculations were conservative and that even with a factor of 10 uncertainty allowed for the full calculation, the sodium activation in the heat exchanger vault would be less than one-third of its allowed value.

1. Abstract of ORNL-TM-4446 (in press).
2. Research supported by AEC-LMFBR program.
3. On assignment from the Australian Atomic Energy Commission.
4. Operations Division.

75. ORNL CROSS-SECTION SENSITIVITY ANALYSIS APPLICATIONS FOR RADIATION SHIELDING[1,2]

D. E. Bartine R. L. Childs[3]
F. R. Mynatt J. V. Pace III[3]
E. M. Oblow J. R. Knight[3]
T. M. Sims[4]

Cross-section sensitivity analysis refers to a determination of how sensitive a calculated quantity or result is to microscopic cross-section data utilized in the calculation. Previous work in this field has employed both direct substitution methods[5-8] and perturbation theory.[9-11] The sensitivity function used in the work discussed here represents an application of earlier perturbation approaches.[12-13] The sensitivity of a result, R, from a discrete-ordinates transport calculation to a particular cross section, x, at energy E may be expressed as

$$P_x(E) = \left\{ \int_{\mathbf{r}} dr \int_{\mathbf{r}} d\Omega\, \rho_x(\mathbf{r}) \left[-\phi^*(\mathbf{r}, \Omega, E)\, \sigma_x(E)\, \phi(\mathbf{r}, \Omega, E) + \int_{\Omega'} d\Omega' \int_{E'} dE'\, \phi^*(\mathbf{r}, \Omega', E')\, \sigma_x(\Omega\cdot\Omega', E \to E')\, \phi(\mathbf{r}, \Omega, E) \right] \right\} \div R\,, \quad (1)$$

where $\phi^*(\mathbf{r}, \Omega, E)$ is the unperturbed adjoint flux, $\phi(\mathbf{r}, \Omega, E)$ is the unperturbed forward flux, $\sigma_x(E)$ is the cross section for reaction type x, $\sigma_x(\Omega\cdot\Omega', E \to E')$ is the differential scattering cross section from angle Ω to Ω' and from energy E to E' for reaction type x, $\rho_x(\mathbf{r})$ is the atomic number density, and R is the integrated response. All of the above quantities are defined for the specific problem under consideration.

R is defined as

$$R = \int_{\mathbf{r}} dr \int_{\Omega} d\Omega \int_{E} dE\, D(\mathbf{r}, \Omega, E)\, \phi(\mathbf{r}, \Omega, E)\,, \quad (2)$$

where $D(\mathbf{r}, \Omega, E)$ is the response function (for example, a flux-to-dose conversion factor) and also the source for the adjoint calculation.

The sensitivity definition of Eq. (1) has been found to be convenient for identification of the most important cross sections for a given problem. A plot of the sensitivity function vs energy is referred to as a sensitivity profile and indicates cross-section importance as a function of the energy of the incident particle. This "fingerprint" of the calculation has many potential uses since it quantitatively focuses attention on the important cross-section data. These uses consist partly of indication of need for specific cross-section evaluation and measurements, the correlation of integral experiments and design problems, and the prediction of overall uncertainty in a design problem.

Equation (1) can also be integrated over the incident energy E to give the total sensitivity of the problem to the cross sections for reaction type x. The effect of Legendre series truncation for a multigroup P_ℓ cross-section set may also be evaluated by examining sensitivity as a function of the number of expansion terms.

This method of analysis is applicable to a wide range of shielding problems and has been used with the one-dimensional discrete-ordinates transport code ANISN[14] for studies involving deep neutron penetration in a sodium-iron system,[15] coupled neutron-gamma transport in air[16] and concrete[17] systems, and neutron transport in a preliminary CTR blanket.[18]

ORNL-DWG 73-12611

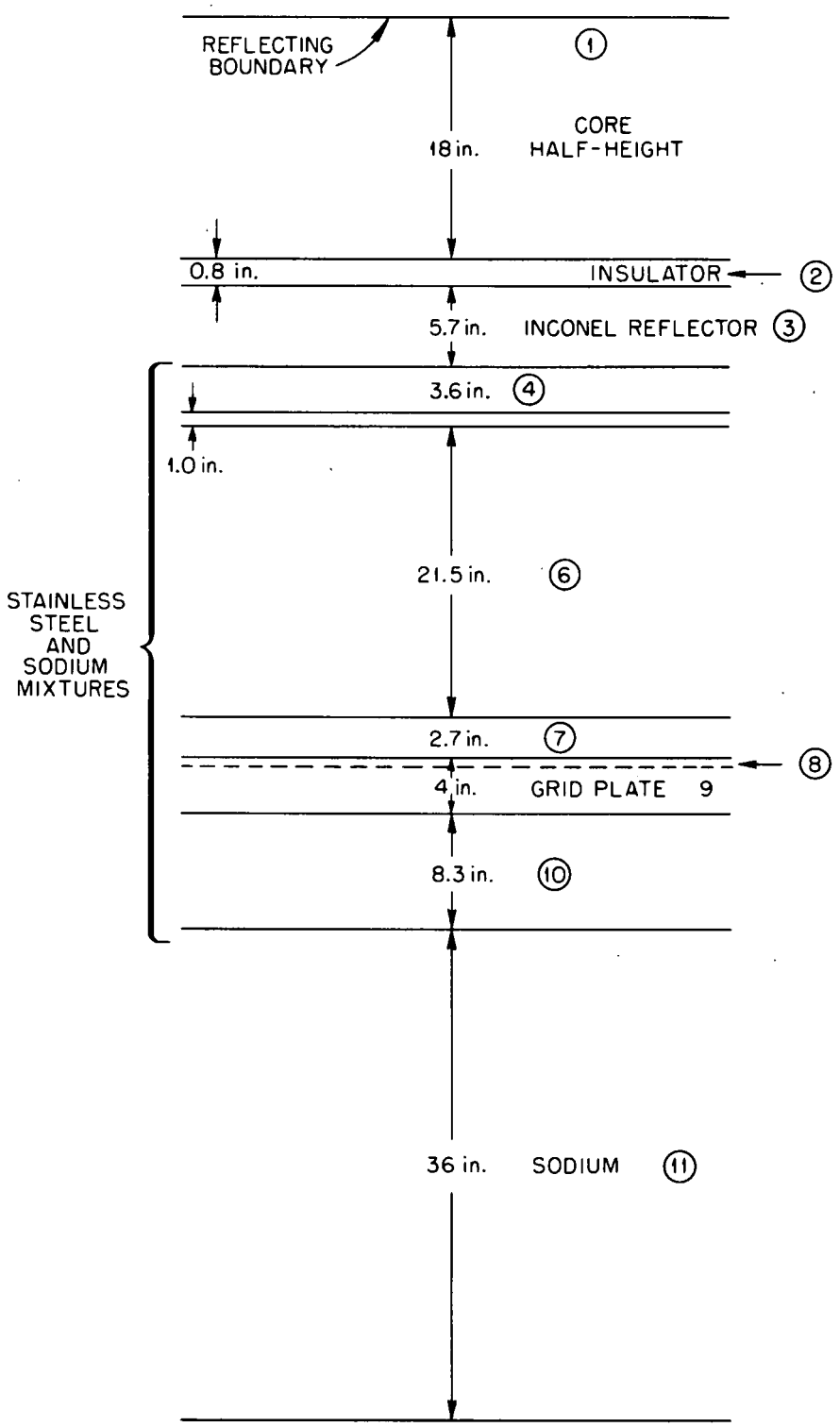

Fig. 75.1. Configuration of the FTR lower axial shield used for one-dimensional slab calculations of neutron damage to the FTR grid plate.

A recent application of interest to the reactor design community is a study of the sensitivity of the calculated neutron-induced damage in the FTR grid plate[19] to nickel cross sections in the lower axial reflector and shield regions as shown in Fig. 75.1. The integral sensitivity of the damage function to all nickel cross sections for this calculation was 1.08 (predicted percent change in calculated damage per percent change in all cross sections). This sensitivity is considered to be low, based on previous studies, but may still be significant in view of the existing uncertainties in nickel cross sections and the need for accurate FTR calculations. As a demonstration of the ability of the sensitivity approach to correlate design calculations with integral experiments, sensitivity studies were performed for an Inconel experimental configuration[20] in which a collimated neutron beam was incident on an assembly consisting of a small spectrum modifier followed by an Inconel slab, and the transmitted neutron spectrum was measured with a neutron spectrometer. A separate sensitivity calculation was made for each of six energy bins which span the energy range covered by the spectrometer. The sensitivity for each energy bin was then normalized to the FTR damage sensitivity in the same energy bin. The resulting normalized flux sensitivity profile (sensitivity per unit lethargy vs energy) is compared with the FTR damage sensitivity curve in Fig. 75.2.

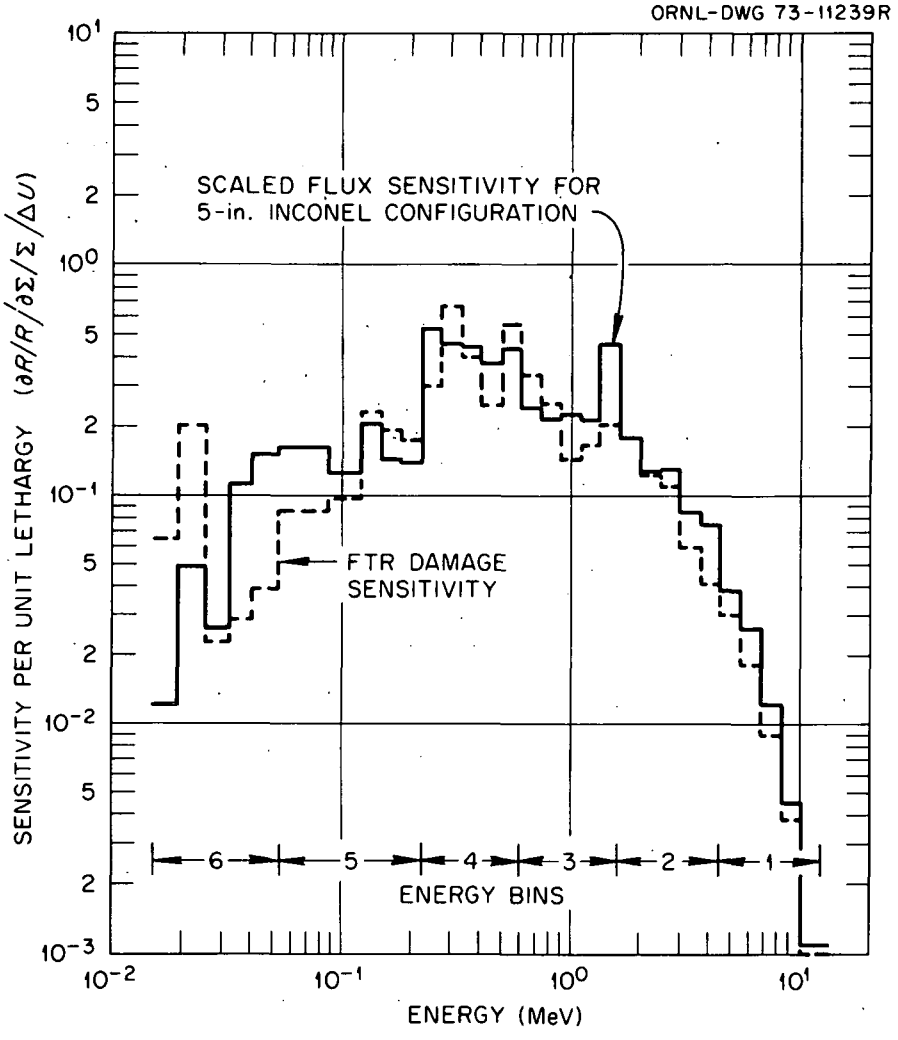

Fig. 75.2. Comparison of FTR grid-plate damage sensitivity to nickel cross sections with the scaled flux sensitivity for an experimental 5-in. Inconel configuration.

The result of this procedure is a weighted response function for the experimental analysis. For this integral response the experiment has approximately the same sensitivity profile as the design problem and is, hence, prototypic in the same sense that one would achieve with an experiment having the same source, configuration, and response function as the design problem. The disagreement between experiment and analysis can then be applied directly to the design problem provided that the dominant uncertainty in the analysis of the experiment is due to cross-section uncertainties rather than other parameters such as geometrical representation.

The full potential of the sensitivity analysis technique will not be realized until the use of the ENDF error files for the prediction of design problem uncertainties is routine and techniques are fully developed to obtain and test error files using integral experiments. Sensitivity analysis routines are being developed for one-dimensional reactor core and two-dimensional shielding problems.

---

1. Summary of paper to be presented at American Nuclear Society Meeting, Atlanta, Ga., September 8–11, 1974.
2. Research jointly sponsored by Defense Nuclear Agency and AEC-LMFBR program.
3. Computer Sciences Division, UCC Nuclear Division.
4. Operations Division.

5. G. E. Hansen and H. A. Sandmeier, *The Effect of Basic Neutron Reaction Cross Sections of Nitrogen (n,n'), (n,2n), (n,γ), (n,p), and (n,α) on High Energy Neutron Penetration in Air,* LA-3810, Los Alamos Scientific Laboratory (1967).
6. E. A. Straker, *Sensitivity of Neutron Transport in Oxygen to Various Cross-Section Sets,* ORNL-TM-2252 (1968).
7. W. E. Preeg, "Flux Sensitivity to Cross-Section Data for Iron and Oxygen," doctoral thesis, Columbia University (1970).
8. S. Hui, D. Spielberg, H. Steinberg, E. S. Troubetzkoy, and M. Kalos, *SAMCEP: An Application of Correlated Monte Carlo to the Simultaneous Solution of Multiple, Perturbed, Time-Dependent Neutron Transport Problems on Complex Three-Dimensional Geometry,* BRL-CR-62, Ballistic Research Laboratories, Aberdeen Proving Ground (1972).
9. L. N. Usachev, "Perturbation Theory for the Breeding Ratio," *J. Nucl. Energy,* A/B 18, 571 (1964).
10. P. C. E. Hemment et al., *The Multigroup Neutron Transport Perturbation Program DUNDEE,* AWRE-040/66, Atomic Weapons Research Establishment, England (1966).
11. D. L. Prezbindowski and H. A. Sandmeier, "The Effects of Cross-Section Inaccuracies on Integral Data," *Trans. Amer. Nucl. Soc.* 11, 193 (1968).
12. D. E. Bartine, F. R. Mynatt, and E. Oblow, *SWANLAKE, a Computer Code Utilizing ANISN Transport Calculations for Sensitivity Analysis,* ORNL-TM-3809 (1973).
13. E. M. Oblow, D. E. Bartine, and F. R. Mynatt, *General Sensitivity Theory,* ORNL-TM-4110 (1973).
14. W. W. Engle, Jr., *A User's Manual for ANISN, a One-Dimensional Discrete Ordinates Transport Code with Anisotropic Scattering,* K-1693, Union Carbide Corp., Oak Ridge, Tenn. (1967).
15. D. E. Bartine, E. Oblow, and F. R. Mynatt, "Sensitivity Analysis: A General Approach Illustrated for a Na-Fe System," *National Topical Meeting on New Developments in Reactor Physics and Shielding,* CONF-720901, vol. 1, p. 512 (1972).
16. D. E. Bartine, E. M. Oblow, and F. R. Mynatt, *Radiation Transport Cross-Section Sensitivity Analysis – a General Approach Illustrated for a Thermonuclear Source in Air,* ORNL-TM-4335 (December 1973); see also paper 91.
17. D. E. Bartine, J. V. Pace III, and J. R. Knight, "A Cross Section Sensitivity Study of Radiation Transport in Concrete," *Trans. Amer. Nucl. Soc.* 18, 381 (1974); see also paper 93.
18. D. E. Bartine, R. G. Alsmiller, Jr., E. M. Oblow, and F. R. Mynatt, "Cross-Section Sensitivity of Breeding Ratio in a Fusion-Reactor Blanket," *Nucl. Sci. Eng.* 53, 304 (1974); see also paper 99.
19. F. R. Mynatt et al., *Fast Reactor Analytical Shielding Progress Report for May and June, 1973,* ORNL-TM-4401 (1973).
20. F. R. Mynatt et al., *Fast Reactor Analytical Shielding Progress Report for July and August, 1973,* ORNL-TM-4402 (1973).

76. AN EVALUATION OF THE ENGINEERING SHIELD DESIGN FOR THE FFTF HEAD COMPARTMENT[1,2]

H. C. Claiborne[3]

The current Westinghouse Advanced Reactor Division (ARD) shield design for the FFTF head compartment was evaluated and found to be generally adequate except in a small area around the drive for the IVHM. This area is amenable to the installation of patch shielding if deemed necessary.

Other problem areas that could develop as a result of underestimation of the dose rates or design changes should be patchable, particularly if one of the primary missions of the steel maintenance floor is considered to be shielding. It represents a potential rack for the installation of patch shielding.

1. Abstract of ORNL-73-8-12 (Aug. 6, 1973).
2. Work supported by AEC-LMFBR program.
3. Chemical Technology Division.

77. THE ORNL LMFBR EXPERIMENTAL SHIELDING PROGRAM[1,2]

C. E. Clifford

The experimental program supporting fast reactor shielding methods development at ORNL can be divided into three major categories. The first of these categories relates to work done in direct support of the FFTF reactor shielding analysis. Five experimental studies were made for the FFTF as follows: (1) studies of grid plate shields consisting of iron and sodium, (2) studies of secondary gamma-ray production in the FFTF top head, (3) studies of neutron streaming in pipe chase configurations, (4) studies of neutron streaming in annular slits in iron shields, (5) studies of the fission rate in fuel storage positions in the FTR shield.

Three major studies have been made to date of shielding problems in the Clinch River Breeder Reactor design. These include (1) a study of the radiation penetration through a simulated radial shield configuration, (2) a study of fission rate at the stored-fuel position in the radial shield, and (3) a determination of the fission rate in a three-dimensional ^{235}U mockup of a stored-fuel experiment in the CRBR radial shield.

In addition to direct project support, there have been basic studies on neutron transport through very thick shields of mild steel, stainless steel, sodium, and boron carbide.

The LMFBR experimental studies have been carried out at the Tower Shielding Facility (TSF) at ORNL by F. J. Muckenthaler, who directs the experimental program, and by L. B. Holland, who operates the TSF. A typical experiment is shown in Fig. 77.1.[3] The neutron source is a spherical 1-MW water-cooled aluminum-uranium reactor approximately 3 ft in diameter. The reactor is usually surrounded by a lead, water, and concrete shield containing a neutron beam port. The absolute energy spectrum and spatial distribution of the beam of neutrons emerging have been carefully measured many times. The shield configuration shown is a simulation of the radial shield for the Clinch River Breeder Reactor. Shield configurations such as this are readily simulated from simple slabs of stainless steel, iron, Inconel, and sodium. The front portion of the configuration contains a "spectral modifier" which alters the neutron spectrum of the beam so that it closely resembles the spectrum leaking from a fast breeder reactor. The modifier consists of the 4 in. of stainless steel, 6 in. of sodium, and 1 in. of Boral that are in front of the blanket in Fig. 77.1. The blanket is simulated by an array of UO_2-filled rods about ½ in. in diameter in a stainless box. The measurements which are routinely taken during these experiments include a determination of the neutron spectrum over the energy region from 10 keV to 20 MeV, a gamma-ray spectral measurement from 200 keV to 11 MeV, and measurements of neutron fluences using Bonner balls and foils. Techniques are being developed for gamma-ray energy deposition measurements.

A typical comparison of the measured and calculated neutron spectra transmitted through 22 in. of iron is presented in Fig. 77.2. The neutron spectra shown here were measured using a Bennet-type hydrogen-filled proportional counter to obtain proton recoil spectra, which were unfolded using the Spect. 4 code developed by Benjamin et al. of the U.K.A.E.C. The calculations were done using the MORSE

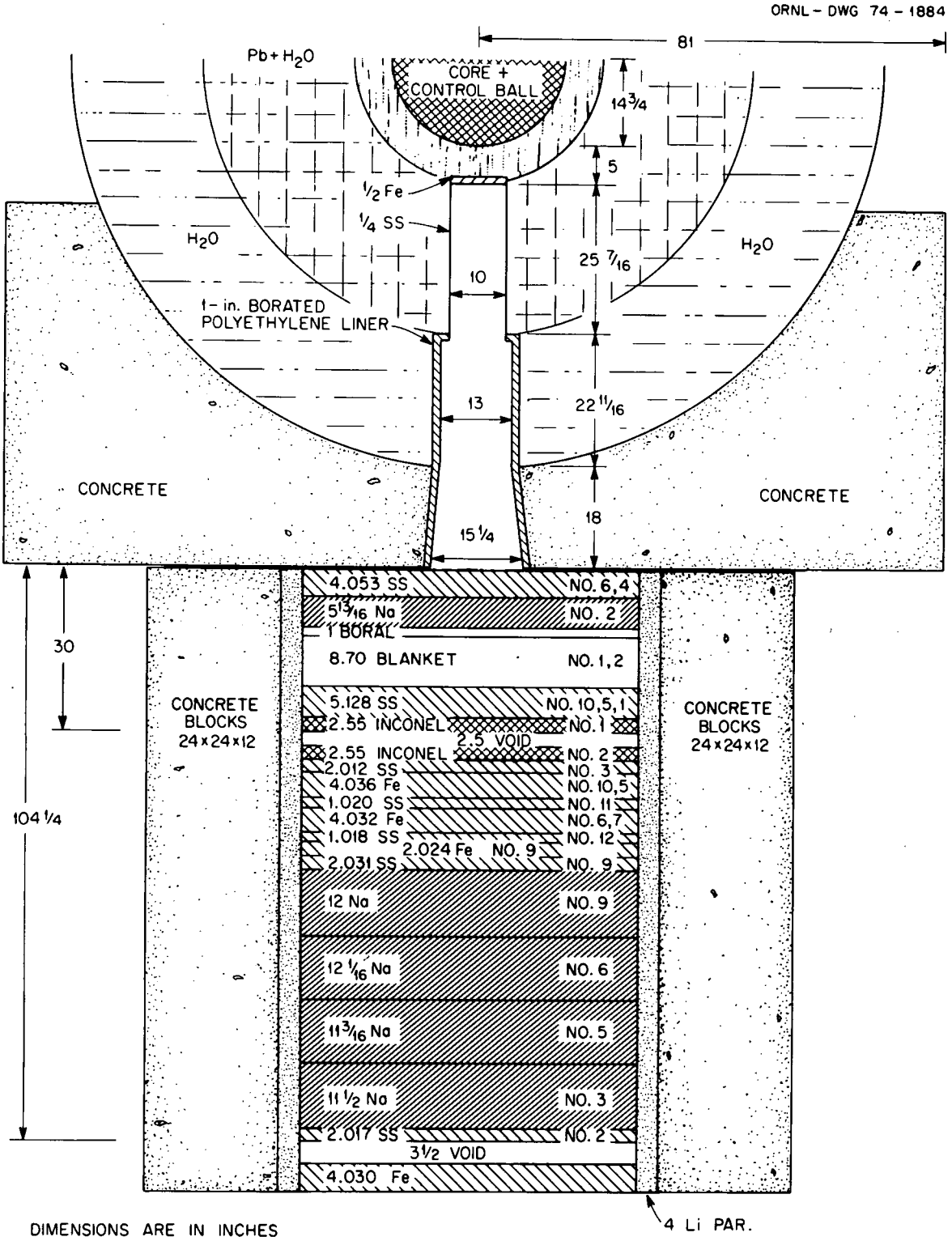

Fig. 77.1. Demo first-fission experiment. Shield configuration 5B, item III-B.

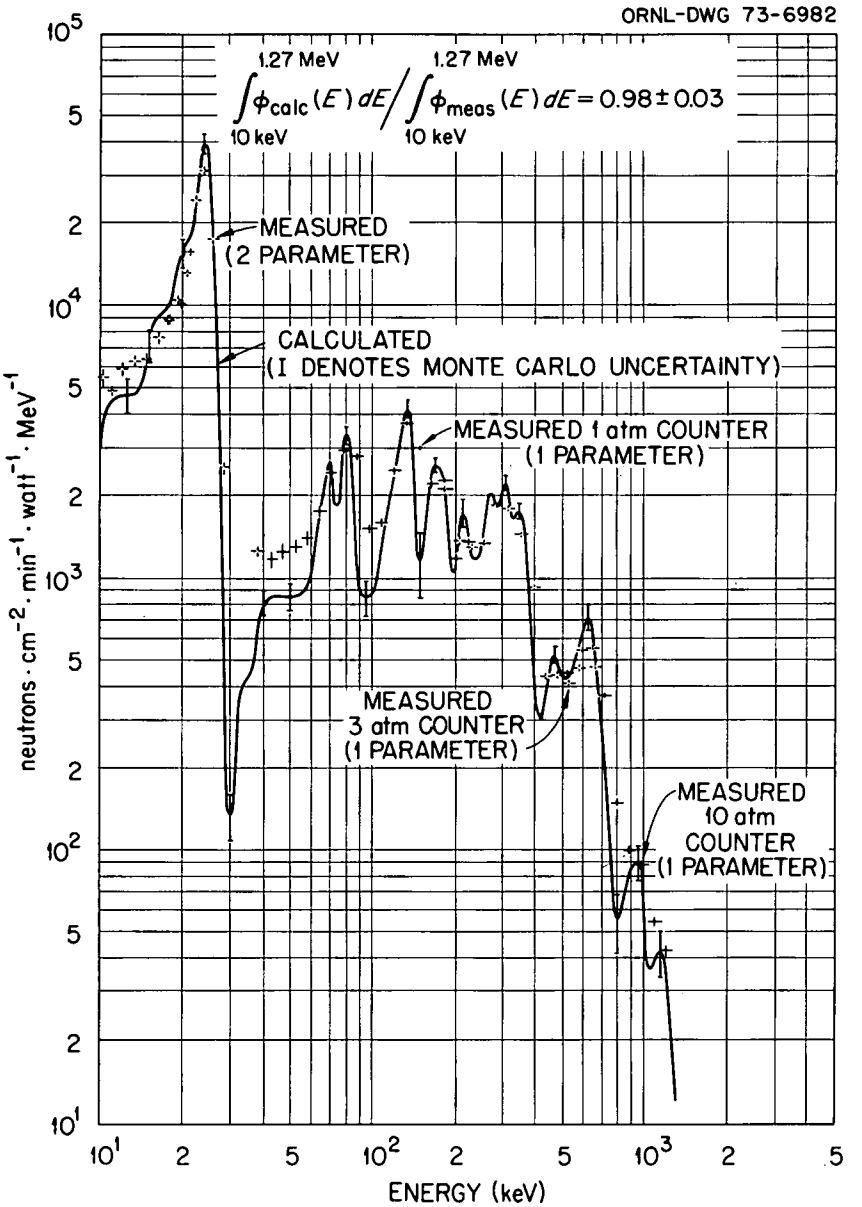

Fig. 77.2. Comparison of MORSE-calculated and measured neutron spectra 18 in. behind 22 in. of iron.

Monte Carlo code and a fine-group cross-section data set (220-group, $1/E_{\sigma_T}$, iron weighted) generated from the ENDF MAT 4180, Mod. 1, data. The excellent agreement resulted only after many measurements were incorporated in the iron total cross sections.

---

1. Paper presented at American Nuclear Society Meeting, Atlanta, Ga., September 8–11, 1974.
2. Work supported by AEC-LMFBR program.
3. C. E. Clifford, F. J. Muckenthaler, P. N. Stevens, and R. M. Freestone, Jr., *Fast Reactor Experimental Shielding Progress Report for January 1974*, ORNL-TM-4592 (May 1974).
4. F. R. Mynatt, *Fast Reactor Analytical Shielding Progress Report for July and August 1973*, ORNL-TM-4402 (November 1973).

78. FAST REACTOR EXPERIMENTAL SHIELDING PROGRESS REPORTS, MAY 1973–FEBRUARY 1974[1]

Reports written by:	Work done by:	T. A. Love
C. E. Clifford	R. M. Freestone, Jr.	J. J. Manning
F. J. Muckenthaler	K. M. Henry	J. N. Money
P. N. Stevens[2]	J. L. Hull	F. J. Muckenthaler
R. M. Freestone, Jr.	F. B. K. Kam[3]	P. N. Stevens[2]
F. B. K. Kam[3]	J. Lewin	

May 1973, ORNL-TM-4284 (July 1973)

This report describes the accomplishments of the ORNL Neutron Physics Division in fast reactor experimental shielding research during May. The Westinghouse and General Electric demonstration plant shielding experiments were essentially completed. The two-parameter hydrogen counter system is described and results compared with earlier single-parameter hydrogen counter data. Additional hydrogen counter measurements were made for comparison with NE-213 results. Uranium foil data are also presented for the Westinghouse radial shield configuration. Some additional measurements designed to improve procedures for determining the background were obtained for the FTR gamma-ray experiments. These latter results differed from earlier measurements by about 20%.

June 1973, ORNL-TM-4343 (August 1973)

This work describes the work done by the ORNL Neutron Physics Division in fast reactor experimental research during June. The results presented include (1) the description and evaluation of two-parameter hydrogen counter spectrum measurements in the energy range 10 to 140 keV, (2) the measurement of gamma-ray heating in a Westinghouse radial shield configuration using thermoluminescent dosimeters, and (3) the calculation and measurement of gamma-ray heating in iron. The latter work was done to evaluate the use of thermoluminescent dosimeters in shielding-type situations.

July 1973, ORNL-TM-4364 (September 1973)

This report describes the work performed by the ORNL Neutron Physics Division in fast reactor experimental shielding research during July 1973. The FTR Inconel experiment was completed during this period and includes shield configurations with Inconel thicknesses of $2\frac{1}{2}$ and 5 in. The experiment was designed to study neutron transport through Inconel and the associated production of secondary gamma rays. Spectral measurements were made with the NE-213 spectrometer and the hydrogen counter, and integral flux measurements with Bonner balls. The gamma-ray spectra were taken with a 5-in. sodium iodide spectrometer. A repeat NE-213 spectral measurement was also performed for the 22-in. iron configuration to resolve a disagreement between the NE-213 and hydrogen counter spectra in the overlap region.

August and September 1973, ORNL-TM-4420 (December 1973)

This report describes the work performed by the ORNL Neutron Physics Division in fast reactor experimental shielding research during August and September 1973. The Fast Test Reactor (FTR) and Demonstration Plant Reactor (Demo) first-fission experiments were completed, which provided data on the fission rate of ^{239}Pu and ^{235}U as a function of shield thickness. Shield mockups for both the FTR and Demo plant reactors were constructed, and plutonium and uranium fission counters were used to obtain

absolute fission rates behind the shields. Experimental results were in disagreement with the results from a parliminary analysis of the experiment. Results were obtained on the effectiveness of a graphite reflector in increasing the counting rate for ex-vessel detectors in both the FTR and Demo configurations. Increases in count rates by factors of about 8.0 resulted in both cases. Also reported are experiments which were intended to evaluate the accuracy of thermoluminescent dosimeters (TLDs). TLD results are compared with calculated results for a ^{60}Co source shielded by iron. Calculations are also compared with spectral measurements using a sodium iodide spectrometer. Two-parameter hydrogen counter data for the Inconel experiment completed in July are also presented, which completes the reporting of the data from Inconel experiments.

October 1973, ORNL-TM-4469 (January 1974)

This report describes the work performed by the ORNL Neutron Physics Division in fast reactor experimental shielding research during October 1973. A program for a total cross-section experimental check was initiated and measurements were performed for the bare beam and 12-in. iron configurations. This experiment was designed to confirm total cross sections primarily in the energy region from 1 MeV to 5 keV for elements of interest to the fast reactor programs. The two-dimensional hydrogen counter neutron spectral data for the FTR and Demo plant stored-fuel experiments are also reported. In addition, gamma spectral measurements were also performed in support of the FFTF gamma-ray experiment. This included a bare beam gamma spectral measurement and a systematic study of side-shield requirements for the 22-in. iron configuration.

November and December 1973, ORNL-TM-4514 (March 1974)

This report describes the work performed by the ORNL Neutron Physics Division in fast reactor experimental shielding research during November and December 1973. The program for a total cross-section experimental check was continued, and NE-213 fast-neutron spectra are reported for the bare beam, a sample of iron 19 in. thick, a 25-in.-thick graphite sample, a 12-in.-thick nickel sample, a 12-in.-thick stainless steel sample, and a 10-in.-thick chromium sample. Low-energy neutron spectra obtained with the hydrogen counter are reported for the 19-in.-thick iron sample and the 12-in.-thick stainless steel sample. Also reported is a brief description of a rod-drop experiment conducted by the Instrumentation and Controls Division of ORNL at the Tower Shielding Facility during the month of December.

January 1974, ORNL-TM-4592 (May 1974)

This report describes the work performed by the ORNL Neutron Physics Division in fast reactor experimental shielding research during the month of January 1974. Additional FTR and Demoplant first-fission measurements were made because of a significant disagreement between earlier measurements and calculated results. Measurements were taken with several ^{235}U fission counters, a bare and a cadmium-covered BF_3 counter, and the 3-in. Bonner ball. A more comprehensive set of shield configurations were analyzed, with two of the configurations being duplicates of experiments conducted during August and September 1973. Care was taken to ensure that the effects of reflected low-energy neutrons from either the ground or the air in back of the shield were eliminated. The new results were found to agree to within about 10% for the two configurations run earlier.

February 1974, ORNL-TM-4611 (June 1974)

This report describes the work performed by the ORNL Neutron Physics Division in fast reactor experimental shielding research during the month of February 1974. The program to verify the accuracy of total cross sections was continued. Single-parameter hydrogen counter spectral measurements and BF_3 radial traverses were made for the bare beam with the beam collimated down to a 1-in. by 1-in. aperture. Single- and two-parameter hydrogen counter measurements were also made with ¼ in. of lead in the bare beam and with ¼ in. of lead plus 1 in. of carbon in the beam. Some difficulties were encountered in the unfolding of the two-parameter data, and these results are not included in this report.

1. Research supported by AEC-LMFBR program.
2. University of Tennessee.
3. Operations Division.

79. ORNL TSF PIPE CHASE NEUTRON STREAMING EXPERIMENT – PHASE 2[1,2]

B. J. McGregor[3] F. J. Muckenthaler

A second ORNL Tower Shielding Facility experiment has been performed and analyzed in the investigation of techniques for predicting the extent of neutron streaming through the sodium coolant pipes of the Fast Flux Test Facility (FFTF). In this second experiment the HTS pipeway of the FFTF was mocked up by a concrete-walled plenum (18 ft by 13.7 ft by 57.5 in.) lined with steel. A beam of reactor neutrons entered through one of the large walls and scattered throughout the plenum. A fraction of the scattered neutrons then entered a 31-in.-diam pipe-chase mockup located near one end of the plenum in the large wall on which the beam was incident. Measurements of neutron intensities were made with Bonner ball detectors along horizontal and vertical traverses within the plenum, and neutron spectra were measured with a Benjamin spectrometer at two locations within the plenum. Bonner ball measurements were also made along the axis of the empty pipe chase and along radial traverses beyond the empty pipe chase outside the plenum. Additional measurements were made beyond the pipe chase containing first a 16-in.-OD sodium-filled pipe and then the pipe surrounded by insulation. For the latter configuration, spectrometer measurements were also made beyond the pipe chase. The analysis consisted of calculations of the Bonner ball and spectrometer responses with the two-dimensional discrete ordinates code DOT-III using 50-group and 14-group cross-section sets and assumptions of both isotropic and anisotropic boundary sources at the pipe-chase entrance. The Monte Carlo codes AMC and MORSE were used to correct the DOT calculations for three-dimensional geometric effects inherent in the experiment. For points inside the plenum, the calculated and experimental Bonner ball responses are in exceptionally good agreement; for points outside the plenum the calculated responses are approximately 20% higher than the experimental results. The calculated and measured neutron spectra agree at all three locations. It is concluded that the same calculational approach would accurately predict, or possibly slightly overpredict, the neutron flux levels that will exist in the heat exchanger vaults of the FFTF.

1. Abstract of ORNL-TM-4283 (in press).
2. Research supported by AEC-LMFBR program.
3. On assignment from the Australian Atomic Energy Commission.

80. FINAL REPORT ON A BENCHMARK EXPERIMENT FOR NEUTRON TRANSPORT IN THICK SODIUM[1,2]

R. E. Maerker R. L. Childs[3]
F. J. Muckenthaler M. L. Gritzner[4]

An experiment concerning deep neutron penetration in sodium is described, and experimental results are presented which provide a basis for verification of the accuracy of sodium cross sections to be used in transport calculations. The experiment was performed at the Tower Shielding Facility of ORNL and included measurements of both the neutron fluence and neutron spectra through a large-diameter sample of sodium up to 15 ft thick. Calculated results for the experiment are presented for comparison with the experimental measurements. These results were obtained using the multigroup Monte Carlo code MORSE and a two-dimensional discrete-ordinates code, DOT III. One-hundred-group data sets were developed from both a preliminary and the final version of the ENDF/III set (MAT-1156) for sodium for use in the calculations. Comparisons of the calculations with experiment indicate that the preliminary version is slightly superior to the final version and that using the preliminary set the total neutron leakage above thermal energies penetrating up through 15 ft of sodium can be calculated to within about 15% and the absolute spectra penetrating up through 12.5 ft of sodium can be calculated to within 20%. Using the final set, the corresponding comparisons are 30% and 60%.

1. Abstract of ORNL-4880 (January 1974); see also *Nucl. Technol.* **22**, 275 (1974) and ORNL-TM-4223 (ENDF-189) (1974).
2. Research sponsored by AEC-LMFBR program.
3. Computer Sciences Division, UCC Nuclear Division.
4. Now with Science Applications, Inc.

81. FINAL REPORT ON A BENCHMARK EXPERIMENT FOR NEUTRON TRANSPORT THROUGH IRON AND STAINLESS STEEL[1,2]

R. E. Maerker F. J. Muckenthaler

An experiment concerning neutron penetration in iron and stainless steel is described, and experimental results are presented which provide a basis for vertification of the accuracy of iron cross sections to be used in transport calculations. The experiment was performed at the Tower Shielding Facility of ORNL and included measurements of both the neutron fluence and neutron spectra through samples of iron up to 3 ft thick and of stainless steel up to 18 in. thick. Calculations of the experiment were performed with a special version of the MORSE multigroup Monte Carlo code which uses point total cross sections. Comparison of the calculations with experiment indicates that the recently evaluated MAT 4180-Mod. 1 iron cross-section set is superior to the older MAT 1101 and MAT 1124 sets. Calculations using this newest set result in total neutron leakages above thermal energies penetrating up to 3 ft of iron or 18 in. of stainless steel that agree with experiment to within about 20%. The calculated leakage spectra above 90 keV arising from scattering through up to 1 ft of iron or 18 in. of stainless steel also agree with experiment to within about 20%. Using any of the three sets, the calculated unscattered component through 1 ft of iron or stainless steel above 1 MeV is only accurate to within about 40%.

1. Abstract of ORNL-4892 (April 1974); see also *Nucl. Sci. Eng.* **52**, 227 (1973).
2. Research sponsored by AEC-LMFBR program.

82. COMPARISONS OF DETAILED MEASURED AND CALCULATED NEUTRON SPECTRA BEHIND THICK SAMPLES OF IRON[1,2]

R. E. Maerker F. J. Muckenthaler

Measurements have been made at the Tower Shielding Facility of neutron spectra in the energy range 10 keV to 1.3 MeV penetrating 22-in.- and 34-in.-thick samples of carbon steel. The detector used was a Benjamin proton-recoil counter with gamma-ray discrimination (i.e., a two-parameter system) in the range 10 keV to 150 keV, and without gamma-ray discrimination (i.e., a one-parameter system) in the range 50 keV to 1.3 MeV. The counter pressures varied between 1 and 10 atm, and good agreement was attained in the overlap regions of the counters. A measurement of the neutron spectrum in the energy region 0.80 to 7 MeV using an NE-213 scintillator was also made behind the 22-in. sample.

Calculations of the absolute spectra were performed with MORSE multigroup Monte Carlo code, using a 220-group set tailored to the total cross-section structure in iron, together with point total cross sections at over 6000 energy points in the range 10 keV to 10 MeV. The downscattering probabilities were handled by the multigroup representation, and the total cross section was sampled within a group from the point data. Iron data based on the latest possible evaluation, MAT 4180-Mod 1, was used.[3] The spectral and angular distribution of the collimated source used in the calculations had been previously measured and described in an earlier experiment.[4] Calculated fluxes at the detector locations were smoothed with the detector resolution functions before compairing with the measured data.[5]

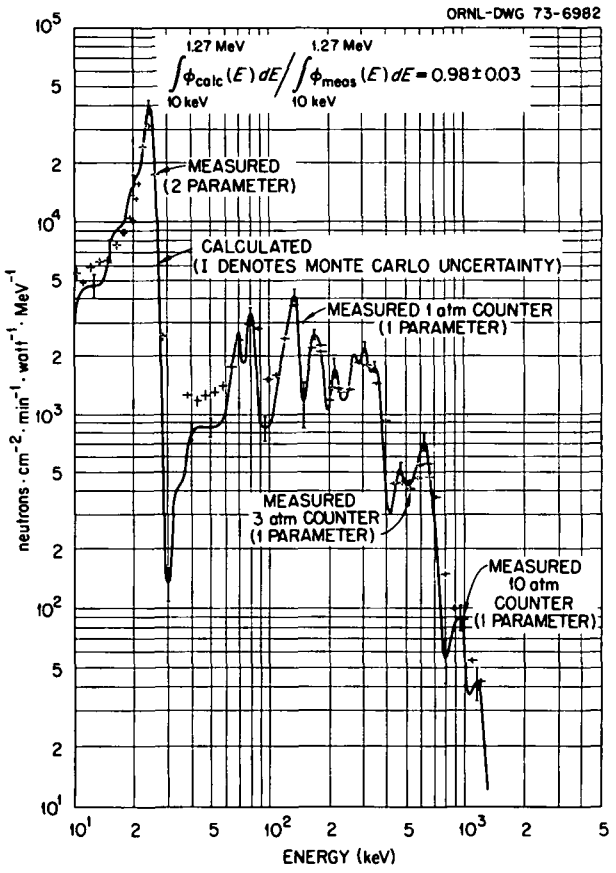

Fig. 82.1. Comparison of calculated and measured spectra behind 22 in. of iron.

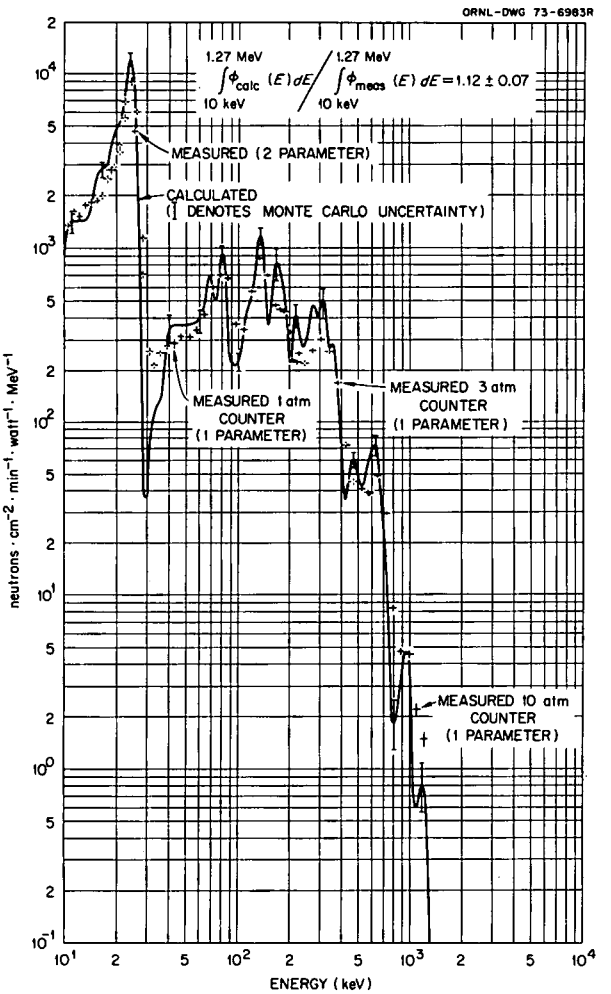

Fig. 82.2. Comparison of calculated and measured spectra behind 34 in. of iron.

Comparisons of the measured and calculated spectra in the range 10 keV to 1.3 MeV are shown in Figs. 82.1 and 82.2. The uncollided contribution at both detector locations was very small (less than 5%), so that the measurements afforded comparisons with calculated slowing-down spectra. It can be seen that, with few exceptions, the MAT 4180-Mod 1 data produce fluxes that agree well with the measurements.

---

1. Summary of paper presented at American Nuclear Society Meeting, San Francisco, November 11–15, 1973; *Trans. Amer. Nucl. Soc.* **17**, 522 (1973).

2. Research sponsored by AEC-LMFBR program.

3. This data set was evaluated by F. G. Perey and includes important changes in the MAT 1180 data set for the total cross sections in the energy range 80 to 500 keV. It will be the basis for version IV of ENDF/B IRON.

4. R. E. Maerker and F. J. Muckenthaler, *The Absolute Neutron Spectrum Emerging through a 15$^1/_4$-in. Collimator from the TSR-II Reactor at the Tower Shielding Facility*, ORNL-TM-4010 (1972).

5. A constant value of 10% FWHM was used for the Benjamin counter system. For the NE-213 system, see R. E. Maerker, *SDT1. Iron Broomstick Experiment an experimental check of neutron total cross sections*, ORNL-TM-3867 (ENDF-166) (Revised), p. 7 (1972).

83. CALCULATION OF ENERGY DEPOSITIONS AND DOSE RATES IN PROPOSED SHIELDING SURROUNDING THE TSR-II REACTOR[1,2]

S. Uchida[3] J. Lewin R. E. Maerker

The spherical distributions of dose rates and energy depositions due to neutrons and gamma rays in several kinds of shields surrounding the TSR-II reactor are presented. The distributions were calculated using ANISN. These results were used to determine an adequate configuration for the proposed new shielding around the TSR-II when an approximately 3-ft-diam collimator is employed.

1. Abstract of ORNL-TM-4450 (December 1973).
2. Research sponsored by AEC-LMFBR program.
3. On assignment from Hitachi Research Laboratory, Hitachi, Limited, Hitachishi, Ibaraki-ken, Japan.

84. EXPERIMENTALLY DETERMINED NEUTRON AND GAMMA-RAY SPECTRA FROM AN ENCAPSULATED CM_2O_3 POWER SOURCE[1,2]

R. M. Freestone, Jr.

The experimentally determined neutron and gamma-ray spectra of a Cm_2O_3 spontaneously fissioning source are presented. The neutron spectrum is given for the energy range 30 keV to 10 MeV, while the gamma-ray spectrum spans the energy range 205 keV to 12 MeV.

1. Abstract of ORNL-TM-4459 (March 1974).
2. Research sponsored by AEC-LMFBR program.

85. TIME-DEPENDENT NEUTRON AND SECONDARY GAMMA-RAY WEAPON OUTPUT, INCLUDING COMPLETE COLLISION KINETICS[1,2]

T. A. Gabriel

A version of MORSE has been developed to incorporate the scattering effect of rapid radial expansion and of high temperature associated with the detonation of a nuclear device on the neutron and gamma-ray leakage spectra. The particular nuclear device considered in these calculations is of the Tamborine type, and the time-dependent system description was obtained from a VERA calculation performed by S^3. All of the neutron and gamma-ray transport calculations were accomplished using a modified version of the time-dependent Monte Carlo code MORSE.[3] The main changes made to MORSE were (1) modifications of the standard spherical geometry routines to accommodate a time-dependent geometry, (2) modifications of the cross-section modules to account for the time-dependent density, and (3) the addition of transformation routines for handling the transformations to and from the rest system and the moving target nuclei at each collision. The coupled neutron and gamma-ray cross sections (75N-18G,P3) were obtained through the use of the code AMPX.[4]

1. Abstract of paper presented at Joint Electromagnetic Pulse Technical Meeting, Air Force Weapons Laboratory, Kirtland Air Force, Base, New Mexico, September 25–27, 1973.

2. Research sponsored by Defense Nuclear Agency.
3. E. A. Straker et al., *The MORSE CODE – a Multigroup Neutron and Gamma-Ray Monte Carlo Transport Code*, ORNL-4585 (1970).
4. N. M. Greene et al., *AMPX: A Modular Code System for Generating Coupled Multigroup Neutron-Gamma Libraries from ENDF/B*, ORNL-TM-3706 (AMPX-1) (to be published).

86. EFFECTS OF AIR-DENSITY PERTURBATIONS ON THE TRANSPORT OF GAMMA RAYS PRODUCED BY POINT GAMMA-RAY SOURCES[1,2]

B. J.McGregor[3] F. R. Mynatt

A series of MORSE Monte Carlo calculations have been performed to determine the effect that changes in the air density produced by one weapon detonation would have on the transport of gamma-ray radiation produced by a second weapon detonated about 1 sec later. The response of interest was the ionization that would be induced in silicon by gamma rays in the vicinity of and beyond the first burst. A gamma-ray emission spectrum was used for the second weapon, and four burst separation distances were considered. The medium was assumed to be infinite air, and spherical geometry was employed with the origin at the center of the second detonation. The changes in density about the first detonation were handled with a pseudocollision technique. Boundary-crossing estimators were used at two radii from the second detonation and within nine solid angles measured from an axis passing through both detonations. Total, uncollided, and time-dependent gamma-ray ionization responses were calculated at each detector position. Total responses calculated for a position in the perturbed air immediately beyond the first burst were about 50% higher than those obtained in unperturbed air; an even greater increase was calculated for the uncollided response, which is a significant portion of the total response at detector positions between 1000 and 1500 m from the source.

The changes in the total ionization due to the perturbations were very similar to the changes in the neutron displacement calculated for a 14-MeV neutron source in a previous study. Changes in the peak ionization rate followed changes in the total ionization for large separation distances but were less for small separations.

1. Abstract of ORNL-TM-4266 (December 1973).
2. Research sponsored by Defense Nuclear Agency.
3. On assignment from the Australian Atomic Energy Commission.

87. CALCULATIONS OF THE PENETRATION OF NUCLEAR WEAPONS RADIATION INTO A MISSILE SILO[1,2]

F. R. Mynatt T. J. Hoffman[3] J. V. Pace III[4] C. E. Burgart[3] L. S. Abbott

A series of calculations have been performed which comprise a study of the vulnerability of missile silos to neutrons and gamma rays streaming through regions of the structure having complex geometries as compared with radiation transmitted through the silo cover. The radiation incident on the silo was obtained from calculations with the two-dimensional discrete ordinates code DOT for a point thermonuclear neutron source in an air-over-ground geometry. Insofar as possible, both the DOT code and the three-dimensional Monte Carlo code MORSE were used to evaluate streaming paths within the silo in order to provide verification through cross-checks. The quantities compared were the ionization induced in silicon by secondary gamma rays produced in the atomsphere and silo structure and the ioniza-

tion and displacement induced by the source neutrons. Most of the comparisons were made at points on the silo axis. The majority of the analysis was on a time-integrated basis, although time-dependent MORSE calculations were performed for the most important streaming problems. This study demonstrated the use of both Monte Carlo and discrete ordinates techniques in the analysis of radiation "streaming" problems in a shielded underground structure.

---

1. Abstract of ORNL-TM-4021 (November 1973); report is classified; abstract is unclassified.
2. Research sponsored by Defense Nuclear Agency.
3. Now with Science Applications, Inc.
4. Computer Sciences Division, UCC Nuclear Division.

88. A ONE-DIMENSIONAL CALCULATIONAL METHOD FOR AN AIR-OVER-GROUND RADIATION FIELD INCIDENT ON AN UNDERGROUND CONCRETE STRUCTURE[1,2]

J. V. Pace III[3] F. R. Mynatt

An approximate method has been developed to calculate the radiation transmitted through the cover shield of an underground structure using a one-dimensional (1-D) air calculation coupled with a one-dimensional (1-D) shield calculation with great savings in computer time over the conventional 2-D calculational approach. In addition, the procedure allows a 1-D sensitivity analysis[4] of an air-over-concrete shield system.

A DOT[5] 2-D calculation on an air-over-ground system with an unclassified thermonuclear source[6] was compared with a 2-D air-over-air (infinite air) calculation. The downward-directed radiation field at various positions on the surface of the ground compared favorably with that of the air-over-air taken at similar positions along an imaginary ground interface. Additionally, from the air-over-ground calculation, the downward-directed fluxes at the ground surface were used in a 2-D calculation of the radiation penetration through 50 in. of concrete at 1500-ft ground range and 1000-ft source height.

Using the results from the 2-D calculation for comparison, a method was devised to transform the 1-D angular fluxes calculated with ANISN[7] for infinite air from a spherical quadrature or coordinate system to a 2-Dcylindrical quadrature or coordinate system. From this transformation, the downward-directed angular fluxes into and underground structure were compared with those of the 2-D calculation, with the following observations: (*a*) the neutron angular fluence was in overall good agreement and (*b*) the gamma-ray fluence deviated from the 2-D calculated fluence by as much as 75% in some groups. However, since the 2-D calculation showed that, for the gamma-ray fluence transmitted through the cover, only 6% originated from sources in the air, the method was still considered to be a good approximation.

The transformed fluences were then available to be input to a DOT cylindrical calculation of the underground structure, or averaged over azimuthal angle and input to an ANISN 1-D calculation. A calculational code identified as SCS (for spherical-to-cylindrical-to-slab) was developed which implemented the second option of the above procedure.

Using this method, neutron responses below a 50-in. concrete lid and at various ground ranges varied from the 2-D calculation by ~10%. Gamma-ray responses were ~20% higher than the 2-D case. The most striking results were that the computer time required to make the 1-D calculation and the resulting transformation of coordinate system was $^1/_{70}$ of that required for a DOT 2-D calculation.

The above comparisons indicate that the method is sufficiently accurate for survey calculations. Moreover, the method is being employed in air-over-concrete sensitivity studies with an adjoint version

being completed. Further refinement of the method will greatly reduce the cost of air-over-ground calculations.

1. Summary of paper presented at American Nuclear Society Meeting, Philadelphia, June 23–27, 1974; published in *Trans. Amer. Nucl. Soc.* **18**, 379 (1974).
2. Research sponsored by Defense Nuclear Agency.
3. Computer Sciences Division, UCC Nuclear Division.
4. D. E. Bartine et al., "A Sensitivity Analysis of Neutron and Gamma Transport in Air," *Trans. Amer. Nucl. Soc.* **15**, 959 (1972).
5. F. R. Mynatt et al., *The DOT III Two-Dimensional Discrete Ordinates Transport Code*, ORNL-TM-4280 (1973).
6. E. A. Straker and M. L. Gritzner, *Neutron and Secondary Gamma-Ray Transport in Infinite Homogeneous Air*, ORNL-4464 (1969).
7. W. W. Engle, *A User's Manual for ANISN – a one-Dimensional Discrete Ordinates Transport Code with Anisotropic Scattering*, K-1693 (Mar. 30, 1967).

89. TRANSPORT CALCULATIONS FOR 14-MeV AND FISSION NEUTRON SOURCES IN AIR/GROUND AND AIR/SEAWATER GEOMETRY[1,2]

J. V. Pace III[3] D. E. Bartine

Calculations have been made for 14-MeV and fission neutron sources in air/ground and air/seawater geometries using ENDF/B Version IV cross sections in 22 neutron groups and 18 gamma-ray groups. The air/ground calculations at various source heights were made available for use in the ATR data base[4] in order that results from updated cross sections, especially those for gamma production, are incorporated in that system. The air/seawater calculation was made at only one source height. Results show that the seawater and ground exhibit approximately the same effects near the ground for neutron and gamma doses from the 14-MeV source. However, for the fission source the seawater reduces the neutron dose and enhances the gamma dose when compared with the air/ground.

The calculations were performed with the DOT code using cylindrical geometry. The cylinder had an upper 1300-m-high region of air and a lower 50-cm-deep region of ground or seawater. The maximum horizontal range was 1500 m, and the source height was fixed at 50 m. The principal results obtained were the Henderson neutron and gamma-ray tissue doses at a height of 0.5 m above the air/ground or air/seawater interface. This study showed that the weighted diamond-difference option in DOT III gave much better results than the diamond-step option used in previous calculations.[5,6]

Neutron dose for the air/seawater due to the 14-MeV source was lower than the air/ground by 10% directly beneath the source and lower by 25% at 1500 m. The gamma dose was approximately 5% higher for the entire 1500 m. The hydrogen in the seawater thermalizes more neutrons, thereby lowering the neutron dose but increasing the gamma dose due to thermal capture.

The neutron dose from the fission source for the air/seawater was from 25% to 30% lower than the air-/ground dose. However, from Fig. 89.1, the gamma-ray dose for the air/seawater was higher than the air/ground by 300% directly beneath the source to 8% at 1500 m. The hydrogen effect is also noticed here; however, the large difference in the gamma dose was found to be due to the thermal capture gammas produced from the trace of chlorine found in the seawater.

The above comparisons indicate the effect hydrogen plays in reducing the neutron dose near the interface of air/seawater. But more important is the fact that the small amount of chlorine present in the seawater has a tremendous effect on the gamma dose at the air/seawater interface.

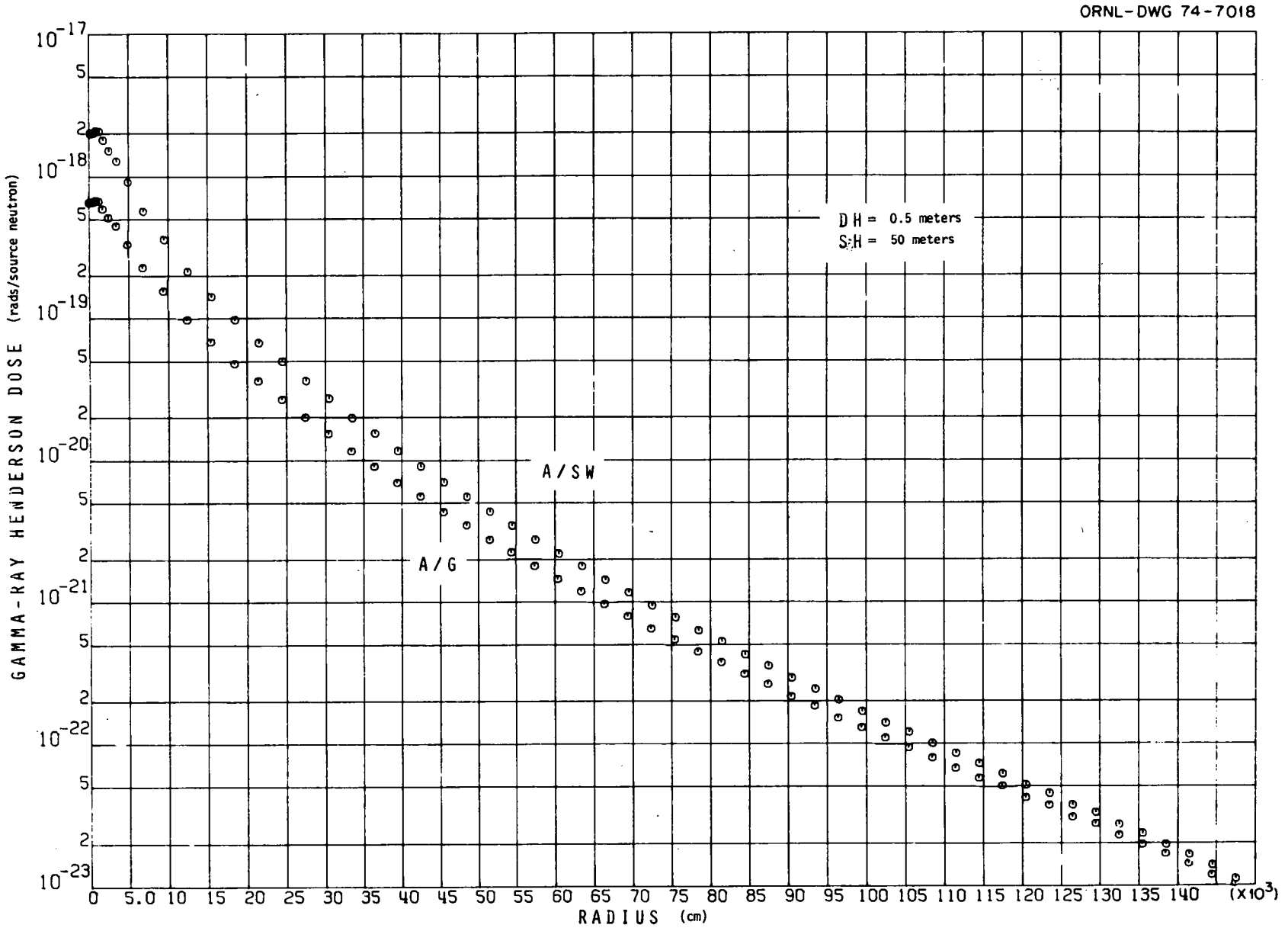

Fig. 89.1. Air-over-ground dose vs air-over-seawater dose. Weapons fission source.

1. Summary of paper to be presented at American Nuclear Society Meeting, Washington, D.C., October 27–November 1, 1974.
2. Research sponsored by Defense Nuclear Agency.
3. Computer Sciences Division, UCC Nuclear Division.
4. L. Huszar, L. J. Nesseler, and W. A. Woolson, *Users' Guide to Version 2 of ATR (Air Transport of Radiation)*, DNA 3144Z (SAI-73-534-LJ) (April 1973).
5. E. A. Straker and M. L. Gritzner, *Neutron and Secondary Gamma Ray Transport in Infinite Homogeneous Air*, ORNL-4464 (December 1969).
6. E. A. Straker, "The Effect of the Ground on the Steady-State and Time-Dependent Transport of Neutrons and Secondary Gamma Rays in the Atmosphere," *Nucl. Sci. Eng.* **46**, 334 (1971).

90. TIME-DEPENDENT NEUTRON AND SECONDARY GAMMA-RAY TRANSPORT IN THE ATMOSPHERE – SENSITIVITY TO CROSS SECTIONS[1,2]

F. R. Mynatt

Recent studies have been performed to test the effects of cross-section data on neutron and secondary gamma-ray transport in the atmosphere. In one of these studies the time-dependent ANISN code (TDA) was used to calculate the radiation environment in infinite air using the ENDF III air cross sections, an older ORNL set, and a combination with the neutron part from ENDF III and the secondary gamma-ray part from the ORNL set. Results were intercompared for a large variety of source spectra and response functions. The consequences of cross-section updating on many calculations performed with the older set can be judged by referring to these intercomparisons. As an example, for a 14-MeV instantaneous source, the air ionization from secondary gamma rays at a range of 1000 m using ENDF III data is a factor of 2 lower at the peak rate ($t \sim 10^{-5}$ sec), the results for the two data sets cross at 4×10^{-5} sec, and the thermalization-induced peak at late times ($10^{-4} < t < 10^{-1}$ sec) is of markedly different shape for the different data sets.

A more comprehensive means of determining the effect of cross-section data errors on transport problems has been developed based on the perturbation theory method of sensitivity analysis. For a given problem, the forward and adjoint flux solutions are used to construct the energy-dependent sensitivity function $S_i(E)$. The fractional change in the answer of the transport problems is given by the product of $S_i(E)\,dE$ and the fractional change in the ith cross section over the energy interval dE. The sensitivity function itself is used to understand the problem in terms of which cross sections and energy ranges are important. The total error or variance of the problem is given by the sensitivity function convoluted with the cross-section errors and summed in a manner such that the correlations of the data errors are treated correctly. The present sensitivity code is used with the one-dimensional steady-state transport code, ANISN, although extension to time dependence and two space dimensions is straightforward. The present sensitivity code has been applied to several air transport problems.

1. Abstract of paper presented at Joint Electromagnetic Pulse Technical Meeting, Air Force Weapons Laboratory, Kirtland Air Force Base, New Mexico, September 25–27, 1973.
2. Research sponsored by the Defense Nuclear Agency.

91. RADIATION TRANSPORT CROSS-SECTION SENSITIVITY ANALYSIS – A GENERAL APPROACH ILLUSTRATED FOR A THERMONUCLEAR SOURCE IN AIR[1,2]

D. E. Bartine E. M. Oblow F. R. Mynatt

A general approach to radiation transport cross-section sensitivity analysis is introduced and its applicability demonstrated for a problem involving neutron and gamma-ray transport in air. The basis for the method is generalized perturbation theory using flux solutions to the transport equation and its adjoint. Both an analytical aspect of the technique, designed for surveying the sensitivity of a result to the entire cross-section data field, and a predictive aspect, designed for predicting the effect of changes in the data field, are presented. The analytic procedure is demonstrated by results that include a determination of important energy regions in the total, partial, and gamma-ray-production cross sections of nitrogen and oxygen for deep-penetration calculations of tissue dose in air. The predictive capability is illustrated for specific cross-section perturbations in the system and the effects of truncating the Legendre expansion of the scattering kernel. In addition, the applicability of the method for predicting variances in a calculated result arising from cross-section data uncertainties is demonstrated. In the sample case, the variance in the total neutron-gamma tissue dose is estimated from preliminary cross-section error files given in the evaluations of the nitrogen and oxygen cross sections.

---

1. Abstract of ORNL-TM-4335 (December 1973); also of paper published in Nucl. Sci. Eng. 55 (1974).
2. Research supported by Defense Nuclear Agency.

92. SELECTION OF GROUP ENERGY BOUNDARIES USING SENSITIVITY THEORY[1,2]

E. Oblow J. Ching* J. Drischler

Considerable interest has been generated recently in selecting a fine-group structure suitable for creating a multigroup cross-section library applicable to a wide range of problems.[3] In addition to these developments, there has always been an interest in reducing the number of energy groups needed to solve particular design problems without sacrificing accuracy or spectral detail beyond reasonable limits. With the successful development of sophisticated methods for sensitivity analysis,[4] an attempt has been made to use the sensitivity approach to develop an automated scheme for selecting multigroup energy boundaries so as to minimize the energy groups required to solve a specific problem. The scheme chosen is related to the importance sampling concept in Monte Carlo calculations. That is, the group boundaries are selected for a problem or class of problems so that the reaction rate, biased by an importance function, is divided equally among the energy groups. In the terminology of sensitivity theory, each energy group is chosen to be equally sensitive in absolute magnitude to the multigroup cross-section data.

To determine the information needed in group boundary selection, a superfine point-energy sensitivity code, combining the transport solution capabilities of MOMANS[5] and the sensitivity calculations of SWANLAKE,[6] has been developed. The code produces a superfine (approximately 1000-point energy grid) total cross-section sensitivity profile for the particular problem being optimized (a problem being defined by a unique geometrical configuration, material composition, source, and response). From this result, a probability function for the cumulative area under the sensitivity profile as a function of energy is generated. A series of optimum group energy boundaries are then chosen from the probability curve

Table 92.1. Optimum 50-group energy boundaries for several problems of neutron transport through iron spheres

Group number	Upper Boundary Energy (MeV)		
	r = 23 cm, 14-MeV source	r = 60 cm, Fission source	r = 100 cm, Fission source
1	1.5000E+01[a]	1.5000E+01	1.5000E+01
2	1.4889E+01	1.9984E+00	1.2579E+00
3	1.4848E+01	1.3461E+00	9.9141E−01
4	1.4815E+01	1.1233E+00	8.2532E−01
5	1.4782E+01	9.8325E−01	6.8515E−01
6	1.4736E+01	8.7740E−01	6.4119E−01
7	1.4656E+01	7.0352E−01	5.4865E−01
8	1.4450E+01	6.2019E−01	4.8238E−01
9	1.3821E+01	5.7343E−01	4.4871E−01
10	2.3850E+00	5.2600E−01	3.9094E−01
11	1.8076E+00	4.7250E−01	3.7584E−01
12	1.5026E+00	4.0643E−01	3.5916E−01
13	1.3658E+00	3.6790E−01	3.4966E−01
14	1.2143E+00	3.4869E−01	3.3150E−01
15	1.1750E+00	3.3198E−01	3.2019E−01
16	1.1087E+00	2.9453E−01	2.8924E−01
17	1.0182E+00	2.7330E−01	2.8009E−01
18	9.5226E−01	2.4901E−01	2.7310E−01
19	8.6083E−01	2.2324E−01	2.4762E−01
20	7.9465E−01	2.0685E−01	2.2085E−01
21	7.1195E−01	1.7799E−01	1.8990E−01
22	6.9979E−01	1.6695E−01	1.7886E−01
23	6.7305E−01	1.5630E−01	1.7085E−01
24	6.5425E−01	1.3773E−01	1.5731E−01
25	6.4482E−01	1.2556E−01	1.4309E−01
26	6.3237E−01	1.1686E−01	1.3905E−01
27	6.1618E−01	1.0587E−01	1.3249E−01
28	6.0273E−01	8.4997E−02	1.1753E−01
29	5.8576E−01	8.0043E−02	9.3104E−02
30	5.5886E−01	7.1203E−02	8.3664E−02
31	5.3631E−01	6.7687E−02	7.9315E−02
32	4.9796E−01	5.9130E−02	7.0841E−02
33	4.6950E−01	4.6911E−02	5.8719E−02
34	3.8418E−01	3.5187E−02	3.7270E−02
35	3.7128E−01	2.5386E−02	2.6701E−02
36	3.5353E−01	2.4813E−02	2.5366E−02
37	3.4311E−01	2.4282E−02	2.4718E−02
38	3.1355E−01	2.3811E−02	2.4104E−02
39	3.0634E−01	2.3325E−02	2.3543E−02
40	2.9271E−01	2.2785E−02	2.2961E−02
41	2.7041E−01	2.2193E−02	2.2328E−02
42	2.4594E−01	2.1559E−02	2.1620E−02
43	2.1880E−01	2.0878E−02	2.0843E−02
44	1.8418E−01	2.0130E−02	1.9980E−02
45	1.6695E−01	1.9285E−02	1.8958E−02
46	1.3757E−01	1.8320E−02	1.7735E−02
47	1.2298E−01	1.7211E−02	1.6238E−02
48	8.1949E−02	1.5919E−02	1.4664E−01
49	3.3244E−02	1.4361E−02	1.2732E−02
50	2.2355E−02	1.2514E−02	1.1119E−02
51	1.0000E−00	1.0000E−02	1.0000E−02

[a]Read as 1.5×10^1 MeV.

so as to have equal sensitivity in each group. Multigroup calculations for the original problem are made with the optimum sets, and comparisons are made with the responses in the original fine-point calculation. An optimum set for any given error requirement can then be chosen from these results. Group boundaries are easily selected for minimizing the error in a class of problems by simply making linear combinations (appropriately weighted) of the cumulative sensitivity curves for a particular set of problems and selecting a grid from the weighted union of all the curves.

As a demonstration of the usefulness of the method, a series of problems involving transport in iron were studied. Group selection for this material has been a particularly difficult problem in the past because of the cross-section structure in the keV range, particularly the existence of a large number of total cross-section minima. The problems calculated were boundary fluence responses (from 10 keV and 14 MeV) for a 14-MeV source in a 23-cm iron sphere and fission sources in 60-cm and 100-cm spheres. In all cases, the point sensitivity calculations used more than 600 energy points to represent the cross-section detail in the keV range.

The optimum boundary response results were rather remarkable, since it was found that the boundary fluence responses could be calculated to about 10% with less than 50 groups and as few as 10 groups in the range 10 keV to 14 MeV. For the 14-MeV source problem, the group structure was more detailed around 14 MeV, while for the 60-cm and 100-cm fission source problems the grid was finer in the vicinity of the 24-keV total cross-section minimum and several higher energy minima in the keV range. Table 92.1 shows the optimized 50-group boundaries for the three problems. A union of the group structures containing about 50 groups appears to be sufficient to calculate fluences out to 100 cm in iron from both a 14-MeV and a fission source to about 10% accuracy. In addition to the accuracy achieved, the group selection process has the desirable property of generating fine energy detail in the most important energy regions of the flux spectrum, as well as converging uniformly to the exact result when increasing the number of groups.

It may be generally concluded that if accurate sets with as few as 10 groups are possible in other problem areas, it should be quite practical to choose a few hundred group boundaries for a multigroup library which will have guaranteed accuracy in calculating a fair number of different problems.

---

1. Summary of paper presented at American Nuclear Society Meeting, San Francisco, November 11–15, 1973; *Trans. Amer. Nucl. Soc.* **17**, 547 (1973).
2. Research sponsored by Defense Nuclear Agency.
3. C. R. Weisbin and R. T. LaBauve, *Specifications of a Generally Useful Multigroup Structure for Neutron Transport*, LA-5277-MS (May 1973).
4. E. M. Oblow, D. E. Bartine, and F. R. Mynatt, *General Sensitivity Theory for Radiation Transport*, ORNL-TM-4110 (March 1973).
5. J. Ching, E. Oblow, and H. Goldstein, "A Discrete Energy Formulation of S_n Transport Theory," *Trans. Amer. Nucl. Soc.* **14**, 335 (1971).
6. D. E. Bartine, F. R. Mynatt, and E. M. Oblow, *SWANLAKE–a Computer Code Utilizing ANISN Radiation Transport Calculations for Cross Section Sensitivity Analysis*, ORNL-TM-3809 (May 1973).

*University of Tennessee.

93. A CROSS-SECTION SENSITIVITY STUDY OF RADIATION TRANSPORT IN CONCRETE[1,2]

D. E. Bartine J. V. Pace III[3]
J. R. Knight[3]

The purpose of this investigation was to determine the sensitivity of calculated neutron and gamma-ray responses at the exit face of a concrete slab to the cross sections used in the transport calculations. The source incident on the concrete slab was a neutron and gamma-ray spectrum calculated at 500 m in air from

a typical thermonuclear source.[4] The 50-in. concrete slab had a composition by atom fraction of 0.52 oxygen, 0.19 silicon, 0.14 hydrogen, 0.04 calcium, 0.04 aluminum, and 0.07 iron, where the iron is a homogeneous representation of reinforcing rods present in the slab. Calculations were made for neutron ionization, neutron displacement, and gamma ionization responses[5] with the one-dimensional discrete ordinates code ANISN,[6] and the sensitivity of each of these calculated responses to the cross sections used in the concrete transport was determined with the SWANLAKE[7] code. A 129-42 coupled neutron-gamma cross-section set was formed from ENDF/B-III data for these calculations. The energy group structure was selected to fit important minima in the neutron total cross sections and important gamma production lines.

Table 93.1 shows the sensitivity of the calculated neutron ionization response to cross sections used in the calculation as a function of element and reaction type. More detailed analysis indicates that the second inelastic levels for oxygen and silicon, inelastic continuum for iron, oxygen (n,α), and silicon (n,p) and (n,α) reactions are especially significant. Sensitivities for the neutron displacement response showed essentially the same trends but indicated increased sensitivity to the hydrogen elastic cross sections and decreased sensitivity to the oxygen inelastic cross sections, probably because lower-energy neutrons have a greater importance for the neutron displacement response than for the neutron ionization response. An investigation of the variation of the neutron ionization response sensitivity with energy shows the dominance of oxygen, with low sensitivity in energy regions where the oxygen total cross section is large and high sensitivity in the energy regions in which the oxygen total cross section is small. In the energy regions corresponding to the oxygen cross-section minima, the sensitivity of the calculated responses to the cross sections for the other elements, especially silicon and hydrogen, becomes dominant. At these energies the low probability of neutron interaction with oxygen increases the probability of interaction with other elements and therefore increases the sensitivity of the response to their cross sections.

The sensitivity of the calculated gamma-ray ionization response to neutron transport (including gamma-ray production) and to gamma transport cross sections was also determined. The results show that with regard to neutron transport cross sections, the gamma-ray ionization response is primarily sensitive to oxygen and silicon at high energies, to hydrogen at intermediate to low energies, and to iron in the thermal energy range. This calculation was also quite sensitive to oxygen, silicon, and iron high-energy gamma transport cross sections. Analysis of the significance of various gamma-ray production mechanisms indicated that 87% of the gamma-ray ionization response was due to gammas produced in concrete by thermal capture, with 71% produced by thermal capture in iron.

In summary, for this problem the calculated neutron ionization, neutron displacement, and gamma-ray ionization responses are quite sensitive to the concrete cross sections. Neutron transport is especially

Table 93.1. Sensitivity of calculated neutron ionization to cross sections for concrete constituents

Cross section	Sensitivity[a]						Total (concrete)
	O	Si	H	Ca	Al	Fe	
Total	−4.71	−2.83	−1.59	−0.78	−0.52	−1.45	−11.88
Elastic	−2.95	−0.55	−1.59	−0.23	−0.14	−0.24	−5.70
Inelastic	−1.01	−1.40		−0.17	−0.32	−1.09	−3.99
Absorption	−0.75	−0.88	−0.00	−0.38	−0.06	−0.09	−2.16
$(n,2n')$		−0.00		0.00	0.00	−0.03	−0.03

[a]Sensitivity values may be viewed as predicted percent change in the neutron ionization per percent increase at all energies for a given cross section.

sensitive to high-energy oxygen and, to a lesser extent, silicon cross sections. Gamma-ray production for this problem is dominated by thermal capture, especially in iron, and the gamma-ray transport cross sections are unusually important.

---

1. Summary of paper presented at American Nuclear Society Meeting, Philadelphia, June 23–27, 1974; *Trans. Amer. Nucl. Soc.* 18, 381 (1974).
2. Research sponsored by Defense Nuclear Agency.
3. Computer Sciences Division, UCC Nuclear Division.
4. E. A. Straker and M. L. Gritzner, *Neutron and Secondary Gamma-Ray Transport in Infinite Homogeneous Air*, ORNL-TM-4464 (1969).
5. W. W. Engle, Jr., and F. R. Mynatt, *Time-Dependent Neutron and Secondary Gamma-Ray Transport in Infinite Homogeneous Air – Comparison of Two Cross Section Sets*, ORNL-TM-3932 (1972).
6. W. W. Engle, Jr., *A User's Manual for ANISN, a One-Dimensional Discrete Ordinates Transport Code with Anisotropic Scattering*, K-1693, Union Carbide Corp., Oak Ridge, Tenn. (1967).
7. D. E. Bartine, F. R. Mynatt, and E. Oblow, *SWANLAKE, a Computer Code Utilizing ANISN Transport Calculations for Sensitivity Analysis*, ORNL-TM-3809 (1973).

94. MONTE CARLO ANALYSIS OF NEUTRON AND GAMMA-RAY TRANSPORT IN CONCRETE[1,2]

G. W. Morrison[3] L. M. Petrie[3]
F. R. Mynatt

To evaluate the calculational techniques of radiation transport codes for neutron and secondary gamma-ray transport in concrete, several calculations have been performed to compare with the experimental studies[4,5] performed at Gulf General Atomic (GGA) for neutron and gamma-ray penetration through thick slabs of concrete. A special session, "Fast-Neutron and Secondary Gamma-Ray Transport through Concrete," was held at the ANS 1971 Winter Meeting to present the results of the calculations performed by the various organizations.[6–8] A significant result of the comparisons was the overall underprediction of the time-dependent gamma count rates by the different codes, with the late-time (3 to 50 μsec) count rates having the largest discrepancy.

A major calculational effort was undertaken to determine the reasons for the discrepancy and to suggest improvements for the calculational models. This effort included several two-dimensional DOT[9] calculations as well as several Monte Carlo sensitivity calculations. The culmination of this work indicated several improvements that should be made in the O6R-OGRE calculational model. Among the improvements made to the model were an improved thermal scattering treatment and the explicit representation of the large NE-213 detector in the model geometry. The time-integrated DOT calculations showed that reflection from the detector produced large perturbations in the thermal spectra inside the concrete. The single-velocity thermal treatment in O6R was replaced with a continuous velocity model in which the velocity of the target nucleus is determined by sampling a Maxwell-Boltzmann distribution of a specified temperature. Improvements were also made to the analysis routines, in which a track-length estimator was added. Finally, the latest evaluated cross sections from the current DNA Working Cross Section Library[10] were used in the calculations. This includes a revised gamma production matrix which consisted of 18 gamma groups determined by a sensitivity analysis.[11]

The results of the calculations indicate that the agreement between the experimental and calculated gamma count rates has been greatly improved. Figure 94.1 shows the comparison between the measured and calculated gamma-ray count rates for the 40.64-cm slab. Other slab thickness calculations will be discussed.

ORNL-DWG 73-11691

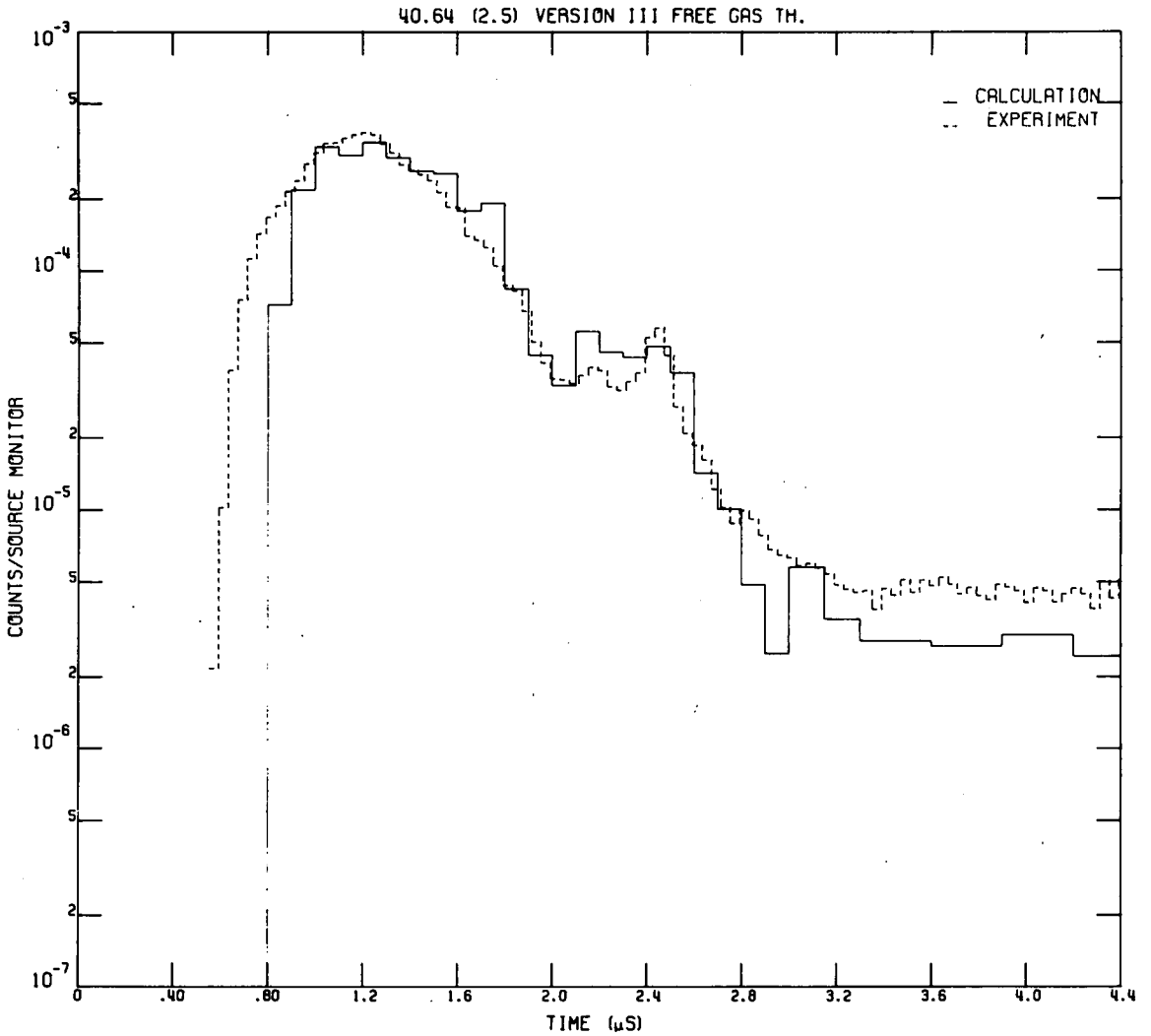

Fig. 94.1. Calculated and measured time-dependent gamma-ray count rates for the 40.64-cm slab.

---

1. Summary of paper presented at American Nuclear Society Meeting, San Francisco, November 11–15, 1973; *Trans. Amer. Nucl. Soc.* 17, 524 (1973).
2. Research sponsored by Defense Nuclear Agency.
3. Computer Sciences Division, UCC Nuclear Division.
4. L. Harris et al., *Time-Dependent Fast Neutron and Secondary Gamma Ray Spectrum Measurements in Concrete,* DASA 2401/GA-9751, Gulf General Atomic (November 1969).
5. L. Harris and H. Kendrick, "Measurements of Fast-Neutron and Secondary Gamma-Ray Transport through Concrete," *Trans. Amer. Nucl. Soc.* 14, 916 (1971).
6. David E. Groce et al., "Analysis of Neutron and Gamma Transport in Concrete Using Multigroup Code," *Trans. Amer. Nucl. Soc.* 14, 918 (1971).
7. E. A. Straker and G. W. Morrison, "Analysis of Neutron and Gamma-Ray Transport Using the O6R and OGRE Codes," *Trans. Amer. Nucl. Soc.* 14, 919 (1971).
8. M. O. Cohen, "Analysis of Neutron and Gamma-Ray Transport Using the SAM-CE Code," *Trans. Amer. Nucl. Soc.* 14, 920 (1971).
9. F. R. Mynatt, *A User's Manual for DOT, a Two-Dimensional Discrete Ordinates Transport Code with Anisotropic Scattering,* K-1694, Union Carbide Corp. (1967).

ORNL-DWG 73-9549

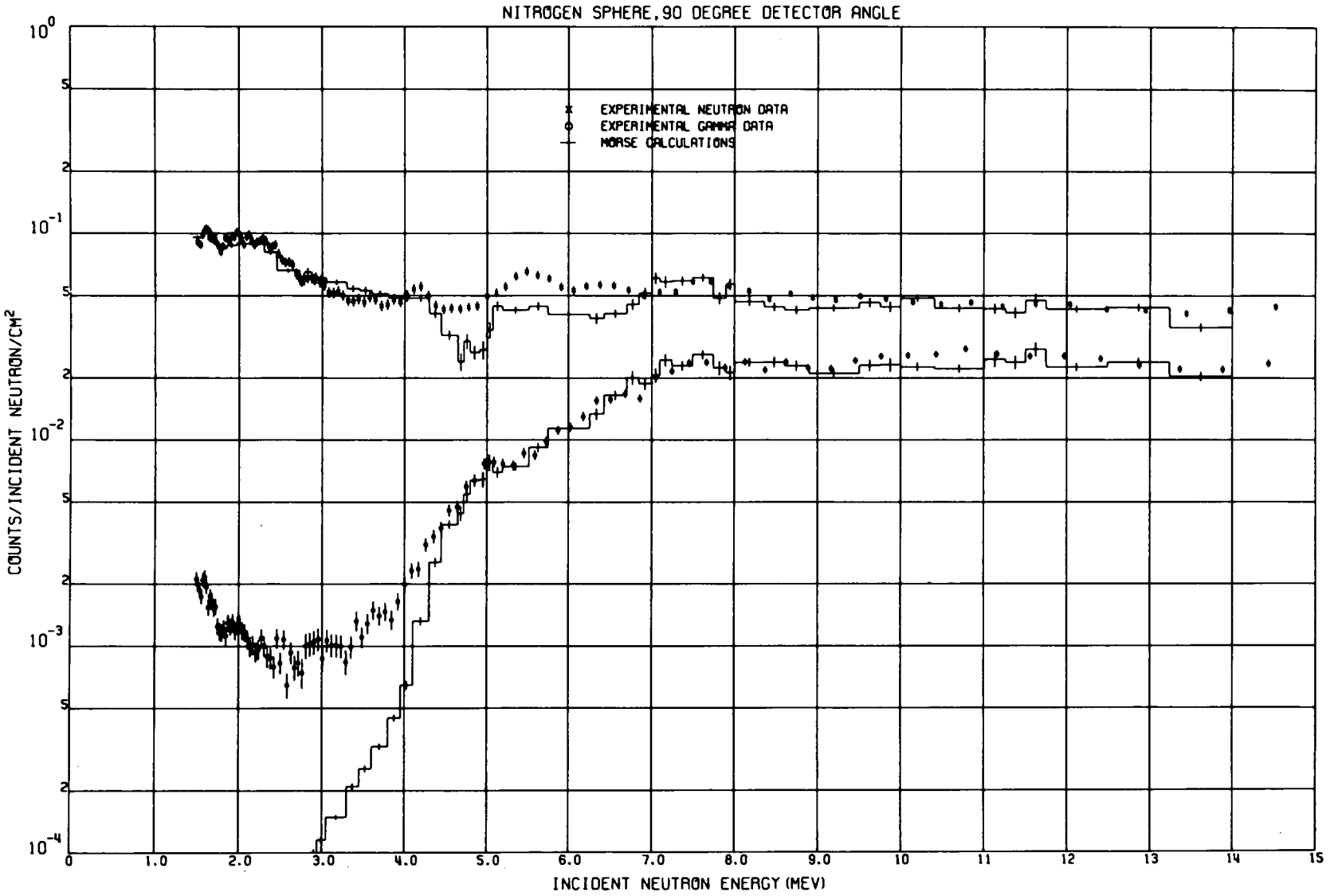

Fig. 95.1. MORSE calculation of IRT nitrogen experiment at 90° detector orientation.

10. R. W. Roussin, *Defense Nuclear Agency Working Cross Section Library – Description and Contents*, ORNL-RSIC-34, vol. I (1972).
11. D. E. Bartine, private communication, 1973.

95. CALCULATIONAL ANALYSIS OF NEUTRON AND GAMMA-RAY TRANSPORT EXPERIMENTS IN NITROGEN[1,2]

S. N. Cramer E. M. Oblow

Calculations have been performed at Intelcom Radiation Technology[3] for comparison with recent integral experiments involving neutron and gamma-ray transport through nitrogen. The IRT experiment consisted of a 15-cm-ID sphere of liquid nitrogen in a 20-cm-OD Styrofoam container pulsed with a monodirectional neutron beam with time-of-flight separation of neutron energies from 1 to 20 MeV. The detectors were located several centimeters away from the sphere at angles of 30, 55, 90, and 125 deg with respect to the incident neutron beam. These were 2 X 2 in. cylindrical NE213 detectors for the simultaneous detection of both neutrons and gamma rays.

Figure 95.1 shows a comparison of the measured and calculated neutron and gamma-ray count rates as a function of incident-neutron energy for the 90-deg detector orientation. The calculations were made using the MORSE multigroup Monte Carlo code, although equivalent results were also obtained with the point-energy O6R Monte Carlo code as a check on the neutron calculations. All calculations were made using the ENDF/B-III nitrogen data, MAT 1133. The comparisons reveal significant disagreements in the neutron count rates in the important region around 5 MeV, which corresponds to the dominant total cross-section minimum in nitrogen. This discrepancy could have important effects on deep-penetration calculations in air. Gamma-ray count rate comparisons, on the other hand, show remarkable agreement, possibly resolving the long standing controversy[4] about the adequacy of the Young[5] evaluation of the nitrogen gamma-ray-production cross sections. The apparent discrepancy below the gamma-ray-production threshold in nitrogen in this figure is due to background corrections not included in the calculations.

In addition to the count spectra for each detector position, detailed sensitivity analyses have been made in an effort to isolate the energy- and angular-dependent data causing disagreement between experiment and calculation at all the detector positions. The sensitivity results include calculations of the unfolded spectra for a series of incident-energy bins, the significance of first and subsequent collisions, the effect of anisotropic inelastic scattering for neutrons, and the effect of anisotropic gamma-ray production.

Integral nitrogen experiments performed at Oak Ridge National Laboratory are also being calculated. An analysis of these two experiments with the two Monte Carlo codes should help in verifying and improving the current nitrogen data files.

---

1. Summary of paper presented at American Nuclear Society Meeting, San Francisco, November 11–15, 1973; *Trans. Amer. Nucl. Soc.* 17, 522 (1973).
2. Research sponsored by Defense Nuclear Agency.
3. L. Harris, Jr., G. D. Trimble, and J. C. Young, *Integral Experiment to Test Carbon and Nitrogen Cross Sections*, Gulf-RT-A12292, Gulf Radiation Technology (September 1972).
4. F. G. Perey and J. K. Dickens, *Is There Still a Nitrogen Cross-Section Discrepancy*? ORNL-TM-4216 (May 1973).
5. P. G. Young and D. G. Foster, Jr., *An Evaluation of the Neutron and Gamma-Ray Production Cross Sections for Nitrogen*, LA-4725, Los Alamos Scientific Lab. (September 1972).

96. NEUTRON AND PHOTON ENERGY SPECTRUM CALCULATIONS FOR NITROGEN INTEGRAL EXPERIMENTS[1,2]

S. N. Cramer E. M. Oblow

In a continuing effort to validate the evaluated cross-section files for nitrogen through analysis of integral experiments, the neutron-energy spectra unfolded from measurements at IRT[3] have been

calculated for the nitrogen integral experiment. In addition, some recent neutron and gamma-ray integral count data and unfolded energy spectra from nitrogen experiments at ORNL have also been calculated. The IRT measurements are described in refs. 3 and 4, and some earlier calculations for the reported integral data are described in ref. 5. Additional experimental data not given in refs. 3 and 4 (i.e., the neutron spectra at the 55° detector angle) have also been unfolded and calculated in wide incident energy bins to try to resolve discrepancies found in earlier calculational comparisons. The ORNL experiment is similar to that at IRT, using an NE213 detector for both neutrons and gamma rays. The ORNL sample was 20 cm of nitrogen contained in a thin Pyrex spherical container. The incident neutron beam did not cover the entire sample as was the case at IRT. The ORNL experiment and calculations consist of integral count rates and spectra at four detector angles for both neutrons and gamma rays. All current calculations used ENDF/B-IV nitrogen data, MAT 1133.

Representative comparisons of the unfolded secondary spectra data from the IRT experiment and the calculations are shown in Fig. 96.1 for four incident neutron energy bins. In the figure the data points and error bars represent the spread in the experimental data, and the continuous lines give the spread (one standard deviation about the mean) of the Monte Carlo calculations. The agreement between calculation and experiment is good in both the elastic and inelastic peaks. In the valley, where the experimental spread is large, the calculational results are due mainly to the empirical detector energy resolution function

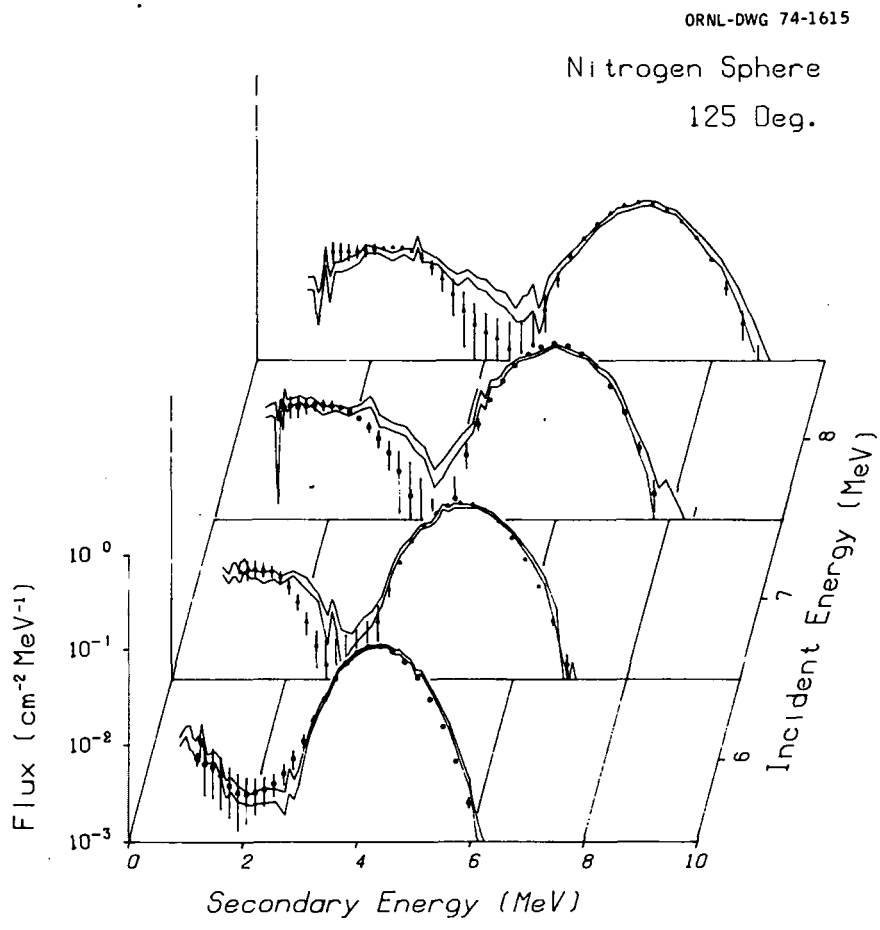

Fig. 96.1. Comparison of IRT unfolded secondary neutron spectra at 125° for various incident neutron energies with Monte Carlo calculations using ENDF/B-IV nitrogen data.

provided by the experimenter. Agreement for the other energy bins from 1 to 20 MeV at 125° is comparable to that shown in the figure. The 55° spectra calculations also analyzed reflect the disagreement between experimental and calculated integral count rate at 55°. The calculations are uniformly low, especially in the inelastic peaks.

The ORNL experiments and calculations are in good general agreement for both neutron and gamma-ray count rates and spectra. A typical spectrum comparison is shown in Fig. 96.2 which gives the secondary gamma-ray spectrum at 55° for the 8–9 MeV incident neutron energy bin. The integral gamma-ray calculations for both experiments indicate there are no inadequacies in the gamma-ray data used. The only significant disagreement uncovered in the analysis of the ORNL results is the failure of the calculated integral neutron count rate to show the minimum in the experimental data near 5 MeV for the

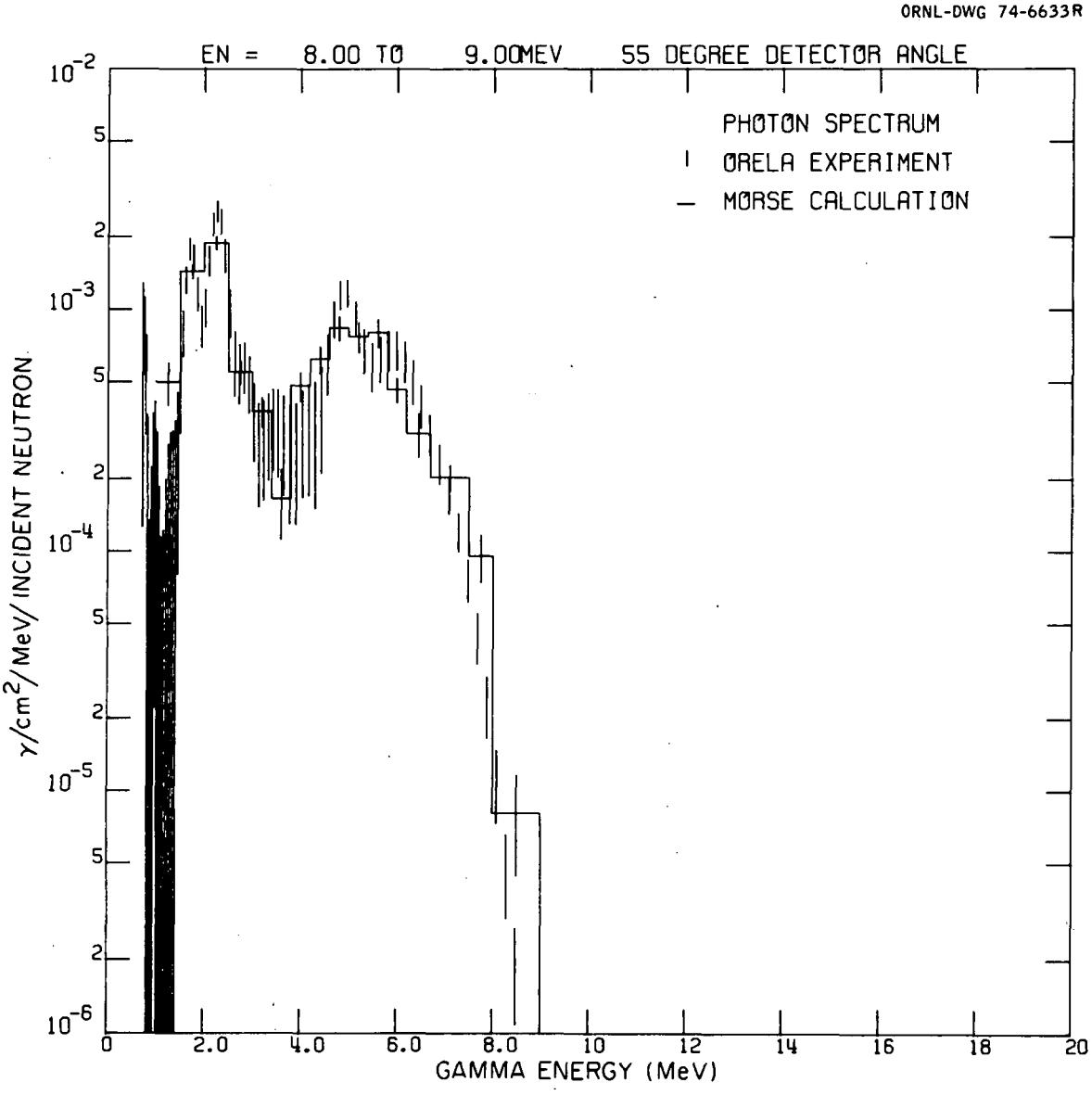

Fig. 96.2. Comparison of 55° ORNL unfolded secondary gamma spectrum from 8 to 9 MeV incident neutrons with Monte Carlo calculation using ENDF/B-IV nitrogen data.

two forward angles. Examination of the secondary spectra for the 4–5 MeV and 5–6 MeV incident energy bins indicates the angular data for elastic scattering is too large in the forward angles at these energies.

1. Summary of paper to be presented at American Nuclear Society Meeting, Washington, D.C., October 27–November 1, 1974.
2. Research sponsored by Defense Nuclear Agency.
3. L. Harris, Jr., et al., *Integral Experiment to Test Carbon and Nitrogen Cross Sections,* Intelcom Rad Tech Report DNA 2986F (1972).
4. L. Harris, Jr., and J. C. Young, "Energy Spectrum Measurements of Scattered Neutrons from Nitrogen," *Trans. Amer. Nucl. Soc.* 17, 550 (1973).
5. S. N. Cramer and E. M. Oblow, "Calculational Analysis of Neutron and Gamma-Ray Transport Experiments in Nitrogen," *Trans. Amer. Nucl. Soc.* 17, 522 (1973).

97. ANALYSES OF NEUTRON SCATTERING AND GAMMA-RAY PRODUCTION INTEGRAL EXPERIMENTS ON CARBON FOR NEUTRON ENERGIES FROM 1 TO 15 MeV[1,2]

S. N. Cramer E. M. Oblow

The results of two integral experiments on carbon, performed at ORNL and IRT, were compared with Monte Carlo calculations to test the evaluated carbon neutron and gamma-ray production data. The experiments were designed to measure with NE-213 detectors the angular dependence of neutron scattering and gamma-ray production from a thick (1 mean free path) carbon sample in the energy range from 1 to 13 MeV. Additional measurements in the ORNL experiment also provided the angular dependence of the secondary energy distribution of scattered neutrons. Multigroup Monte Carlo calculations modeling the two experimental arrangements were made to compare with the measured data. Both ENDF/B-III and ENDF/B-IV carbon data were used in the computations. The results indicate that such experiments are adequate for testing processed neutron scattering and gamma-production data (both integral and double differential) to within 15% over the entire range of incident neutron energies (1 to 15 MeV). Also, on the whole, the carbon ENDF/B-IV data gave fairly good agreement between the calculated and the measured results over the energy range tested. The only notable exception was the disagreement in the neutron result comparisons above 9 MeV, which was attributed to the $C(n,n')3\alpha$ being too low in this range.

1. Abstract of ORNL-TM-4494 (in press).
2. Research sponsored by Defense Nuclear Agency.

98. PRODUCTION AND TESTING OF THE DNA FEW-GROUP CROSS-SECTION LIBRARY[1,2]

D. E. Bartine R. W. Roussin
F. R. Mynatt J. R. Knight[3]
R. Q. Wright[3]

A coupled neutron–gamma-ray multigroup cross-section library was created for use in performing defense-related radiation transport calculations. Coupled P_3 cross sections consisting of 37 neutron groups and 21 gamma-ray groups have been processed in the ANISN[4] format with the AMPX[5] code for H, ^{9}Be, ^{10}B, ^{12}C, N, O, Na, Mg, Al, Si, K, Ca, Cu, Fe, ^{181}Ta, ^{182}W, ^{183}W, ^{184}W, ^{186}W, Pb, ^{238}U, and ^{239}Pu. Neutron energies range from 19.64 to 1.0×10^{-11} MeV, and gamma-ray energies range from 14.0 to 0.01 MeV. The weighting spectrum for neutron groups was $1/E$ with a thermal group Maxwellian weighting spectrum with a 300°K temperature.

Table 98.1. Comparison of 37-21 and 129-43 coupled neutron-gamma calculations

Cross section	Snyder-Neufeld neutron tissue dose (millirems/hr)	Neutron displacement (equiv 1-MeV neutrons per square centimeter)	Neutron ionization (rads-Si)	Henderson gamma tissue dose (rads/hr)	Gamma ionization (rads-Si)
Air transport problem (2000 m of air, thermonuclear source, P_3S_{16}, spherical)					
A. 129-43	1.61(−23)[a]	3.87(−15)	2.72(−25)	8.28(−24)	8.80(−24)
B. 37-21	1.66(−23)	3.94(−15)	2.74(−25)	8.28(−26)	9.25(−24)
% difference[b]	+3.3%	+1.8%	+0.7%	0.0%	+5.1%
Concrete transport problem (40 in. of concrete, thermonuclear source, P_3S_8, slab)					
A. 129-43	2.26(−14)	4.97(−6)	4.69(−16)	4.72(−14)	4.66(−14)
B. 37-21	2.11(−14)	4.61(−6)	4.49(−16)	4.47(−14)	4.76(−14)
% difference[b]	−6.6%	−7.2%	−4.3%	−5.3%	+2.1%

[a]Read: 1.61×10^{-23}.
[b]$(A - B) \times 100/B$.

The neutron and gamma-ray group structures employed for this library are quite high-energy biased due to the importance of high-energy particles for the calculation of tissue dose and silicon damage in electronics.[6] In addition, the neutron group structure is tailored to allow for the major peaks and valleys in the total neutron cross sections of nitrogen, oxygen, silicon, and iron. The gamma-ray group structure is tailored to allow accurate calculation of pair production, annihilation photon transport, hydrogen capture, and backscatter photon transport. There is also sufficient low photon energy structure to allow for rapidly changing cross sections and response functions.

Calculations were performed through 2000 m of air and through 40 in. of concrete to determine the ability of the 37-21 library to solve problems of basic interest. Transport calculations for both air and concrete using both 14-MeV and typical thermonuclear sources were performed using the 37-21 group structure and a 129-43 group structure. The results are given for the thermonuclear source case in Table 98.1. The 129-43 results were selected as standards for comparison because energy group boundaries for this structure were specifically chosen to fit in detail the peaks and valleys in the neutron cross sections and to bracket major gamma production lines for elements involved in transport through air and concrete. The comparisons are very favorable overall and agree within 10% for all responses. A study was also made of the effect of the weighting function ($1/E$ vs $1/E\Sigma_T$) used in the neutron cross section processing. The results indicated no significant variation in the calculated responses for the 129-43 group structure. The results for the 37-21 group structure indicated a small improvement in the calculated responses for the concrete problem due to the use of $1/E\Sigma_T$ weighting (less than 10% change). In the calculation through air, however, the use of $1/E\Sigma_T$ weighting for 37-21 cross sections resulted in overpredicting the neutron tissue dose by 19% and the neutron displacement by 14%. This effect is probably due to an overemphasis on relative minima contained in relatively broad energy groups in the 1.8 to 0.1 MeV range, so that resulting downscatter is too low.

In summary, the testing of the 37-21 coupled neutron-gamma cross-section sets in this library indicates that they are quite satisfactory for many basic defense calculations.

1. Summary of paper to be presented at American Nuclear Society Meeting, Washington, D.C., October 27–November 1, 1974.
2. Research sponsored by Defense Nuclear Agency.
3. Computer Sciences Division, UCC Nuclear Division.

4. W. W. Engle, Jr., *A Users Manual for ANISN, a One-Dimensional Discrete Ordinates Transport Code with Anisotropic Scattering,* K-1693, Computing Technology Center, Union Carbide Corporation (1967).
5. N. M. Greene, J. L. Lucius, W. E. Ford III, J. E. White, and R. Q. Wright, *AMPX: An Interface System to Generate Coupled Multigroup Neutron-Gamma Cross Sections from ENDF/B,* ORNL-TM-3706 (to be published).
6. D. E. Bartine, E. M. Oblow, and F. R. Mynatt, *Radiation Transport Cross-Section Sensitivity Analysis – a General Approach Illustrated for a Thermonuclear Source in Air,* ORNL-TM-4335 (1973).

99. CROSS-SECTION SENSITIVITY OF BREEDING RATIO IN A FUSION-REACTOR BLANKET[1,2]

D. E. Bartine E. M. Oblow
R. G. Alsmiller, Jr. F. R. Mynatt

For a particular fusion-reactor blanket configuration, the changes in the tritium breeding ratio – that is, in the number of tritium nuclei produced in the blanket per incident neutron – due to changes in nuclear cross-section data are calculated on the basis of linear perturbation theory. Results are presented for the changes in the breeding ratio due to changes in specific energy ranges of various partial cross sections of ^{6}Li, ^{7}Li, Nb, and C. The breeding ratio is found to be most sensitive to changes in the ^{7}Li$(n,n')\alpha,t$ cross section, but the sensitivity to changes in this cross section is not large.

1. Abstract of ORNL-TM-4208 (October 1973); also of paper published in *Nucl. Sci. Eng.* 53, 304 (1974).
2. Research sponsored by AEC Division of Physical Research.

100. COMPARISON OF CROSS-SECTION SENSITIVITIES OF BREEDING RATIOS IN FUSION-REACTOR BLANKETS[1,2]

R. G. Alsmiller, Jr. T. A. Gabriel
J. Barish[3] R. T. Santoro

In a recent paper,[4] calculated results of the cross-section sensitivity of the breeding ratio in a particular fusion-reactor blanket configuration were presented and discussed. In this paper, cross-section sensitivity results are presented and compared for three recently proposed fusion-reactor blanket designs. The designs considered here are that proposed at ORNL and studied by Steiner[5] and the reference theta-pinch reactor design proposed at LASL and studied by Dudziak.[6] For the ORNL design, results are presented separately for the cases when niobium and vanadium are used as structural material.

The calculated results presented here were obtained using perturbation theory as described in ref. 4. The transport calculations were carried out with the one-dimensional discrete ordinates code ANISN,[7] using P_3S_{12}, and the perturbation calculations were carried out with the code SWANLAKE.[8] The cross-section data for vanadium were obtained from the work of Penny and Owen,[9] and the cross-section data for the other materials were taken from ENDF/B III.[10]

The sensitivities of the ^{6}Li, ^{7}Li, and total breeding ratios to increases in the various partial cross sections of ^{7}Li are given in Table 100.1 for the three configurations considered. The quantity given in the table, $\delta R_j/R$, where j takes values of ^{6}Li, ^{7}Li, and ^{6}Li + ^{7}Li and $R = R_{^6\mathrm{Li}} + R_{^7\mathrm{Li}}$, is the percent change in the breeding ratio for a 1% increase at all energies in a particular partial cross section (see ref. 4 for more details). For all three configurations considered, the sensitivities to the partial cross section of ^{7}Li are found to be small except that in all three configurations the ^{7}Li breeding ratio shows an appreciable sensitivity to the ^{7}Li$(n,n')\alpha,t$ cross section, that is, to the tritium production cross section in ^{7}Li.

The sensitivity of the breeding ratios to the partial cross sections of ^{6}Li, C, Be, and Cu has also been obtained. For those partial cross sections which have been found to introduce appreciable uncertainties in

Table 100.1. Percent change in breeding ratio due to a 1% increase at all energies in the indicated partial cross sections of ^{7}Li

$(R = R_{^6Li} + R_{^7Li})$

^{7}Li cross-section type	Breeding material, j	$\delta R_j/R$ (%) ORNL design with Nb	ORNL design with V	LASL design
$(n,n')\alpha,t$	^{6}Li	1.7×10^{-2}	2.2×10^{-2}	3.1×10^{-3}
	^{7}Li	2.8×10^{-1}	2.7×10^{-1}	1.2×10^{-1}
	^{6}Li + ^{7}Li	3.0×10^{-1}	2.9×10^{-1}	1.2×10^{-1}
Absorption	^{6}Li	-5.9×10^{-3}	-6.0×10^{-3}	-2.3×10^{-3}
	^{7}Li	-3.4×10^{-3}	-3.4×10^{-3}	-2.8×10^{-4}
	^{6}Li + ^{7}Li	-9.3×10^{-3}	-9.4×10^{-3}	-2.6×10^{-3}
Elastic	^{6}Li	1.8×10^{-2}	2.9×10^{-2}	6.4×10^{-3}
	^{7}Li	-1.8×10^{-2}	-1.9×10^{-2}	2.4×10^{-4}
	^{6}Li + ^{7}Li	0.0	1.0×10^{-2}	6.6×10^{-3}
Inelastic	^{6}Li	4.3×10^{-3}	5.5×10^{-3}	1.3×10^{-3}
	^{7}Li	-1.1×10^{-2}	-1.1×10^{-2}	-3.9×10^{-4}
	^{6}Li + ^{7}Li	-6.7×10^{-3}	5.5×10^{-3}	-6.5×10^{-3}
$(n,2n)$	^{6}Li	3.7×10^{-2}	3.9×10^{-2}	1.1×10^{-2}
	^{7}Li	-1.9×10^{-2}	-1.9×10^{-2}	-1.6×10^{-3}
	^{6}Li + ^{7}Li	1.8×10^{-2}	2.0×10^{-2}	9.4×10^{-3}
Total collision	^{6}Li	7.0×10^{-2}	9.0×10^{-2}	2.0×10^{-2}
	^{7}Li	2.3×10^{-1}	2.2×10^{-1}	1.1×10^{-1}
	^{6}Li + ^{7}Li	3.0×10^{-1}	1.3×10^{-1}	1.3×10^{-1}

the total breeding ratio, cross-section uncertainty estimates as a function of energy have been made, and the change in the breeding ratio due to these energy-dependent cross-section uncertainties has been obtained and will be presented.

1. Summary of paper to be presented at American Nuclear Society Meeting, Washington, D.C., October 27–November 1, 1974.
2. Research sponsored by AEC Division of Physical Research.
3. Computer Sciences Division, UCC Nuclear Division.
4. D. E. Bartine, R. G. Alsmiller, Jr., E. M. Oblow, and F. R. Mynatt, *Nucl. Sci. Eng.* **53**, 304 (1974).
5. D. Steiner, *Nucl. Fusion* **14**, 33 (1974).
6. D. J. Dudziak, *Discrete Ordinates Neutronic Analysis of a Reference Theta-Pinch Reactor (RTPR)*, LA-DC-72-1427, Los Alamos Scientific Laboratory (1972).
7. W. W. Engle, Jr., *A Users Manual for ANISN, a One-Dimensional Discrete Ordinates Transport Code with Anisotropic Scattering*, K-1693, Computing Technology Center, Union Carbide Corporation (1967).
8. D. E. Bartine, F. R. Mynatt, and E. Oblow, *SWANLAKE, a Computer Code Utilizing ANISN Transport Calculations for Cross-Section Sensitivity Analysis*, ORNL-TM-3809, (1973).
9. S. K. Penny and L. W. Owen, *A Re-evaluation of Vanadium Neutron and Gamma-Ray Production Cross Sections*, ORNL-TM-4007 (1972).
10. O. Ozer and D. Garber, *ENDF/B Summary Documentation*, BNL-17541, National Cross Section Center, Brookhaven National Laboratory (1973).

101. SHIELDING DESIGN CALCULATIONS FOR ORMAK-F/BX[1,2]

T. A. Gabriel R. T. Santoro
W. W. Engle, Jr.

Calculations are presented which are oriented toward the initial shielding design for the ORMAK-F/BX, the Oak Ridge National Laboratory version of a first-generation injection-heated *d*-T ("wetwood") burning

Table 101.1. Calculated results for the toroidal field coil region

Peak heating rate	7.3×10^{-5} W/cm^3 per megawatt of fusion power
Dose in insulation material	11 rads per megajoule of fusion energy
Fast fluence ($E_n \geq 0.1$ MeV)	2.4×10^9 neutrons/cm^2 per megajoule of fusion energy
Residual gamma-ray dose	35 mR/hr

tokamak-type thermonuclear reactor. The prime purposes of the ORMAK-F/BX are threefold: (1) to obtain plasma containment for a reasonable amount of time (5 to 10 sec); (2) to obtain as much energy from the *d*-T fusion as is introduced into the plasma through the neutral ion injectors ($Q = 1$); and (3) to carry out vital experiments in a high-energy, high-flux neutron environment.

Since the prime energy release is in the form of a 14-MeV neutron, the shielding of personnel and equipment from these high-energy particles is of major importance. To implement the shield design, the calculations reported include heating rates in the reactor system with special interest on the heating in the superconducting magnet regions; radiation-damage studies in insulating and current-conduction material; shield and interior-wall activation and personnel dosimetry; building and wall composition and thickness; and void-streaming problems associated with entry ports into the reactor plasma region. The calculated transport results were obtained with the one-dimensional discrete ordinates code ANISN,[3] the two-dimensional discrete ordinates code DOT,[4] and the one-dimensional optimization code ASOP,[5] using P_3S_{12}. The coupled neutron and gamma-ray cross-section data (52 neutron, 21 gamma) were obtained from the Kriese CTR library,[6] the kerma factors from MACK[7] and MUG,[8] and the activation cross sections from refs. 9–11.

Some of the results are presented in Table 101.1 and are for the 40-cm reference design shield – 35 cm of stainless steel (65% by volume) and borated water (35% by volume), and 5 cm of lead on the outside. The reference shield is totally adequate for shielding the superconducting magnet system and for radiation damage to conductors and insulation. However, the residual gamma-ray dose from the major radioactive nuclides (^{56}Mn, ^{54}Mn, ^{58}Co, and ^{60}Co) in a work area several meters away from the shield after two years of operation and 15×10^3 pulses at 10^{19} neutrons per pulse is somewhat higher than desirable.

---

1. Summary of paper to be presented at American Nuclear Society Meeting, Washington, D.C., October 27–November 1, 1974.

2. Research sponsored by AEC Division of Physical Research.

3. W. W. Engle, Jr., *A Users Manual for ANISN, a One-Dimensional Discrete Ordinates Transport Code with Anisotropic Scattering,* K-1693, Computing Technology Center, Union Carbide Corporation (1967).

4. W. A. Rhoades and F. R. Mynatt, *The DOT III Two-Dimensional Transport Code,* ORNL-TM-4280 (1973).

5. W. W. Engle, Jr., *A User's Manual for ASOP, ANISN Shield Optimization Program,* CTC-INF-941, Union Carbide Corporation, Nuclear Division (1969).

6. J. T. Kriese, *Coupled Neutron and Gamma-Ray Cross-Section Sets for Fusion Reactor Calculations,* ORNL-TM-4277 (1973).

7. M. A. Abdou, C. W. Maynard, and R. Q. Wright, *MACK: A Computer Program to Calculate Neutron Energy Release Parameters (Fluence-to-Kerma Factors) and Multigroup Neutron Reaction Cross Sections from Nuclear Data in ENDF Format,* ORNL-TM-3994 (1973).

8. J. R. Knight and F. R. Mynatt, *MUG, a Program for Generating Multigroup Photon Cross Sections,* CTC-17, Computing Technology Center, Union Carbide Corporation, Nuclear Division (1970).

9. O. Ozer and D. Garber, *ENDF/B Summary Documentation,* BNL-17541, National Cross Section Center, Brookhaven National Laboratory (1973).

10. W. E. Alley and R. M. Lessler, *Semiempirical Neutron-Induced Reaction Cross Sections,* UCRL-50484, Rev. 1, Lawrence Livermore Laboratory (1972).

11. G. W. Cunningham III, ORNL, private communication.

102. SERVICES TO THE CTR COMMUNITY BY THE RADIATION SHIELDING INFORMATION CENTER[1,2]

R. W. Roussin D. K. Trubey
B. F. Maskewitz

The Radiation Shielding Information Center, established in 1962 to collect, package, analyze, and distribute information, computer codes, and data in the area of radiation transport related to fission, is now being utilized to support fusion reactor technology. The major activities include: (1) operating a computer-based information system and answering inquiries on radiation analysis, (2) collecting, checking out, packaging, and distributing large computer codes, and (3) evaluated and processed data libraries. The data packages include multigroup coupled neutron–gamma-ray cross sections and kerma coefficients, other nuclear data, and radiation transport benchmark problem results. Future plans include clearinghouse functions for CTR evaluated and processed multigroup data libraries.

1. Abstract of paper presented at American Nuclear Society Topical Meeting on the Technology of Controlled Nuclear Fusion, San Diego, California, April 16–18, 1974.
2. Work supported by AEC Division of Controlled Thermonuclear Research.

103. BIBLIOGRAPHY, SUBJECT INDEX, AND AUTHOR INDEX OF THE LITERATURE EXAMINED BY THE RADIATION SHIELDING INFORMATION CENTER (REACTOR AND WEAPONS RADIATION SHIELDING)[1,2]

D. K. Trubey J. Gurney
R. W. Roussin A. B. Gustin

An indexed bibliography is presented of literature selected by the Radiation Shielding Information Center since the previous volume was published in 1971 in the area of radiation transport and shielding against radiation from nuclear reactors, x-ray machines, radioisotopes, nuclear weapons (including fallout), and low-energy accelerators (neutron generators). The bibliography was printed by computer from magnetic tape files. In addition to lists of literature titles by subject categories (accessions 2301–3500), author and key-work indexes are given for the entire file, which includes citations listed in the previous volumes (I–III).

Most of the literature selected for Vol. IV was published in the years 1971–1973.

1. Abstract of ORNL-RSIC-5 (Vol. IV) (March 1974).
2. Work jointly supported by the AEC Division of Reactor Research and Development, the AEC Division of Controlled Thermonuclear Research, and the Defense Nuclear Agency.

104. MATERIALS INFORMATION IN THE RADIATION SHIELDING INFORMATION CENTER[1,2]

B. F. Maskewitz D. K. Trubey
R. W. Roussin

The Radiation Shielding Information Center (RSIC), established in 1962, serves the shielding community by collecting, organizing, processing, evaluating, packaging, and disseminating information mainly related to reactor and weapons radiation. The scope includes the physics of interaction of radiation

with matter, radiation production, transport, and energy deposition, radiation detectors and measurements, engineering design techniques, shielding materials properties, computer codes useful in research and design, and shielding data compilations. This information is analyzed, evaluated, synthesized, and repackaged in a form more authoritative, timely, and useful.

Promoting exchange and improvement of nuclear data, computer codes, and radiation transport information, RSIC provides strong support for the technology areas of its sponsors. The goal is to save time and prevent duplication of effort, to advance the state of the art, to increase the value and content of information by correlating it with other information, and to implement government information-dissemination policy. Materials information is an integral part of all information in the subject areas covered by the Center.

1. Abstract of paper presented at Materials Information Programs, an Interagency Review of Federal Agency Activities on Technical Information about Materials, Gaithersburg, Maryland, April 16–17, 1974.

2. Work jointly supported by the AEC Division of Reactor Research and Development, the AEC Division of Controlled Thermonuclear Research, and the Defense Nuclear Agency.

105. THE DEVELOPMENT OF RADIATION SHIELDING STANDARDS IN THE U.S.A.[1,2]

D. K. Trubey

The American Nuclear Society (ANS) is a standards-writing organization member of the American National Standards Institute (ANSI). The ANS Standards Committee has a subcommittee denoted ANS-6, Shielding, whose charge is to establish standards in connection with radiation shields, to provide shielding information to other standards-writing groups, and to prepare recommended sets of shielding data and test problems. This paper is a progress report of this subcommittee.

The purpose of a standard is to set forth acceptable practices, procedures, dimensions, material properties, specifications, etc., which have been agreed upon by representatives of a broad segment of the subject activity.

The organization responsible for promulgating voluntary standards is ANSI. The Institute, a nonprofit corporation, is a federation of leading trade, technical, and professional organizations, government agencies, and consumer groups. ANSI's principal functions are to coordinate standards development, minimize duplication and overlap, and provide a neutral forum to consider and identify standards needs.

The standards-writing organization of interest here is the ANS. Among its several administrative committees is one on standards composed of 27 subcommittees. The subcommittees, in turn, have established ad hoc working groups for preparation of individual standards.

The Subcommittee on Shielding Standards, ANS-6, now composed of seven working groups, was established in 1964. The goals and accomplishments of the working groups are briefly described below.

1. Summary of paper to be presented at International Symposium on Radiation Physics, 1974, Bose Institute, Calcutta, India, November 30–December 4, 1974.

2. Work supported by the AEC Division of Reactor Research and Development.

106. CALCULATIONS RELATED TO THE APPLICATION OF NEUTRONS, PROTONS, NEGATIVELY CHARGED PIONS, AND HEAVY IONS IN CANCER RADIOTHERAPY[1,2]

R. G. Alsmiller, Jr.

This report describes some of the most significant aspects of the research which has been conducted during the past year (September 1, 1972, to August 31, 1973) on the NSF/RANN-supported projects: A

Comparative Study of the Use of Photons, Neutrons, Protons, Negatively Charged Pions, and Heavy Ions in Cancer Radiotherapy and Calculations for Cancer Radiotherapy with Negatively Charged Pions. The report contains the information presented to the Grantees Conference on Instrumentation Technology held by the National Science Foundation on September 25 and 26, 1973, at Washington, D.C., as part of the RANN program.

1. Abstract of paper presented at the Grantees Conference on Instrumentation Technology, September 25–26, 1973, Washington, D.C.; published in *Proc. of the Grantees Conference on Instrumentation Technology*, p. 43, Grant No. GI-39844; prepared by Neus, Inc., Santa Monica, Calif., 1974.
2. Work funded by the National Science Foundation under Order NSF/RANN AG-399.

107. CALCULATIONS RELATED TO THE USE OF PHOTONS, NEUTRONS, NEGATIVELY CHARGED PIONS, PROTONS, AND ALPHA PARTICLES IN CANCER RADIOTHERAPY[1,2]

R. G. Alsmiller, Jr. J. Barish[3]
R. T. Santoro K. C. Chandler[3]
T. W. Armstrong G. T. Chapman

Calculated results are presented for absorbed dose, LET spectrum, and cell-survival probability as a function of position when photons, neutrons, negatively charged pions, protons, and alpha particles are incident on a tissue phantom. The beam parameters for each type of incident particle were chosen to be approximately those appropriate to the single-port irradiation of a small cylindrical volume (1 cm in radius and 2 cm in height) centered about a depth of 15 cm in the 30-cm-thick tissue slab. Both monoenergetic (15 MeV) neutrons and neutrons produced by 35-MeV ^{2}H on beryllium are considered. The cell-survival-probability calculations are carried out using the model developed by R. Katz et al., and results are presented for both aerobic and anoxic T-1 kidney cells. Spatially dependent OER's and RBE's for each type of particle considered are also given.

1. Abstract of ORNL-TM-4369 (January 1974) and of paper submitted for journal publication.
2. Work funded by the National Science Foundation under Order NSF/RANN AG-399.
3. Computer Sciences Division, UCC Nuclear Division.

108. CALCULATIONS PERTAINING TO THE USE OF FAST ($\lesssim$50 MeV) NEUTRONS IN CANCER RADIOTHERAPY[1,2]

R. G. Alsmiller, Jr. J. Barish[3]

Calculated results are presented for a variety of neutron spectra incident on a tissue-equivalent phantom. The neutron spectra considered are those produced by 35- and 50-MeV deuterons in a thick beryllium target and by 67-MeV protons in a thick lithium target. Results are presented for the absorbed doses, LET spectra, cell-survival probabilities, OER's, and RBE's as a function of position in the phantom. The cell-inactivation calculations were carried out using the model of Katz et al., and parameters for T-1 kidney cells.

In the case of incident neutrons from 35-MeV ^{2}H on beryllium, experimental and calculated absorbed-dose data are compared as a function of position in the phantom and are shown to be in good agreement.

1. Abstract of ORNL-TM-4442 (February 1974) and of paper to be published in *Medical Physics*; paper also presented at Fifth International Congress of Radiation Research Seattle, July 14–20, 1974.
2. Work jointly funded by the National Science Foundation under Order NSF/RANN AG-399 and the AEC Division of Physical Research.
3. Computer Sciences Division, UCC Nuclear Division.

109. THE EFFECTS OF BONE IN THE USE OF NEGATIVELY CHARGED PIONS IN CANCER RADIOTHERAPY[1,2]

R. T. Santoro R. G. Alsmiller, Jr.
K. C. Chandler[3]

The effects of bone in the use of negatively charged pions in cancer treatment planning have been estimated using Monte Carlo methods. The influence of bone along the pion path and also the influence of a bone-tissue interface parallel to the direction of motion of the pions have been considered. Calculated results of absorbed dose, cell-survival probability, oxygen enhancement ratio, and relative biological effectiveness as a function of spatial coordinates in a 30-g/cm^2-thick tissue phantom with bone both included and excluded are presented. All of the biological data reported here are for T-1 human kidney cells. The extent to which the effects of bone in the path of the pion beam can be approximated by using results for tissue and measuring depth in the phantom in grams per square centimeter is considered and discussed.

1. Abstract of ORNL-TM-4407 (February 1974) and of paper submitted for journal publication; paper also presented at Fifth International Congress of Radiation Research, Seattle, July 14–20, 1974.
2. Work funded by the National Science Foundation under Order NSF/RANN AG-399.
3. Computer Sciences Division, UCC Nuclear Division.

110. CALCULATIONS RELATED TO THE APPLICATION OF NEGATIVELY CHARGED PIONS IN RADIOTHERAPY: ABSORBED DOSE, LET SPECTRA AND CELL SURVIVAL[1,2]

T. W. Armstrong K. C. Chandler[3]

Calculations using a Monte Carlo radiation transport code and a model for cell inactivation have been carried out to estimate the spatial distributions of the absorbed dose, LET spectra, and the cell survival, RBE, and OER for T-1 human kidney cells produced by a beam of negatively charged pions incident on a slab of tissue.

1. Abstract of ORNL-TM-4294 (September 1973) and of *Radiat. Res.* 58, 293 (1974).
2. Work funded by the National Science Foundation under Order NSF/RANN AG-399.
3. Computer Sciences Division, UCC Nuclear Division.

111. CALCULATED PHYSICAL AND BIOLOGICAL RESULTS WHEN NEGATIVELY CHARGED PIONS ARE USED TO IRRADIATE A SMALL AND A LARGE "TUMOR" VOLUME IN A TISSUE PHANTOM[1,2]

R. T. Santoro R. G. Alsmiller, Jr.

The calculated absorbed doses, LET spectra, cell-survival probabilities, oxygen enhancement ratios, and relative biological effectiveness are presented and compared for two negatively charged pion beams, each incident on a 30-cm-thick tissue phantom. All of the biological results were obtained using the cell-inactivation model of Katz et al. and parameters for T-1 human kidney cells. The beam parameters were chosen to produce an approximately uniform absorbed dose in a small (2 cm in depth and 1 cm in radius) and in a large (5 cm in depth and 2.5 cm in radius) cylindrical tissue volume, each centered about a depth of 15 cm in the phantom.

1. Abstract of ORNL-TM-4490 (March 1974).
2. Work funded by the National Science Foundation under Order NSF/RANN AG-399.

112. CALCULATED PARTICLE-PRODUCTION SPECTRA FROM π^- CAPTURES IN TISSUE, TISSUE-EQUIVALENT PLASTIC, SILICON, AND GERMANIUM[1,2]

T. W. Armstrong K. C. Chandler[3]

An intranuclear-cascade–evaporation model has been applied to predict the energy spectra of the products (neutrons, protons, deuterons, tritons, ^{3}He's, alpha particles, and residual nuclei) from π^- capture in several materials (tissue, tissue-equivalent plastic, silicon, and germanium) of interest in pion dosimetry. Also, the energy spectra of the products from 90-MeV π^- interactions in tissue are computed.

1. Abstract of ORNL-TM-4462 (February 1974) and of *Nucl. Instrum. Methods* **118**, 515 (1974).
2. Work jointly funded by the National Science Foundation under Order NSF/RANN AG-399 and the AEC Division of Physical Research.
3. Computer Sciences Division, UCC Nuclear Division.

113. CALCULATIONS ON TISSUE EQUIVALENCE FOR STOPPING π^- MESONS[1,2]

T. W. Armstrong K. C. Chandler[3]

Calculations have been made of the energy deposition in tissue-equivalent plastic (Shonka type A-150) and tissue when both are placed in the stopping region of a negatively charged pion beam. The configuration considered is that of relatively small pieces of tissue-equivalent plastic (thicknesses of 50 and 3000 μ) placed in a large π^- capture region. The multiplicities and energies of the π^- capture products were determined using an intranuclear-cascade–evaporation model, and the energy deposition was obtained using computed stopping powers and ranges.

1. Abstract of ORNL-TM-4499 (March 1974) and of *Nucl. Instrum. Methods* **119**, 125 (1974); paper also presented at Fifth International Congress of Radiation Research, Seattle, July 14–20, 1974.
2. Work funded by the National Science Foundation under Order NSF/RANN AG-399.
3. Computer Sciences Division, UCC Nuclear Division.

114. CALCULATIONS RELATED TO THE APPLICATION OF SILICON DETECTORS IN PION RADIOBIOLOGY[1,2]

T. W. Armstrong K. C. Chandler[3]

Calculations have been made of the pulse-height spectrum and energy deposition in silicon detectors of various thicknesses (10, 50, 300, 1000, and 3000 μ) placed in a large region of π^- mesons stopping in tissue. The contribution of π^- captures within the detectors is determined, and the energy deposition in the detector is compared with the actual energy deposition in the tissue with the detector removed. A method for inferring the energy deposition in the tissue by various types of particles from the pulse-height spectra of the thin detectors is discussed and evaluated.

1. Abstract of ORNL-TM-4530 (May 1974) and of paper submitted for journal publication; paper also presented at Fifth International Congress of Radiation Research, Seattle, Washington, July 14–20, 1974.
2. Work funded by the National Science Foundation under Order NSF/RANN AG-399.
3. Computer Sciences Division, UCC Nuclear Division.

115. CALCULATION OF THE RESPONSE OF SILICON DETECTORS OF FINITE RADIUS TO π^- MESONS STOPPING IN TISSUE[1,2]

T. W. Armstrong K. C. Chandler[3]

Calculated results are presented for the response of silicon detectors of various radii placed in a large region of π^- mesons stopping in tissue.

1. Abstract of ORNL-TM-4614 (June 1974).
2. Work jointly funded by the National Science Foundation under Order NSF/RANN AG-399 and by the AEC Division of Physical Research.
3. Computer Sciences Division, UCC Nuclear Division.

116. CALCULATION OF RESIDUAL NUCLEI PRODUCTION BY A BEAM OF NEGATIVELY CHARGED PIONS INCIDENT ON A TISSUE PHANTOM[1,2]

T. W. Armstrong K. C. Chandler[3]

Monte Carlo calculations have been carried out to determine the depth dependence of the residual nuclei produced in tissue by a negatively charged pion beam. In addition, the depth dependence of those residual nuclei which are β^+ emitters and the photon energy produced by π^0 decay and nuclear deexcitation are computed since these photon sources have been proposed as a possible means of monitoring the treatment volume during radiotherapy using π^- beams.

1. Abstract of ORNL-TM-4590 (June 1974).
2. Work jointly funded by National Science Foundation under Order NSF/RANN AG-399 and by the AEC Division of Physical Research.
3. Computer Sciences Division, UCC Nuclear Division.

117. RESPONSE OF A LARGE ALL-LIQUID SCINTILLATION SPECTROMETER AND OF A 24-LAYER IRON-PLASTIC SPECTROMETER TO CHARGED PIONS AND PROTONS IN THE LOW-GeV ENERGY RANGE[1,2]

T. A. Gabriel J. D. Amburgey[3]

To aid in the design of a particular class of ionization spectrometers, calculations have been carried out to determine the response of a large all-liquid scintillation spectrometer to incident protons and charged pions in the low-GeV energy range. Included for comparative purposes is the calculated response of a 24-layer iron-plastic sandwich spectrometer of comparable g/cm^2 thickness. The calculated data include spatially dependent energy deposition, spatially integrated contributions to the total energy deposition, leakage and binding energies, scintillation pulse-height distributions including and excluding saturation effects, and correlations between different variables. Also included for several cases is the calculated Cherenkov response.

1. Abstract of ORNL-TM-4349 (December 1973) and of paper published in *Nucl. Instrum. Methods* **116**, 333 (1974).
2. Research sponsored by AEC Division of Physical Research.
3. Computer Sciences Division, UCC Nuclear Division.

118. ENERGY DEPOSITION BY HIGH-ENERGY ELECTRONS (50 TO 200 MeV) IN WATER[1,2]

R. G. Alsmiller, Jr. J. Barish[3]
S. R. Dodge[4]

The data presented here are intended for use in studying the effects of electron contamination in negatively charged pion beams which are used in cancer radiotherapy. Electron-photon cascade calculations have been carried out for zero-width beams of electrons with kinetic energies of 50, 100, 150, and 200 MeV normally incident on a water phantom. The energy deposition per unit volume as a function of depth and

radius in the phantom is given. To make the results more accessible for treatment planning, a quasi-analytic representation of the energy-deposition data has been obtained and is presented.

1. Abstract of ORNL-TM-4419 (February 1974) and of paper submitted for journal publication.
2. Work jointly funded by the National Science Foundation under Order NSF/RANN AG-399 and by the AEC Division of Physical Research.
3. Computer Sciences Division, UCC Nuclear Division.
4. Oak Ridge Associated Universities Undergraduate Research Trainee. Present address: Chapman College, Orange, Calif.

119. ENERGY DEPOSITION BY 45-GeV PHOTONS IN HYDROGEN, BERYLLIUM, ALUMINUM, COPPER, AND TANTALUM[1,2]

R. G. Alsmiller, Jr. J. Barish[3]

Electron-photon cascade calculations have been carried out for zero-width beams of 45-GeV photons normally incident on semi-infinite slabs of hydrogen, beryllium, aluminum, copper, and tantalum. The energy deposition is given as a function of both depth and radius in the slabs.

1. Abstract of ORNL-4933 (January 1974).
2. Research sponsored by the AEC Division of Physical Research.
3. Computer Sciences Division, UCC Nuclear Division.

120. PHOTON SPECTRA FROM INDUCED ACTIVITY IN AN ORBITING SPACECRAFT[1,2]

R. G. Alsmiller, Jr. J. W. Wachter[3]
G. T. Chapman J. Barish[4]

The results of nucleon-meson and photon transport calculations are presented, and an estimate is given of the photon spectrum from the induced activity in a spacecraft orbiting the earth and periodically passing through the Van Allen proton belt. A simplified slab model of the spacecraft is considered, but a realistic time dependence of the proton flux per unit energy for the orbit assumed is used. Results are given for a variety of times ($\leqslant$23.5 hr + 720 days) after the spacecraft has been in orbit.

1. Abstract of ORNL-TM-4345 (May 1974).
2. Work funded by the National Aeronautics and Space Administration under Order H-38280A.
3. Chemical Technology Division.
4. Computer Sciences Division, UCC Nuclear Division.

121. A TECHNIQUE TO DETERMINE THE SHAPE OF A MINIMUM-WEIGHT SHIELD[1,2]

W. W. Engle, Jr. F. R. Mynatt

The conceptual design for a 5-kW(e) power system for space applications consists of a small reactor power source, a shadow shield to protect the payload from neutron and photon radiation, and a thermoelectric system for converting the heat generated by the reactor into usable electrical energy. Because the system is to be used for space applications, the first consideration in the design of the radiation shield is minimum weight. This paper describes a technique which uses forward and adjoint two-dimensional discrete ordinates calculations to determine the optimum shape of a minimum-weight shield.

In the configuration used in this analysis, the shadow shield is located between the reactor and the power conversion system. The shield consists of two components, a heavy-metal gamma-ray shield next to the reactor followed by a lithium hydride neutron shield. The overall shape of the system is conical with a

half angle of approximately 8°. Several of the components in the power conversion system contain a significant amount of stainless steel; and within the mechanical constraints of the design, these components are arranged to take advantage of their potential as a gamma-ray shield. In order to incorporate the gamma-ray shielding effectiveness of the power conversion system in the shape of the heavy-metal gamma-ray shield, the following procedure was devised.

A DOT-III[3] adjoint calculation using the gamma-ray flux-to-dose conversion factors as a source at the bottom of the power conversion system was performed in *R-Z* geometry. The geometry included the entire power conversion system and the lithium hydride neutron shield. Forward DOT calculations including the reactor and shield were run for several heavy-metal shield configurations.

The integral over angle, energy, and surface area of the product of the forward and adjoint fluxes at a common surface is the average dose at the bottom of the power conversion system. To shape the heavy-metal shield, the integration was performed over angle and energy only by the FACT code at the bottom surface of the heavy-metal shield. These results then show the relative contribution per unit area to the average dose at the bottom of the power conversion system as a function of radial position beneath the heavy-metal shield. Because the gamma-ray shield is disk shaped, a constant dose contribution per unit area is equivalent to a constant dose contribution per unit weight, which is a necessary condition in a weight-optimized shield. By assuming an exponential attenuation in the shield and using the dose contribution data from two different shield configurations, it is possible to calculate the shield thickness as a function of radius which yields a constant dose contribution per unit area.

Figure 121.1 shows dose contribution data for three configurations – no gamma-ray shield, a simple heavy-metal disk geometry, and a shaped heavy-metal shield calculated from the first two configurations. It is apparent that beyond 21 cm radius the unshaped heavy metal acts as a source of secondary gamma rays

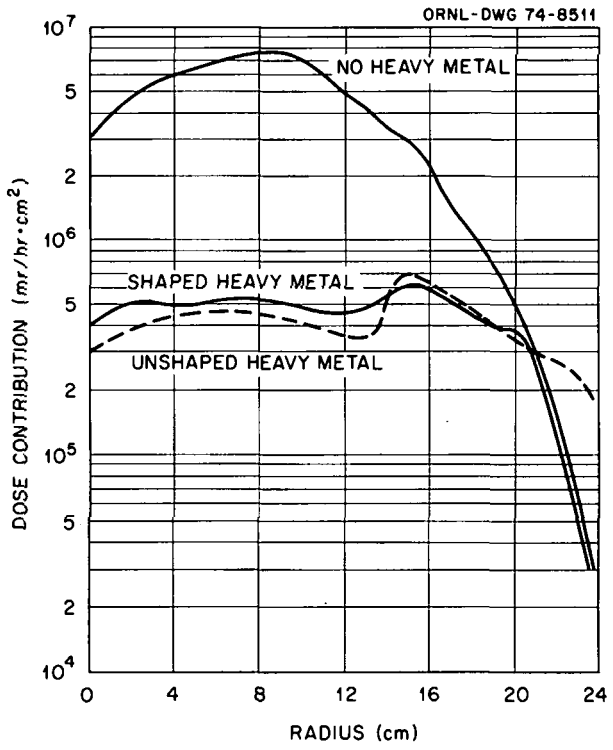

Fig. 121.1. Dose contribution per unit area for different shield configurations.

rather than as a shield. The undulations in the shaped shield data occur at places where the rectangular DOT mesh does not closely coincide with the desired curved surface. The shaped shield weighs 37% less than the unshaped shield, and further DOT calculations confirmed that the shields provide the same average dose rate.

---

1. Summary of paper presented at American Nuclear Society Meeting, San Francisco, November 11–15, 1973; *Trans. Amer. Nucl. Soc.* 17, 556 (1973).
2. Research sponsored by AEC Division of Space Nuclear Systems.
3. W. A. Rhoades and F. R. Mynatt, *The DOT III Two-Dimensional Discrete Ordinates Transport Code*, ORNL-TM-4280 (1973).

122. NUCLEAR ACCIDENT DOSIMETRY IN A SIMULATED CRITICALITY ACCIDENT[1]

R. T. Santoro G. C. Cain
R. G. Affel J. H. Greene

A criticality accident was simulated using the Health Physics Research Reactor (HPRR) to determine the response of three Union Carbide Nuclear Division health physics teams[2] in analyzing exposed personnel dosimeters (film badges) and area dosimeters to determine the magnitude of the accident and the radiation dose received by personnel working at the site of the accident. Since the recovery of exposed personnel may depend on early medical treatment, it is essential that reliable estimates of dose received by each victim be obtained as rapidly as possible. Continuous reanalyses of the exposed dosimeters combined with clinical procedures must, of course, continue to define the actual radiation dose accumulated by the exposed individuals.

In the simulated criticality accident reported here, personnel doses were defined as the dose received by four saline-solution-filled polyethylene manikins (phantoms). Three of the phantoms were placed in line of sight with the reactor at distances from the reactor of 1, 2, and 6 m. These distances were chosen to assure a wide range of doses to the phantoms. Film badges were placed chest high on each phantom on both the anterior and posterior surfaces to simulate persons facing toward and away from the reactor. The fourth phantom was placed at a distance of 2 m from the reactor but in the shadow of the phantom nearest the reactor. Film badges were placed at waist level on the anterior surface of this manikin.

Area dosimeters were placed 10 m from the reactor at a height of 1.5 m. Threshold detectors were positioned adjacent to each phantom and alongside the area dosimeters.

The criticality accident was simulated by a single burst of the HPRR that resulted in a total yield of 6×10^{16} fissions. Following the burst, film badges and saline-solution samples taken from each phantom along with one of the area dosimeters were given to each health physics team. Each team was asked to provide, in minimum time, dose estimates and their uncertainties. The teams were also asked to report revised dose data as they became available. No information other than the sodium concentration in the saline solution was provided to each team.

The results of the test are summarized in Table 122.1. The initial dose estimates vary widely but, within the limits of error, suggest the magnitude and seriousness of the dose received. The final dose values are within ±25% error bands – a value consistent with AEC requirements[3] for defining exposure doses. Comparison of the final dose values with the doses obtained from the reference threshold detectors and sodium activation in the saline solution show the results to be consistent within the limits of uncertainty.

Table 122.1. Summary of results for the simulated criticality accident

Phantom	Distance from reactor to phantom mid-plane (m)	Dosimeter location[b] (m)	Initial total dose[a]			Final total dose[a]			Threshold detector (rad)[a,e]	Dose from Na activation[f] (rad)
			Team A[c] (rad)	Team B[d] (rad)	Team C[d] (rad)	Team A[d] (rad)	Team B[d] (rad)	Team C[d] (rad)		
1	1.02	A – 0.92	7900	4185	1700	2506	1769	1510	1906	1398
1		P – 1.12	1200	870	1500	2230	1634	1560		
2	2.11	A – 2.01	158	1256	530	1056	662	570	252	555
2		P – 2.21	250	331	610	767	575	590		
3	6.13	A – 6.03	190	213	90	156	145	95	77	98
3		P – 6.23	45	110	95	107	89	92		
4	2.09	A – 1.99	1000	960	200	205	129	195	165[g]	164
Final area dosimeter total dose (at 10-m)						33	31	33		
Elapsed time (hr)[h]			2.2	2.0	2.1	19.5	14.5	7.0		

[a]Total dose = neutron dose plus gamma ray dose.
[b]A = anterior, P = posterior; numeric value is the distance from reactor to film badge plane.
[c]Uncertainty in these data = ± factor of 3.33.
[d]Uncertainty in these data = ± 25%.
[e]These are doses at a distance corresponding to the mid-plane of the phantom.
[f]Neutron dose only.
[g]The threshold detector adjacent to this phantom was not shielded from the reactor by phantom number 1. Correcting for the shielding of phantom 1, the value obtained is 165 rad.
[h]Time from burst to report of results.

1. Summary of paper to be presented at 1974 Winter Meeting of American Nuclear Society, Washington, D.C., October 27–November 1, 1974.
2. Health physics teams from the Oak Ridge National Laboratory, the Y-12 Plant, and the Oak Ridge Gaseous Diffusion Plant participated in the test.
3. United States Atomic Energy Commission Manual, chap. 0545.

123. DIFFERENTIAL CROSS SECTIONS FOR CHARGED-PARTICLE EMISSION IN REACTIONS OF 58-MeV ALPHA PARTICLES WITH ^{12}C, ^{16}O, AND ^{54}Fe; COMPARISON WITH THE EXCITON MODEL OF PRE-EQUILIBRIUM PARTICLE EMISSION[1,2]

F. E. Bertrand[3] R. W. Peelle
C. Kalbach-Cline[4]

Cross sections differential in energy and angle are presented for the proton, deuteron, triton, and alpha particles from reactions of 58-MeV alpha particles on C, O, and ^{54}Fe, and the angle-integrated differential spectra are compared with the predictions of an extended exciton model of pre-equilibrium reactions. The experimental results were obtained with a semiconductor telescope and cover the whole energy range above a few MeV. Except for oxygen, the results are given with uncertainties of 5 to 10%; for oxygen, relative intensities are valid at a given angle, but the absolute uncertainty is about 50%. The high-energy segment of the spectrum is highly anisotropic for all emitted particles, but for low energies the evaporation mechanism may be important for proton and perhaps alpha-particle emission. The inelastic alpha spectra from ^{54}Fe are more similar in shape to previous observations of the ^{54}Fe(p,xp) spectra than to the presently reported ^{12}C($\alpha,x\alpha$) results.

1. Abstract of *Phys. Rev.* **C10**, 1028 (1974).

2. Research jointly sponsored by National Aeronautics and Space Administration, the U.S. Atomic Energy Commission, and the National Science Foundation.
3. Physics Division.
4. Nuclear Structure Research Laboratory and Chemistry Department, University of Rochester, Rochester.

124. FEASIBILITY STUDY OF A HONEYCOMB VACUUM WALL FOR FUSION REACTORS[1,2]

S. N. Cramer E. M. Oblow

Honeycombing the vacuum first wall of plasma devices has been proposed at ORNL to reduce the sputtering and refluxing of neutral impurities into the plasma. A preliminary evaluation of the feasibility of such a honeycomb wall concept has been performed using a series of Monte Carlo simulations of sputtering interactions in a cylindrical honeycomb cell. These calculations parameterized the length-to-diameter ratio (L/D) of the cell and the sputtering yield data (because of the unavailability of the data in some important areas) to determine (1) the sensitivity of the design to sputtering data, (2) the optimum L/D of the cell, and (3) whether a significant reduction in sputtering yield results from honeycombing the wall. The preliminary results obtained so far are encouraging in that small L/D ratios (close to unity) appear to be optimum and a factor of 3 to 4 reduction in sputtering yields appears feasible. In addition, these results do not appear to be unduly sensitive to the sputtering data within reasonable uncertainty bounds.

1. Work supported by the AEC Controlled Thermonuclear Research Program.
2. Abstract of ORNL-TM-4708 (in publication).

PUBLICATIONS AND PAPERS PRESENTED AT SCIENTIFIC MEETINGS

PUBLICATIONS*

ABDOU, M. A.,** AND R. W. ROUSSIN

"MACKLIB: 100-Group Neutron Fluence-to-Kerma Factors and Reaction Cross Sections Generated by the MACK Computer Program from Data in ENDF Format," ORNL-TM-3995 (August 1974). (52)

ALLEN, B. J.,** R. L. MACKLIN,** R. R. WINTERS,** AND C. Y. FU

"Neutron-Capture Cross Sections of the Stable Lead Isotopes," *Phys. Rev.* C8(4), 1504 (1973). (10)

ALSMILLER, R. G., JR., AND J. BARISH**

"The Calculated Response of ^{6}LiF Albedo Dosimeters to Neutrons with Energies $\leqslant$400 MeV," *Health Phys.* **26**, 13 (1973). (1973)

"Shielding against the Neutrons Produced When 400-MeV Electrons Are Incident on a Thick Copper Target," *Particle Accel.* **5**, 155 (1973). (1973)

"Energy Deposition by 45-GeV Photons in H, Be, Al, Cu, and Ta," ORNL-4933 (January 1974). (119)

"Calculations Pertaining to the Use of Fast ($\lesssim$50 MeV) Neutrons in Cancer Radiotherapy," ORNL-TM-4442 (February 1974); *Med. Phys.* **1**(2), 51 (1974). (108)

ALSMILLER, R. G., JR., G. T. CHAPMAN, J. W. WACHTER,** AND J. BARISH**

"Photon Spectra from Induced Activity in an Orbiting Spacecraft," ORNL-TM-4345 (May 1974). (120)

ALSMILLER, R. G., JR., J. BARISH,** AND S. R. DODGE**

"Energy Deposition by High-Energy Electrons (50 to 200 MeV) in Water," ORNL-TM-4419 (February 1974). (118)

ALSMILLER, R. G., JR., R. T. SANTORO, T. W. ARMSTRONG, J. BARISH,**
K. CHANDLER,** AND G. T. CHAPMAN

"Calculations Related to the Use of Photons, Neutrons, Negatively Charged Pions, Protons, and Alpha Particles in Cancer Radiotherapy," ORNL-TM-4369 (January 1974). (107)

ARMSTRONG, T. W., R. G. ALSMILLER, JR., AND K. C. CHANDLER**

"Calculation of the Dose Induced in Tissue by Negatively Charged Pion Beams," *Phys. Med. Biol.* **18**(6), 830 (1973). (1973)

ARMSTRONG, T. W., AND K. C. CHANDLER**

"Calculations Related to the Application of Negatively Charged Pions in Radiotherapy: Absorbed Dose, LET Spectra, and Cell Survival," ORNL-TM-4294 (September 1973); *Radiat. Res.* **58**, 293 (1974). (110)

"Calculated Particle-Production Spectra from π^- Captures in Tissue, Tissue-Equivalent Plastic, Silicon, and Germanium," ORNL-TM-4462 (February 1974); *Nucl. Instrum. Methods* **118**, 515 (1974). (112)

"Calculation of the Response of Silicon Detectors of Finite Radius to π^- Mesons Stopping in Tissue," ORNL-TM-4614 (June 1974). (115)

"Calculations on Tissue Equivalence for Stopping π^- Mesons," ORNL-TM-4499 (March 1974); *Nucl. Instrum. Methods* **119**, 125 (1974). (113)

---

*Numbers between 1 and 124 shown in parentheses following the publication correspond to an abstract included in this report. In most cases, abstracts not included here were published in a previous annual report for which the year is indicated.

**Non-Division personnel.

"Calculations of Residual Nuclei Production by a Beam of Negatively-Charged Pions Incident on a Tissue Phantom," ORNL-TM-4590 (June 1974). (116)

"Stopping Powers and Ranges for Muons, Charged Pions, Protons, and Heavy Ions," *Nucl. Instrum. Methods* **113**, 313 (1973). (1973)

"Calculation of the Absorbed Dose and Dose Equivalent from Neutrons and Protons in the Energy Range from 3.5 GeV to 1.0 TeV," *Health Phys.* **24**, 277 (1973). (1972)

ARMSTRONG, T. W., K. C. CHANDLER,** AND J. BARISH**

"Calculations of Neutron Flux Spectra Induced in the Earth's Atmosphere by Galactic Cosmic Rays," *J. Geophys. Res.* 78(16), 2715 (1973). (1973)

BARTINE, D. E., R. G. ALSMILLER, JR., E. M. OBLOW, AND F. R. MYNATT

"Cross-Section Sensitivity of Breeding Ratio in a Fusion-Reactor Blanket," ORNL-TM-4208 (October 1973); *Nucl. Sci. Eng.* **53**, 304 (1974). (99)

BARTINE, D. E., E. M. OBLOW, AND F. R. MYNATT

"Radiation Transport Cross-Section Sensitivity Analysis – a General Approach Illustrated for a Thermonuclear Source in Air," ORNL-TM-4335 (December 1973). (91)

BERTINI, H. W., T. A. GABRIEL, AND R. T. SANTORO

"Predicted Proton Spectrum at Forward Angles for 29.4-GeV Nitrogen on Carbon Collisions," ORNL-TM-4311 (September 1973). (29)

"Predicted Proton Spectrum at Forward Angles for 29.4-GeV Nitrogen on Carbon," *Phys. Rev.* **C9**(2), 522 (February 1974). (29)

BERTINI, H. W., T. A. GABRIEL, R. T. SANTORO, O. W. HERMANN,**
N. M. LARSON,** AND J. M. HUNT**

"HIC-1: A First Approach to the Calculation of Heavy-Ion Reactions at Energies $\gtrsim$50 MeV/Nucleon," ORNL-TM-4134 (January 1974). (31)

BERTINI, H. W., G. D. HARP,** AND F. E. BERTRAND**

"Comparisons of Predictions from Two Intranuclear Cascade Models with Measured Secondary Proton Spectra at Several Angles from 62- and 39-MeV Protons on Various Elements," ORNL-TM-4638 (August 1974). (30)

"Differential Cross Sections for Charged-Particle Emission in Reactions of 58-MeV α Particles with ^{12}C, ^{16}O, and ^{54}Fe; Comparison with the Exciton Model of Preequilibrium Particle Emission," *Phys. Rev.* **C10**, 1028 (1974). (123)

BUHL, A. R., J. C. ROBINSON,** AND E. T. TOMLINSON**

"Intercomparison of Nonperturbing Techniques for Inferring the Reactivity of Fast Reactors," *Nucl. Technol.* **21**, 67 (January 1974). (1973)

CLAIBORNE, H. C.**

"An Evaluation of the Engineering Shield Design for the FFTF Head Compartment," ORNL-CF-73-8-12 (Aug. 6, 1973). (76)

CLIFFORD, C. E., F. J. MUCKENTHALER, AND P. N. STEVENS**

"Fast Reactor Experimental Shielding Progress Report for February 1974, 189a No. 10028, Activity No. HN 04 01 01 1," ORNL-TM-4611 (June 1974). (78)

CLIFFORD, C. E., F. J. MUCKENTHALER, P. N. STEVENS,** AND R. M. FREESTONE, JR.

"Fast Reactor Experimental Shielding Monthly Progress Report for May, 1973, 189a No. 10028, Activity 40 01 03 1," ORNL-TM-4284 (July 1973). (78)

"Fast Reactor Experimental Shielding Monthly Progress Report for July 1973, 189a No. 10028, Activity No. HN 04 01 01 1," ORNL-TM-4364 (September 1973). (78)

"Fast Reactor Experimental Shielding Progress Report for August and September 1973, 189a No. 10028, Activity No. HN 04 01 01 1," ORNL-TM-4420 (December 1973). (78)

"Fast Reactor Experimental Shielding Progress Report for October 1973, 189a No. 10028, Activity No. HN 04 01 01 1," ORNL-TM-4469 (January 1974). (78)

"Fast Reactor Experimental Shielding Progress Report for November and December 1973, 189a No. 10028, Activity No. HN 04 01 01 1," ORNL-TM-4514 (March 1974). (78)

"Fast Reactor Experimental Shielding Progress Report for January 1974, 189a No. 10028, Activity No. HN 04 01 01 1," ORNL-TM-4592 (May 1974). (78)

CLIFFORD, C. E., F. J. MUCKENTHALER, P. N. STEVENS,** R. M. FREESTONE, JR., AND F. B. K. KAM**

"Fast Reactor Experimental Shielding Monthly Progress Report for June 1973, 189a No. 10028, Activity No. 40 01 03 1," ORNL-TM-4343 (August 1973). (78)

COMOLANDER, H. E., AND R. K. GRYDER**

"MANYFILE: A Computer Program for Use in the Manipulation of Data Sets between Various Input/Output Devices," ORNL-TM-4377 (October 1973). (53)

CRAMER, S. N., AND E. M. OBLOW

"Analyses of Neutron Scattering and Gamma-Ray Production Integral Experiments on Carbon for Neutron Energies from 1 to 15 MeV," ORNL-TM-4494 (1974). (97)

CROSS, N. F.,** P. B. FOX,** AND G. E. WHITESIDES**

"Criticality Calculations for Cylindrical Billets of Uranium-Aluminum Alloy," ORNL-CF-74-4-21 (Apr. 9, 1974). (67)

De SAUSSURE, G.

"Resonance Reaction Formalisms for Fissile Nuclei," in Proceedings of the CSEWG Resonance Region Subcommittee Meeting Held at Brookhaven National Laboratory May 8, 1972, M. R. Bhat (editor), p. 5 (April 1973). (1972)

De SAUSSURE, G., AND R. B. PEREZ

"Multilevel Effects in the Unresolved Resonances Region of the Cross Sections of Fissile Nuclides," *Nucl. Sci. Eng.* 52, 382 (1973). (3)

"The Transformation of a Set of Multilevel Resonance Parameters into an Equivalent Set of Single-Level Pseudoparameters and a 'Smooth' Background," *Nucl. Sci. Eng.* 52, 412 (1973).

De SAUSSURE, G., E. G. SILVER, R. B. PEREZ, R. INGLE,** AND H. WEAVER

"Measurement of the Uranium-238 Capture Cross Section for Incident Neutron Energies up to 100 keV," *Nucl. Sci. Eng.* 51, 385 (1973). (1973)

DICKENS, J. K.

"Neutron-Induced Gamma-Ray Production in Titanium for Incident-Neutron Energies of 4.9, 5.4, and 5.9 MeV," Technical Note, *Nucl. Sci. Eng.* **54**, 191 (1974). (6)

"Gamma-Ray Production Due to Neutron Interactions with ^{68}Zn and the Level Structure of ^{68}Zn," ORNL-4985 (August 1974). (18)

DICKENS, J. K., T. A. LOVE, AND G. L. MORGAN

"Neutron-Induced Gamma-Ray Production in Calcium in the Energy Range $0.7 \leqslant E_n \leqslant 20$ MeV," *Nucl. Sci. Eng.* 53, 277 (1974). (15)

"Gamma-Ray Production from Neutron Interactions with Nickel for Incident Neutron Energies between 1.0 and 10 MeV: Tabulated Differential Cross Sections," ORNL-TM-4379 (November 1973). (13)

"Gamma-Ray Production from Neutron Interactions with Silicon for Incident Neutron Energies between 1.0 and 20 MeV: Tabulated Differential Cross Sections," ORNL-4389 (December 1973). (20)

"Gamma-Ray Production Due to Neutron Interactions with Tin for Incident Neutron Energies between 0.75 and 20 MeV: Tabulated Differential Cross Sections," ORNL-TM-4406 (November 1973). (21)

"Gamma-Ray Production Due to Neutron Interactions with Zinc for Incident Neutron Energies between 0.85 and 20 MeV: Tabulated Differential Cross Sections," ORNL-TM-4464 (February 1974). (16)

"Gamma-Ray Production Due to Neutron Interactions with Fluorine and Lithium for Incident Neutron Energies between 0.55 and 20 MeV: Tabulated Differential Cross Sections," ORNL-TM-4538 (April 1974). (23)

"Gamma-Ray Production Due to Neutron Interactions with Magnesium for Incident Neutron Energies between 0.8 and 20 MeV: Tabulated Differential Cross Sections," ORNL-TM-4544 (May 1974). (22)

DICKENS, J. K., AND G. L. MORGAN.

"^{28}Si($n,n'\gamma$) Photon Production Cross Sections for E_γ = 1.78 MeV, 5.0 $\leqslant E_n \leqslant$ 9.5 MeV," *Phys. Rev.* **C10**, 958 (1974).

DICKENS, J. K., G. L. MORGAN, AND F. G. PEREY.

"Neutron-Induced Gamma-Ray Production in Iron for the Energy Range 0.8 $\leqslant E_n \leqslant$ 20 MeV," *Nucl. Sci. Eng.* **50**, 311 (1973). (1973)

FREESTONE, R. M., JR.

"Experimentally Determined Neutron and Gamma-Ray Spectra from an Encapsulated Cm_2O_3 Power Source," ORNL-TM-4459 (March 1974). (84)

FU, C. Y., D. C. LARSON, AND F. G. PEREY

"ENDF/B Evaluation of Neutron and Gamma-Ray-Production Cross Sections for Fluorine," published in ENDF-201, ENDF/B Summary Documentation, National Neutron Cross Section Center, Brookhaven National Laboratory, BNL-17541 (May 1973 plus updates). (39)

FU, C. Y., AND F. G. PEREY

"ENDF/B Evaluation of Neutron and Gamma-Ray-Production Cross Sections for Calcium," published in ENDF-201, ENDF/B Summary Documentation, National Neutron Cross Section Center, Brookhaven National Laboratory, BNL-17541 (May 1973 plus updates). (35)

"ENDF/B Evaluation of Neutron and Gamma-Ray-Production Cross Sections for Lead," published in ENDF-201, ENDF/B Summary Documentation, National Neutron Cross Section Center, Brookhaven National Laboratory, BNL-17541 (May 1973 plus updates). (37)

GABRIEL, T. A., AND J. D. AMBURGEY**

"Response of a Large All-Liquid Scintillation Spectrometer and of a 24-Layer Iron-Plastic Spectrometer to Charged Pions and Protons in the Low-GeV Energy Range," ORNL-TM-4349 (December 1973); *Nucl. Instrum. Methods* **116**, 333 (1974). (117)

GABRIEL, T. A., AND K. C. CHANDLER**

"Energy Deposition and Energy-Deposition Fluctuations in an Ionization Spectrometer and a Total-Absorption Nuclear-Cascade Counter," *Particle Accel.* **5**, 161 (1973). (1973)

GABRIEL, T. A., R. T. SANTORO, H. W. BERTINI, AND N. M. LARSON**

"Calculated Secondary-Particle Spectra from Alpha-Particle- and Carbon-Induced Nuclear Reactions," ORNL-TM-4334 (October 1973); *Nucl. Sci. Eng.* **53**, 323 (1974). (28)

GABRIEL, T. A., R. T. SANTORO, AND W. W. ENGLE, JR.

"Shielding Design Calculations for ORMAK-F/BX," ORNL-TM-4619 (August 1974). (101)

HOLLAND, L. B.

"Procedures Manual for the Tower Shielding Facility," revised (no number) (July 1974).

"Procedures Manual for the Health Physics Research Reactor," ORNL-3519 Rev. (August 1974).

KINNEY, W. E., AND F. G. PEREY

"Natural Chromium and ^{52}Cr Neutron Elastic and Inelastic Scattering Cross Sections from 4.07 to 8.56 MeV," ORNL-4806 (ENDF-198) (January 1974). (4)

"Natural Nickel and ^{60}Ni Neutron Elastic and Inelastic Scattering Cross Sections from 4.07 to 8.56 MeV," ORNL-4807 (ENDF-198) (January 1974). (12)

"Natural Titanium Neutron Elastic and Inelastic Scattering Cross Sections from 4.07 to 8.56 MeV," ORNL-4810 (October 1973). (5)

"^{54}Fe Neutron Elastic and Inelastic Scattering Cross Sections from 5.50 to 8.50 MeV," ORNL-4907 (ENDF-203) (February 1974). (7)

"^{63}Cu and ^{65}Cu Neutron Elastic and Inelastic Scattering Cross Sections from 4.07 to 8.50 MeV," ORNL-4908 (ENDF-204) (February 1974). (8)

"^{206}Pb, ^{207}Pb, and ^{208}Pb Neutron Elastic and Inelastic Scattering Cross Sections from 5.50 to 8.50 MeV," ORNL-4909 (ENDF-206) (June 1974). (9)

LARSON, D., S. M. AUSTIN,** AND B. H. WILDENTHAL**

"Inelastic Proton Scattering from ^{138}Ba and ^{144}Sm at 30 MeV," *Phys. Rev.* **C9**(4), 1574 (1974). (26)

LARSON, D. C., AND F. G. PEREY

"ENDF/B Evaluation of Neutron and Gamma-Ray-Production Cross Sections for Silicon," published in ENDF-201, ENDF/B Summary Documentation, National Neutron Cross Section Center, Brookhaven National Laboratory, BNL-17541 (May 1973 plus updates). (38)

MAERKER, R. E.

"SDT12. The ORNL Benchmark Experiment for Neutron Transport through Sodium," ORNL-TM-4223 (August 1974). (80)

MAERKER, R. E., AND F. J. MUCKENTHALER

"Final Report on a Benchmark Experiment for Neutron Transport through Iron and Stainless Steel," ORNL-4892 (April 1974); see also *Nucl. Sci. Eng.* **52**, 227 (1973). (81)

MAERKER, R. E., F. J. MUCKENTHALER, R. L. CHILDS,** AND M. L. GRITZNER**

"Final Report on a Benchmark Experiment for Neutron Transport in Thick Sodium," ORNL-4880 (January 1974); see also *Nucl. Technol.* **22**, 275 (1974). (80)

McGREGOR, B. J.,** AND F. R. MYNATT

"Effects of Air-Density Perturbations on the Transport of Gamma Rays Produced by Point Gamma-Ray Sources," ORNL-TM-4266 (December 1973). (86)

MYNATT, F. R., T. J. HOFFMAN,** J. V. PACE III,** C. E. BURGART,** AND L. S. ABBOTT

"Calculations of the Penetration of Nuclear Weapons Radiation into a Missile Silo," ORNL-TM-4021 (November 1973) (classified). (87)

MYNATT, F. R., AND L. S. ABBOTT

"Fast Reactor Analytical Shielding Progress Report for March and April 1973, 189a No. 10318, Activity No. 04 40 01 03 1," ORNL-TM-4400 (February 1974). (72)

"Fast Reactor Analytical Shielding Progress Report for May and June 1973, 189a No. 10318, Activity No. 04 40 01 03 1," ORNL-TM-4401 (February 1974). (72)

"Fast Reactor Analytical Shielding Progress Report for September and October 1973, 189a No. 10318, Activity No. 04 40 01 03 1," ORNL-TM-4482 (May 1974). (72)

MYNATT, F. R., L. S. ABBOTT, R. L. CHILDS,** W. W. ENGLE, Jr., AND R. E. MAERKER

"Fast Reactor Analytical Shielding Progress Report for July and August 1973, 189a No. 10318, Activity No. HN 04 01 01 1," ORNL-TM-4402 (November 1973). (72)

OBLOW, E. M.

"Reactor Cross-Section Sensitivity Studies Using Transport Theory," ORNL-TM-4437 (April 1974). (69)

OBLOW, E., K. KIN,** H. GOLDSTEIN,** AND J. J. WAGSHAL**

"Effects of Highly Anisotropic Scattering on Monoenergetic Neutron Transport at Deep Penetrations," ORNL-TM-4408 (December 1973); also *Nucl. Sci. Eng.* **54**, 72 (1974). (49)

PEREY, C. M., AND F. G. PEREY

"Compilation of Phenomenological Optical-Model Parameters, 1971–1972," *At. Data and Nucl. Data Tables* **13**, 293 (1974) (27)

PEREY, F. G., C. Y. FU, S. K. PENNY,** W. E. KINNEY, AND R. Q. WRIGHT**

"ENDF/B Evaluation of Neutron and Gamma-Ray-Production Cross Sections for Iron," published in ENDF-201, ENDF/B Summary Documentation, National Neutron Cross Section Center, Brookhaven National Laboratory, BNL-17541 (May 1973 plus updates). (36)

PEREY, F. G.

"Report to the U.S. Nuclear Committee," ORNL-TM-4390 (November 1973). (40)

"Report to the U.S. Nuclear Data Committee," ORNL-TM-4589 (June 1974). (40)

PEREY, F. G., AND W. E. KINNEY

"Nitrogen Neutron Elastic and Inelastic Scattering Cross Sections from 4.34 to 8.56 MeV," ORNL-4805 (ENDF-205) (February 1974). (11)

PEREZ, R. B.

"General Formalism for the Transition Matrix of Nuclear Reaction Theory and Its Application to the Study of Potential Scattering," *Phys. Rev.* **C8**(1), 8 (1973). (1972)

PEREZ, R. B., AND G. De SAUSSURE

"Treatment of Large Perturbations of the Hamiltonian and the Boundary Conditions of a Quantum Mechanical System as an Initial Value Problem," *Phys. Rev.* **C10**(1), 187 (1974). (1973)

PEREZ, R. B., G. De SAUSSURE, E. G. SILVER, R. W. INGLE,** AND H. WEAVER

"Simultaneous Measurements of the Neutron Fission and Capture Cross Sections for Uranium-235 for Neutron Energies from 8 eV to 10 keV," *Nucl. Sci. Eng.* **52**, 46 (1973). (1972)

PERRY, A. M.,** F. C. MAIENSCHEIN, AND D. R. VONDY

"Fission-Product Afterheat – a Review of Experiments Pertinent to the Thermal-Neutron Fission of ^{235}U," ORNL-TM-4197 (October 1973). (24)

RHOADES, W. A., M. B. EMMETT,** G. W. MORRISON,** J. V. PACE III,** AND L. M. PETRIE**

"Vehicle Code System (VCS) User's Manual," ORNL-TM-4648 (August 1974). (58)

RHOADES, W. A., AND F. R. MYNATT

"The DOT III Two-Dimensional Discrete Ordinates Transport Code," ORNL-TM-4280 (June 1973). (56)

ROUSSIN, R. W., AND J. B. WRIGHT

"Defense Nuclear Agency Working Cross Section Library: Description and Contents," ORNL-RSIC-34, Vol. I (Rev.) (June 1974). (41)

SAHIN, S.**

"Comparison of Transport and Diffusion Theory for Fast Reactor Shielding Calculations," *Atomkernenergie* 22(1), 24 (1973). (1973)

SANTORO, R. T., AND R. G. ALSMILLER, JR.

"Calculated Physical and Biological Results When Negatively Charged Pions Are Used to Irradiate a Small and a Large 'Tumor' Volume in a Tissue Phantom," ORNL-TM-4490 (March 1974). (111)

SANTORO, R. T., R. G. ALSMILLER, JR., AND K. C. CHANDLER**

"Shielding of Manned Space Vehicles against Galactic Cosmic-Ray Protons and Alpha Particles," *Nucl. Sci. Eng.* 52, 124 (1973). (1973)

"The Effects of Bone in the Use of Negatively Charged Pions in Cancer Radiotherapy," ORNL-TM-4407 (February 1974). (109)

SLAUGHTER, G. G.,** AND J. K. DICKENS

"Gamma-Ray Production Due to Neutron Interactions with Zinc. Tabulated Differential Cross Sections for 31 Gamma Rays for Incident Neutron Energies between 0.9 and 6 MeV," ORNL-TM-4523 (April 1974). (17)

TOMLINSON, E. T.**

"Approximate Numerical Solutions to the Time-Dependent Neutron Transport Equation Using the TASK Algorithm," ORNL-TM-4595 (July 1974). (55)

TRUBEY, D. K.

"The MAINTAIN Code for Use in Maintaining and Revising Card Image Files on Tape," ORNL-TM-4291 (August 1973). (1973)

TRUBEY, D. K., AND S. V. KAYE**

"The EXREM III Computer Code for Estimating External Radiation Doses to Populations from Environmental Releases," ORNL-TM-4322 (December 1973). (1973)

TRUBEY, D. K., R. W. ROUSSIN, J. GURNEY, AND A. B. GUSTIN

"Bibliography, Subject Index, and Author Index of the Literature Examined by the Radiation Shielding Information Center (Reactor and Weapons Radiation Shielding)," ORNL-RSIC-5 (Vol. IV) (March 1974). (103)

UCHIDA, S.,** J. LEWIN, AND R. E. MAERKER

"Calculation of Energy Depositions and Dose Rates in Proposed Shielding Surrounding the TSR-II Reactor," ORNL-TM-4450 (December 1973). (83)

WACHTER, J. W.,** R. T. SANTORO, T. A. LOVE, AND W. ZOBEL

"Fast Forward Neutron Production in the $^{7}Li(p,n)^{7}Be$ Reaction for 41- and 64-MeV Protons," *Nucl. Instrum. Methods* 113, 185 (1973). (1973)

WEISBIN, C. R., AND R. J. LaBAUVE**

"Specification of a Generally Useful Multigroup Structure for Neutron Transport," LA-5277-MS (May 1973).

WESTON, L. W., AND J. H. TODD**

"Fission-Neutron Multiplicity and Total Prompt Gamma-Ray Energy for Resonances in ^{239}Pu," *Phys. Rev.* **10**(4) (1974). (1971)

WHITE, J. E.,** C. Y. FU, AND K. J. YOST**

"Neutron Capture Gamma-Ray Yields in Iron," Technical Note, *Nucl. Sci. Eng.* **51**, 496 (1973). (1971)

WRIGHT, R. Q.,** S. N. CRAMER, AND D. C. IRVING**

"UKE-III: A Computer Program for Translating Neutron Cross Section Data from the UKAEA Nuclear Data Library to the Evaluated Nuclear Data File Format," ORNL-TM-2880 (Rev.) (ENDF 134R) (October 1973). (51)

PAPERS PRESENTED AT SCIENTIFIC MEETINGS*

European-American Committee on Reactor Physics, Argonne National Laboratory, June 4–8, 1973

MAIENSCHEIN, F. C., "Studies of Sensitivity of Shield Performance to Nuclear Data Variations" (71)†

Grantees Conference on Instrumentation Technology, National Science Foundation, Washington, D.C., September 25–26, 1973

ALSMILLER, R. G., JR., "Calculations Related to the Application of Neutrons, Protons, Negatively Charged Pions, and Heavy Ions in Cancer Radiotherapy" (106)

Joint Electromagnetic Pulse Technical Meeting, Air Force Weapons Laboratory, Kirtland Air Force Base, New Mexico, September 25–27, 1973

GABRIEL, T. A., "Time-Dependent Neutron and Secondary Gamma-Ray Weapon Output Including Complete Collision Kinetics" (85)

MYNATT, F. R., "Time-Dependent Neutron and Secondary Gamma-Ray Transport in the Atmosphere – Sensitivity to Cross Sections" (90)

International Symposium on Physics of Fast Reactors, Tokyo, Japan, October 16–23, 1973

STACEY, W. M.,** B. J. TOPPEL,** R. N. HWANG,** H. HENRYSON II,** K. D. LATHROP,** AND F. R. MYNATT, "The U.S. Theoretical and Computational Program" (62)

American Physical Society Meeting, Division of Nuclear Physics, Bloomington, Indiana, November 1–3, 1973

DICKENS, J. K., T. A. LOVE, AND G. L. MORGAN, "Ca($n,x\gamma$) Gamma-Ray Production Cross Sections for E_n between 0.7 and 20 MeV," *Bull. Amer. Phys. Soc.*, Ser. II **18**(10), 1402 (1973)

1973 Winter Meeting of the American Nuclear Society, San Francisco, California, November 11–15, 1973; Trans. Amer. Nucl. Soc. **17** *(1973)*

CRAMER, S. N., AND E. M. OBLOW, "Calculational Analysis of Neutron and Gamma-Ray Transport Experiments in Nitrogen," p. 552 (95)

EMMETT, M. B.,** W. W. ENGLE, JR., AND F. R. MYNATT, "Calculation of Penetrations in the FTR Radial Cavity Shield," p. 561 (73)

ENGLE, W. W., JR., AND F. R. MYNATT, "A Technique to Determine the Shape of a Minimum Weight Shield," p. 556 (121)

FLANAGAN, G. F., N. M. GREENE,** W. W. ENGLE, JR., AND E. T. TOMLINSON,** "Comparison of Transport Approximations for Reactor Physics Calculations in a Fast Reactor," p. 486 (63)

FORD, W. E., III,** "The Testing of ^{238}U Photon Production Data from ENDF/B Materials 58, 702, and 4187," p. 545 (47)

GREENE, N. M.,** "Anisotropic Inelastic Scattering Matrices from ENDF Data," p. 549 (48)

JAMES, G. D.,** G. De SAUSSURE, AND R. B. PEREZ, "Intermediate Structure in the Neutron-Induced ^{235}U Cross Sections," p. 495 (32)

MAERKER, R. E., AND F. J. MUCKENTHALER, "Comparisons of Detailed Measured and Calculated Neutron Spectra behind Thick Samples of Iron," p. 522 (82)

MORRISON, G. W.,** L. M. PETRIE,** AND F. R. MYNATT, "Monte Carlo Analysis of Neutron and Gamma-Ray Transport in Concrete," p. 524 (94)

---

*Compiled July 19, 1974; includes papers submitted for future presentation.
†Numbers in parentheses indicate related paper number in this report.
**Non-Division personnel.

OBLOW, E., J. CHING,** AND J. DRISCHLER, "Selection of Group Energy Boundaries Using Sensitivity Theory," p. 547 (92)

WEISBIN, C. R., J. S. HENDRICKS,** D. E. CULLEN,** E. M. OBLOW, AND P. D. SORAN,** "Multigroup Cross-Section Dependence on Weighting Function Model," p. 483 (42)

CULLEN, D. E.,** AND C. R. WEISBIN, "Determination of Multigroup Weighting Spectra and Cross Sections," p. 488

SORAN, P. D.,** R. J. LaBAUVE,** C. R. WEISBIN, AND J. S. HENDRICKS,** "Multiplication Factor Dependence on Number of Multigroups and Weighting Function Model," p. 484

KLEIN, M.,** C. R. WEISBIN, R. J. LaBAUVE,** AND O. OZER,** "Efficient Representation of Nuclear Cross Sections on a Common Energy Mesh," p. 489

Seminar on Codes for Nuclear Data Processing, NEA-CPL, Ispra, December 5–7, 1973

HARRIS, D. R.,** R. J. LaBAUVE,** R. E. MacFARLANE,** P. D. SORAN,** C. R. WEISBIN, AND J. E. WHITE,** "MINX, a Modular Code System for Processing Multigroup Cross Sections from Nuclear Data in ENDF/B Format" (43)

American Physical Society Meeting, Berkeley, California, December 27–29, 1973

WACHTER, J. W.,** R. T. SANTORO, T. A. LOVE, AND W. ZOBEL, "Differential Cross Sections for the Production of Neutrons from the Bombardment of ^{12}C, ^{27}Al, ^{54}Fe, and ^{208}Pb by 40-MeV Protons" (25)

Materials Information Programs, an Interagency Review of Federal Agency Activities on Technical Information about Materials, Gaithersburg, Maryland, April 16–17, 1974

MASKEWITZ, B. F., D. K. TRUBEY, AND R. W. ROUSSIN, "Materials Information in the Radiation Shielding Information Center" (104)

American Nuclear Society Topical Meeting on the Technology of Controlled Nuclear Fusion, San Diego, California, April 16–18, 1974

ROUSSIN, R. W., D. K. TRUBEY, AND B. F. MASKEWITZ, "Services to the CTR Community by the Radiation Shielding Information Center" (102)

Specialists Meeting on Resonance Parameters of Fertile Nuclei (^{232}Th, ^{238}U, and ^{240}Pu) and of ^{239}Pu, Saclay, France, May 20–22, 1974

De SAUSSURE, G., "Recent Measurements on U-238 at ORNL" (1).

De SAUSSURE, G., "Recent U.S. Experimental Data and Evaluation for Pu-239"

1974 Annual Meeting of the American Nuclear Society, Philadelphia, Pennsylvania, June 23–27, 1974; Trans. Amer. Nucl. Soc. **18** *(1974)*

BARTINE' D. E., J. V. PACE III,** AND J. R. KNIGHT,** "A Cross-Section Sensitivity Study of Radiation Transport in Concrete," p. 381 (93)

CRAMER, S. N., "Next Flight Estimation for the Fictitious Scattering Monte Carlo Method," p. 400 (54)

FLANAGAN, G. F., D. B. SIMPSON, D. L. SELBY,** AND J. T. MIHALCZO,** "Transport Calculations for Reactivity Measurements in Subcritical Configurations of the FFTF Engineering Mockup Core," p. 268 (64)

PACE, J. V., III,** AND F. R. MYNATT, "A One-Dimensional Calculational Method for an Air-over-Ground Radiation Field Incident on an Underground Concrete Structure," p. 379 (88)

PEREY, F. G., "Estimated Uncertainties in Evaluated Data," p. 337 (33)

PETRIE, L. M.,** AND N. F. CROSS,** "Energy- and Region-Dependent Bucklings for the FFTF Engineering Mockup Core from Monte Carlo," p. 348 (66)

SILVER, E. G., E. M. OBLOW, J. M. KALLFELZ,** C. R. WEISBIN, D. E. BARTINE, G. F. FLANAGAN, AND F. R. MYNATT, "Generalized Reactor Sensitivity Analysis Program at ORNL," p. 341 (68)

Fifth International Congress of Radiation Research, Seattle, Washington, July 14–20, 1974

ALSMILLER, R. G., JR., AND J. BARISH,** "Calculations Pertaining to the Use of Fast ($\lesssim$50 MeV) Neutrons in Cancer Radiotherapy" (108)

ARMSTRONG, T. W., AND K. C. CHANDLER,** "Calculations Related to the Application of Silicon Detectors in Pion Radiotherapy" (114)

CHANDLER, K. C.,** AND T. W. ARMSTRONG, "Calculations on Tissue Equivalence for Stopping π^--Mesons" (113)

SANTORO, R. T., R. G. ALSMILLER, JR., AND K. C. CHANDLER,** "The Effects of Bone in the Use of Negatively Charged Pions in Cancer Radiotherapy" (109)

American Nuclear Society Topical Meeting for Advanced Reactors: Physics, Design, and Economics, Atlanta, Georgia, September 8–11, 1974

BARTINE, D. E., F. R. MYNATT, E. M. OBLOW, R. L. CHILDS,** J. V. PACE,** J. R. KNIGHT,** AND T. M. SIMS,** "ORNL Cross Section Sensitivity Analysis Applications for Radiation Shielding" (invited paper) (75)

CLIFFORD, C. E., "The ORNL LMFBR Experimental Shielding Program" (invited paper) (77)

De SAUSSURE, G., AND R. B. PEREZ, "Present Status of Cross Section Data of the Fissile and Fertile Isotopes for Fast Reactors" (invited paper) (1)

FLANAGAN, G. F., W. W. ENGLE, JR., L. R. WILLIAMS, AND F. R. MYNATT, "Analysis of Stored Fuel, Control Rod and Inherent Source Effects on the CRBR Ex-Vessel Source Range Monitoring System" (65)

KALLFELZ, J. M.,** M. L. WILLIAMS,** D. LAI,** AND G. F. FLANAGAN, "Sensitivity Studies of the Breeding Ratio for the Clinch River Breeder Reactor" (70)

PEREY, F. G., G. De SAUSSURE, AND R. B. PEREZ, "The Formalism for Data Covariance Representation in ENDF/B and Application to the ^{238}U Capture Cross Section Sensitivity Study" (34)

WEISBIN, C., N. M. GREENE,** H. HENRYSON III,** R. J. LaBAUVE,** C. DURSTON,** D. E. CULLEN,** AND R. B. KIDMAN,** "Fast Reactor Processing Codes – Is There a Dollars Worth of Difference between Them?" (invited paper) (46)

Second Symposium on Neutron Dosimetry in Biology and Medicine, Munich, Germany, September 30–October 4, 1974,

ALSMILLER, R. G., JR., "Calculations of the Transport of Fast Neutrons ($\lesssim$50 MeV) through Matter" (59)

1974 Winter Meeting of the American Nuclear Society, Washington, D.C., October 27–November 1, 1974

ALSMILLER, R. G., JR., J. BARISH,** T. A. GABRIEL, AND R. T. SANTORO, "Comparison of Cross-Section Sensitivities of Breeding Ratios in Fusion-Reactor Blankets" (100)

BARTINE, D. E., F. R. MYNATT, R. W. ROUSSIN, J. R. KNIGHT,** AND R. Q. WRIGHT,** "Production and Testing of the DNA Few-Group Cross-Section Library" (98)

CRAMER, S. N., AND E. M. OBLOW, "Neutron and Photon Energy Spectrum Calculations for Nitrogen Integral Experiments" (96)

GABRIEL, T. A., R. T. SANTORO, AND W. W. ENGLE, JR., "Shielding Design Calculations for ORMAK–F/BX" (101)

KEE, C. W.,** C. R. WEISBIN, AND R. E. SHENTER,** "Processing and Testing of ENDF/B-IV Fission Product and Transmutation Data" (50)

PACE, J. V.,** AND D. E. BARTINE, "Transport Calculations for 14-MeV and Fission Neutron Sources in Air/Ground and Air/Seawater Geometry" (89)

SANTORO, R. T., R. G. AFFEL,** G. C. CAIN,** AND J. H. GREENE,** "Nuclear Accident Dosimetry in a Simulated Criticality Accident" (122)

International Symposium on Radiation Physics, 1974, Bose Institute, Calcutta, India, November 30–December 4, 1974

TRUBEY, D. K., "Recent Trends in Reactor Shielding in the U.S.A." (61)

TRUBEY, D. K., "The Development of Radiation Shielding Standards in the USA" (105)

TRUBEY, D. K., B. F. MASKEWITZ, AND R. W. ROUSSIN, "Computer Codes and Data Available from the Radiation Shielding Information Center" (60)

NEUTRON PHYSICS DIVISION

SEPTEMBER 1, 1974

DIRECTOR F. C. MAIENSCHEIN
R. RICKMAN

FINANCE OFFICER
C. T. LONG[c]

QUALITY ASSURANCE COORDINATOR
W. R. CASTO[h]

ELECTRON LINEAR ACCELERATOR
R. W. PEELLE[1]
L. K. LOVETTE

NEUTRON CROSS SECTIONS – FISSILE AND FERTILE NUCLIDES
G. de SAUSSURE
J. K. DICKENS
F. C. DIFILIPPO[k]
R. GWIN
R. W. INGLE[d]
T. A. LOVE[g]
D. K. OLSEN
R. B. PEREZ
E. G. SILVER[i]
R. R. SPENCER
J. H. TODD[d]
H. WEAVER
L. W. WESTON

LINAC OPERATIONS
H. A. TODD[d]
T. A. LEWIS[d]
D. W. BIBLE[d]
- - - - - - - - - -
G. M. ARGO
C. C. BARRINGER
E. BECKHAM
O. W. CHRISTIAN
W. R. FINNELL

DATA SYSTEMS
J. G. CRAVEN[a]
C. R. STEWART[a]
C. H. THOMPSON[a,j]

NEUTRON CROSS SECTIONS – LIGHT AND MEDIUM A NUCLIDES
F. G. PEREY
J. C. GENTRY
G. T. CHAPMAN[7]
C. Y. FU
W. E. KINNEY
D. C. LARSON
G. L. MORGAN
J. W. McCONNELL
E. NEWMAN[f]
C. M. PEREY[a]

REACTOR SHIELDING EXPERIMENTS
C. E. CLIFFORD[2]
J. H. LUCKETT

TSF AND HPRR OPERATIONS
L. B. HOLLAND
E. S. HOWE[i]
J. L. HULL
J. LEWIN
J. J. MANNING
J. N. MONEY
D. R. WARD

TSF MEASUREMENTS
F. J. MUCKENTHALER
R. M. FREESTONE
L. W. GILLEY
K. M. HENRY
P. N. STEVENS[a]
- - - - - - - - - - -
D. L. REED[b]
F. J. SLAGLE[b]
W. YOON[b]

SHIELDING ANALYSIS AND REACTOR PHYSICS
F. R. MYNATT
V. D. GLIDEWELL
S. M. PIERCE
L. S. ABBOTT[9]
D. E. BARTINE[4]
T. J. BURNS
G. P. CAVANAUGH
R. L. CHILDS[a]
J. CHING[b]
S. N. CRAMER
G. W. CUNNINGHAM[a]
J. D. DRISCHLER
M. B. EMMETT[a]
G. F. FLANAGAN[3]
W. W. ENGLE
T. B. FOWLER
S. K. FRALEY[a]
W. E. FORD[a]
N. M. GREENE[a]
J. M. KALLFELZ[a]
R. A. LILLIE
J. L. LUCIUS[a]
R. E. MAERKER
J. H. MARABLE
E. M. OBLOW[6]
J. V. PACE[a]
W. A. RHOADES
J. C. ROBINSON[a]
D. B. SIMPSON
D. R. VONDY
C. R. WEISBIN
M. L. WEISS[a]
J. E. WHITE[a]
L. R. WILLIAMS
M. L. WILLIAMS
R. Q. WRIGHT[a]
- - - - - - - - - - - - -
D. L. SELBY[b]
J. S. TANG[b]
E. T. TOMLINSON[b]

RADIATION SHIELDING INFORMATION CENTER
B. F. MASKEWITZ
E. N. BERRIER
M. W. LANDAY
F. S. ALSMILLER[a]
C. M. ANTHONY
C. P. COKER
H. E. COMOLANDER
J. GURNEY
A. B. GUSTIN[i]
N. A. HATMAKER
H. R. HENDRICKSON
R. W. ROUSSIN
D. K. TRUBEY
J. B. WRIGHT

HIGH AND MEDIUM ENERGY RADIATION TRANSPORT
R. G. ALSMILLER, JR.[5]
H. D. COOK
J. D. AMBURGEY[a]
J. BARISH[a]
H. W. BERTINI
T. A. GABRIEL
R. T. SANTORO[10]

1. ORELA CODIRECTOR WITH J. A. HARVEY
2. LMFBR AND GCBR COORDINATOR
3. LMFBR ALTERNATE COORDINATOR
4. GCBR ALTERNATE COORDINATOR
5. TN COORDINATOR
6. TN ALTERNATE COORDINATOR

STAFF FUNCTIONS

7. SAFETY AND RADIATION CONTROL OFFICER
8. AFFIRMATIVE ACTION REPRESENTATIVE
9. ALTERNATE FINANCE OFFICER
10. DIVISION OMBUDSMAN

- -

a. ADJUNCT RESEARCH PARTICIPANT
b. CONTRACT ASSIGNEE, U. OF TENNESSEE
c. ON ASSIGNMENT FROM FINANCE AND MATERIALS DIVISION
d. ON LOAN FROM INSTRUMENTATION AND CONTROLS DIVISION
e. ON ASSIGNMENT FROM COMPUTER SCIENCES
f. ON ASSIGNMENT FROM PHYSICS DIVISION
g. ON ASSIGNMENT FROM GE-SUNNYVALE
h. ON ASSIGNMENT PART TIME FROM OPERATIONS DIVISION
i. ON LEAVE TO INSTITUTE FOR ENERGY ANALYSIS
j. PART TIME
k. ON ASSIGNMENT FROM IAEA AND CNEA, ARGENTINA

ORNL-4997
UC-34c – Physics–Nuclear

INTERNAL DISTRIBUTION

1–5. L. S. Abbott
6. R. G. Affel
7. R. G. Alsmiller, Jr.
8. J. D. Amburgey
9. J. Barish
10. D. E. Bartine
11. H. W. Bertini
12. F. E. Bertrand
13. H. P. Carter
14. G. C. Cain
15. G. T. Chapman
16. R. L. Childs
17. J. Ching
18. H. C. Claiborne
19. C. E. Clifford
20. H. E. Comolander
21. S. N. Cramer
22. F. L. Culler
23. G. de Saussure
24. J. K. Dickens
25. J. Drischler
26. M. B. Emmett
27. W. W. Engle, Jr.
28. G. F. Flanagan
29. W. E. Ford, III
30. P. B. Fox
31. R. M. Freestone
32. T. B. Fowler
33. C. Y. Fu
34. T. A. Gabriel
35. J. H. Greene
36. N. M. Green
37. R. K. Gryder
38. J. Gurney
39. A. B. Gustin
40. R. Gwin
41. W. O. Harms
42. G. L. Haynes
43. K. M. Henry
44. O. W. Hermann
45. R. F. Hibbs
46. R. J. Hinton
47. L. B. Holland
48. J. L. Hull
49. F. B. K. Kam
50. C. W. Kee
51. W. R. Kinney
52. J. R. Knight
53. D. Larson
54. N. M. Larson
55. J. Lewin
56. R. A. Lillie
57. C. T. Long
58. T. A. Love
59. B. K. Lyon
60. R. L. Macklin
61. R. E. Maerker
62–71. F. C. Maienschein
72. J. J. Manning
73. B. F. Maskewitz
74. J. T. Mihalczo
75. J. N. Money
76. G. L. Morgan
77. G. W. Morrison
78. F. J. Muckenthaler
79. F. R. Mynatt
80. J. W. McConnell
81. E. M. Oblow
82. J. V. Pace, III
83–84. R. B. Parker
85. R. W. Peelle
86. S. K. Penny
87. C. M. Perey
88. F. G. Perey
89. R. B. Perez
90. A. M. Perry
91. L. M. Petrie
92. H. Postma
93. W. A. Rhoades
94. R. W. Roussin
95. R. T. Santoro
96. D. L. Selby
97. R. D. Sharp
98. E. G. Silver
99. D. B. Simpson
100. T. M. Sims
101. M. J. Skinner
102. P. N. Stevens
103. G. G. Slaughter
104. J. H. Swank
105. E. T. Tomlinson
106. D. R. Vondy
107. J. W. Wachter
108. C. R. Weisbin
109. L. W. Weston
110. J. E. White

111. G. E. Whitesides
112. L. R. Williams
113. R. R. Winters
114. J. B. Wright
115. R. Q. Wright
116. A. Zucker
117. H. Feshbach (consultant)
118. P. F. Fox (consultant)
119. W. W. Havens (consultant)
120. A. F. Henry (consultant)
121–123. Central Research Library
124. ORNL – Y-12 Technical Library Document Reference Section
125–174. Laboratory Records Department
175. Laboratory Records, ORNL R.C.

EXTERNAL DISTRIBUTION

176. B. J. Allen, Australian Atomic Energy Commission, Lucas Heights, AUSTRALIA
177. W. Zobel, 110 Stanton Lane, Oak Ridge, Tennessee 37830
178. S. M. Austin, Michigan State University, Lansing, Michigan
179. B. H. Wildenthal, Michigan State University, Lansing, Michigan
180. G. D. Harp, Chemistry Department, Brookhaven National Laboratory, Upton, N. Y.
181. J. M. Hunt, University of Wisconsin Medical School, Madison, Wisconsin
182. G. D. James, Nuclear Physics Division 7.21, Atomic Energy Establishment, Harwell, Didcot, Berkshire, ENGLAND
183. J. S. Hendricks, Massachusetts Institute of Technology, Cambridge, Mass. 02139
184. H. Goldstein, Division of Nuclear Science & Engineering, Columbia University, New York, New York 10027
185. J. J. Wagshal, Hebrew University, Jerusalem, ISRAEL
186. R. E. Schenter, Hanford Engineering Development Laboratory, Richland, Washington
187. D. C. Irving, Science Applications, Inc., Box 2351, La Jolla, California 92037
188. M. A. Abdou, Nuclear Engineering Department, University of Wisconsin, Madison, Wisconsin 53706
189. A. R. Buhl, U. S. Atomic Energy Commission Division of Reactor Research and Development, Washington, D.C.
190. T. J. Hoggman, Science Applications, Inc., 2109 Clinton Avenue West, Huntsville, Alabama 35806
191. D. E. Cullen, University of California Lawrence Livermore Laboratory, P.O. Box 808, Livermore, California 94550
192. P. D. Soran, Los Alamos Scientific Laboratory, Group T-2, Los Alamos, New Mexico 87544
193. D. R. Harris, Los Alamos Scientific Laboratory, Group T-2, Los Alamos, New Mexico 87544
194. R. J. LaBauve, Los Alamos Scientific Laboratory, Group T-2, Los Alamos, New Mexico 87544
195. R. E. MacFarlane, Los Alamos Scientific Laboratory, Group T-2, Los Alamos, New Mexico 87544
196. H. Henryson, II, Argonne National Laboratory, 9700 South Cass Avenue, Argonne, Illinois 60439
197. Charles O. Slater, 4975 Clairmont Mesa Blvd., Apartment 104, San Diego, California 92117
198. C. Durston, Argonne National Laboratory, Applied Physics Laboratory, 9700 South Cass Avenue, Argonne, Illinois 60439
199. R. B. Kidman, Hanford Engineering Development Laboratory, Richland, Washington
200. K. Kin, Division of Nuclear Science & Engineering, Columbia University, New York, N. Y. 10027
201. W. M. Stacey, Argonne National Laboratory, 9700 South Cass Avenue, Argonne, Illinois 60439
202. B. J. Toppel, Argonne National Laboratory, 9700 South Cass Avenue, Argonne, Illinois 60439
203. R. N. Hwant, Argonne National Laboratory, 9700 South Cass Avenue, Argonne, Illinois 60439
204. K. D. Lathrop, Los Alamos Scientific Laboratory, Los Alamos, New Mexico 87544
205. J. M. Kallfelz, Georgia Institute of Technology, Atlanta, Georgia
206. M. M. Williams, Georgia Institute of Technology, Atlanta, Georgia
207. D. Lal, Georgia Institute of Technology, Atlanta, Georgia
208. B. J. McGregor, Physics Division, A.A.E.C. Research Establishment, P. M. B. Sutherland 2232, AUSTRALIA
209. S. Uchida, Hitachi Research Laboratory, Hitachi, Limited, Hitachishi, Ibarakiken, JAPAN
210. M. L. Gritzner, Science Applications, Inc., 2109 Clinton Avenue West, Huntsville, Alabama 35805

211. C. E. Burgart, Science Applications, Inc., 122 Le Veta Drive, Albuquerque, New Mexico 87108
212. T. W. Armstrong, Science Applications, Inc., P.O. Box 2351, 1200 Prospect Street, La Jolla, California 92037
213. K. C. Chandler, Tennessee Eastman Corp., Kingsport, Tennessee
214. S. R. Dodge, Chapman College, Orange, California
215. A. M. Weinberg, Institute for Energy Analysis, P.O. Box 117, Oak Ridge, Tennessee 37830
216–347. Given special NPD Progress Report Distribution
348. Research and Technical Support Division, AEC, ORO
349–465. Given distribution as shown in TID-4500 under Physics–Nuclear category (25 copies – NTIS)